Cyclic and acyclic oligopyrrole derivatives towards anion binding

A Thesis Submitted for the Degree of

DOCTOR OF PHILOSOPHY

By

Sanjeev Pran Mahanta

School of Chemistry
University of Hyderabad
Hyderabad-500 046
INDIA

January 2013

Dedicated

to

Maa and Deuta

CONTENTS

DECLARATION

I hereby declare that the matter embodied in the thesis entitled "***Cyclic and acyclic oligopyrrole derivatives towards anion binding"*** is the result of investigations carried out by me in the School of Chemistry, University of Hyderabad, Hyderabad, India under the supervision of **Dr. Pradeepta K. Panda** and it has not been submitted elsewhere for the award of any degree or diploma or membership, etc.

In keeping with the general practice of reporting scientific investigations, due acknowledgements have been made wherever the work described is based on the findings of other investigators. Any omission or error that might have crept in is sincerely regretted.

January 2013 **Sanjeev Pran Mahanta**

UNIVERSITY OF HYDERABAD

Central University (P.O.), Hyderabad-500 046, INDIA

Dr. Pradeept K Panda
Associate Professor
School of Chemistry

Tel: 91-40-23134818 (Office)
Fax: 91-40-23012460
E-mail: pkpsc@uohyd.ernet.in
pradeepta.panda@gmail.com

CERTIFICATE

This is to certify that the work described in this thesis entitled "***Cyclic and acyclic oligopyrrrole derivatives towards anion binding***" has been carried out by Mr. Sanjeev Pran Mahanta under my supervision and the same has not been submitted elsewhere for any degree.

Dean
School of Chemistry
University of Hyderabad
Hyderabad-500 046
India

Dr. Pradeepta K Panda
(Thesis supervisor)

PREFACE

The present thesis entitled "Cyclic and acyclic oligopyrrole derivatives towards anion binding" has been divided into seven chapters. The thesis is principally concerned with the synthesis and anion binding studies of some neutral cyclic and acyclic oligopyrrole based anion receptors, which can recognize anions primarily on the basis of their H-bonding ability. **Chapter 1** provides a brief introduction on the chemical, biochemical and environmental relevance of anions and an overview of various classical synthetic anion receptors. In addition it describes some of the analytical techniques used in the anion recognition study. **Chapter 2** gives a brief account of various solvents, chemicals used in the study and different instruments and computational methods employed for characterization in our investigation. In addition, it presents an overview of the theory of the various methods used in calculating the binding constants along with the synthetic procedures of the precursor materials employed in the subsequent investigations. **Chapter 3** deals with our efforts to synthesize various biscalix[4]pyrroles. This chapter describes the synthesis of bisdipyrromethanes from diketones with different organic scaffolds, along with several unexpected and interesting products. **Chapter 4** deals with the *meso* acylation of the basic calix[4]pyrrole skeleton with the goal of generating receptors with improved dihydrogenphosphate affinity and selectivity. This chapter describes the anion binding affinity of the calix[4]pyrrole w.r.t. the position and conformation of the two acyl substituents placed at their *meso* positions. **Chapter 5** deals with the synthesis and anion binding studies of calix[2]bispyrrolylethenes, an expanded calix[4]pyrrole where the two dialkyldipyrromethane units are linked via ethene bridges. **Chapter 6** describes the synthesis of pyrrole-benzimidazole conjugates and presented them as a new H-bonding motif towards anion binding. Finally, **Chapter 7** summarizes the findings of the present investigations along with the future scopes.

January 2013 **Sanjeev Pran Mahanta**

Acknowledgement

I would like to acknowledge all the people who helped me along my seven year's journey in the University of Hyderabad.

First of all, I would like to thank my supervisor, Dr. Pradeepta K Panda. Thank you so much for your constant cooperation, encouragement and kind guidance. I am also indebted to you for the work freedom you have given me during the last six years.

I would like to thank the former and present Dean, School of Chemistry, for their constant inspiration and for allowing me to use the available facilities. I am extremely thankful individually to all the faculty members of the School for their kind help and cooperation at various stages of my stay in the campus.

I thank all the non-teaching staff of the School of Chemistry and CIL for their assistance on various occasions.

I am grateful to CSIR, New Delhi, ACHREM and School of Chemistry Development Fund for providing financial support. I also would like to record my thanks to DST-PURSE programme for funding towards my presentation at ICPP-6, New-Mexico, USA.

I would wish to thank our collaborators Dr. Chainnappan Sivasankar and Mr. Sambath Baskaran, Pondicherry University for their contribution in some of our computational study. I wish also to thank Dr. Akkaladevi Narahari, Dr. Sushanta Ghanta, Mr. Shashikant Reddy and Mr. Deepak K Tosh for their help during different part of my Ph.D. work.

I would like to thank all the group members in Panda lab for their non-conservative help and candid discussion regarding my research work. Thank you, Naren, Tridib, Ritwik, Brijesh, Nandakishore, Anup, Sathish, Obaiah, Vikranth, Dr. Raju, Dr. Balakrishna, Dr. Santosh, Prameela, Sandip and Prity. I would also wish to thank the project students Kiran Kumar, Chinnaayyaswamy, Shamimul, Rajesh, Promod, Rajasekhar, Samatha, Sathish, Mahesh, Vidyasagar, Shantimoy, Sauradip, Srinivas, Preety, Sabhapati, Suganya, Archana, Sanjib, Arghya, Pramit, Bilash, Arpita, Subham, Sreedhar, Shravani and Gopi Sudheer.

My pleasant association with some friends in UOH such as Ranjit, Tridib, Gauranga, Bipul Da, Naba Da, Abdul, Pabitra, Bipul, Satya, Prasenjit, Alankar, Jahnu, Debabrot, Mouchumi, Barnali, Monima, Sapan, Tiken, Kamble, Taya, Jayanta, Milan, Gokul, Bhokti, Debanath, Sumit, Nobojyoti, Amir and Bhanu is unforgettable.

I would like to thank my school of chemistry friends Dinu da, Rahul Da, Binoy Da, Archan Da, Abhijit da, Prashant da, Teja bhai, Lucky Bhai, Tapan Bhai, Chetan sir, Sanjeev bhai, Sudhanshu, Dinu, Satyajit, Raja, Nayan, Rajeswar, Arindam, Arun, Sandeep, Ghanta, Satyajit, Mehboob, Ganesh, Shrinivas, Ravindra, Krishnachary, Tanmoy, Praveen, Sanatan, Srinivas, Karunakar, Sekhar, Tirupati, Kishore, Gupta, Hari, Ramesh, Anji, Srinivas, D. K., Krishnachaitanya, and all others whose names are not mentioned due to limited space.

I would like to thank Subrata Barooah sir, for his constant guidance throughout my life. I also like to thank Dhruba sir and Diganta sir for their constant support. Special thanks to the institution, B. Borooah College where I spent my golden days with my friends like Ranjit, Ganesh, Naba, Sanjay, Dhruba, Prem, Samiran, Anupam, Dipankar, Nabanita and Mouchumi. I am grateful to all the faculty members of the Department of Chemistry, B. Barooah College and Gauhati University.

I wish to thank my juniors Gauranga, Dipjyoti, Bidyut, Kashyap, Bilash, Prajwalita, Anamika and Upama who visited our department under different programes with whom I spent some unforgettable moment.

I would like to thank all my family members. Thank you, my beloved Maa, Deuta, Kakati Khura, Kalyani Khuri, Sun Da, Biju Khuri, Dada, Bou, Bhonti, Dibya, Harihar, Karabi, Tulika, Biju, Sikha, Eva, Bikash and my two sweet nieces (Kristi and Preksha).

Finally, I would like to express my love and gratitude to my parents for their unconditional love and blessings. They made me what I am today and I owe everything to them. Dedicating this thesis to them is a minor recognition for their relentless support and love.

January 2013 **SanjeevPran Mahanta**

University of Hyderabad

Hyderabad-500 046

India

List of abbreviations

Anhyd.	anhydrous
2D	Two-dimensional
BisDPM	Bisdipyrromethane
br	Broad
C4P	Calix[4]pyrrole
Calcd.	Calculated
COSY	Correlated spectroscopy
Conc	Concentaration
d	Doublet
DCM	Dichloromethane
DMSO	Dimethylsulfoxide
DFT	Density functional theory
DMF	N,N-Dimethylformamide
DMAc	N,N-Dimethylacetamide
EPR	Electron paramagnetic resonance
Equiv.	Equivalent
HRMS	High resolution-mass spectrometry
HOMO	Highest occupied molecular orbital
h	Hour (s)
ITC	Isothermal titration calorimetry
LUMO	Lowest unoccupied molecular orbital
LCMS	Liquid chromatography mass spectrometry
L	Ligand and/or guest
m	Multiplet
m	Meta
m/z	Mass/charge
min	Minute (s)
NMR	Nuclear magnetic resonance
MSA	Methane sulphonic acid

NOESY	Nuclear Overhauser effect spectroscopy
o	Ortho
ORTEP	Oak Ridge thermal ellipsoid program
p	Para
PCM	Polarizable continuum model
PXRD	Powder X-ray diffraction
S	Substrate and/or Host
s	Singlet
TBAF	Tetrabutylammonium fluoride
TBACl	Tetrabutylammonium chloride
TBA(CH_3COO)	Tetrabutylammonium acetate
$TBAH_2PO_4$	Tetrabutylammonium phosphate
TFA	Trifluoroacetic acid
THF	Tetrahydrofuran
TLC	Thin layer chromatography
t	Triplet
TTF	Tetrathiafulvalene
TEA	Triethylamine
UV-Vis	Ultraviolet-Visible
XRD	X-Ray diffraction
COSY	Correlated spectroscopy
Conc	Concentaration
d	Doublet
DCM	Dichloromethane
DMSO	Dimethylsulfoxide
DFT	Density functional theory
DMF	N,N-Dimethylformamide
DMAc	N,N-Dimethylacetamide
EPR	Electron paramagnetic resonance

CHAPTER 1

Introduction

1.1 Anions and life

The selective recognition of anions has emerged as an attractive field of research in supramolecular chemistry since anions are ubiquitous in nature *e.g.* chloride ion is present in large quantities in the oceans, nitrate and sulfate are present in acid rain, carbonates are in bio-mineralized materials and most importantly more than two third of enzyme substrates and cofactors are anionic in nature.[1,2] The selective recognition and sensing of anions has been the subject of intense research activities, motivated by their applications in medical diagnostics, environmental and industrial monitoring, and nuclear waste remediation. The role of some of the anions in biology and environment is discussed below.

Fluoride ion is important to study owing to its duplicitous nature. It has many industrial applications, and also been used in human diet, however, it has been accused of several human pathologies. Addition of fluoride to water is a general practice in USA since about 1950s.[3] Fluoride can be effective in improvement of overall dental health through a very basic chemical process, where it converts hydroxyapatite to fluorapatite, which is comparatively hard and hence prevents corrosion of teeth by acids.[4] Fluoride is also used as an ingredient in several drugs, to treat the brittle-bone disease called osteoporosis.[5] With appropriate dose, the fluoride appears to stimulate the formation of new bone tissue. However on the darker side, dental and skeletal fluorosis have been reported in many countries, in particular the developing nations, associated with high level of fluoride content in drinking water due to geogenic origin. Moreover, some anthropogenic activities in relation to the use of phosphate containing fertilizers and aluminum processing industries also introduce fluoride ion into the environment. Fluoride is also responsible for causing osteosarcoma.[6] Inhibition of neurotransmitter biosynthesis in fetuses, owing to high concentration of fluoride ion has also been documented.[7] Chloride is a prominent anion in blood, together with sodium, potassium and bicarbonate serves as electrolyte in our body and help in maintaining the blood's pH level.[8] Anions, in particular, are crucial to many processes as they help to regulate cellular pH, maintain cell volume, osmotic balance and serve as cellular signals. The transmembrane transport of anions is also important, since defective anion transport has been linked to various diseases for example, the malfunction of natural chloride channels has been associated with Bartter syndrome,[9] Dent's disease[10] and cystic fibrosis.[11] Similarly, defects in proteins that facilitate transmembrane bicarbonate transport have been linked to diseases of brain, heart and bones, as well as cystic fibrosis.[12] Iodide plays an important role in biological activities such as neurological activity and thyroid function. The iodide deficiency could lead

to disorders in physiological functions. Hence the iodide content of urine and milk is often analyzed for nutritional, metabolic, and epidemiological studies of thyroid disorder.[13] Moreover, elemental iodine has been used in many areas of chemistry for synthesizing valuable molecules such as drugs and dyes.

Cyanide is used in many chemical processes such as electroplating, plastic manufacturing, gold and silver extraction, tanning and metallurgy.[14] In addition, cyanide is a chemical warfare agent and thus, responsible for the cyanide pollution in environment.[15] Biological sources of cyanide include bacteria, fungi, and algae, which produce this ion as part of their nitrogen metabolic pathways. Vegetables containing cyanogenic glycosides are also sources of cyanide ingestion in humans and animals. Other potential sources of cyanide in humans and animals are sodium nitroprusside, succinonitrile and organic thiocyanates.[14b] Cyanide is extremely toxic and can affect many functions in the body, including the vascular, visual, central nervous, cardiac, endocrine, and metabolic systems. Perhaps, the best known effect of cyanide is its inhibition of respiration, which is caused by the inhibition of terminal oxidase (cytochrome oxidase) of the mitochondrial respiratory chain.[14a,15] Cyanide can also cause a decrease in the rate of glycolysis and inhibit the operation of the Krebs cycle and also act as an inhibitor of metalloenzymes and of some non-metalloenzymes that function through the intermediacy of Schiff bases.

Oxoanions as a group are characterized by high aqueous solubility. Among oxoanions, phosphates are the most important constituent of living systems. In conjunction with heterocyclic bases and sugars, phosphate makes the hereditary elements of living system *i.e.* DNA.[16] In addition, phosphate ion and its derivatives play crucial roles in energy storage and transduction in biological systems. Protein phosphorylation is a key mechanism for signaling, and phosphorylated proteins are a significant source of ingested phosphate. Phosphate has also important medical implications, for example, hyperphosphatemia, caused due to an abnormally high concentration of serum phosphate levels, and affects nearly all hemodialysis patients.[17] The adverse effects of hyperphosphatemia, include the development of hyperparathyroidism, soft tissue calcification, cardiovascular complications and increased morbidity and mortality.[18] Anthropogenic phosphates from agricultural fertilizers and other human activities, constitutes the eutrophication of natural water resources, leading to a dangerous increase in toxic algal boom.[19] Perchlorate is naturally occurring, as well as can be made artificially and extensively used as rocket fuel, fireworks, flares, and explosives. Perchlorate can also be present in some bleach and fertilizers. Perchlorate is also of concern

to human health, as it interferes with the ability of the thyroid gland, to utilize iodine to produce thyroid hormones.[20a] On the other hand, owing to this, it has been used to treat hyperthyroidism.[20b] Oxoanions such as nitrate and aluminate also contributed to eutrophication of water bodies. Oxoanions of As, Sb, Pb and Cr present locally in high concentrations from industrial or mining activities are very toxic to environment.[21] The accumulating concentrations of $^{188}ReO_4^-$ and $^{99}TcO_4^-$ or other radioactive anions generated in consequence of radiopharmaceutical use and/or in the nuclear industry need adequate monitoring to avoid their harmful ramifications.[22]

Given the above role anions play in environment and in biology, the objective of achieving strong and selective complexation of anions has become very significant.

1.2 Natural anion binding receptors

The influence of anions on biological processes is usually affected *via* macromolecular receptors, often made of proteins. The protein-anion interactions serve specific purposes, for example enzymatic transformations (where majority of enzymes bind anions as either substrates or cofactors), transport and signal transduction. The complexation occurs through interactions that are usually noncovalent in nature such as hydrogen bond, electrostatic interaction, metal ligand coordination, hydrophobic interaction etc. The structures of some of the natural anion receptors and their mode of interaction are discussed below.

Several X-ray crystal structures have been reported that provide direct visualization of enzyme-anionic substrate complexes, stabilized via multiple hydrogen bonding interactions. The X-ray crystal structure, of the DNS helicase RepA sulfate complex shows seven hydrogen bonding interactions between the sulfate ion and RepA protein scaffold. The anion

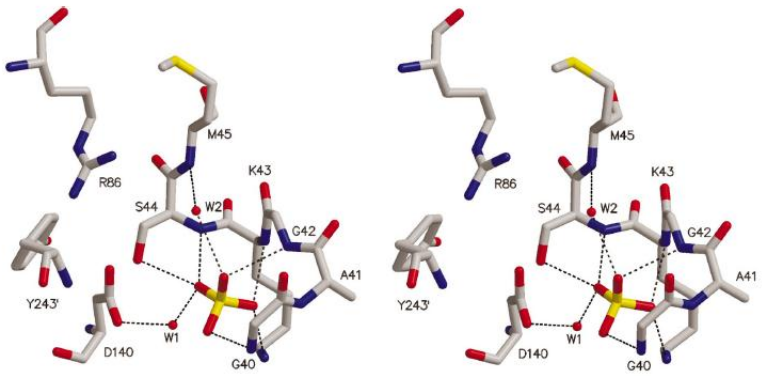

Figure 1.1 Stereo view of the ATPase active site showing the interaction of sulfate anion and P-loop residues.[23]

is further hydrogen bonded to Asp 140 via an intervening water molecule (Figure 1.1).[23] In another report, the X-ray crystal structure of the sulfate binding protein found in *Salmonella typhimurium*, which is involved in sulfate transport, shows that the sulfate ion is forming seven hydrogen bonds, five of which from peptide NH groups, one from a serine OH residue with the remaining residue coming from the tryptophan NH group (Figure 1.2).[24] The charge on the sulfate ion is stabilized through several hydrogen bond relay system that presumably serve to spread well into the protein matrix.

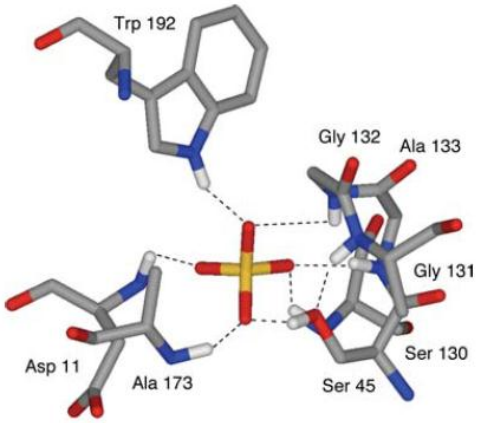

Figure 1.2 The X-ray crystal structure and schematic of the sulfate binding site in the sulfate-binding protein.[1b]

The guanidinium group present in the side chain of arginine is ubiquitous in enzymes that bind anionic substrates and also involved in stabilization of protein tertiary structures via internal salt bridges with carboxylate functions. This motif is realized in phosphatases and phosphorylases, which selectively bind phosphate, as well as in decarboxylases, dehydrogenases, isomerases, and in some proteases that bind carboxylates. The crystal structure of the histone octamer-phosphate complex, by Baldwin *et al.* shows how the phosphate ion is binding with several basic amino-acid residues (Figure 1.3).

Smith and colleagues reported the crystal structures of the anion binding sites of the nitrate (NrtA) and bicarbonate (CmpA) transporters from cyanobacteria (Figure 1.4).[25,26] The two proteins are homologous, being 48 % identical in sequence. However, each protein is selective towards its own substrate. The difference in anion selectivity is attributed to changing a single amino acid from a hydrogen bond donor in NrtA to a hydrogen bond acceptor CmpA (Figure 1.4). In NrtA, nitrate is bound within a cleft by a combination of

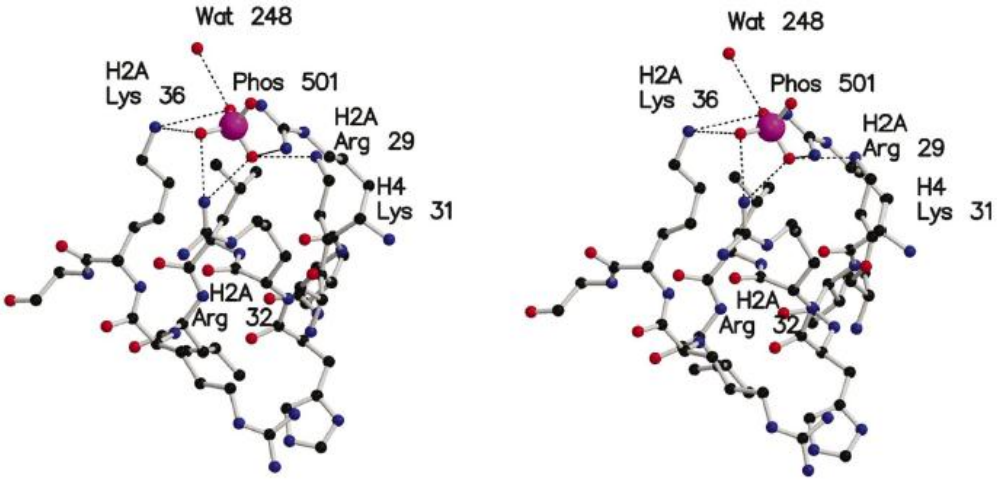

Figure 1.3 Stereo structures of amino-acid residues interacting with phosphate in histone octamer-phosphate complex.[24]

hydrogen bonds and electrostatic interactions. On the other hand, in CmpA, bicarbonate ion is bound by hydrogen bonds and electrostatic interactions, which are provided by the Ca^{2+} ion, not by positively charged amino acid side chain.

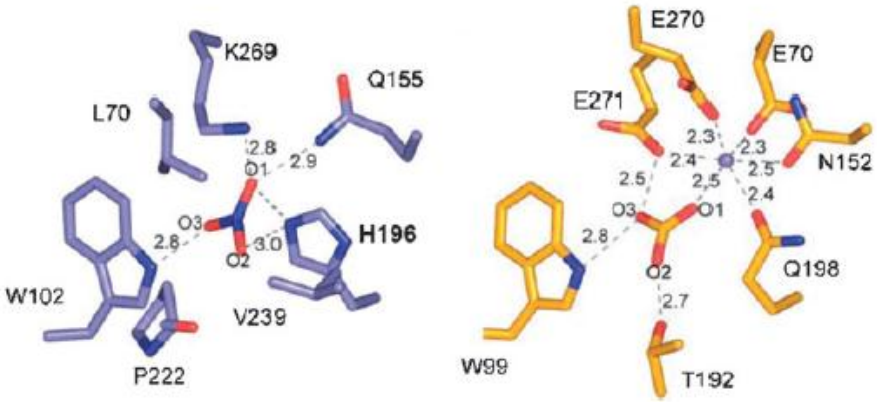

Figure 1.4 Depiction of the anion binding sites of nitrate-binding protein NrtA (left), and bicarbonate-binding protein CmpA (right) showing the electrostatic interactions between protein amino acid residues and anionic substrates NO_3^- and HCO_3^- respectively.[27]

In 1992, Jordan and coworkers reported the crystal structure of porphobilinogen deaminase, a key enzyme in the biosynthesis of the linear tetrapyrrole precursor of protoporphyrin IX.[28] The structure shows that the pyrrolic NH protons of the dipyrromethane

substrate is hydrogen bonded with the carboxylate side chain of Asp 84 (Figure 1.5). Further, the four carboxyl groups at the *β*-pyrrolic positions are seen to interact with the positively charged enzyme residues of Arg 11, Arg 131, Arg 132, Arg 155 and Lys 55 and Lys 83 and to be involved in hydrogen bond interactions with Ser 13. The replacement of Asp 84 by Glu causes the enzyme to loss 99% of its activity and prevents the enzyme from catalyzing the formation of pre-europorphyrinogen. This result underscores the importance of the interactions between the two pyrrole units and the Asp 84 carboxylate anion, thus providing a further incentive to design and study pyrrole based anion receptors.

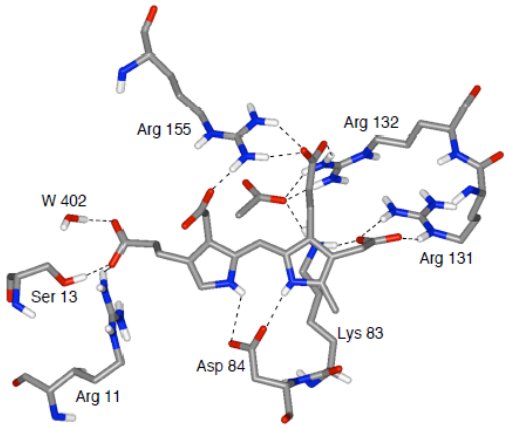

Figure 1.5 Partial view of the X-ray structure of the enzyme porphobilinogen deaminase showing the binding of a dipyrromethane cofactor.[28]

Dutzler and MacKinnon combinedly reported the X-ray crystal structure of two prokaryotic ClC chloride channels (which catalyses the selective flow of Cl^- ions across cell membranes) in 2002 from *Salmonella enterica serovar typhimurium* and *Escherichia coli* at 3.0 and 3.5 Å, respectively. Both structures reveal two identical pores, each pore being formed by a separate subunit contained within a homodimeric membrane protein (Figure 1.6). Individual subunits are composed of two repeated halves that span the membrane with opposite orientations.[29] At the anion binding sites the Cl^- ion is coordinated by main-chain amide nitrogen atoms from amino acids Ile 356 and Phe 357 and by the side-chain oxygen atoms from Ser 107 and Tyr 445 (Figure 1.7). The nitrogen atoms are not involved in hydrogen bonding with the protein, and are available for ion binding. The side chains of Ser 107 and Tyr 445 contact the Cl^- ion opposite the nitrogen cradle. In addition to the interactions with polar functional groups, the Cl^- ion is surrounded by a number of hydrophobic amino-acid side chains (Figure 1.7). The structure of conduction pore indicates

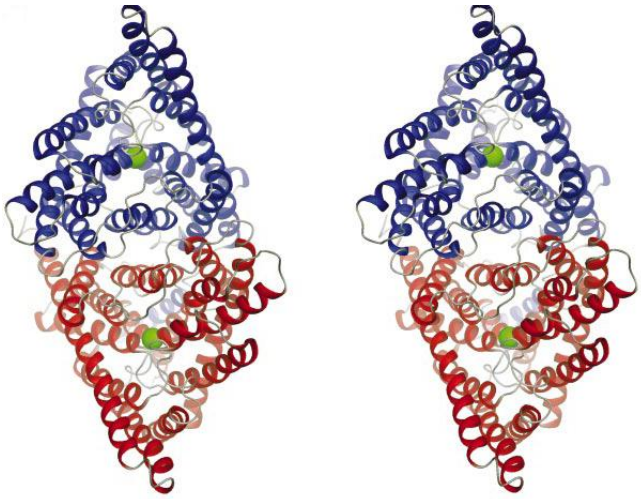

Figure 1.6 Structure of the ClC dimer. Stereo view of a ribbon representation of the ClC dimer from the extracellular side. The two subunits are blue and red. A Cl^- ion in the selectivity filter is represented as a green sphere.[30]

the presence of negatively charged glutamate side chain, just above the channel entrance. This residue acts as an anion-regulating gate.[30] By swinging out to open the channel, it allows chloride ions to enter the channel pore from where they are directed towards the confined center of the channel by positively polarized residues. In spite of these significant

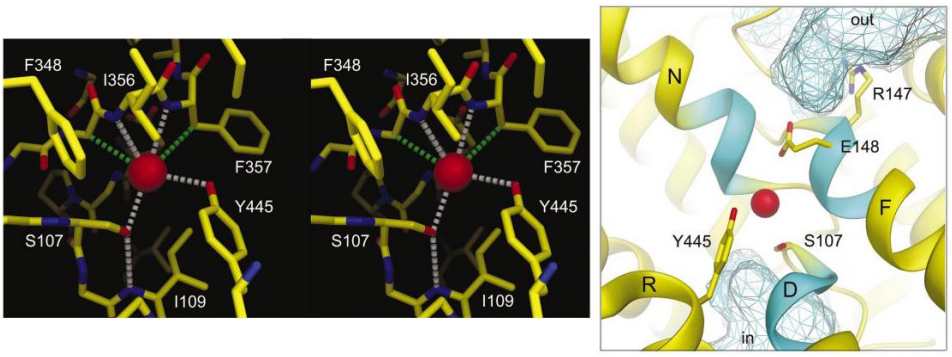

Figure 1.7 Left: Stereo view of the Cl^- ion-binding site. Distances (<3.6 Å) to the Cl^- ion (red sphere) are shown for polar (white dashed lines) and hydrophobic (green dashed lines) contacts. A hydrogen bond between Ser 107 and the amide nitrogen of Ile 109 is shown (white dashed line). Right: Ion conduction pathway. The ion-binding site viewed from the dimer interface, along the pseudo two-fold axis, with foreground α-helices removed for clarity.[30]

developments, still further work is needed to understand how anion transporters gate and how the gating processes are coupled to ion conduction through the pore. One way of addressing this, is through the synthesis and study of synthetic anion receptors and artificial anion channels, to mimic such systems.

In contrast to the many natural products that transport cations across lipid membranes, there are only few natural products that have been reported to be anion carriers.[31] Since the structural complexity of proteins is beyond the reach of most synthetic chemist, it is important to design and synthesize small molecules that could serve as models for synthetic anion transporters. Prodigiosine, a tripyrrolic alkaloid (Figure 1.8), produced by microorganism such as *Streptomyces* and *Serratia,* acts as an efficient transmembrane chloride transporter. It can function either as an H^+/Cl^- co-transporter or as a Cl^-/A^- antiporter depending on the conditions.[32] Although its mechanism of action remains unclear, prodigiosin and its analogues (Figure 1.8) have shown promising anticancer, antimicrobial, and immunosuppressive activities.[33] Obatoclax, an abiotic prodigiosin, which is an inhibitor of the Bcl-2 family of proteins, is undergoing Phase II clinical trials for the treatment of lung cancer.[34]

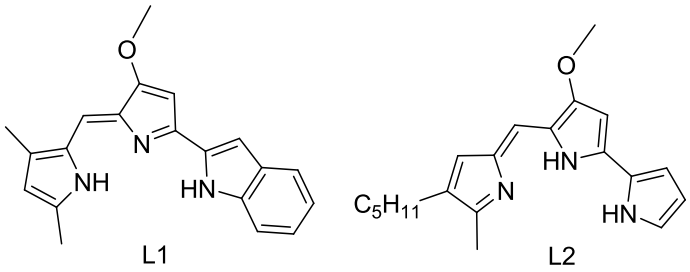

Figure 1.8 Left: Prodigiosin a natural ionophore. Right: Obatoclax a synthetic ionophore.

1.3 Artificial anion binding receptors

The design of artificial host molecules for anion recognition has attracted the attention of many research groups, owing to the important roles it play. Generally, the term host describes the ability of a molecular species to bind another one, with preference over the rest and with greater strength than is commonly found, as a result of noncovalent interactions. Recently, Scmidtchen termed another definition of host: the attribute "host" denotes some purposefully planned architecture, if not already some application, and *a priori* excludes all of the non-modified natural systems.[35] The quantitative thermodynamic term representing the molecular association, the binding constant K_a comprises all direct mutual interactions between the binding partners as well as changes in the environment (*e.g.* in the solvent). Both

contributions are predominantly dependent on the inherent structure of the binding partners and as a consequence, are subject to molecular design. The design of any synthetic host for anion relies on the optimal attractive interactions between the host and the guest, to drive complexation and this can be either driven by favorable enthalpy or entropy or a combination of both.[36] In order to achieve enhanced selectivity towards targeted guest, fine tuning of interaction sites are required, which in turn needs appropriate functionalization, such that the complementarity of interacting sites, size and shape between the receptor and the guest is achieved. Generally the host-anion complexation process involves electrostatic interaction, hydrogen bonding, metal or Lewis acid coordination, the hydrophobic effect, anion-π interactions and van der Waals interactions along with the solvent contributions. Hence the major challenge in anion recognition is to maximize negative favorable free energy change (ΔG) of complexation and the free-energy difference ($\Delta\Delta G$) between the competing guests upon complexation, by the host. Very recently, Ursu *et al.* demonstrated selective host-guest binding of anions, without auxiliary hydrogen bonds, in contrast to classical host-guest design tactics. Here the aid in selectivity comes from the overwhelming positive entropy of association.[37]

1.3.1 Challenges during the design of host for anions

The design of receptor, for anions is particularly challenging compared to that for cations. This is because of the following reasons: (i) Shape: Anions exist in a variety of shapes and sizes. Even simple anions can occur in a large range of shapes and geometries (Table 1.1) and hence a higher degree of design is required to make receptors complementary to the shape or topology of their anionic guest.[38] (ii) Anions are larger in size than its isoelectronic cations

Table 1.2 Structural varieties of anions.

Anions	Geometry
F^-, Cl^-, Br^-, I^-	spherical
N_3^-, CN^-, SCN^-, OH^-	linear
CO_3^{2-}, NO_3^-	Trigonal planar
PO_4^{3-}, VO_4^{3-}, SO_4^{2-}, MoO_4^{2-},SeO_4^{2-}, MnO_4^-	tetrahedral
$[Fe(CN)_6]^{4-}$, $[Co(CN)_6]^{3-}$	octahedral

(Table 1.2) and therefore have a lower charge to radius ratio due to which anions can offer less electrostatic binding interactions than the corresponding isoelectronic cations. Again owing to the larger size of the anion, it requires receptors of considerably bigger size than the

Table 1.2 Ionic sizes, experimental enthalpies and Gibb's enthalpies of hydration for selected ions.[35]

Anions	R [Å]	ΔH_{hyd} [kJ.mol^{-1}]	ΔG_{hyd} [kJ.mol^{-1}]
F^-	1.33	-510	-465
Cl^-	1.81	-367	-340
Br^-	1.96	-336	-315
I^-	2.20	-291	-275
$HCOO^-$	1.56	-432	-335
NO_3^-	1.79	-312	-300
$H_2PO_4^-$	2.00	-522	-465
ClO_4^-	2.50	-246	-430
CO_3^{2-}	1.78	-1397	-1315
SO_3^{2-}	2.00	-1376	-1295
SO_4^{2-}	2.30	-1035	-1080
$PdCl_6^{2-}$	3.19	-730	-695
PO_4^{3-}	2.38	-2879	-2765
Li^+	0.69	-531	-475
Na^+	1.02	-416	-365
K^+	1.38	-334	-295
Cs^+	1.70	-283	-250
NH_4^+	1.48	-329	-285
$(C_2H_5)_4N^+$	3.37	-73	0
Ca^{2+}	1.00	-1602	-505
Zn^{2+}	0.75	-2070	-1955
Al^{3+}	0.53	-4715	-4525
Fe^{3+}	0.65	-4462	-4265
La^{3+}	1.05	-3312	-3145
Th^{4+}	1.00	-6057	-5815

isoelectronic cation.[35,38] (iii) Role of solvent: Solvent plays a crucial role in controlling anion binding strength and selectivity. Electrostatic interactions generally dominate in anion solvation and protic solvents in particular, form strong hydrogen bonds with anions. In comparison to cations of similar size, anions have high free energies of solvation (Table 1.2) and hence need to be compensated while forming anion-host complexes. (iv) Existence of anions: another very obvious but frequently ignored characteristic of anions is that they exist in a relatively narrow pH range, which can cause problems, especially, in the case of receptors based on polyammonium salts where the host may not be fully protonated in the desired pH region. Therefore the receptors must function within the pH range of their targeted anion. (v) Hydrophobicity: hydrophobicity can also influence the selectivity of a receptor. Hydrophobic anions are generally bound more strongly in hydrophobic binding sites.[38]

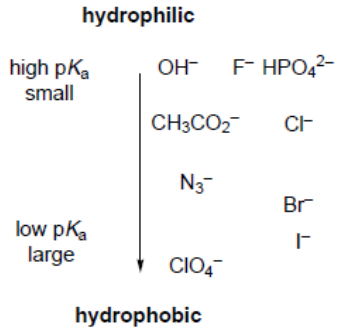

Figure 1.9 Hydrophilic/hydrophobic series of anions.[38]

1.3.2 Abiotic receptors for anions

In 1968, Park and Simmons described the first example of a bicyclic diammonium host, katapinand for chloride anion.[39] A decade later, Lehn *et al.* made a similar bicyclic

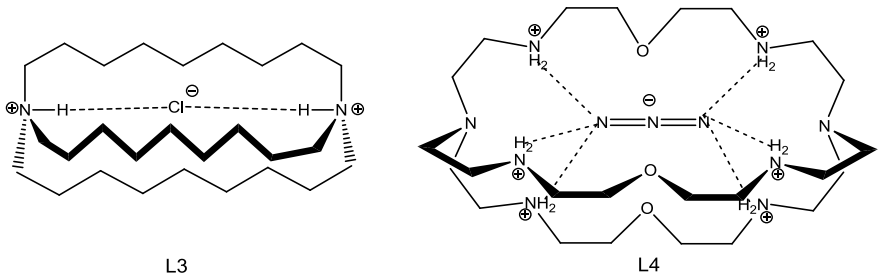

Figure 1.10 Left: bicyclic diammonium host-chloride complex reported by Simmons *et al.*[39] Right: bicyclic azacryptand-azide complex reported by Lehn *et al*.[40]

azacryptand, [bis-tren](ClO$_4$)$_6$, capable of binding a linear azide ion through its six protonated amine functions.[40] Since these pioneering discoveries, the field of anion recognition drew increasing attention from the scientific community.[1,36] As a result a variety of anion receptor motifs such as polyamines,[41] amides,[42] ureas and thioureas,[43] guanidiums,[44] steroids,[45] metal-based systems[46] and heterocycles were developed subsequently. Among heterocycles, pyrroles,[47] indoles,[48] and imidazoles[49] are quite popular anion binding motifs, which interacts via N-H…anion hydrogen bonding. Further, Flood *et al.* reported triazole-based heterocyclic anion binding motif, which uses preorganized C-H moiety as the hydrogen bond donor.[50]

1.3.2.1 Ammonium and Guanidium based receptors

Ammonium and guanidium based receptors bind anions, with a combination of electrostatic and hydrogen bonding interactions. Protonation increases positive charge density and consequently increases the anion affinity. Incidentally, the first anion receptor was reported by Park and Simmons in 1968, the diazabicyclo katapinands **L3**, ammonium based hosts for halide ions in aqueous media.[39] Simultaneously, Lehn and coworkers began to explore the opportunities behind anion coordination chemistry of polyammonium macrocycles.[40] Many of these systems are multiply protonated at physiological pH (*i.e.* the polyammonium form), to display significant anion binding under neutral condition. A number of researchers are now involved in this field, and contributed towards the development of a wide variety of receptors including the azacrowns and the cryptands (Figure 1.11).[51]

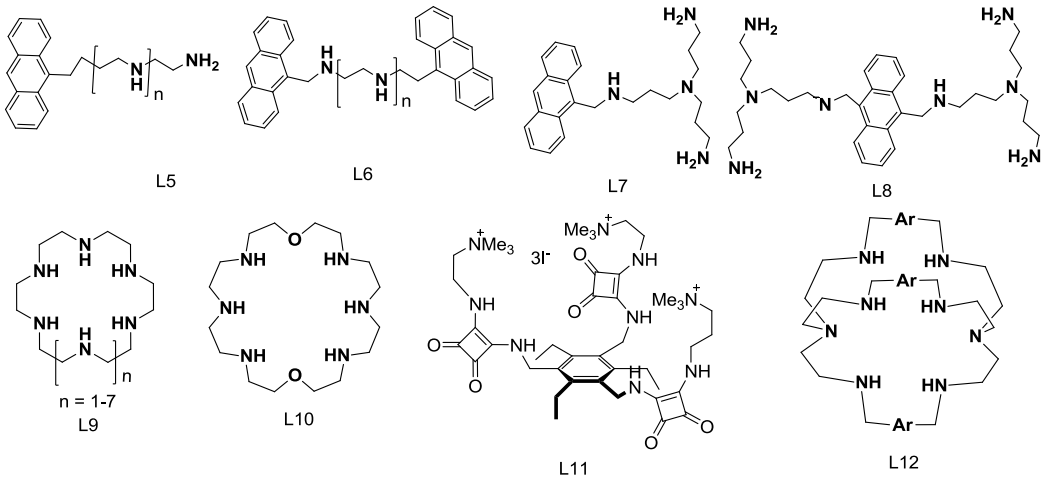

Figure 1.11 Some of the literature reported ammonium based receptors.

The ability of guanidinium moiety to bind anions arises from several factors. Most significant is its ability to remain protonated over a wide range of pH, including physiological pH, as it has a very high pK_a value of 13.6. Further, the geometrical orientation of this functional group complements well with the oxoanions such as carboxylate, phosphate, nitrate and sulphate. Following the publication of the synthesis of **L13** by McKay and Kreling in 1957,[52] Schmidtchen and coworkers reported that compounds containing the substructure **L14** bound anions including *p*-nitrobenzoate in acetonitrile.[53] This drew wide attention of researcher and as a consequence, a plethora of guanidinium based receptors has emerged in literature (Figure 1.12).[5]

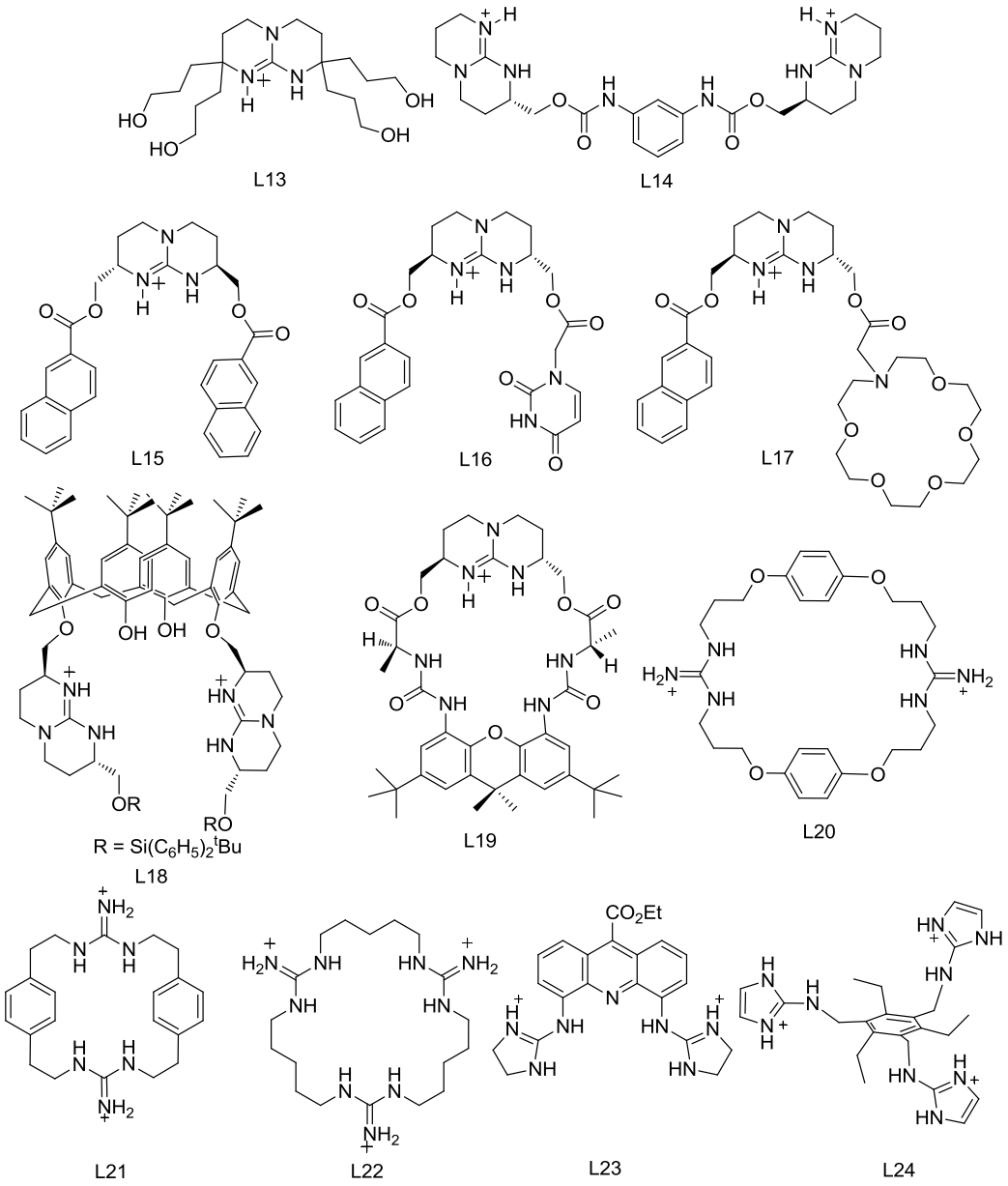

Figure 1.12 Some of the literature reported guanidium based receptors.

1.3.2.2 Amide based receptors

The use of secondary amides as H-bond donors to anions has wide application in nature.[55] The pK_a of primary or secondary amides are usually well above 15 (in DMSO) which implies that it is not easily deprotonated. Amide receptors constructed on an organic scaffold most often utilize solely H-bonding and sometimes additional electrostatic interactions to bind anions. The first example of a synthetic amide containing receptor, reported in 1986 by Pascal and coworkers, was a cryptand like tris-amide **L25**, which displayed interaction with fluoride ion in DMSO-d_6.[56] Subsequently in 1993, Reinhoudt and coworkers reported a series of tris-amides and tris-sulphonamides based upon *tren* skeleton and these (**L26** and **L27**) receptors show selectivity towards phosphate in acetonitrile.[57] In another study, Carbtree and coworkers reported a very simple system containing isophthalamide **L28** as halide ion receptors, especially for chloride in organic media, whereas Smith and coworkers demonstrated its boron functionalized derivatives as excellent receptors for anions.[58] In this regard, so far a lot of neutral amide based receptors with different organic scaffold has been reported in literature,[59] some of their structures are shown in figure 1.13 and 1.14.

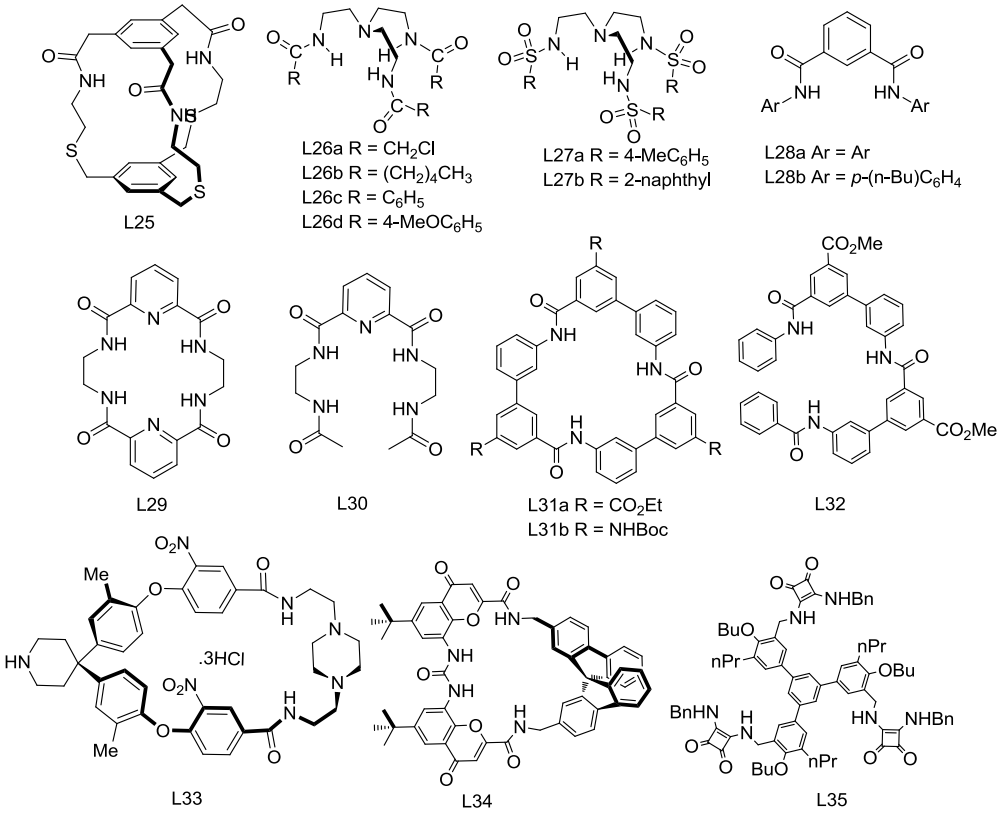

Figure 1.13 Some of the literature reported amide based receptors.

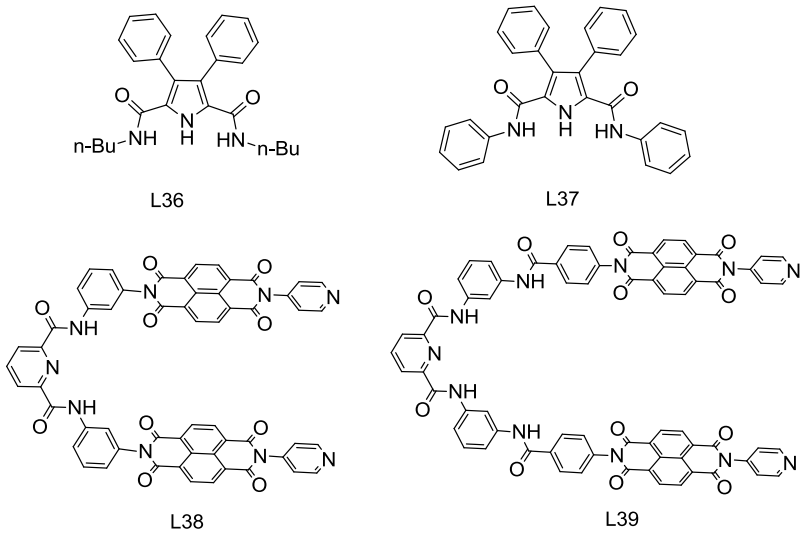

Figure 1.14 Some of the literature reported amide based receptors.

1.3.2.3 Urea and thiourea based receptor

Urea and thiourea have been shown to provide a strong binding sites for anions, in particular oxoanions, especially carboxylates, using a bidentate hydrogen bonding motif.[60] The key factors that govern the design of (thio)urea based anion receptors are the strength of the hydrogen bonding, *cis*- and *trans*- conformation of the two (thio)ureido N-H bonds versus C=O or C=S bonds and the topology of the (thio)urea binding sites in the receptor molecule. Wilcox was the first to utilize urea and thiourea based receptors **L40** for carboxylate binding.[61]

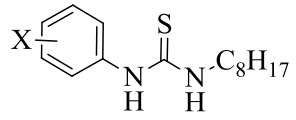

X = H, p-NO_2, p-CN, p-CF_3, P-$COOC_2H_5$, p-C_6H_5, p-OC_2H_5, p-$N(CH_3)_2$

L40

The geometrical arrangement, of the acetate complex, of a thiourea based receptor is illustrated in figure 1.15.

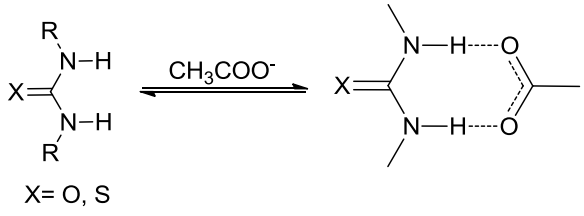

Figure 1.15 Complementary H-bonding interactions between (thio)urea and an acetate anion.

Hamilton examined the binding of ureas and thioureas in polar solvents such as DMSO. They reported that 1,3-dimethyl urea and thiourea bind tetramethylammonium acetate in DMSO-d_6 and the binding affinity of 1,3-dimethylurea is 45 M^{-1} while that of 1,3-dimethylthiourea is ~8 fold higher *i.e.* 340 M^{-1}. This is attributed to the higher acidity of the H-bonding sites in case of thiourea (p*Ka* = 21.1) than urea (p*Ka* =26.9).[62] Teramae *et al*. have explored the anion recognition of N-alkyl-N′-(*p*-nitrophenyl)thioureas, **L41** in cationic vesicle solution and found that the anion binding site of receptor (n=1) is buried deep within the nonpolar vesicle core and shows the selectivity towards anions in the order $Br^- > H_2PO_4^- > Cl^- >> HCO_3^-$, CH_3COO^-.[63] Some of the urea and thiourea based receptors reported in literature are shown in figure 1.16.[64]

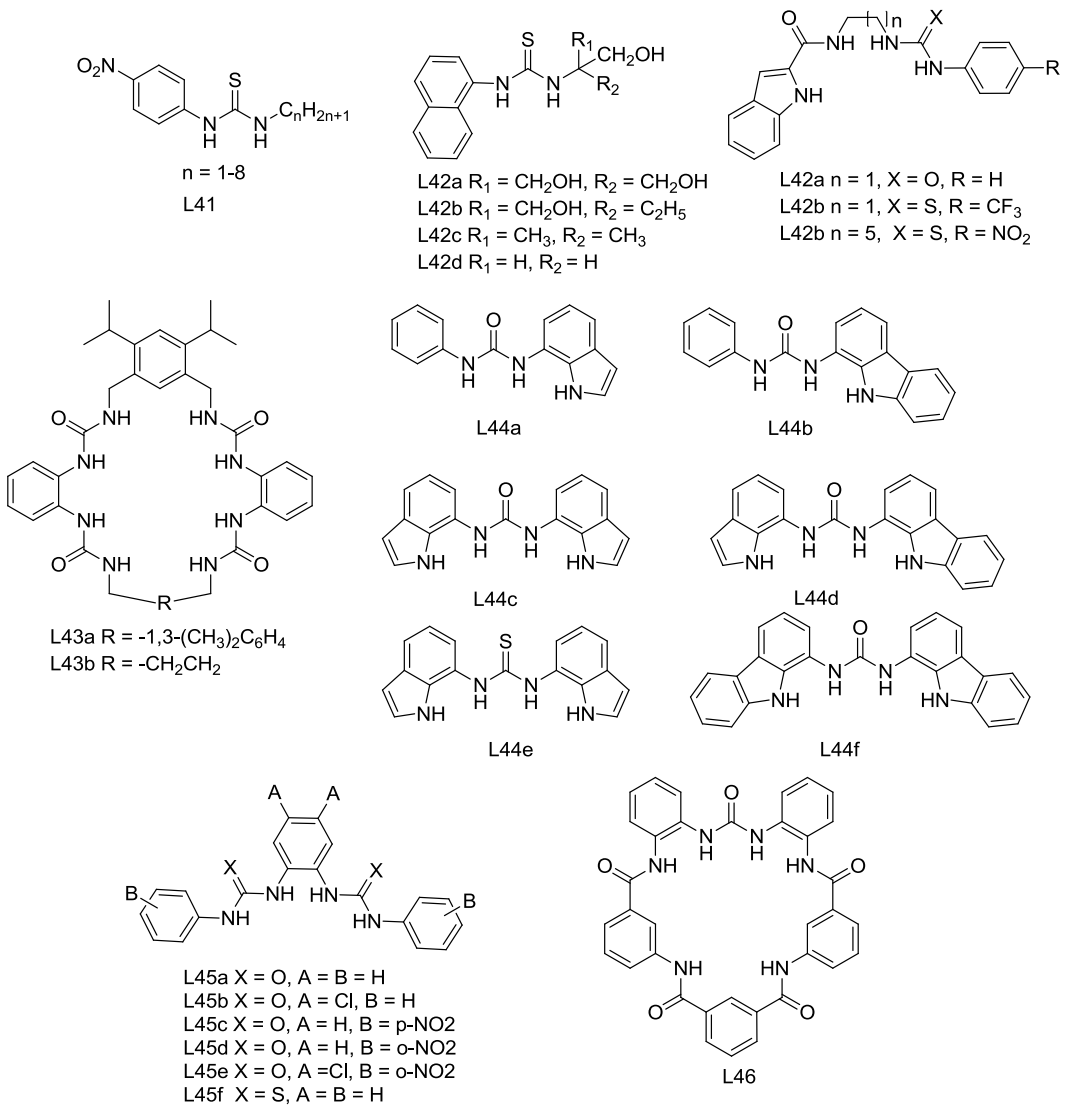

Figure 1.16 Some of the literature reported urea and thiourea containing receptors.

1.3.2.4 Aromatic heterocycles as anion receptors

There is a lot of interest in receptors composed of aromatic heterocycles. The heteroaromatic unit can act as H-bond donor as in the case of the pyrrole NH or acceptor as in the case of the pyridine nitrogen. pK_a values of some of the nitrogen containing heterocycles in DMSO are reported by Bordwell.[65]

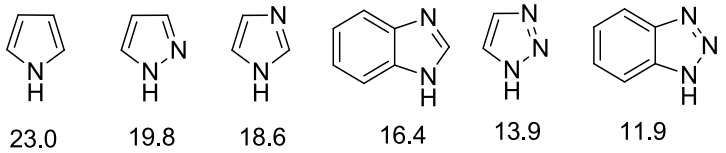

1.3.2.4.1 Pyrrole based receptors

The use of pyrrole as anion receptor was pioneered and developed by Sessler's group. Pyrrole is an ideal group to bind anions because it does not contain a hydrogen bond acceptor that could compete with a putative anionic guest for hydrogen bond formation with the NH group. A wide variety of cyclic and acyclic pyrrole based receptors have been reported in literature. Gale and coworkers have recently demonstrated that pyrrole itself can stabilize an anion, at least in the solid state.[66]

1.3.2.4.1.1 Macrocyclic pyrrole based receptor

The serendipitous discovery of protonated sapphyrin **L47** by Sessler's group in 1993 as a strong fluoride acceptor, introduced the idea of taking advantage of the properties of pyrrole

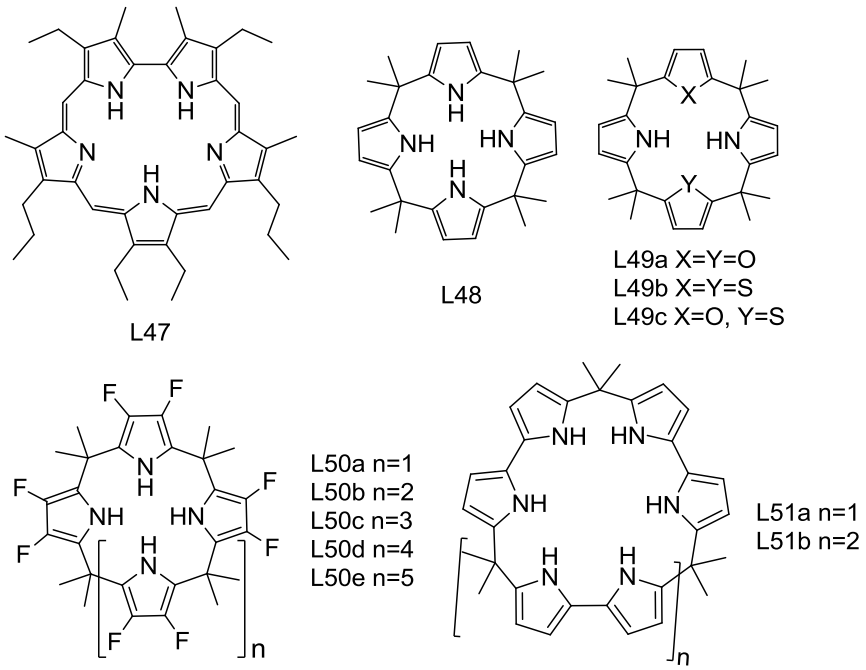

Figure 1.17 Some of the literature reported pyrrole based macrocyclic receptors.

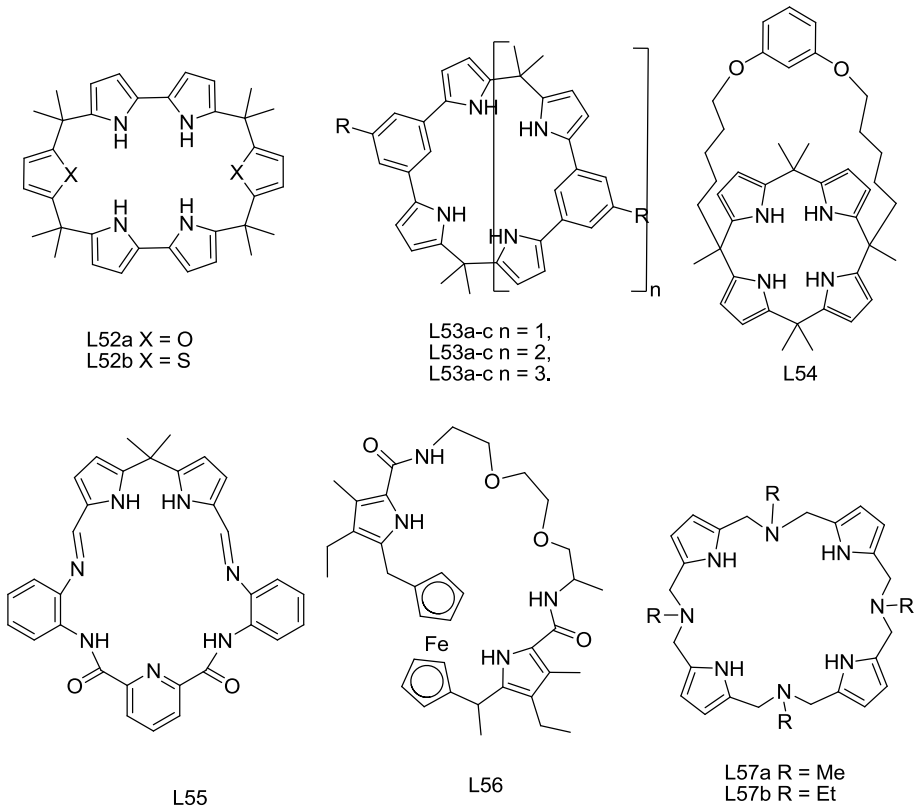

Figure 1.18 Some of the literature reported pyrrole based macrocyclic receptors.

as a H-bond donor.[67] In 1996, the same group presented another porphyrinogen *i.e.* calix[4]pyrrole **L48** as a neutral halide receptor and showed that anions such as chloride and fluoride were complexed by four pyrrole NH groups through hydrogen bonds.[68] Subsequently a lot of structural modification has been performed on this molecule to fine tune its anion binding w.r.t. affinity and selectivity. Some of its modification and some other oligopyrrolic macrocycles reported in literature are shown in figure 1.17 and 1.18.[69]

1.3.2.4.1.2 Acyclic pyrrole based receptors

The discovery of prodigiosin, an open chain pyrrolylpyrromethene type oligopyrrole, as an antineoplastic and immunosuppressive agent and its protonation-counter anion binding

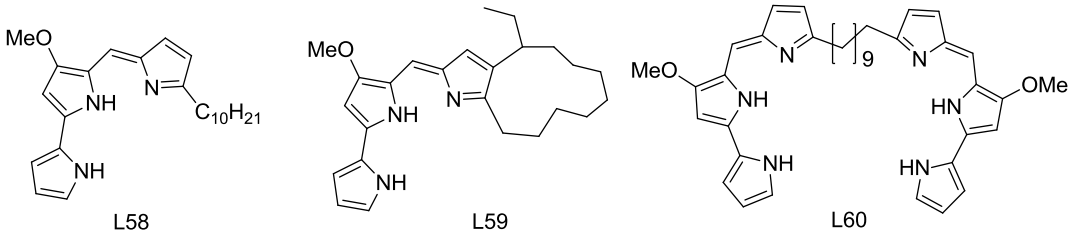

Figure 1.19 Some of the literature reported prodigiosin receptors.

mode of action, led to enhanced curiosity towards the anion binding study of oligopyrroles and in this context, in 2005 Sessler and Gale started exploring some modified prodigiosin and other oligopyrroles as anion binding hosts (Figure 1.19).[34,70] Subsequently researchers had synthesized a library of functionalized acyclic pyrroles and pyrrole coupled with other anion binding motifs and studied their anion binding properties. Some of the receptors are shown in figure 1.20.[71]

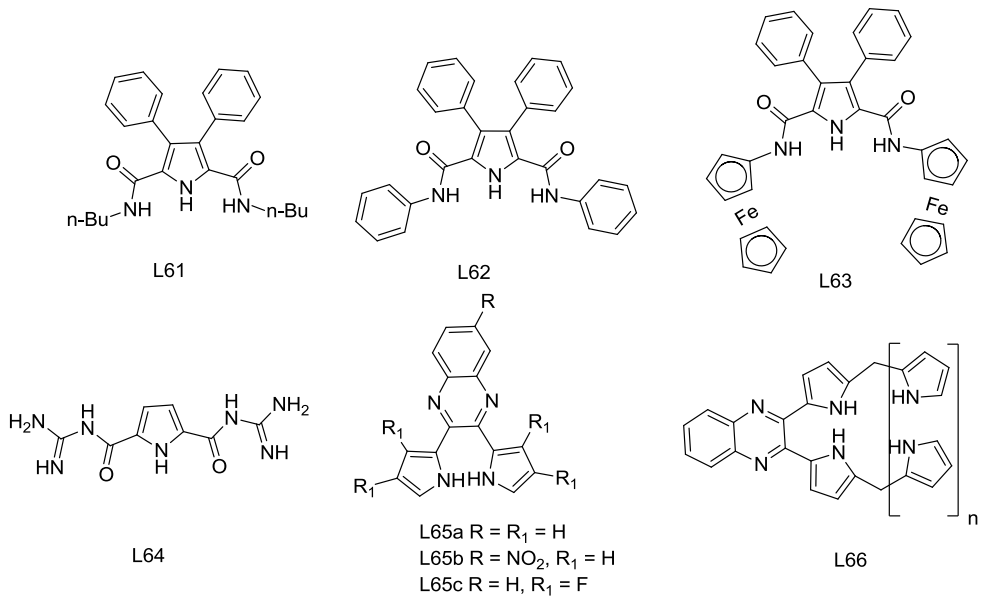

Figure 1.20 Some of the literature reported acyclic pyrrole containing receptors.

1.3.2.4.2 Indole and carbazole based receptors

Indole moiety has been exploited by nature, as tryptophan, to bind anion in the sulfate binding proteins and haloalkane dehalogenase.[72] In spite of this, it was only in 2004 that the first reports of the use of indoles and carbazoles as the synthetic anion receptors appeared.[73] Like pyrroles, indoles and carbazoles contain a single NH hydrogen bond donor and are more acidic (pK_a in DMSO: pyrrrole 23.0, indole 21.0 and carbazole 19.9) in nature, so whilst indole and carbazole are better hydrogen bond donors than pyrrole, they are also more prone to deprotonation, which may not be desirable when trying to complex with anionic guests. In 2004, Beer and coworkers and Jurczak and coworkers independently reported carbazoles, as an anion receptor.[73] Beer *et al.* synthesized indolocarbazole derivatives **L67** and their binding studies in acetone show fluorescence enhancement with fluoride, chloride and

dihydrogenphosphate ions while benzoate quenches the fluorescence. Some of the reported indole and carbazole based receptors are shown in figure 1.21.[74]

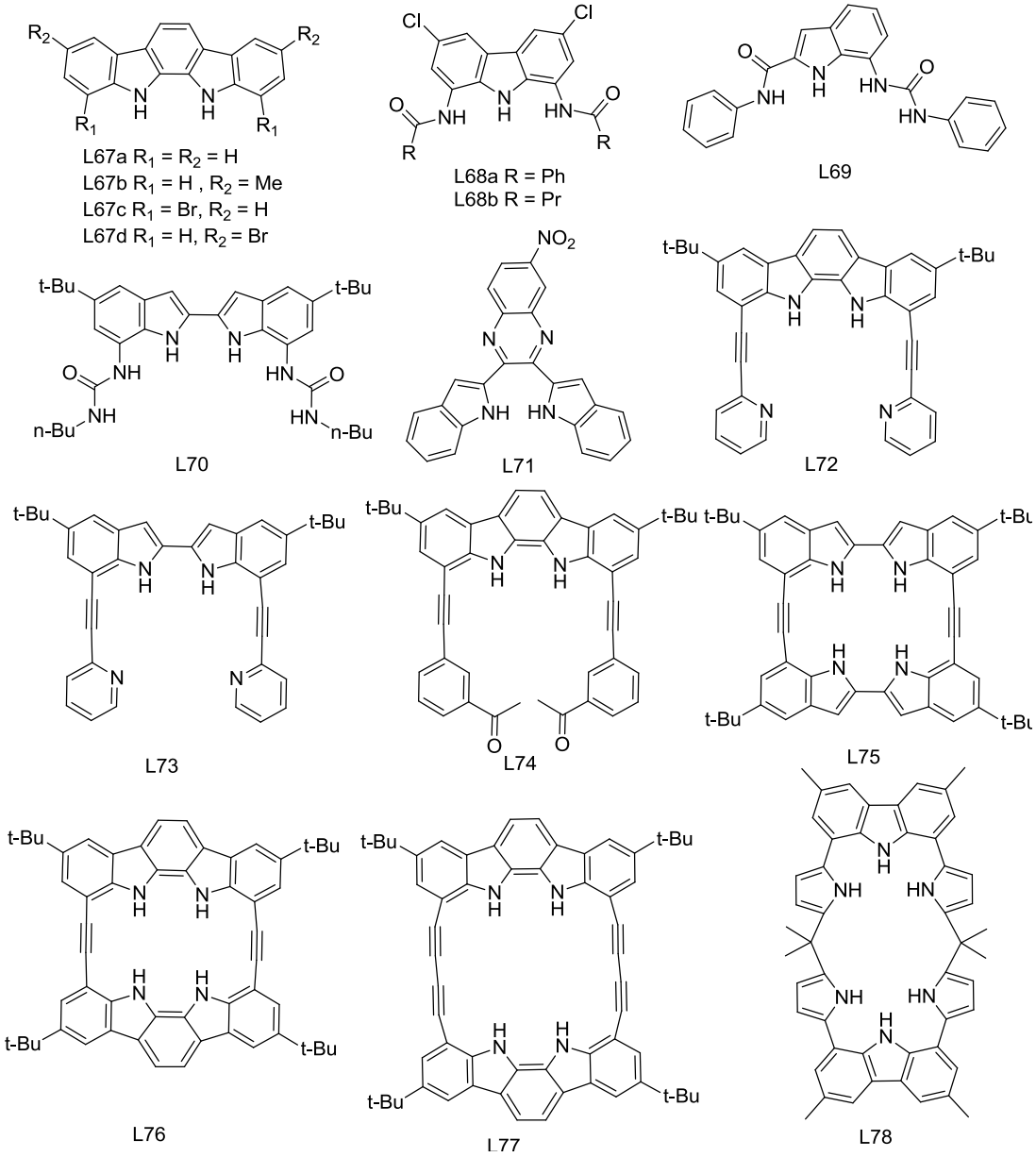

Figure 1.21 Some of the literature reported indole and carbazole containing receptors.

1.3.2.4.3 Imidazole based receptors

The first report of imidazole containing artificial anionic host, appeared in 1999, by Sato *et al.* They have prepared a receptor **L79** where three imidazolium groups are connected through a 1,3,5-trimethylbenzene spacer and explored it as a halide ion receptor.[75a] Subsequently, in 2002 Kim and coworker reported another tripodal nitro-imidazolium

receptor **L80** which shows high affinity and selectivity for chloride ion. In this system the affinity is driven by $(C\text{-}H)^{+}\ldots X^{-}$ interactions. In a subsequent report, Allen and coworker

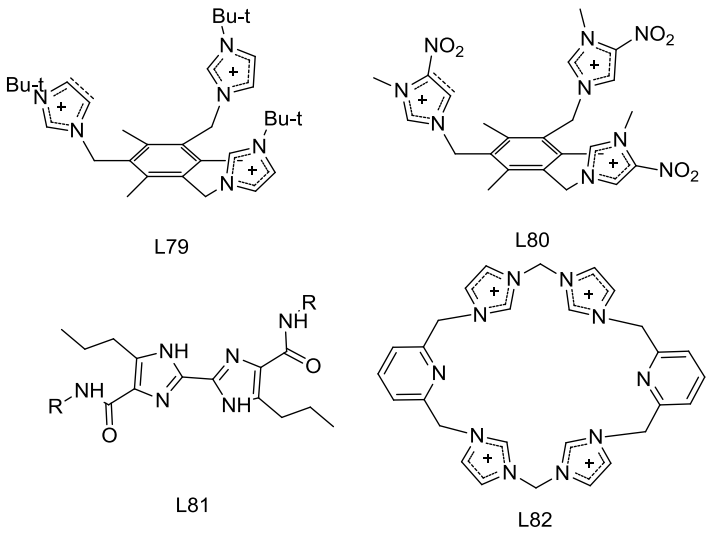

Figure 1.22 Some of the literature reported imidazole and imidazole based receptors.

synthesized biimidazole diamide **L81** derivatives, a neutral amide-imidazole conjugate system and studied its anion binding properties w.r.t. phosphate and chloride ions (Figure 1.22). They found it as an electrically neutral, relatively unselective sensor for anions in organic media.

Benzimidazole where a benzene ring is fused with an imidazole ring occurs in nature as part of the vitamin B_{12} molecule. In 2005, Jang and coworkers reported this moiety as an anion receptor and since then very little work is done on this molecule.[75] Some of the literature reported imidazole and benzimidazole based receptors are shown in figure 1.23.

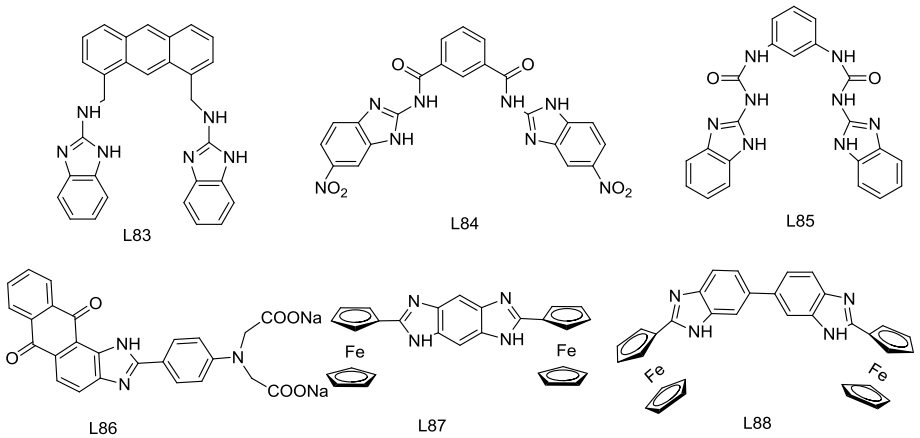

Figure 1.23 Some of the literature reported imidazole and benzimidazole based receptors.

1.4 Detection methods

The interaction of anions with artificial receptor systems can be monitored and quantified using several methods, the choice of which has been largely dependent on the nature of the receptor in question. These are carried out by using different analytical techniques, including ^{1}H NMR spectroscopy, UV-Vis and fluorescence spectroscopy, mass spectrometry (especially ESI-MS), reaction kinetics, potentiometry, solubility measurement, liquid-liquid partitioning, dialysis, chromatography, calorimetry, refractometry, polarimetry etc.[76] Each of the techniques depends on the understanding of the intermolecular forces responsible for the complexation from a chemical point of view. For instance, NMR spectroscopic titrations monitor changes in the chemical shift of one or more resonances present in the spectrum of the interacting partners. On the contrary, optical spectroscopy records changes in optical properties of the receptor such as molar absorptivity or emissivity as a consequence of complex formation. On the other hand, calorimetry provides information about the heat change of the system as a whole.[77]

The measurements are often made using a variety of solvents and the binding behavior depends on the permittivity, refractive index (polarizability), dielectric constant, donor or acceptor strength of the solvent. Therefore, in order to compare the binding constants, it is necessary that the binding studies be conducted under identical conditions *e.g.* temperature, solvent, concentration, and even measurement method.[76a] Some of the methods, which will be employed in the latter half of the thesis are outlined below, to facilitate the ensuing discussion of receptor design.

1.4.1 Nuclear magnetic resonance (NMR)

NMR spectroscopic titration constitute one of the most widely used techniques to determine the association constant (K_a) for host-guest interactions. This method is particularly useful when there is an involvement of hydrogen bonding interaction and can be used to gain both structural and thermodynamic information. ^{1}H NMR spectroscopic titration, generally monitor the effect of an added substrate *i.e.* guest has on the chemical shift of one or more proton signals of the receptor *i.e.* host when subjected to titration. Under conditions of fast exchange and for a simple 1:1 binding equilibrium, the chemical shift of the signal in question is the average of the chemical shifts of the nucleus in the free and in the complexed form. Thus, by monitoring the chemical shift as a function of added substrate, it is possible to construct binding profiles, from which apparent K_a values may be derived.[76,78] The effective range for which NMR titrations can provide reliable values for 1:1 binding equilibrium is *ca.*

$10< K_a<10^4$ M^{-1}. However, it should be kept in mind that relatively high concentrations (usually 10^{-2}-10^{-3} M) are required in this method.

1.4.2 Optical methods

Optical techniques require comparatively much lower concentration of receptor than the NMR method and hence, relatively are more sensitive than the latter. In these methods, the main requirement is that there should be some binding/complexation induced changes in the absorption or emission properties of the receptor. Therefore, the system must have a combination of a substrate recognition functionality (receptor) and optical signaling (absorption or emission) reporter, which, may be either directly linked or appropriately associated in a non-covalent manner. In well behaved systems, the association constant corresponding to complex formation can be determined, by using curve-fitting program, using different equations. Further, binding stoichiometry can be evaluated from the method of continuous variation method.[76]

1.4.2.1 Covalently attached chromophore

In this case, a chromophore is covalently attached to receptor that undergoes a change in the absorption profile when binds with a guest (Figure 1.24). The change in the absorption spectrum, generally originates from the anion induced change in HOMO-LUMO gap or anion induced modulation in key charge transfer bands.

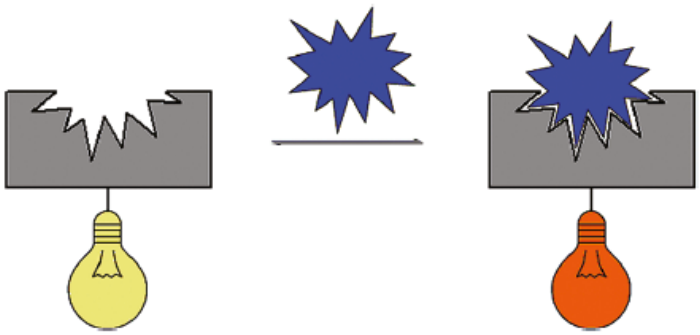

Figure 1.24 Covalently attached reporter-receptor system. The reporter unit is represented by the bulbs with the receptor in gray and the guest in blue.[18]

1.4.2.2 Covalently attached fluorophore

This method involves the covalent attachment of a fluorogenic reporter, which can show guest induced change in the emission profile (Figure 1.24). This technique is very important,

analytically owing to its high sensitivity. This method generally utilizes photo-induced electron transfer (PET), electronic energy transfer, metal-to-ligand charge transfer (MLCT), excimer/ exciplex formation, internal charge transfer (ICT), and excited state proton transfer (ESPT) to respond to the complexation and/or recognition event.

1.4.2.3 Indicator displacement assay

It is a competition experiment, where two guests compete for a particular receptor and among them one is a reporter unit. In this method the reporter or indicator group is connected to the receptor via non-covalent interactions which is eventually displaced by the guest. The molecular ensemble used, consists of a recognition unit, designed for selective interaction with a desired guest along with an external indicator that associates with the recognition unit, in the absence of guest. When the guest is added, the indicator is displaced from the binding cavity, producing a measurable change in the optical properties of the indicator.

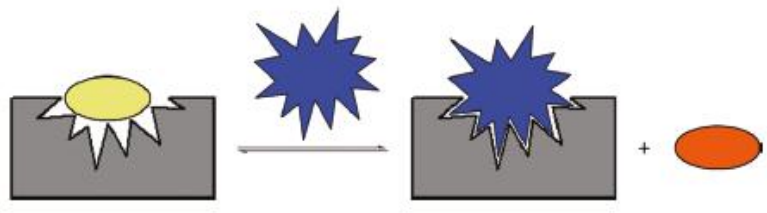

Figure 1.25 Indicator displacement assay (IDA). The indicator is represented by the oval, while the receptor unit is gray and the guest is blue.[18]

1.4.3 Isothermal titration calorimetry (ITC)

ITC analysis provides a measure of the overall heat change, during the complexation process. Thus, it provide ready access to the energetics (*i.e.* ΔH, ΔS and ΔG) of the recognition event without retreating into a structural probe (*e.g.*, a NMR signal), which may or may not reflect the entirety of the associative process. Therefore, calorimetry accounts for the individual contributions of all simultaneous processes in solution. Since the output is an ensemble of all these processes, the analysis of ITC data in terms of an interpretable binding model is not so easy and hence is a major challenge. In ITC, only ΔH is obtained directly, whereas ΔG and K_a are computed from the modeling of the experimental data to a binding profile, a process that permits the calculation of TΔS. Thus, the choice of curve fitting methods and models, for the proposed equilibrium events underlying the experimental observations is absolutely critical. If this is not done correctly, ITC can produce numbers that

have little physical significance. So it is necessary to get knowledge about binding stoichiometry. In spectroscopic techniques, this is easily calculated by continuous variation method or Job's plot. However, in ITC, inverse titrations should be performed, where the guest is titrated into the host solution. If both the normal and the inverse titration methods, produce identical energetics and binding constants, than the results can be fit into a 1:1 binding stoichiometry. Deviation from this indicates additional events and/or presence of higher order binding events. The effective K_a range for which ITC can provide reliable values for 1:1 binding is *ca*. 10^2-10^7 M^{-1}.[36f,79]

1.5 References

1. (a) In *Supramolecular Chemistry of anions* Eds. Bianchi, A.; Garcia-Epsána, E.; Bowman-James, K. Wiley-VCH, New York, 1997. (b) In *Anion Receptor Chemistry* Sessler, J. L.; Gale, P. A.; Cho, W. -S. RSC Publishing, Cambridge, UK, 2006. (c) Gale, P. A. *Chem. Commun.* **2011**, 82.
2. (a) Wright, E. M.; Diamond, J. M. *Physiol. Rev.* **1977**, *57*, 109. (b) Bauduin, P.; Renoncourt, A.; Touraud, D.; Kunz, W.; Ninham, B. W. *Curr. Opin. Colloid Interface Sci.* **2004**, *9*, 43.
3. (a) Connet, P. *Fluoride* **2007**, *40*, 155. (b) Foulkes, R. G. *Fluoride* **2007**, *40*, 229. (c) Carton, R. J. *Fluoride* **2006**, *39*, 163.
4. Matsuo, S.; Kiyomiya, K.; Kurebe, M. *Arch. Toxicol.* **1998**, *72*, 798.
5. (a) Briancon, D. *Rev. Rheum*. **1997**, *64*, 78. (b) Kirk, K. L. In *Biochemistry of the Halogens and Inorganic Halides*, Plenum: New York, 1991.
6. Bassin, E. B.; Wypij, D.; Davis, R. B. *Cancer Causes Control* **2006**, *17*, 421.
7. Yu, Y.; Yang, W.; Dong, Z.; Wan, C.; Zhang, J.; Liu, J.; Xiao, K.; Huang, Y.; Lu, B. *Fluoride* **2008**, *41*, 134.
8. Jentsch, T. J.; Stein, V.; Weinreich, F.; Zdebik, A. A. *Physiol. Rev.* **2002**, *82*, 503.
9. Simon, D. B.; Bindra, R. S.; Mansfield, T. A.; Nelson-Williams, C.; Mendonca, E.; Stone, R.; Schurman, S.; Nayir, A.; Alpay, H.; Bakkaloglu, A.; Rodriguez-Soriano, J.; Morales, J. M.; Sanjad, S. A.; Taylor, C. M.; Pilz, D.; Brem, A.; Trachtman, H.; Griswold, W.; Richard, G. A.; John, E.; Lifton, R. P. *Nature Genet.* **1997**, *17*, 171.
10. Devuyst, O.; Christie, P. T.; Courtoy, P. J.; Beauwens, R.; Thakker, R. V. *Human Molec. Genetics* **1999**, *8*, 247.
11. (a) Anderson, M. P.; Rich, D. R.; Gregory, R. J.; Smith, A. E.; Welsh, M. J. *Science* **1991**, *251*, 679. (b) Riordan, J.; Bear, C.; Rommens, J.; Reyes, E.; Ackerly, C.; Sun,

S.; Nalsmith, A.; Jensen, T.; Hanraha, J.; Kartner, N. *Cell* **1991**, *64*, 681. (c) Welsh, M.; Smith, A.; Manavalan, P.; Gregory, R.; Anderson, M.; Rich, D. *Science* **1991**, *253*, 205.

12. (a) Choi, J. Y.; Muallem, D.; Kiselyov, K.; Lee, M. G.; Thomas, P. J.; Muallem, S. *Nature* **2001**, *410*, 94. (b) Bok, D.; Galbraith, G.; Lopez, I.; Woodruff, M.; Nusinowitz, S.; Beltrandel-Rio, H.; Huang, W.; Zhao, S.; Geske, R.; Montgomery, C.; Van Sligtenhorst, I.; Friddle, C.; Platt, K.; Sparks, M. J.; Pushkin, A.; Abuladze, N.; Ishiyama, A.; Dukkipati, R.; Liu, W.; Kurtz, I. *Nat. Genet.* **2003**, *34*, 313. (c) Rousselle, A. V.; Heymann, D. *Bone* **2002**, *30*, 533. (d) Vaughan-Jones, R. D.; Spitzer, K. W.; Swietach, P. *J. Mol. Cell. Cardiol.* **2009**, *46*, 318.
13. (a) Haldimann, M.; Zimmerli, B.; Als, C.; Gerber, H. *Clin. Chem.* **1998**, *44*, 817 and references cited therein. (b) Aumont, G.; Tressol, J.-C. *Analyst* **1986**, *3*, 841. (c) Jalali, F.; Rajabi, M. J.; Bahrami, G.; Shamsipur, M. *Anal. Sci.* **2005**, *21*, 1533.
14. (a) Kulig, K. W. In *Cyanide Toxicity, U.S. Department of Health and Human Services, Atlanta*, GA, 1991. (b) In Guidelines for Drinking Water Quality, World Health Organization, Geneva, 1996.
15. Baskin, S. I.; Brewer, T. G. In *Medical Aspects of Chemical and Biological Warfare*, Eds Sidell, F.; Takafuji, E. T.; Franz, D. R. TMM Publication, Washington, DC, 1997; Chapter 10.
16. (a) Adams, R. L. P.; Knowler, J. T.; Leader, D. P. In *The Biochemistry of the Nucleic Acids*, 10th ed.; Chapman and Hall: New York, 1986. (b) Saenger, W. In *Principles of Nucleic Acid Structure*; Springer-Verlag: New York, 1984.
17. (a) Charra, B.; Calemard, E.; Ruffet, M.; Chazot, C.; Terrat, J. C.; Vanel, T.; Laurent, G. *Kidney Int.* **1992**, *41*, 1286. (b) Gutzwiller, J. -P.; Schneditz, D.; Huber, A. R.; Schindler, C.; Gutzwiller, F.; Zehnder, C. E. *Nephrol., Dial., Transplant*. **2002**, *17*, 1037.
18. Hargrove, A. E.; Nieto, S.; Zhang, T.; Sessler, J. L.; Anslyn, E. V. *Chem. Rev.* **2011**, *111*, 660.
19. (a) Mason, C. F. In *Biology of Freshwater Pollution*; Longman: New York, 1991. (b) In *Phosphorus in the Global Environment: Transfers, Cycles, and Management*; Tiessen, H., Ed.; Wiley: New York, 1995.
20. (a) Wolff, J. *Pharmacol Rev.* **1998**, *50*, 89. (b) Godley, A. F.; Stanbury, J. B. *J. Clin. Endocrinol. Metab.* **1954**, *14*, 70.

21. McKee,V.; Nelson, J.; Town, R. M. *Chem. Soc. Rev.* **2003**, *32*, 309.
22. Katayev, E. A.; Ustynyuk, Y. A.; Sessler, J. L. *Coord. Chem. Rev.* **2006**, *250, 3004.*
23. Xu, H.; Straèter, N.; Schroèder, W.; Boèttcher, C.; Ludwig, K.; Saenger, W. *Acta Cryst. D* **2003**, *59*, 815.
24. Chantalat, L.; Nicholson, J. M.; Lambert, S. J.; Reid, A. J.; Donovan, M. J.; Reynolds, C. D.; Wood, C. M.; Baldwin, J. P. *Acta Cryst. D* **2003**, *59*, 1395.
25. Koropatkin, N. M.; Pakrasi, H. B.; Smith, T. J. *Proc. Natl. Acad. Sci. U. S. A.* **2006**, *103*, 9820.
26. Koropatkin, N. M.; Koppenaal, D. W.; Pakrasi, H. B.; Smith, T. J. *J. Biol. Chem.* **2006**, *282*, 2606.
27. Davis, J. T.; Okunola, O.; Quesada, R. *Chem. Soc. Rev.* **2010**, *39*, 3843.
28. Louie, G. V.; Brownlie, P. D.; Lambert, R.; Cooper, J. B.; Blundell, T. L.; Wood, S. P.; Warren, M. J.; Woodcock, S. C.; Jordan, P. M. *Nature* **1992**, *359*, 33.
29. Dutzler, R.; Campbell, E. B.; Cadene, M.; Chait, B. T.; MacKinnon, R. *Nature* **2002**, *45*, 287.
30. Dutzler, R.; Campbell, E. B.; MacKinnon, R. *Nature* **2003**, *300*, 108.
31. (a) Sheth, T. R.; Henderson, R. M.; Hladky, S. B.; Cuthbert, A. W. *Biochim. Biophys. Acta, Biomembr.* **1992**, *179*, 1107. (b) Jeong, E. J.; Kang, E. J.; Sung, L. T.; Hong, S. K.; Lee, E. *J. Am. Chem. Soc.* **2002**, *124*, 14655. (c) Tanigaki, K.; Sato, T.; Tanaka, Y.; Ochi, T.; Nishikawa, A.; Nagai, K.; Kawashima, H.; Ohkuma, S. *FEBS Lett.* **2002**, *37*, 524.
32. (a) Sato, T.; Konno, H.; Tanaka, Y.; Kataoka, T.; Nagai, K.; Wasserman, H. H.; Ohkuma, S. *J. Biol. Chem.* **1998**, *273*, 21455. (b) Seganish, J. L.; Davis, J. T. *Chem. Commun.* **2005**, 5781.
33. (a) Pèrez-Tomá, R.; Montaner, B.; Llagostera, E.; Soto-Cerrato, V. *Biochem. Pharmacol.* **2003**, *66*, 1447. (b) Pandey, R.; Chander, R.; Sainis, K. B. *Curr. Pharm. Des.* **2009**, *15*, 732. (c) Williamson, N. R.; Fineran, P. C.; Gristwood, T.; Chawrai, S. R.; Leeper, F. J.; Salmond, G. P. C. *Future Microbiol.* **2007**, *2*, 605.
34. Yamamoto, D.; Kiyozuka, Y.; Uemura, Y.; Yamamoto, C.; Takemoto, H.; Hirata, H.; Tanaka, K.; Hioki, K.; Tsubura, A. *J. Cancer Res. Clin. Oncol.* **2000**, *126*, 191.
35. Schmidtchen, F. P.; Berger, M. *Chem. Rev.* **1997**, *97*, 1609.
36. (a) Bazzicalupi, C.; Bencini, A.; Bianchi, A.; Cecchi, M.; Escuder, B.; Fusi, V.; Garcia-Espána, E.; Giorgi, C.; Luis, S. V.; Maccagni, G.; Marcelino, V.; Paoletti, P.;

Valtanocoli, B. *J. Am. Chem. Soc.* **1999**, *121*, 6807. (b) Arranz, P.; Bencini, A.; Bianchi, A.; Diaz, P.; Garcia-Espána, E.; Luis, S. V.; Querol, M.; Valtancoli, B. *J. Chem. Soc., Perkin Trans.* **2001**, *2*, 1765. (c) Beer, P. D.; Bayly, S. R. *Top. Curr. Chem.* **2005**, *255*, 125. (d) Bowman-James, K. *Acc. Chem. Res.* **2005**, *38*, 671. (e) Metrangolo, P.; Neukrich, H.; Pilati, T.; Resnati, G. *Acc. Chem. Res*. **2005**, *38*, 386. (f) Sessler, J. L.; Gross, D. E.; Cho, W. –S.; Lynch, V. M.; Schmidtchen, F. P.; Bates, G. W.; Light, M. E.; Gale, P. A. *J. Am. Chem. Soc.* **2006**, *128*, 12281. (g) Schmidtchen, F. P. *Coord. Chem. Rev.* **2006**, *250*, 2918. (h) Schottel, B. L.; Chifotides, H. T.; Dunbar, K. R. *Chem. Soc. Rev.* **2008**, *37*, 68. (i) Frontera, A.; Gamez, P.; Mascal, M.; Mooibroek, T. J.; Reddijk, J. *Angew. Chem. Int. Ed.* **2011**, *50*, 9564.

37. (a) Ursu, A.; Schmidtchen, F. P. *Angew. Chem. Int. Ed.* **2012**, *51*, 242. (b) Piguet, C. *Dalton Trans*. **2011**, *40*, 8059.
38. Beer, P. D.; Gale, P. A. *Angew. Chem. Int. Ed.* **2001**, *40*, 486.
39. (a) Simmons, H. E.; Park, C. H. *J. Am. Chem. Soc.* **1968**, *90*, 2428. (b) Park, C. H.; Simmons, H. E. *J. Am. Chem. Soc.* **1968**, *90*, 2429. (c) Park, C. H.; Simmons, H. E. *J. Am. Chem. Soc.* **1968**, *90*, 2431.
40. Lehn, J. M.; Sonveaux, E.;Willard, A. K. *J. Am. Chem. Soc.* **1978**, *100*, 4914.
41. (a) Garcia-Espańa, E.; Díaz, P.; Llinares, J. M.; Bianchi, A. *Coord. Chem. Rev.* **2006**, *250*, 2952. (b) Wichmann, K.; Antonioli, B.; Söhnel, T.; Wenzel, M.; Gloe, K.; Gloe, K.; Price, J. R.; Lindoy, L. F.; Blake, A. J.; Schröder, M *Coord. Chem. Rev.* **2006**, *250*, 2987.
42. (a) Bondy, C. R.; Loeb, S. J. *Coord. Chem. Rev.* **2003**, *240*, 157. (b) Kang, S. O.; Hossain, Md. A.; Bowman-James, K. *Coord. Chem. Rev.* **2006**, *250*, 3038.
43. Li, A. -F.; Wang, J.-H.; Wang, F.; Jiang, Y. -B. *Chem. Soc. Rev.* **2010**, *39*, 3729.
44. (a) Best, M. D.; Tobey, S. L.; Anslyn, E. V. *Coord. Chem. Rev.* **2003**, *240*, 3. (b) Schmuck, C. *Coord. Chem. Rev.* **2006**, *250*, 3053.
45. (a) Davis, A. P.; Joos, J. -B. *Coord. Chem. Rev.* **2003**, *240*, 3. (b) Davis, A. P. *Coord. Chem. Rev.* **2006**, *250*, 2939.
46. (a) Beer, P. D.; Hays, E. J. *Coord. Chem. Rev.* **2003**, *240*, 167. (b) O'Neil, E. J.; Smith, B. D. *Coord. Chem. Rev.* **2006**, *250*, 3068. (c) Rice, C. R. *Coord. Chem. Rev.* **2006**, *250*, 3190.

47. (a) Sessler, J. L.; Camiolo, S.; Gale, P. A. *Coord. Chem. Rev.* **2003**, *240*, 17. (b) Sessler, J. L.; Davis, J. M. *Acc. Chem. Res.* **2001**, *34*, 989.
48. Gale, P. A. *Chem. Commun.* **2008**, 4525.
49. Sato, K.; Arai, S.; Yamagishi, T. *Tetrahedron Lett.* **1999**, *40*, 5219.
50. Mc. Donald, K. P.; Hua, Y.; Lee, S.; Flood, A. H. *Chem. Commun.* **2012**, 5065.
51. (a) Clifford, T.; Mason, S.; Linares, J. M.; Bowman-Jamess, K. *J. Am. Chem. Soc.* **2000**, *122*, 1814. (b) Cullinane, J.; Gelb, R. I.; Margulis, T. N.; Zompa, L. J. *J. Am. Chem. Soc.* **1982**, *104*, 3048. (c) Huston, M. E.; Akkaya, E. U.; Czarnik, A. W. *J. Am. Chem. Soc.* **1989**, *40*, 8735. (d) Albelda, M. T.; Bernardo, M. A.; Garcia-Espana, E.; Godino-Salido, M. L.; Luis, S. V.; Llinares, J. M.; Pina, F.; Ramirez, J. A.; Soriano, C. *J. Chem. Soc., Perkin Trans. 2*, **1996**, 2335. (e) Papoyan, G.; Gu, K.; Wiórkiewicz-Kuczera, J.; Kuzera, K.;, Bowman-James, K. *J. Am. Chem. Soc.* **1996**, *118*, 1354. (f) Clifford, T.; Mason, S.; Linares, J. M.; Bowman-Jamess, K. *J. Am. Chem. Soc.* **2000**, *122*, 1814. (g) Lakshminarayanan, P. S.; Kumar, D. K.; Ghosh, P. *Inorg. Chem.* **2005**, *44*, 7540. (h) Frontera, A.; Morey, J.; Oliver, A.; Pina, M. N.; Quinonero, D.; Costa, A.; Ballester, P.; Deya, P. M.; Anslyn, E. V. *J. Org. Chem.* **2006**, *71*, 7185. (i) Bose, P.; Ravikumar, I.; Ghosh, P. *Inorg. Chem.* **2011**, *50*, 10693.
52. McKay, A. F.; Kreling, M. E. *Can. J. Chem.* **1957**, *35*, 1438.
53. (a) Schmidtchen, F. P. *Chem. Ber.* **1980**, *113*, 2175. (b) Müller, G.; Reide, J.; Schmidtchen, F. P. *Angew. Chem. Int. Ed.* **1988**, *27*, 1516.
54. (a) Dietrich, B.; Flyes, T. M.; Lehn, J. -M.; Pease, L. G.; Fyles, D. L. *J. Chem. Soc. Chem. Commun.* **1978**, 934. (b) Schmidtchen, F. P. *Tetrahedron Lett.* **1989**, *30*, 4493. (c) Echavarren, A. M.; Galan, A.; Lehn, J. -M.; de Mendoza, J. *J. Am. Chem. Soc.* **1989**, *111*, 4994. (d) Galán, A.; Pueyo, E.; Salmerón, A.; de Mendoza, J. *Tetrahedron Lett.* **1991**, *15*, 1827. (e) Galán, A.; Andreu, D.; Echavarren, A. M.; Prados, P.; de Mendoza, J. *J. Am. Chem. Soc.* **1992**, *114*, 1511. (f) Alázar, V.; Segura, M.; Prados, P.; de Mendoza, J.; *Tetrahedron Lett.* **1998**, *39*, 1033. (g) Ariga, K.; Anslyn, E. V. *J. Org. Chem.* **1992**, *57*, 417. (h) Kneeland, D. M.; Ariga, K.; Lynch, V. M.; Huang, C. -Y.; Anslyn, E. V. *J. Am. Chem. Soc.* **1993**, *115*, 10042. (i) Metzger, A.; Lynch, V. M.; Anslyn, E. V. *Angew. Chem. Int. Ed.* **1997**, *36*, 862. (j) Metzger, A.; Anslyn, E. V. *Angew. Chem. Int. Ed.* **1998**, *37*, 649. (k) Fang, L.; Lu, G. -Y.; He, W. -J.; Wang, Z. -S.; Zhu, L. -G. *Chin. J. Chem.* **2001**, *19*, 317.
55. Bates, G. W.; Gale, P. A. *Structure Bonding* **2008**, *129*, 1.

56. Pascal, R. A.; Spergel, J.; Van Engen, D. *Tetrahedron Lett.* **1986**, *27*, 4099.

57. Valiyaveettil, S.; Engbersen, J. F. J.; Verboom, W.; Reinhoudt, D. *Angew. Chem. Int. Ed.* **1993**, *32*, 900.

58. (a) Kavalleieratos, K.; de Gala S. R.; Austin, D. J.; Crabtree, R. H. *J. Am. Chem. Soc.* **1997**, *119*, 2325. (b) Hughes, M. P.; Smith, B. D. *J. Org. Chem.***1997**, *62*, 4492.

59. (a) Hinzen, B.; Seiler, P.; Diederich, F. *Helv. Chim. Acta* **1996**, *79*, 942. (b) Prohens, R.; Tomas, S.; Morey, J.; Deya, P. M.; Ballester, P.; Costa, A. *Tetrahedron Lett.* **1998**, *39*, 1063. (c) Tejeda, A.; Olivia, A. I.; Simon, L.; Grande, M.; Caballero, M. C.; Moran, J. R. *Tetrahedron Lett.* **2000**, *41*, 4563. (d) Szumna, A.; Jurczak, J. *Eur. J. Org. Chem.* **2001**, *66*, 4031. (c) Choi, K.; Hamilton, A. D. *J. Am. Chem. Soc.* **2001**, *123*, 2456. (f) Gale, P. A.; Camiolo, S.; Tizzard, G. J.; Chapman, C. P.; Light, M. E.; Coles, S. J.; Hursthouse, M. B.; *J. Org. Chem.* **2001**, *66*, 7849. (g) Gale, P. A.; Camiolo, S.; Chapman, C. P.; Light, M. E.; Hursthouse, M. B. *Tetrahedron Lett.* **2001**, *42*, 5095. (h) Camiolo, S.; Gale, P. A.; Hursthouse, M. B.; Light, M. E. *Tetrahedron Lett*. **2002**, *43*, 6995. (i) Lakshminarayanan, P. S.; Suresh, E.; Ghosh, P. *Inorg. Chem.* **2006**, *45*, 4372. (j) Arunachalam, M.; Ghosh, P. *Inorg. Chem.* **2010**, *49*, 943. (k) Guha, S.; Saha, S. *J. Am. Chem. Soc.* **2010**, *132*, 17674.

60. Fitzmaurice, R. J.; Kyne, G. M.; Douheret, D.; Kilburn, J.D. *J. Chem. Soc. Pekin Trans. 1* **2002**, 841.

61. Smith, P. J.; Reddington, M. V.; Wilcox, C. S. *Tetrahedron Lett.* **1992**, *33*, 6085.

62. Fan, E.; Van Arman, S. A.; Kincaid, S.; Hamilton, A. D. *J. Am. Chem. Soc.* **1993**, *115*, 369.

63. Hayashita, T.; Onodera, T.; Kato, R.; Nishizawa, S.; Teramae, N. *Chem. Commun.* **2000**, 755.

64. (a) Qian, X.; Liu, F. *Tetrahedron Lett.* **2003**, *44*, 795. (b) Snellink-Ruël, B. H. M.; Antonisse, M. M. G.; Engbersen, J. F. J.; Timmerman, P.; Reinhoudt, D. N.; *Eur. J. Org. Chem.* **2000**, 165. (c) Jose, D. A.; Kumar, D. K.; Ganguly, B.; Das, A. *Tetrahedron Lett.* **2005**, *46*, 5343. (d) Brooks, S. J.; Edwards, P. R.; Gale, P. A.; Light, M. E. *New J. Chem.* **2006**, *30*, 65. (e) Brooks, S. J.; Gale, P. A.; Light, M. E. *Chem. Commun.* **2006**, 4344. (f) Jose, D. A.; Kumar, D. K.; Ganguly, B.; Das, A. *Inorg. Chem.* **2007**, *46*, 5817. (g) Pfeffer, F. M.; Lim, K. M.; Sedgwik, K. J. *Org. Biomol. Chem.* **2007**, 1795. (h) Edwards, P. R.; Hiscock, J. R.; Gale, P. A. *Tetrahedron Lett.* **2009**, *50*, 4922. (i) Jose, D. A.; Singh, A.; Das, A.; Ganguly, A.

Tetrahedron Lett. **2007**, *48*, 3695. (j) Ghosh, A.; Ganguly, B.; Das, A. *Inorg. Chem.* **2007**, *46*, 9912. (k) Caltagirone, C.; Hiscock, J. R.; Hursthouse, M. B.; Light, M. E.; Gale, P. A. *Chem. Eur. J.* **2008**, *14*, 10236. (l) Ravikumar, I.; Ghosh, P. *Chem. Commun.* **2010**, 1082. (m) Ravikumar, I.; Ghosh, P. *Chem. Commun.* **2010**, 6741.

65. Bordwell, F. G. *Acc. Chem. Res.* **1988**, *21*, 456.
66. Coles, S. J.; Gale, P. A.; Hursthouse, M. B. *Cryst. Engg. Commun.* **2001**, 53.
67. Sessler, J. L.; Cyr, M. J.; Lynch, V.; McGhee, E.; Ibers, J. A. *J. Am. Chem. Soc.* **1990**, *112*, 2810.
68. Gale, P. A.; Sessler, J. L.; Kra´l, V.; Lynch, V. *J. Am. Chem. Soc.* **1996**, *118*, 5140.
69. (a) Scherer, M.; Sessler, J. L.; Gebauer, A.; Lynch, V. *Chem. Commun.* **1998**, 1. (b) Kr´al, V.; Gale, P. A.; Anzenbacher Jr., P.; Jursíkoúa, K.; Lynch, V.; Sessler, J. L. *Chem. Commun.* **1998**, 9. (c) Sessler, J. L.; Anzenbacher, Jr., P.; Shriver, J. A.; Jursíkoúa, K.; Lynch, V. M.; Marquez, M. *J. Am. Chem. Soc.* **2000**, *122*, 12061. (d) Yoon, D. W.; Hwang, H.; Lee, C. H. *Angew. Chem. Int. Ed.* **2002**, *41*, 1757. (e) Sessler, J. L.; An, D.; Cho, W.-S.; Lynch, V. *Angew. Chem., Int. Ed.* **2003**, *42*, 2278. (f) Sessler, J. L.; An, D.; Cho, W.-S.; Lynch, V. *J. Am. Chem. Soc.* **2003**, *125*, 13646. (g) Sessler, J. L.; An, D.; Cho, W. -S.; Lynch, V.; Yoon, D. -W.; Hong, S. -J.; Lee, C. -H. *J. Org. Chem.* **2005**, 70, 1511. (h) Sessler, J. L.; An, D.; Cho, W. -S.; Lynch, V.; Marquez, M. *Chem. Eur. J.* **2005**, *11*, 2001. (i) Panda, P. K.; Lee, C. -H. *J. Org. Chem.* **2005**, *70*, 3148. (j) Katayev, E, A.; Sessler, J. L.; Khrustalev, V. N.; Ustynyuk Y. A. *J. Org. Chem.* **2007**, *72*, 7244. (k) Mani, G.; Jana, D.; Kumar, R.; Ghorai, D. *Org. Lett.* **2010**, *12*, 3212. (l) Mani, G.; Guchhait, T.; Kumar, R.; Kumar, S. *Org. Lett.* **2010**, *12*, 3910.
70. (a) Okhuma, S.; Sato, T.; Okamoto, M.; Matsuya, H.; Arai, K.; Kataoka, T.; Nagai, K.; Wassermann, H. H. *Biochem. J.* **1998**, *334*, 731. (b) Sato, T.; Konno, H.; Tanaka, Y.; Kataoka, T.; Nagai, K.; Wasserman, H. H.; Ohkuma, S. *J. Biol. Chem.* **1998**, *273*, 2145. (c) Yamamoto, D.; Kiyozuka, T.; Uemura, Y.; Yamamoto, C.; Takemot, H.; Hirata, H.; Tanaka, K.; Hiokoi, K.; Tsubura, A. J. *Cancer Res. Clin. Oncol.* **2000**, *126*, 191. (d) Sessler, J. L.; Eller, L. R.; Cho, W. -S.; Nicolaou, S.; Aguilar, A.; Lee, J. T.; Lynch, V. M.; Magda, D. J. *Angew. Chem. Int. Ed.* **2005**, *44*, 5989. (e) Gale, P. A.; Light, M. E.; McNally, B.; Navakhun, K.; Sliwinski, K. E.; Smith, B. D. *Chem. Commun.* **2005**, 3773.

71. (a) Schumuck, C. *Chem. Commun.* **1999**, 843. (b) Anzenbacher Jr., P.; Try, A. C.; Miyaji, H.; Juriskova, K.; Lynch, V. M.; Marquez, M.; Sessler, J. L. *J. Am. Chem. Soc.* **2000**, *122*, 10268. (b) Denault, G.; Gale, P. A.; Hursthouse, M. B.; Light, M. E.; Warriner, C. N. *New J. Chem.* **2002**, 811. (c) Sessler, J. L.; Maeda, H.; Mizuno, T.; Lynch, V. M.; Furuta, H. *Chem. Commun.* **2002**, 862. (d) Aleáković, M.; Basarić, N.; Mlinarić-Majerski, K.; Molćanov, K.; Kojić-Prodić, B.; Kesharwani, M. K.; Ganguly, B. *Tetrahedron* **2010**, *66*, 1689. (e) Sreedevi, K. C. G.; Thomas, A. P.; Salini, P. S.; Ramakrishnan, S.; Anju, K. S.; Holaday, M. G. D.; Reddy, M. L. P.; Suresh, C. H.; Srinivasan, A. *Tetrahedron Lett.* **2011**, *52*, 5995.

72. (a) He, J. J.; Quiocho, F. A. *Science* **1991**, *251*, 1479. (b) Verschueren, K. H. G.; Seljee, F.; Rozeboom, H. J.; Kalk, K. H.; Dijkstra, B. W. *Nature* **1993**, *363*, 693.

73. (a) Chmielewski, M. J.; Charon, M.; Jurczak, J. *Org. Lett.* **2004**, 6, 3501. (b) Cureil, D.; Cowley, A.; Beer, P. D. *Chem. Commun.* **2005**, 236.

74. (a) Piatek, P.; Lynch, V. M.; Sessler, J. L. *J. Am. Chem. Soc.* **2004**, *126*, 16073. (b) Chang, K. -J.; Moon, D.; Lah, M. S.; Jeong, K. S. *Angew. Chem. Int. Ed.* **2005**, *44*, 7926. (c) Sessler, J. L.; Cho, D. -G.; Lynch, V. *J. Am. Chem. Soc.* **2006**, *128*, 16518. (d) Kwon, T. -H.; Jeong, K. -S. *Tetrahedron Lett.* **2006**, *47*, 8539. (d) Chang, K. -Y.; Chae, M. K.; Lee, C.; Lee, J. -L.; Jeong, K. S. *Tetrahedron Lett.* **2006**, *47*, 6385. (e) Bates, G. W.; Light, M. E.; Albrecht, M.; Gale, P. A. *J. Org. Chem.* **2007**, *72*, 8921. (f) Lee, J. -Y.; Lee, M. -H.; Jeong, K. -S *Supramol. Chem*, **2007**, *19*, 257. (g) Kim, N. -K.; Chang, K. -J.; Moon, D.; Lah, M. S.; Jeong, K. -S. *Chem. Commun.* **2007**, 3401. (h) Ju, J.; Park, M.; Suk, J. -M.; Lah, M. S.; Jeong. K. -S. *Chem. Commun.* **2008**, 3546.

75. (a) Kang, G.; Kim, H. S.; Jang, D. O. *Tetrahedron Lett.* **2005**, *46*, 6079. (b) Peng, X.; Wu, Y.; Fan, J.; Tian, M.; Han, K. *J. Org. Chem.* **2005**, *70*, 10524. (c) Kim, H. S.; Moon, K. S.; Jang, D. O. *Supramol. Chem.* **2006**, *18*, 97. (d) Singh, N.; Jang, D. O. *Org. Lett.* **2007**, *9*, 1991. (e) Moon, K. S.; Singh, N.; Lee, G. W.; Jang, D. O. *Tetrahedron* **2007**, *63*, 9106. (f) Lee, G. W.; Singh, N.; Jang, D. O. *Tetrahedron Lett*. **2008**, *49*, 1952. (g) Zapata, F.; Caballero, A.; Tarraga, A.; Molina, P. *J. Org. Chem.* **2010**, *75*, 162 (h) Kumari, N.; Jha, S.; Bhattacharya, S. *J. Org. Chem.* **2011**, *76*, 8215. (i) Abraham, Y.; Salman, H.; Suwinska, K.; Eichen, Y. *Chem. Commun.* **2011**, 6087.

76. (a) Connors, K. A. In *Binding Constant Determination*; Wiley, New York, 1987. (b) Schalley, C.; Hirose, K. In *Analytical Methods in Supramolecular Chemistry*; Wiley-VCH, 2007. (c) Hirose, K. *J. Incl. Phenom. Macrocycl. Chem* **2001**, *39*, 193.
77. Wadso, I.; Goldberg, R. N. *Pure Appl. Chem.* **2001**, *73*, 1625.
78. (a) Wilcox, C. S. *Design, Synthesis and Evaluation of an Efficacious Functional Group Dyad. Methods and Limitations in the Use of NMR for Measuring Host-guest Interactions*. In *Frontiers in Supramolecular Organic Chemistry and Photochemistry*, Schneider, H.-J.; Dürr, H., Eds. VCH: Weinheim, 1991. (b) Wilcox, C. S. *Tetrahedron Lett.* **1985**, *26*, 5749. (c) Wilcox, C. S. *Tetrahedron Lett.* **1986**, *27*, 5563.
79. In *ITC Data Analysis in Origin-Tutorial Guide; MicroCal*, LLC, Northampton, Version *7.0*, 2004.

CHAPTER 2

Materials and methods

In this chapter, the materials used and the procedures employed during the course of our investigation are outlined. Purification procedures adopted for the chemicals and the solvents are described. A brief outline of the various physicochemical techniques used in the present study has also been given.

2.1 General Experimental

2.1.1 Solvents

2.1.1.1 Solvent for reactions

Pyrrole was distilled before use. Dichloromethane and 1,2-dichloroethane was dried by distillation over calcium hydride. Tetrahydrofuran was dried by passage through columns of activated alumina followed by refluxing with sodium metal. Nitrobenzene was dried by vacuum distillation over $CaCl_2$.[1]

2.1.1.2 NMR solvents

Chloroform-d_1, acetonitrile-d_3 and DMSO-d_6 was purchased from Cambridge isotope Inc. and used as such.

2.1.1.3 ITC solvents

Acetonitrile (HPLC grade) were purchased from Sigma-Aldrich® and Hi-Pure fine chem industries and used as such.

2.1.1.4 UV-Vis and fluorescence titration solvents

DMSO (spectroscopy grade) was purchased from Merck and used as such.

2.1.2 Reagents

Anions for binding study were used in the form of their tetrabutylammonium salts (fluoride as its trihydrate). The salts were purchased from Sigma-Aldrich® and used as such in the titration experiments. Pyrrole was purchased from Sisco research laboratories. 2,3-Butandione, acetylacetone, acetonylacetone, cuprous chloride, BF_3-OEt_2 and TFA were purchased from Sigma-Aldrich® and used as such. THF, 1,2-dichloroethane, nitrobenzene, acetonitrile and other reagent grade solvents were purchased from Finar chemicals. Zn and $TiCl_4$ were purchased from Finar chemicals. *o*-Phenylenediamine and 4-nitro-*o*-phenylenediamine were purchased from Merck India and Sigma-Aldrich® respectively. All

the inorganic salts and solvents used for the routine laboratory work were purchased from Merck and Standard reagents respectively.

2.2 Chromatography

Thin layer chromatography was performed on TLC Silica gel 60 F_{254} purchased from Merck. Column chromatography was carried out on silica gel (100-200 mesh size) purchased from Merck. HPLC was carried out by Shimadzu LC-20AT chromatogram with SPD detector using Daicel Chiralcel AS-H column.

2.3 Characterization and analytical instrumentation

Melting points were determined by open capillary tubes on a BIO-TECH, India apparatus and on MR-Vis$^+$ visual melting point range apparatus from LABINDIA instruments private limited. IR spectra were recorded on a JASCO FTIR model 5300 and NICOLET 5700 FT-IR spectrometer. NMR spectra were obtained on Bruker 400 MHz and 500 MHz FT-NMR spectrometer operating at ambient temperature. TMS was used as internal standard for ^{1}H NMR spectra. LCMS were carried out by Shimadzu-LCMS-2010 mass spectrometer and HRMS data were recorded with Bruker Maxis spectrometer. Elemental analyses were obtained through Thermo Finnigan Flash EA 1112 analyzer. DSC data were collected in Pyris Diamond DSC, Perkin Elmer Calorimeter. EPR measurements were done on Bruker EMX microX spectrometer. X-ray powder diffraction were recorded on Bruker D8 Advance diffractometer using Cu-Kα X-radiation (λ = 1.54056 Å) at 40 kV and 30 mA. Diffraction patterns were collected over a 2θ range of 5-50° at a scan rate of 1° min^{-1}. Powder Cell 2.4 was used for Rietveld refinement.

Some of the crystallographic data were collected on BRUKER SMART-APEX CCD diffractometer. Mo-Kα (λ = 0.71073 Å) radiation was used to collect X-ray reflections on the single crystal. Data reduction was performed using Bruker SAINT[2] software. Intensities for absorption were corrected using SADABS[3] and refined using SHELXL-97[4] with anisotropic displacement parameters for non-H atoms. Hydrogen atoms on O and N were experimentally located in difference electron density maps. All C−H atoms were fixed geometrically using HFIX command in SHELX-TL. A check of the final CIF file using PLATON[5] did not show any missed symmetry. Some other crystallographic data were also collected on Oxford Gemini A Ultra diffractometer with dual sources. Mo-K$_\alpha$ (λ = 0.71073 Å) radiation was used to collect the X-ray reflections of the crystal. Data reduction was performed using CrysAlis^{Pro}

171.33.55 software.[6] Structures were solved and refined using Olex 2-1.0, with anisotropic displacement parameters for non-H atoms. Hydrogen atoms on N were located from the Fourier map in all of the crystal structures. All C-H atoms were fixed geometrically. Empirical absorption correction was done using spherical harmonics, implemented in SCALE3 ABSPACK scaling algorithm. A check of the final CIF file using PLATON[5] did not show any missed symmetry.

UV-Vis spectra were recorded on Perkin Elmer Lambda 35 UV-Vis spectrophotometer. Fluorescence spectra were recorded on Horiba Zobin Yovan Fluoromax-4 instrument. The titration data were fitted to a 1:1 binding profile in MATLAB 7.0 package and Origin 8 software to evaluate the affinity constant (K_a) .

Microcalorimetric titrations were performed using isothermal titration calorimeter (ITC), purchased from Microcal Inc., MA. The Origin software provided by Microcal Inc. was used to calculate the binding constant (K_a) and the enthalpy change (ΔH). [7]

2.4 Computational details

The quantum mechanical DFT calculations were performed with the Gaussian 03 program package.[8] The Becke three-parameter hybrid (B3) functional was used along with Lee-Yang-Parr (LYP) correction.[9,10] The 6-311++G (d, p) basis set is employed in all calculations reported below. Solvation is accounted with the help of PCM model.[11]

2.5 Sample preparation for analytical purpose

In our study, the guest involved are anions (L) and the receptors or host (S) are neutral oligopyrrole based acyclic and cyclic derivatives, where the prime driving force for the affinity between the receptor-anion came from H-bonding interactions.

Due to the poor solubility of these synthetic receptors in aqueous environment, studies with the tetrabutylammonium salts of various anions were carried out in organic solvents.

However, these salts were difficult to keep dry, being extremely hygroscopic, in some cases. These salts may form ion pair in solution *e.g.* 1mM solutions of tetrabutylammonium chloride in dichloromethane are less than 20% dissociated. Therefore, change of solvent polarity can change not only the strength of the interaction between the receptor and anions, but also the extent of ion pairing in solution between the tetrabutylammonium cation and the anion.[12] That's why when comparing the binding constants, it is necessary that the binding

studies be conducted under identical conditions *e.g.* temperature, solvent, concentration, and even measurement method.

To account for the dilution effect, in case of NMR and optical spectroscopic techniques, the guest solutions used to effect the titrations, containing the receptor at the same concentration as the receptor solution, into which they were being titrated.

Isothermal titration calorimetry (ITC) measurements were performed with a solution of the chosen receptor in HPLC grade acetonitrile. These solutions were then individually titrated with the appropriate tetrabutylammonium salts at 30 ± 0.01°C. The original heat pulses were normalized using reference titrations carried out using the same salt solution but pure solvent, as opposed to a solution containing the receptor.

There are dangerous sources of systematic error that are often encountered in host-guest complexation, that is, the danger of carrying out titrations at concentrations unsuitable for the equilibrium being measured. In case of standard ^{1}H NMR spectroscopic titrations, wherein, the change in the chemical shift of one or more ^{1}H signals are monitored as a function of anion (actually salt) concentration, Wilcox proposed that a better titration curve can be obtained by moving the entire experiment towards lower concentration.[13] The best results are obtained in a NMR titration when the minor component (the fixed component) is maintained at a concentration equal to about one-tenth of the dissociation constant K_d and the titrant is varied from that concentration to a concentration of ten times the dissociation constant.[13] Similarly, the optimum concentration of the material in the sample cell in ITC is $K_a \times [S] = 10\ to\ 50$.[14] A relevant comparison of results obtained from these two methods is possible, by choosing an appropriate concentration of the receptor from the outset.[7]

2.6 Evaluation of binding constant

2.6.1 ^{1}H NMR titration

2.6.1.1 Connor equation

$$\frac{1}{\delta_{obs}} = \frac{1}{(\delta_{SL}-\delta_S)K_a[L]} + \frac{1}{(\delta_{SL}-\delta_L)}$$

From the ratio of the slope and intercept of the linear plot, the binding constant K_a can be evaluated.[12]

2.6.1.2 Wilcox equation[13]

$$\delta_{obs} = \delta_S + \frac{\delta_{SL} - \delta_S}{2[S]}\left[\frac{1}{K_a} + [S] + [L] - \sqrt{\left(\left(\frac{1}{K_a} + [L] + [S]\right)^2 - 4[L][S]\right)}\right]$$

K_a can be evaluated by nonlinear curve fitting of the titration data in this equation.[13]

Where, δ_{obs}: the observed chemical shift in the experiment (ppm),

$[S]$: Host concentration (M),

$[L]$: Guest concentration (M),

K_a: Binding constant (M^{-1}),

δ_S: Chemical shift of the free host (ppm),

δ_{SL}: Chemical shift of the host-guest complex (ppm).

2.6.2 UV-Vis titration

2.6.2.1 Connor equation

$$\frac{\Delta A}{b} = \frac{S_t K_a \Delta\varepsilon [L]}{1 + K_a[L]}$$

From the nonlinear curve fitting analysis of the above equation on the experimental data, we can evaluate the binding constant K_a.[12]

2.6.2.2 Benesi-Hildebrand plot

$$\frac{1}{\Delta A} = \frac{1}{S_t K_a b \Delta\varepsilon [L]} + \frac{1}{S_t b \Delta\varepsilon}$$

From the ratio of the slope and intercept of the linear plot the binding constant K_a can be evaluated.[12]

Where, $\Delta A = A - A_\circ$

$A_\circ$, A: Measured absorbance of the substrate in absence and in presence of guest

S_t: Total host concentration (M),

$[L]$: Guest concentration (M),

K_a: Binding constant (M^{-1}),

$\Delta\mathcal{E}$: Molar absorptivity of the host-guest solution,

b: Path length.

2.6.3 Isothermal titration calorimetry (ITC)

In ITC it is only ΔH that is obtained directly, with ΔG and K_a coming as the result of modeling the experimental data to a binding profile, a process that permits the calculation of TΔS.[7,14]

For a single identical sites, binding constant,

$$K_a = \frac{\theta}{(1-\theta)[L]} \qquad \ldots\ldots\ldots\ldots\ldots\ldots\ldots\ldots\ldots\ldots\ldots\ldots 1$$

Where θ= fraction of sites occupied by guest L.

$$[L]_t = [L] + n\theta[S]_t \qquad \ldots\ldots\ldots\ldots\ldots\ldots\ldots\ldots\ldots\ldots 2$$

Combining equation 1 and 2,

$$\theta^2 - \theta\left[1 + \frac{[L]_t}{n[S]_t} + \frac{1}{nK_a[S]_t}\right] + \frac{[L]_t}{n[S]_t} = 0 \qquad \ldots\ldots\ldots\ldots\ldots\ldots 3$$

$$Q = n\theta[S]_t\Delta HV_\circ \ldots\ldots\ldots\ldots\ldots\ldots\ldots\ldots\ldots\ldots 4$$

Where, n= number of sites; $V_\circ$= active cell volume; and $[S]$, $[L]$, $[S]_t$, $[L]_t$ are the free and bulk concentration of S and L respectively.

$$Q = \frac{n[S]_t\Delta HV_\circ}{2} \times \left[1 + \frac{[L]_t}{n[S]_t} + \frac{1}{nK_a[S]_t} - \sqrt{\left(1 + \frac{[L]_t}{n[S]_t} + \frac{1}{nK_a[S]_t}\right)^2 - \frac{4[L]_t}{n[S]_t}}\right] \ldots\ldots\ldots 5$$

Where, Q is the total heat content of the solution contained in $V_\circ$ and H is the molar heat of binding.

$$\Delta Q(i) = Q(i) + \frac{\Delta V_i}{V_\circ}\left[\frac{Q(i)+Q(i-1)}{2}\right] - Q(i-1) \ldots\ldots\ldots\ldots\ldots\ldots 6$$

Where, ΔV_i is the injection volume and $\Delta Q(i)$ is the heat content from the i^{th} injection.

Once the experimental data are in hand, four steps are required to complete the analysis. The first involves putting initial guesses for the values of K_a, and ΔH into equation 5; the second, is the calculation of ΔQ(i) for each injection and comparison of these values with the observed heats (equation 6); the third step involves putting improved values of K_a and ΔH to

equation 5 and the fourth step needs repeating these first three steps iteratively, until no further significant change in the value of the parameters is observed. This iteration was performed with the Origin® software provided by the manufacturer.

2.7 Preparation of starting materials

The following compounds were prepared by following literature method, in order to utilize them as the starting material for our investigation. Their identification was further confirmed, by matching the analytical data with that reported in the literature.

2.7.1 Synthesis of acetone N,N-dimethylhydrazone[15]

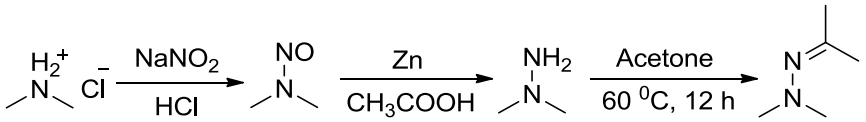

2.7.1.1 Synthesis of nitrosodimethylamine

In a 2 L round-bottomed flask equipped with a mechanical stirrer, dimethylamine hydrochloride (100 g, 1.2 mol), water (50 mL), and ~2N HCl (4 mL) were added. The resulting solution was stirred vigorously and maintained at 70-75 °C by heating on a water bath, then sodium nitrite (93 g, 1.3 mol) suspended in water (60 mL) was added from a dropping funnel over a period of 1 h. The reaction mixture was tested frequently and maintained slightly acidic to litmus, by further additions of 2N HCl when necessary. Stirring and heating were continued for another 2 h, after all the sodium nitrite has been added. The reaction mixture is then distilled under slightly reduced pressure, until the residue was practically dry. To the residue, 50 mL of water was added and the process of distillation to dryness is repeated. The distillates were combined and saturated with potassium carbonate; the upper layer of dimethylnitrosoamine was removed, and the water layer was extracted with ether. The combined nitrosoamine and ethereal extracts were dried over anhyd. potassium carbonate and the removal of solvent under reduced pressure yields the desired product (90 g, 97 %; lit. 90 %) as yellow oil.

2.7.1.2 Synthesis of unsym. dimethylhydrazine

In a 500 mL round-bottomed flask, equipped with a mechanical stirrer, dropping funnel, and thermometer, nitrosodimethylamine (20 g, 0.27 mol) in water (300 mL) and zinc dust (65

g) were added. While the mixture was stirred and maintained at 25-30 °C, by immersion in a water bath, acetic acid (85mL, 1.5 mol) was added from the dropping funnel over a period of 1h. Subsequently the reaction mixture was heated for one hour at 60 °C, allowed to cool, and the excess zinc dust was filtered out and then washed with a little water. The aqueous layers were combined and transferred to a 2 L flask. The flask was fitted with a dropping funnel. The solution was made distinctly alkaline by adding a concentrated solution of sodium hydroxide (150 g) through the dropping funnel, and the mixture was then steam distilled until a test portion of the distillate shows only a faint reduction with Fehling's solution. The aqueous distillate was treated with conc. hydrochloric acid (65 mL) and then concentrated under reduced pressure, until the residual liquor becomes a syrupy mass. The syrupy mass was allowed to drop onto a large excess of solid sodium hydroxide and distilled until the temperature reaches 100 °C. To obtain the anhydrous base, the concentrated aqueous solution is redistilled after standing over potassium hydroxide. By distillation the desired product was obtained as a white liquid (10 g, 64 %; lit. 69-73 %).

2.7.1.3 Synthesis of acetone N,N-dimethylhydrazone

A mixture of dry acetone (10 mL, 136 mmol) and N,N-dimethylhydrazine (10 mL, 136 mmol) was refluxed overnight. To this, NaOH (4.2 g, 104 mmol) was added and then the upper layer was decanted, dried with CaH_2 overnight and distilled to give the pure product (9.5 g, 69.5 %; lit. 68 %).

2.7.2 Synthesis of 2,8-nonanedione

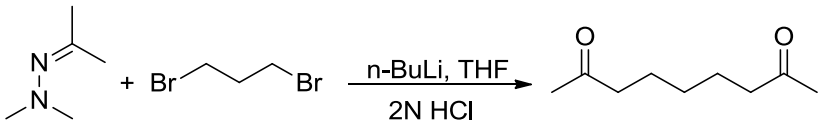

1.6 M *n*-BuLi (19 mL, 30.4 mmol, 2 equiv.) was added to a solution of N,N-dimethyl-hydrazone (4 mL, 40 mmol, 2.2 equiv.) in THF (120 mL) at -5 °C under nitrogen atmosphere and the mixture was stirred for 1 h. 1,3-Dibromopropane (1.6 ml, 15.8 mmol, 1 equiv.) was added at -5 °C and the reaction mixture was stirred for 15 h at room temperature, then 2 M HCl (120 mL) was added and left standing for 15 h. The reaction mixture was further diluted with water and extracted with ethylacetate. After removal of the solvent, the compound was purified over a silica gel column using ethylacetate:hexane (30:70) as the eluent. Evaporation

of the eluent afforded the desired product as white oil (2.2 g, 47 %; lit. 54 %), which solidifies on keeping at low temperature.

2.7.3 Synthesis of 2,6-heptanedione[16]

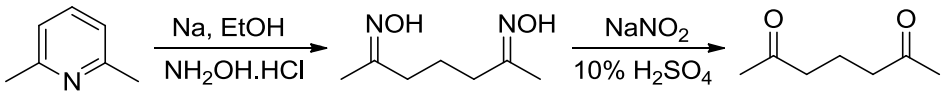

2.7.3.1 Synthesis of heptanedione-2,6-dioxime

A solution of dry 2,6-lutidine (2 mL, 17.2 mmol,1 equiv.) in dry ethanol (8 mL) was heated to reflux temperature and subsequently sodium (390 mg, 17.2 g atom, 1 equiv.) was added slowly as freshly cut pieces. When all the sodium had dissolved, the flask was cooled and a slurry of hydroxylamine hydrochloride (1.2 g, 17.2 mmol) in water (1 mL) and 95% ethanol (1 mL) was added. Again, a solution of conc. HCl (1 mL) in ethanol (1 mL) was added immediately. The mixture was heated at reflux for 1.5 h and filtered to remove sodium chloride while warm. Excess lutidine and ethanol was removed from the filtrate under reduced pressure. The residue was cooled, made alkaline with aq. NaOH and was extracted with ether. The ether layer was discarded and the aqueous layer was acidified with 5 N HCl, keeping the temperature of the solution at 0-5 °C. The product was extracted with diethyl ether and the ether solution was dried over anhyd. sodium sulfate. Evaporation of the solvent afforded the desired product as red color viscous liquid (504 mg, 19 %; lit. 40 %).

2.7.3.2 Synthesis of 2,6-heptandione

A solution of heptanedione-2,6-dioxime (1.2 g, 1.8 mmol) dissolved in 10% aq. H_2SO_4 (1.5 mL) was cooled below 0 °C, to this sodium nitrite (0.24 g, 3.4 mmol) was added slowly with vigorous stirring for 1 h. The temperature was kept below 0 °C during the addition, and then was allowed to rise to ~20 °C. The solution was neutralized by adding sodium carbonate with stirring for 15 minutes then filtered, extracted with diethyl ether and the ether solution was dried with anhyd. sodium sulfate. Evaporation of the solvent afforded the desired product as a red color viscous liquid (530 mg, 54 %; lit. 48 %), which solidifies on cooling.

2.7.4 Synthesis of dipyrromethane[17]

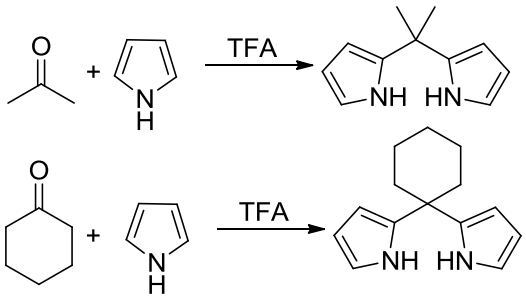

Pyrrole (25 equiv.) and ketone (1 equiv.) were added to a dry round-bottom flask and degassed with a stream of N_2 for 5 min. To the reaction mixture, TFA (0.1 equiv.) was added, and the solution was stirred under N_2 at room temperature for 5 min and quenched immediately with excess triethylamine. Excess pyrrole was removed under vacuum and subsequently the desired dipyrromethane was purified by column chromatography over silica gel. 5,5-Dimethyldipyrromethane **(**59 %; lit. 53 %); 5,5-cyclohexyldipyrromethane **(**70 %; lit. 43 %).

2.7.5 Synthesis of pyrrole-2-carboxaldehyde[18]

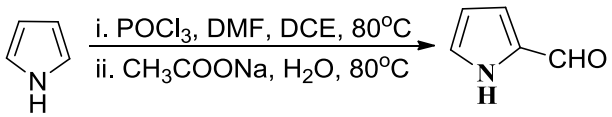

$POCl_3$ (7 mL, 80 mmol), was added slowly to DMF (6 mL, 80 mmol) at 0-5 °C under nitrogen atmosphere. The mixture was then allowed to warm to room temperature and stirred for 20 min. Then 1,2-dichloroethane (50 mL) was added and again cooled to 0 °C. To this mixture, a solution of the freshly distilled pyrrole (5 mL, 72 mmol) in 1,2-dichloroethane (50 mL) was added over a period of 15 min. The resulting mixture was heated to reflux for 30 min and cooled to room temperature. To the reaction mixture, sat. aq. NaOAc (20 g) was carefully added and again heated to reflux for 1 h. Upon cooling, the mixture was extracted with dichloromethane, and the combined organic phase was then washed with sodium bicarbonate solution. The organic phase was then dried over anhyd. sodium sulfate and evaporated to dryness. The product was purified by vacuum distillation, using kugelrohr to afford pyrrole-2-carboxaldehyde as white viscous liquid (4.8 g, 71 %; lit. 79 %) which solidifies at low temperature.

2.7.6 Synthesis of 2,3-Dipyrrol-2-ylquinoxaline[19]

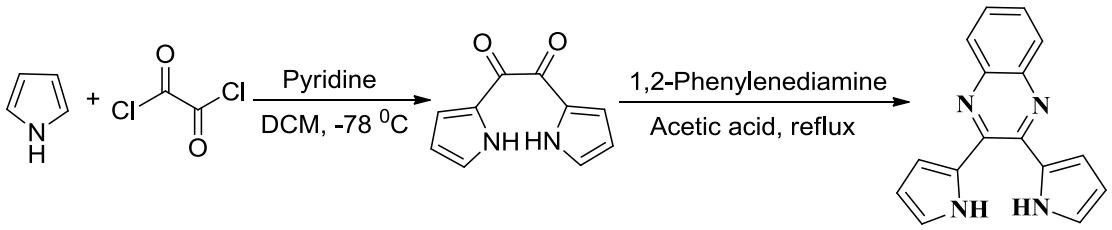

2.7.6.1 Synthesis of 2,3-Dipyrrol-2-ylethanedione

Oxalyl chloride (15 g, 115 mmol) and dichloromethane (200 mL) were placed in a round bottomed flask, under nitrogen atmosphere and stirred. Upon cooling to -78 °C, dry pyridine (18 g, 227 mmol) was added, resulting in the formation of a yellow precipitate. To this cooled suspension, a solution of freshly distilled pyrrole (15g, 230 mmol) in dichloromethane (50 mL) was added by using a dropping funnel. Immediately, the reaction mixture was seen to turn from yellow to brown. The reaction mixture was stirred for 15 min, followed by addition of hydrochloric acid (5N, 200mL) to quench the reaction. The biphasic system was then separated off and the organic phase was collected. The aqueous phase was extracted with dichloromethane and the combined organic phases was washed with water (100 mL), dried over anhyd. sodium sulfate, filtered and evaporated to dryness. This afforded a green precipitate which was purified on silica gel chromatography using chloroform as eluent, to afford the desired product as a yellow powder (6.3 g, 29 %; lit. 38 %).

2.7.6.2 Synthesis of 2,3-Dipyrrol-2-ylquinoxaline

2,3-Dipyrrol-2-ylethandione (3 g, 15.3 mmol) was dissolved in glacial acetic acid (250 mL) and to this, a solution of *o*-phenylenediamine (5.2 g, 48 mmol) in acetic acid (50 mL) was added while stirring under nitrogen atmosphere. The reaction mixture was refluxed for 3 h. After cooling the reaction mixture, the majority of the acetic acid was removed under vacuum and the residue was taken up in a mixture of water (100 mL) and dichloromethane (100 mL). The organic phase was separated off and the aqueous phase was further extracted with dichloromethane. All organic phases were combined and washed with sat. aq. sodium bicarbonate solution. After drying over anhyd. sodium sulfate, the solution was filtered and evaporated to dryness. The residue was purified using silica gel column chromatography, using chloroform as eluent to afford the desired product (3.8 g, 91 %; lit. 94 %).

2.7.7 Synthesis of 2,3-Bis(5′-formylpyrrol-2′-yl)quinoxaline[20]

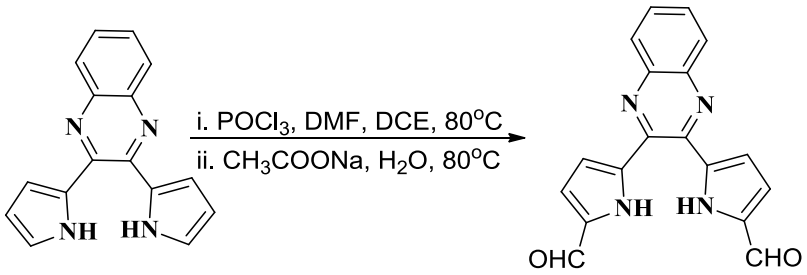

$POCl_3$ (480 µL, 5.1 mmol), was added slowly to DMF (400 µL, 5.1 mmol) at 0-5 °C under nitrogen atmosphere. The mixture was then allowed to warm to room temperature and 1,2-dichloroethane (6 mL) was added. The reaction mixture was cooled to 0 °C and a solution of the unsubstituted dipyrrolylquinoxaline (520 mg, 2 mmol) in 1,2-dichloroethane (30 mL) was added over a period of 15 min. The resultant reaction mixture was heated to reflux for 30 min before being cooled to room temperature. Sat. aq. NaOAc (2g in 5 mL water) was carefully added, and the mixture was again heated to reflux for 1 h. Upon cooling, the mixture was extracted with dichloromethane, and the combined organic phase was washed with sodium bicarbonate solution. The organic phase was dried over anhyd. sodium sulfate and evaporated to dryness. The residue was subject to chromatography over silica gel using 1% MeOH in $CHCl_3$ as eluent, to afford 2,3-bis(5′-formylpyrrol-2′-yl)quinoxaline as greenish yellow solid (405 mg, 65 %; lit. 80 %).

2.8 Summary

A brief account of various solvents, chemicals used in the synthesis and different spectrometers and other physical and computational methods employed for characterization in our investigation, is given in this chapter. Syntheses of the already reported compounds, which are employed as starting materials for the dissertation work, were also described here.

2.9 References

1. Armarego, W. L. F.; Chai, C. In *Purification of laboratory chemicals*; sixth edition, Elsevier, Burkington**,** 2003.
2. SAINT, version 6.45 /8/6/03, Bruker AXS, **2003**.
3. Sheldrick, G. M.; *SADABS, Program for Empirical Absorption Correction of Area Detector Data,* University of Göttingen, Germany, **1997**.

4. Sheldrick, G. M.; *SHELXS-97* and *SHELXL-97, Programs for the Solution and Refinement of Crystal Structures,* University of Göttingen, Germany, **1997**.
5. (a) Spek, A. L.; *PLATON, A Multipurpose Crystallographic Tool,* Utrecht University, Utrecht, The Netherlands, **2002**; (b) Spek, A. L. *J. Appl. Cryst.* **2003**, *36*, 7.
6. Oxford Diffraction. CrysAlis CCD and CrysAlis RED. Versions 1.171.33.55. Oxford Diffraction Ltd, Yarnton, Oxfordshire, England, **2008**.
7. ITC Data Analysis in Origin-Tutorial Guide; MicroCal, LLC, Northampton, Version 7.0, **2004**.
8. Frisch, M. J. *Gaussian 03, Revision B.05,* Gaussian, Inc., Pittsburgh PA. **2003**.
9. Becke, A. D. *J. Chem. Phys.* **1993**, *98*, 5648.
10. Lee, C.; Yang, W.; Parr, R. G. *Phys. Rev. B.* **1988**, *37*, 785.
11. (a) Tomasi, J.; Mennucci, B.; Cammi, R. *Chem. Rev.* **2005**, *105*, 2999. (b) Cossi, M.; Rega, N.; Scalmani, G.; Barone, V. *J. Comput. Chem.* **2003**, *24*, 669.
12. (a) Connors, K. A. In *Binding Constant Determination*; Wiley, New York, 1987. (b) Schalley, C.; Hirose, K. In *Analytical Methods in Supramolecular Chemistry;* Wiley-VCH, 2007.
13. (a) Wilcox, C. S. In *Frontiers in Supramolecular Organic Chemistry and Photochemistry*, Eds. Schneider, H.-J.; Dürr, H., VCH: Weinheim, 1991. **(**b) Wilcox, C. S. *Tetrahedron Lett.* **1985**, *26*, 5749. (c) Wilcox, C. S. *Tetrahedron Lett.* **1986**, *27*, 5563. (d) Sessler, J. L.; Gross, D. E.; Cho, W. S.; Lynch, V. M.; Schmitdtchen, F. P.; Bates, G. W.; Light, M. E.; Gale, P. A. *J. Am. Chem. Soc.* **2006**, *128*, 12281.
14. (a) Wadso, I.; Goldberg, R. N. *Pure Appl. Chem.* **2001**, *73*, 1625.
15. (a) Hatt, H. H. *Org. Synth.* **1936,** *16*, 22. (b) Yamashita, M.; Matsumiya, K.; Morimoto, H.; Seumitsu, R. *Bull. Chem. Soc. Jpn.* **1989**, *62*, 1668. (c) Bai, X.; Eliel, L. E. *J. Org. Chem.* **1991**, *56,* 2087.
16. Overbergert, C. G.; Gibb Jr., T. B.; Chibnik, S.; Huang, P.; Monagle, J. J. *J. Am. Chem. Soc.* **1952**, *74*, 3290.
17. Littler, B. J.; Miller, M. A.; Hung, C. -H.; Wagner, R. W.; O'Shea, D. F.; Boyle, P. D.; Lindsey, J. S. *J. Org. Chem.* **1999**, *64*, 1391.
18. Silverstein, R. M.; Ryskiewicz, E. E.; Willard, C. *Org. Synth.* **1956**, *36*, 734.
19. (a) Oddo, B. *Gazz. Chim. Ital.* **1911**, *41*, 248. (b) Behr, D.; Brandänge, S.; Lindström, B. *Acta Chem. Scand.* **1973**, *27*, 2411. (c) Black, C. B.; Andrioletti, B.; Try, A. C.; Ruiperez, C.; Sessler, J. L. *J. Am. Chem. Soc.* **1999,** *121*, 10438.

20. Sessler, J. L.; Maeda, H.; Mizuno, T.; Lynch, V. M.; Furuta H. *J. Am. Chem. Soc.* **2002,** *124*, 13474.

CHAPTER 3

Towards Biscalix[4]pyrroles…

3.1 Introduction

Meso-functionalized dipyrromethanes are widely used as the precursor material for the synthesis of porphyrinogens (viz. porphyrins, corroles, calixpyrroles, calixphyrins etc.).[1,2] The importance of porphyrins and its analogues (conjugated porphyrinogens) in the field of biological, medical and material science has been well archived.[1] There are two types of dipyrromethanes firstly **L89** which is formed by condensation of pyrrole with aldehyde and can be further oxidized to dipyrrin and secondly **L90** which is formed from the condensation of pyrrole with ketone and cannot be oxidized. 5-Substituted dipyrromethanes are in general used as the building blocks for aromatic porphyrinoids, whereas 5,5-dipyrromethanes are employed as the building blocks for non-conjugated porphyrinogens such as calixpyrrole and calixphyrin which shows potential application in guest recognition and coordination chemistry respectively.[3,4]

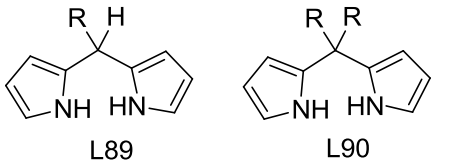

The direct synthesis of dipyrromethanes from pyrrole and aldehydes/ketones results a mixture of statistically distributed oligopyrromethanes whose separation is always a cause of concern. This is because the initially formed 2-(α-hydroxy-α-methyl)pyrrole is more nucleophilic than pyrrole itself. In addition, in presence of acid, α-protonation of pyrrole occurs, thereby creating a good electrophile, which can be attacked by another pyrrole molecule, affording the so called pyrrole trimer **L91** (Scheme 3.1). The coupling reaction can be repeated many times, leading to a mixture of oligopyrroles and insoluble polymeric material.[5] Further, acidolysis of dipyrromethanes also increases its complexity. Many researchers had contributed towards the development of the methodology for the synthesis of dipyrromethanes[6] but the most popular protocol was developed by Lindsey and Lee in 1994, where they have used a large excess of pyrrole without solvent to avoid the formation of oligopyrromethane.[7] Soon after Lindsey and coworkers modified that methodology and used pyrrole:aldehyde ratio of 25:1 and column chromatographic purification was replaced by Kugelrohr distillation.[8] Further, they had reported that reaction catalyzed by TFA afforded less *N*-confused dipyrromethane (*i.e.* analogue of dipyrromethane in which one pyrrole unit is linked via α-position and the second pyrrole unit via β-position) compared to BF_3-OEt_2

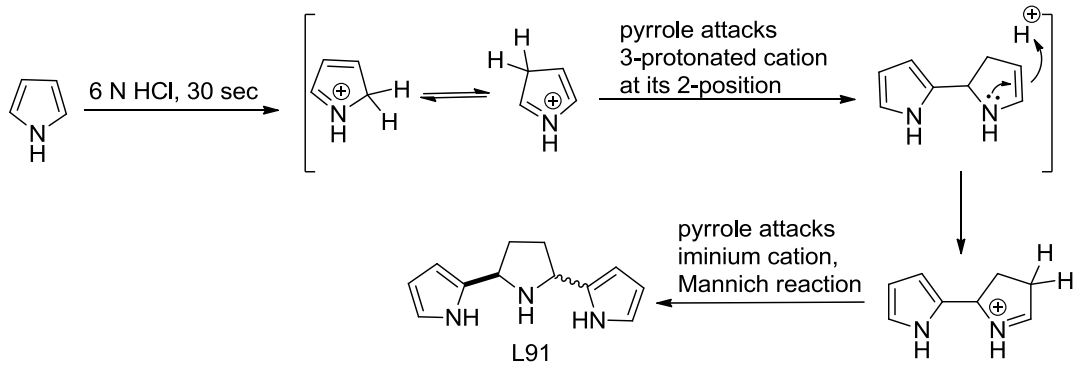

Scheme 3.1 Reaction of pyrrole in the presence of acids.[5]

catalyzed reaction.[8] In another study, Dudić *et al.* proposed increasing the ratio of pyrrole to aldehyde to 60:1 and used BF_3-OEt_2 as a catalyst.[9] This modification gave very high yields but required chromatographic separation. In another study, Sobral *et al.* reported an environmentally benign aq. HCl catalyzed synthesis of dipyrromethanes in water, which involves little or no subsequent purification procedures and needs no excess quantity of pyrrole (2 equiv. w.r.t. aldehyde or ketone).[10] In addition to the abovementioned catalysts, $TiCl_4$,[11] *p*-TsOH,[12] $SnCl_4$,[13] $MgBr_2$,[14] $InCl_3$[15] were also successfully tested as the catalyst on different pyrrole and aldehyde and/or ketone systems.

In the last two decades, non-conjugated porphyrinogen *e.g.* calix[4]pyrrole **L48** and its modified and/or functionalized analogues has emerged as a promising supramolecular neutral host for anions.[3] This molecule was first synthesized by Baeyer by simple acid catalyzed

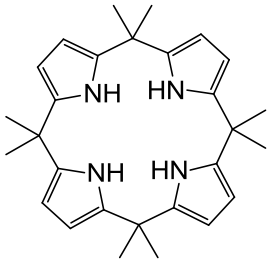

L48

condensation of pyrrole with acetone.[16] In 1996, Sessler and coworkers reported, this macrocycle can act as a neutral host to small anions, such as fluoride and chloride and also neutral guest in common aprotic solvents.[17] Subsequent efforts to increase the binding affinity or selectivity towards anions, has prompted many transformations and modifications on macrocycle **L48**, that includes *meso*-sustitution(s), *β*-substitution(s), single side strapping, core modification and core expansion.[18]

Recently Sessler *et al.* showed that functionalized calixpyrrole such as TTF-C4P (tetrathiafulvalenecalix[4]pyrrole) and *cis*/*trans*-DNP-C4P (*cis*/*trans*-bis(dinitrophenyl)-calix[4]pyrroles) can act as heterocomplimentary monomer towards supramolecular alternating copolymers (Figure 3.1).[19] This polymer shows different response for charged chloride ion and neutral trinitrobenzene (TNB) w.r.t. colorimetric, electrochemical and polymer structural response.

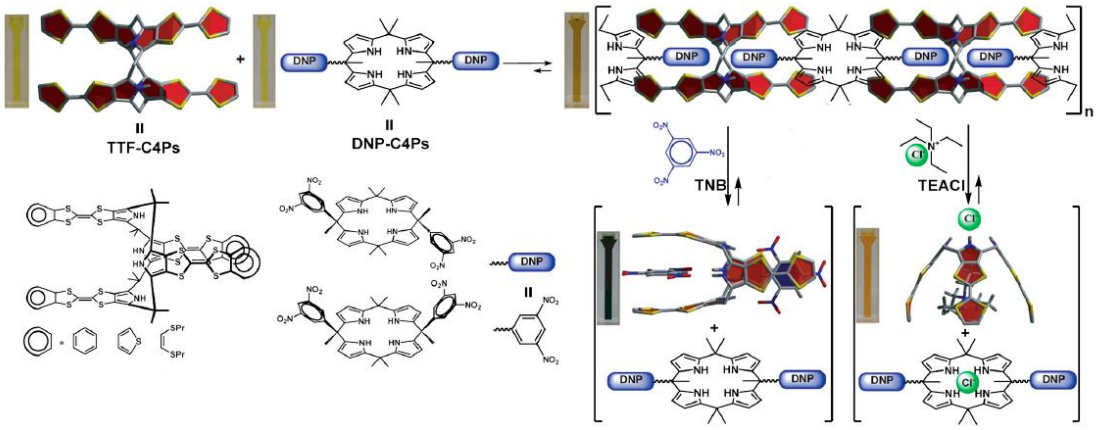

Figure 3.1 Schematic representation of the self-association between the TTF-C4P monomers and the heterocomplementary DNP-C4P monomers. Also shown is the chemoresponsive behavior observed upon the addition of either TEACl or TNB.[19]

Over the last few decades, considerable effort has been put forward towards the development of neutral host molecules bearing rigid spacers that can bind guest molecules in a cooperative manner, however systems that can effect cooperative binding of anions, still remains rare.[20] In 1997, Sessler and coworkers reported that dimeric sapphyrins if appropriately constructed, can carry out this function in their protonated state.[21] So it is presumed that calix[4]pyrroles, an alternative series of pyrrole-based anion receptors, are easy to make and functionalize and therefore, can serve the purpose as a neutral receptor. In

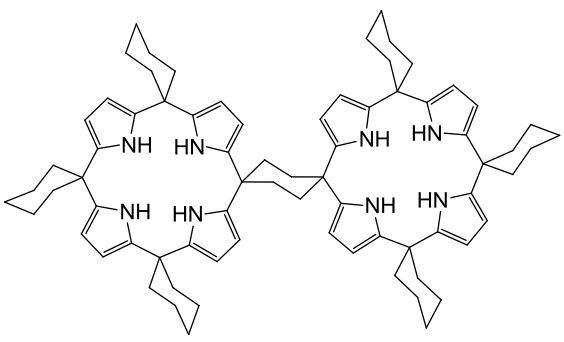

L92

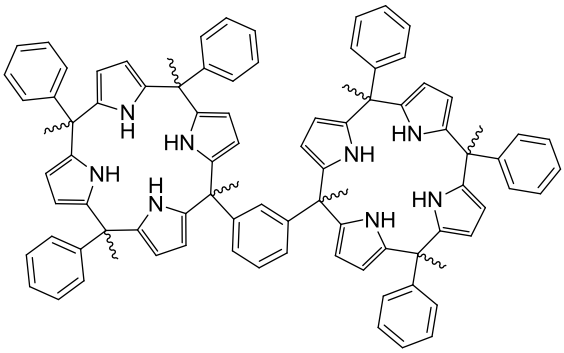

L93

1998, Sessler and coworker proposed two calix[4]pyrrole dimers **L92** and **L93** as a prospective cooperative homoditopic anion and neutral substrate receptors for diols and dicarboxylates.[2a] In another report in 2000, Sessler and coworkers prepared three calix[4]pyrrole dimers **L94**-**96** by following a post modification strategy, which involves palladium (0) catalyzed C-C bond formation and detailed anion binding study of the dimers linked via di-ethynyl spacer, revealed higher binding affinity towards isophthalate, phthalate and benzoate ion compared to octamethylcalix[4]pyrrole monomer **L48** owing to cooperative

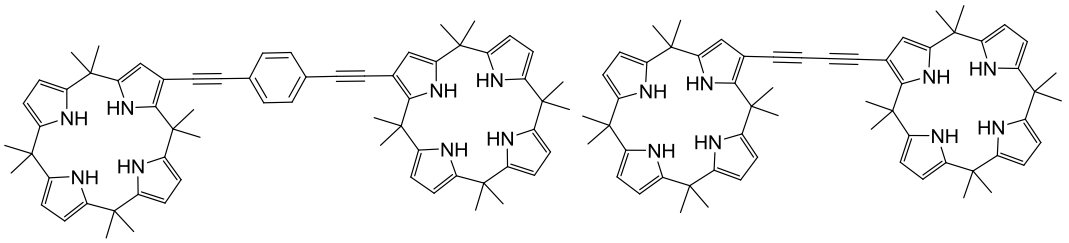

L94

L95

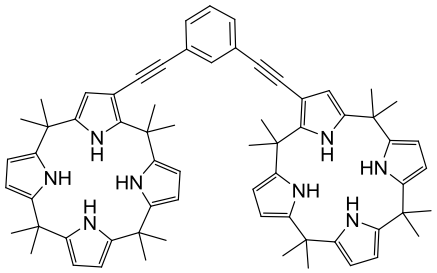

L96

binding.[22] Therefore, it is envisaged that biscalixpyrroles where the calixpyrrole units are bridged by appropriate spacers may display improved anion affinity and/or selectivity accompanied by cooperativity. However, unlike porphyrinoids,[23] very little is known about biscalixpyrrole systems, which can find application as a dianionic host or as supramolecular building block (anion directed supramolecular polymer), along with their potential utility as a host, towards cooperative anion binding, due to the associated synthetic difficulties. In general synthesis of stable nonaromatic porphyrinogens involves either condensation of pyrroles with ketone containing different functional groups or mixed condensation of more than one ketones with pyrrole in acidic media.[2a] Another route involves the [2+2] condensation of dipyrromethanes with ketones.[17,2c,2d] Lindsey and co-worker developed the [2+2] condensation of dipyrromethane dicarbinol and dipyrromethane methodology towards porphyrins.[24] Further Lee and coworkers used this methodology to synthesize hybrid calixpyrrole.[25] While dipyrromethanes were useful in making monomeric porphyrinoid macrocycles; development of dimeric and oligomeric porphyrinoids, in particular calixpyrroles involve a lot of tedious processes.

The reported methods for constructing biscalix[4]pyrrole (**L94**-**L96**) involves functionalization of calix[4]pyrrole in order to be used as building block towards the target.[22] However, this approach only introduces fixed linkers among the calixpyrrole units, which seriously undermines the possible diversification of the multicalixpyrrole arrays. The synthesis of biscalixpyrroles can be targeted by mixed condensation of pyrrole with acetone

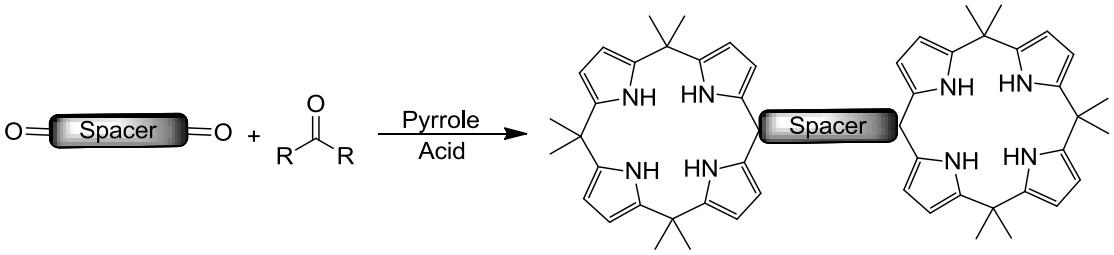

Scheme 3.2 Schematic representation of mixed condensation strategy towards biscalixpyrrrole.

and a diketone and Sessler *et al.* has briefly noted about this strategy as a convenient way towards biscalixpyrrole (Scheme 3.2).[2a] However, this approach will result in the formation of multiple products which needs tedious chromatographic purification and thus seriously limits its utility. In order to simplify the above targets it is envisaged that bisdipyrromethanes (bisDPMs) will be very good building blocks. Lindsey and coworkers used bisdipyrromethanes as a precursor for the synthesis of bisporphyrinoids,[26] however, so far nobody has tried this in calixpyrrole chemistry. The condensation of bisDPMs with

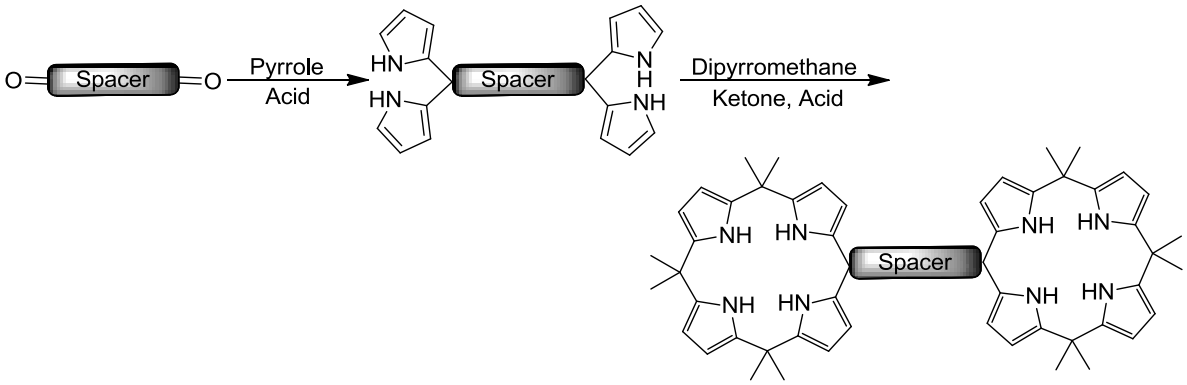

Scheme 3.3 Schematic representation of condensation of DPM and bisDPM by [2+2] strategy towards biscalixpyrrole.

dipyrromethanes by the [2+2] approach would be a potentially important route towards the design and synthesis of novel biscalixpyrrole moieties (Scheme 3.3). Another way to achieve biscalixpyrrole with a pre-organised cavity is by acid catalysed self-condensation of bisDPMs with ketones (Scheme 3.4).This strategy can lead to flexible preorganized binding domain and hence may lead to some interesting encapsulation due to cooperative effect.

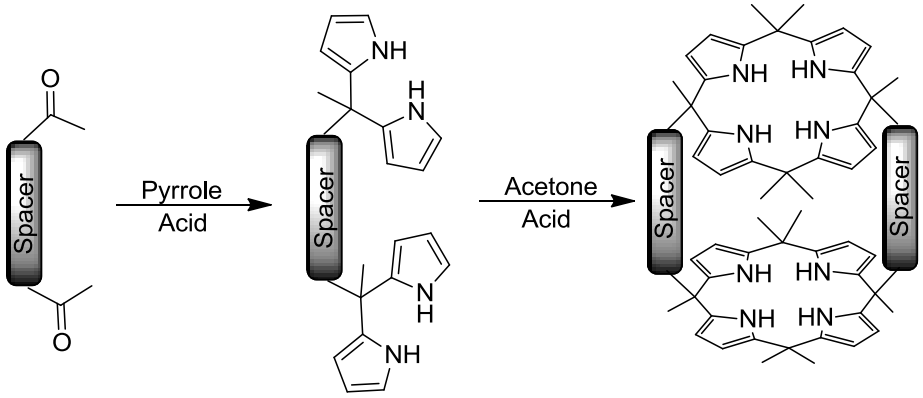

Scheme 3.4 Schematic representation of self-condensation of bisDPM by [2+2] strategy towards biscalixpyrrole.

3.2 Research Goal

We choose acyclic diketones to make biscalix[4]pyrroles, where one calix[4]pyrrole unit is strapped over another through flexible linker, *meso-meso* linked biscalixpyrroles and cyclohexanediones to have two calix[4]pyrroles at closer proximity with comparatively

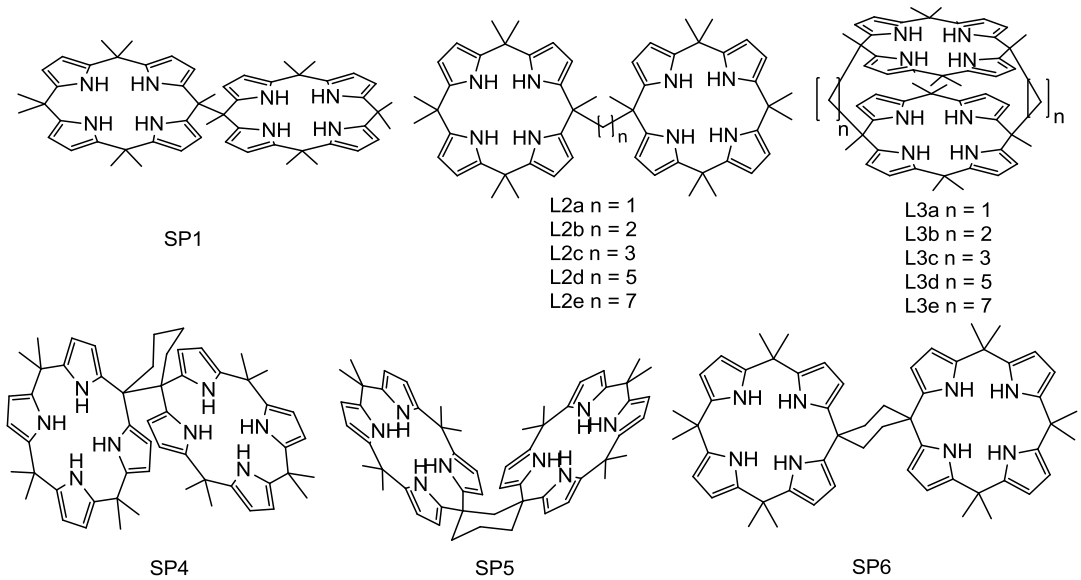

Scheme 3.5 Structure of the proposed biscalix[4]pyrroles.

lesser flexibility (Scheme 3.5). In order to synthesize these systems, we envisage suitable bisDPMs would be useful precursors. In this direction bisDPMs **SP7-11** (Scheme 3.6) were designed to be synthesized at first. The basic idea of making bisDPMs from a diformyl compound was demonstrated first by Chang in the 1980s and exploited later by Sessler, McLendon, Osuka, Lindsey and others.[28] Most of the reported bisDPMs were utilized to synthesize diporphyrins via condensation of each bisDPM with two dipyrromethane units, by [2+2] approach. Several bisDPMs from diketones were reported in literature; they are of convergent type and employed for making single side strapped calix[4]pyrroles.[27] On the other hand, the key precursors towards the synthesis of biscalixpyrroles are the divergent type bisDPMs, containing appropriate linkers between the two dipyrromethane units which

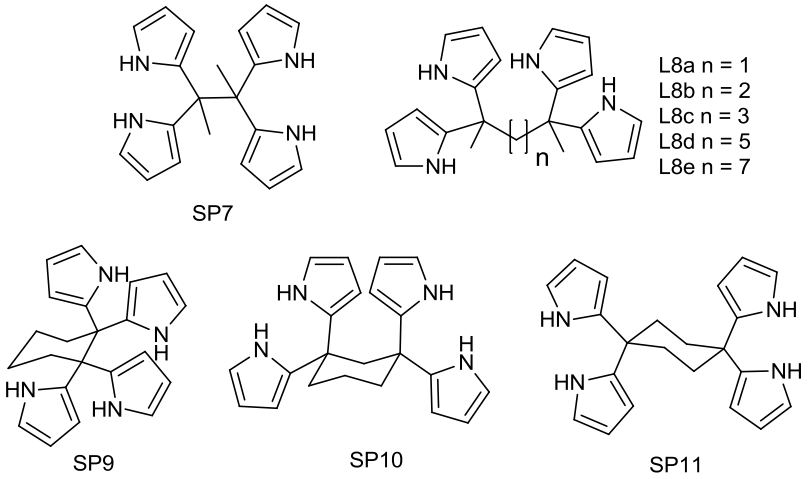

Scheme 3.6 Structure of the proposed bisDPMs.

prevents intramolecular cyclization. However, to the best of our knowledge, only two reports are available on the synthesis of divergent bisdipyrromethanes[29] and those are with rigid linkers and till date the synthesis of biscalixpyrroles is not achieved. Aware of this challenge, here we have tried to synthesize several bisDPMs by using various diketones, where the two carbonyl groups are bridged by alkyl linkers (both acyclic and cyclic type) or directly linked. Although as discussed earlier many acid catalysts can be used for the desired transformations, we mainly focused on trifluoroacetic acid (TFA) as the desired catalyst, because it reduces the formation of N-confused derivative compared to BF_3-OEt_2 and hence purification will be easier (Method A).[8a] In this case pyrrole will be employed as a solvent in order to rule out the formation of tripyrromethane and higher oligomers. The second method, we considered is the HCl catalyzed, aqueous method, owing to its environmentally benign nature. Moreover only

stoichiometric amount of pyrrole is needed in this case (Method B).[10] Subsequently, we have explored the synthesis of the targeted biscalixpyrroles.

3.3 Results and discussion

Pyrrole was distilled before use. 2,6-Heptanedione, 2,8-nonanedione and 2,10-undecanedione were synthesized by the reported procedure in literature as discussed in chapter 2.[30,31]

3.3.1 Reaction of acyclic diketones with pyrrole

The reaction of 2,3-butandione with 10 equiv. of pyrrole and 0.1 equiv. of trifluoroacetic acid (TFA) at room temperature for 5 min showed two spots in TLC. Isolation of the product by Kugelrohr distillation followed by column chromatography and ^{1}H NMR analysis revealed the presence of two methyl (-CH_3) groups at 2.13 and 1.85 ppm indicating that one acyl group remains unreacted. This was further supported by ^{13}C NMR (signal at 210.04 for the carbonyl-C), IR (stretching at 1705 cm^{-1} for carbonyl group) and mass spectroscopic analysis (m/z 202 for mono-acyldipyrromethane). *Meso*-acyldipyrromethane **SP12** was obtained as the major product (40%) instead of the desired bisDPM **SP7**. On the other hand,

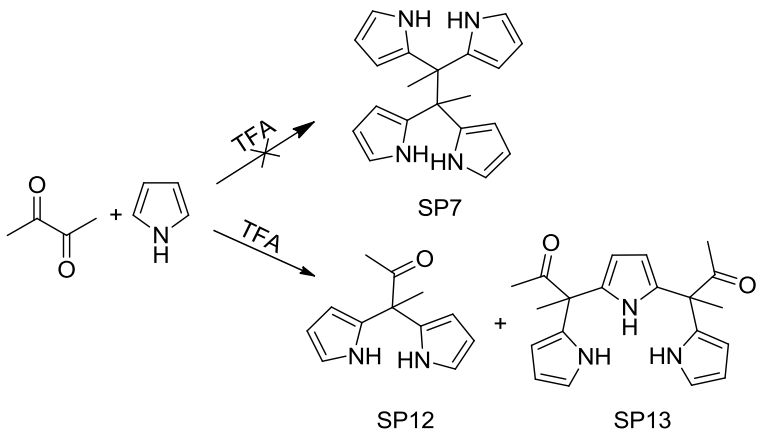

Scheme 3.7 Reaction of 2,3-butandione with pyrrole.

meso-diacyltripyrromethane **SP13** (Scheme 3.7) also formed simultaneously as the minor product (characterised by spectral analysis, further details will be discussed in next chapter). Single crystal analysis of the crystal grown by slow evaporation of ethyl acetate solution, unequivocally confirmed our assumption (Figure 3.2). The solid state structure revealed alternate orientation of the pyrrole nitrogens. To our knowledge, previously only one report was there where only one of the carbonyl functional groups of a dicarbonyl compound could be selectively converted to dipyrromethane without using any protecting group, which deals

with the conversion of a sterically rigid acenaphthenequinone to its corresponding monodipyrromethane.[32] Increasing the amount of pyrrole, upto 50 equiv. led to a slight increase in the yield of **SP12** (upto 43%), however there was no indication of formation of **SP7**. We increased the amount of pyrrole further, to 100 equiv. and the TFA to 0.25 equiv. and extended the reaction time upto 12 h. All our attempts led to an increase in the yield of

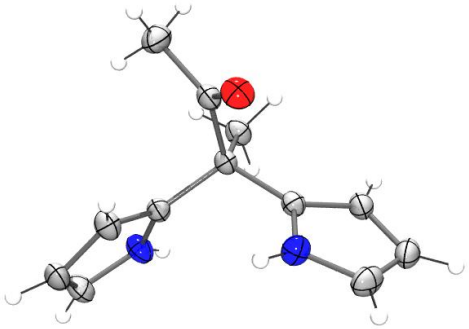

Figure 3.2 ORTEP diagram of **SP12**. Thermal ellipsoids are scaled upto 35% probability level.

SP12 only (65%) without any traces of **SP7**. Interestingly, Method B (HCl catalyzed aqueous method), produced **SP12** in higher yield (67%) as the only product. The failure of 2,3-butandione condensation with pyrrole, to form bisDPM **SP7** may be attributed to the steric restriction imposed by the two pyrrole units to the third one to react with the remaining CO group. To get rid of the steric restriction, we checked the same reaction with 2,4-pentanedione *i.e.* acetylacetone, where the two carbonyl groups were separated by a methylene moiety.

The reaction of acetylacetone with pyrrole (10 equiv.) and TFA (0.25 equiv.) as catalyst, after regular workup and purification by column chromatography over silica gel yielded a white crystalline product. However, to our surprise the ^{1}H NMR spectrum was quite complicated and the mass spectrum showed a peak at 266 (for bisDPM **SP8a** m/z 332). The

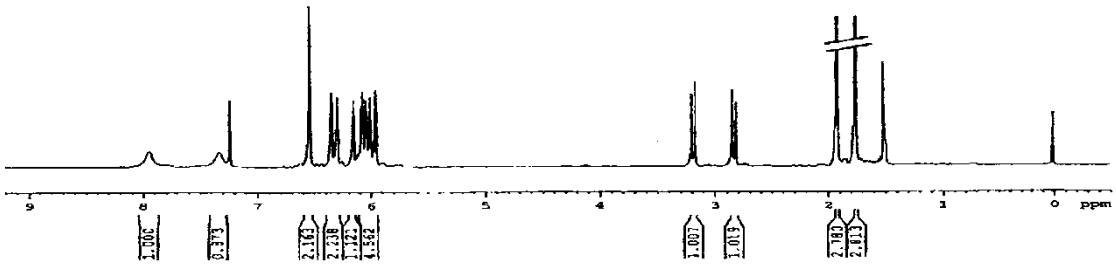

Figure 3.3 ^{1}H-NMR spectrum of the condensation product of 2,4-pentanedione with pyrrole.

^{1}H NMR showed two broad NH peaks at 7.25 and 7.95 ppm, along with eight multiplets between 5.95 and 6.54 ppm (seven with equal intensity whereas eighth one at 6.54 with approximately double the intensity than the others), apart from this there were two more symmetrical doublets at 2.83 and 3.18 ppm with J value of 3.3Hz indicating geminal coupling and two signal for the methyl groups at 1.76 and 1.92 ppm (Figure 3.3). The above result confirmed that the desired bisDPM **SP8a** has not formed and the product is quite unsymmetrical in nature. In order to ascertain the exact structure, single crystal of the compound was grown from slow evaporation of hexane:ethyl acetate (90:10) solution. While the ^{1}H NMR of the crystal confirmed the above observation, ascertaining its purity, the solid state structure obtained by single crystal X-ray diffraction (XRD) analysis (Figure 3.4) revealed unusual occurrence of ring annulation resulted in the formation of a bipyrrole moiety **SP14**, bridged via 2,3-dihydro-1H-pyrrolizine through its 1,3- position. The structure showed that the 2,3-dihydropyrrolizine unit is almost planar while the other two pyrrole units are aligned orthogonal to each other. The structure now could explain clearly the appearance of two NH signals and eight set of multiplets for pyrrolic protons in ^{1}H NMR and having molecular mass 265, also confirmed the mass analysis. To the best of our knowledge this type of ring annulation in pyrrole chemistry is unprecedented. The pyrrolizine and its derivatives were in general synthesized via multi-step reactions and these bicyclic heterocycles are

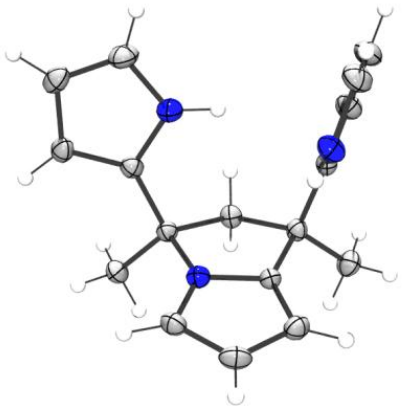

Figure 3.4 ORTEP diagram of **SP14.** Thermal ellipsoids are scaled upto 35% probability level.

present in naturally occurring alkaloids, attracting growing interest from synthetic chemists for their various biological activities.[33] Further, increasing the amount of pyrrole upto 100 equiv. and reaction time upto 12 h improved the yield of **SP14** to 33%, although formation of the desired bisDPM **SP8a** could not be realized (Scheme 3.8). Again the HCl catalyzed

reaction resulted in only compound **SP14** in 25% yield. Though the yield is moderate, but the simplicity of the synthetic method and purification and the presence of two unsubstituted pyrrole units having potential sites for necessary substitution (both at 1- and 5-positions) make this molecule attractive for further modulation.

The plausible mechanism for the formation of **SP14** is followed via the formation of dipyrromethane through the general acid catalyzed synthesis of one of the carbonyl group of acetylacetone (Scheme 3.9).

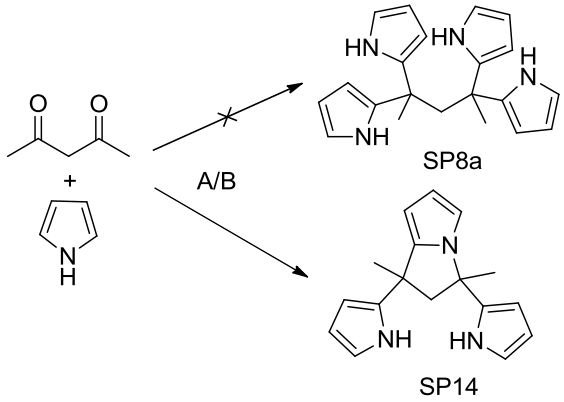

Scheme 3.8 Reaction of 2,5-pentanedione with pyrrole.

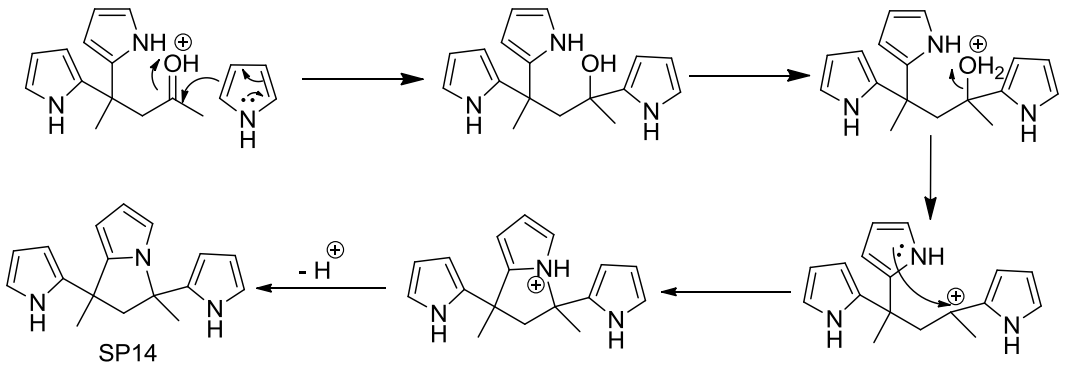

Scheme 3.9 Plausible mechanism for the formation of **SP14**.

The unexpected formation of the pyrrazoline moiety by intramolecular ring annulation increased our curiosity towards other diketones. Therefore, we started exploring the reactivity of various other diketones separated by different length of aliphatic scaffold under acidic condition. The objective was to see if the ring annulation occurred in case of 2,4-pentanedione is due to the conjugated nature of the diketone and also, if at all we can achieve the desired divergent bisDPMs. In this direction, next we explored the condensation reactions

with 2,5-hexanedione, 2,6-heptanedione, 2,8-nonanedione and 2,10-undecanedione where the carbonyl groups are separated by 2, 3, 5 and 7 -CH_2 groups respectively (Scheme 3.10).

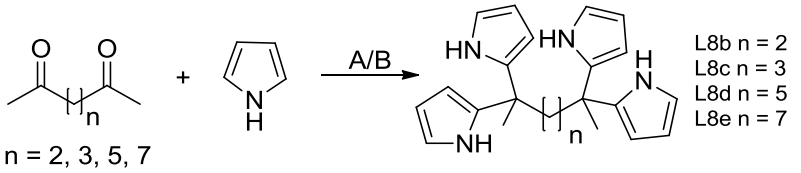

Scheme 3.10 Proposed reaction scheme.

The reaction of 2,5-hexanedione (n=2) with pyrrole in presence of TFA (0.2 equiv.) was carried out for 5 min. After regular work up, thin layer chromatographic (TLC) analysis revealed formation of many products and hence separation was very difficult. However, method B *i.e.* the aqueous method resulted in the formation of again a highly unsymmetrical compound, showing three different type of NH peaks 7.88, 7.79 and 7.62 ppm and five peaks

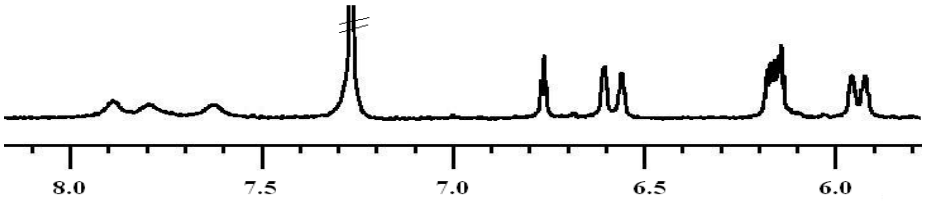

Figure 3.5 Selected protons of ^{1}H NMR of **SP15** in $CDCl_3$.

for the pyrrole protons in ^{1}H NMR spectrum (Figure 3.5) and also the observed mass spectrum (m/z 280) did not match with the desired product (m/z 346). These results, confirmed that the desired bisDPM **SP8b** has not formed. To resolve the exact structure of the compound, single crystal was grown by slow evaporation of dichloromethane and hexane

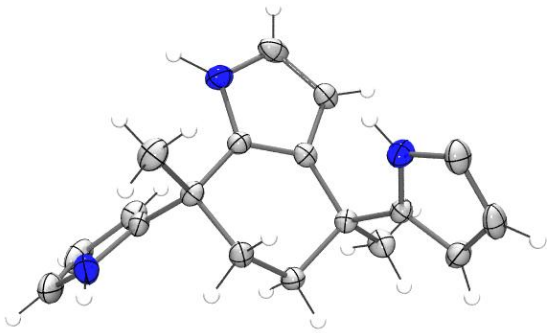

Figure 3.6 ORTEP diagram of **SP15**. Thermal ellipsoids are scaled upto 35% probability level.

solution of the compound and the solid state structure obtained by XRD analysis revealed again the occurrence of ring annulation **SP15**, like in the case of acetylacetone, however, the linking mode is different as depicted in Figure 3.6 (42%, Table 3.1, entry 3). Here the ring annulation resulted in the formation of a 4,5,6,7-tetrahydroindole ring, whose 4- and 7-positions were directly linked to the α-position of two pyrrole moieties. In **SP15**, the two pyrrole rings are located on either side of the plane of the tetrahydroindole moiety, unlike **SP14** where the two pyrrole units are located on the same side of the pyrrolizine unit. The structure now could easily explain the origin of three type of NHs in ^{1}H NMR (7.88, 7.79 and 7.62 ppm) along with other peaks at 6.75, 6.60 ppm (for the pyrrole α-Hs), 6.55, 6.15, 5.94 ppm (for the pyrrole β-Hs), 1.91-1.75 ppm (for the methylene Hs of tetrahydronindole ring), 1.62 ppm (for the methyl-Hs) and further mass data also complied with the new structure. Comparison of the TLC of this compound with the earlier mixture obtained via method A, showed the formation of **SP15** as one of the components. However, purification of the desired product was very difficult. Therefore, we tried to optimize the conditions of method A, by varying the time, quantity of acid catalyst (TFA) and also equivalents of pyrrole. Longer reaction time (12 h) led to increase in yield of **SP15** upto 50% and the product could be isolated very easily by column chromatography, which led us to conclude that the unidentified products were either undergoing interconversion (if it is an intermediate) or decomposition under the reaction condition. The obtained product was a mixture of diastereomers, (^{13}C NMR, Figure 3.7, top) from which only one diastereomer could be selectively crystallized out (in 44% yield, Figure 3.7, bottom) by dissolving the product in a minimum amount of chloroform followed by addition of few drops of hexane and keeping the resultant solution in refrigerator for overnight. Also we could able to resolve only two

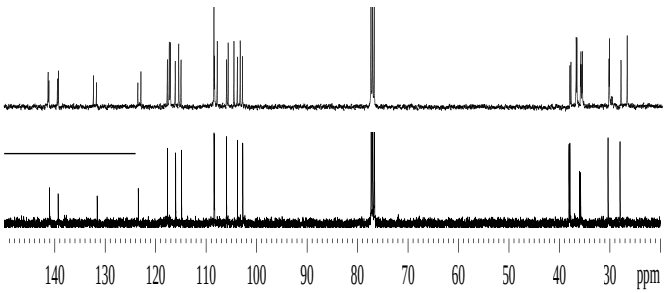

Figure 3.7 ^{13}C NMR of **SP15** in $CDCl_3$: top- mixture of diastereomers; bottom-pure diastereomer isolated by crystallization.

enantiomers in chiral HPLC, whereas the remaining two could not be achieved (Figure 3.8). By increasing the concentration of acid catalyst (upto 1 equiv.) the reaction completed in lesser time (4 h), however, the yield decreased to 44%. While increasing the amount of pyrrole upto 50 equiv. only resulted in a marginal increase in yield (51%). Further increase in the quantity of pyrrole (100 equiv.) did not alter the yield appreciably (50%). As ketone groups are less reactive compared to aldehydes, therefore the formation of larger oligopyrromethanes are less probable in our case, hence we presume, increase in pyrrole content did not alter the yield significantly. The proposed mechanism for the formation of **SP15** (Scheme 3.11) is via the formation of monocondensed DPM through the general acid catalysed condensation of one of the carbonyl group of 2,5-hexanedione.

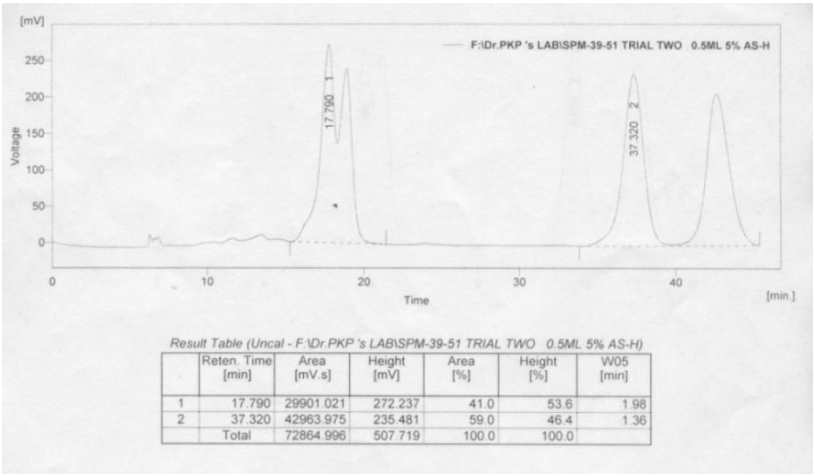

Result Table (Uncal - F:\Dr.PKP 's LAB\SPM-39-51 TRIAL TWO 0.5ML 5% AS-H)

	Reten. Time [min]	Area [mV.s]	Height [mV]	Area [%]	Height [%]	W05 [min]
1	17.790	29901.021	272.237	41.0	53.6	1.98
2	37.320	42963.975	235.481	59.0	46.4	1.36
	Total	72864.996	507.719	100.0	100.0	

Figure 3.8 HPLC profile for the separation of the diastereomers of **SP15** with DAICEL CHIRALCEL AS-H COLUMN in 5% hexane + 95% isopropanol.

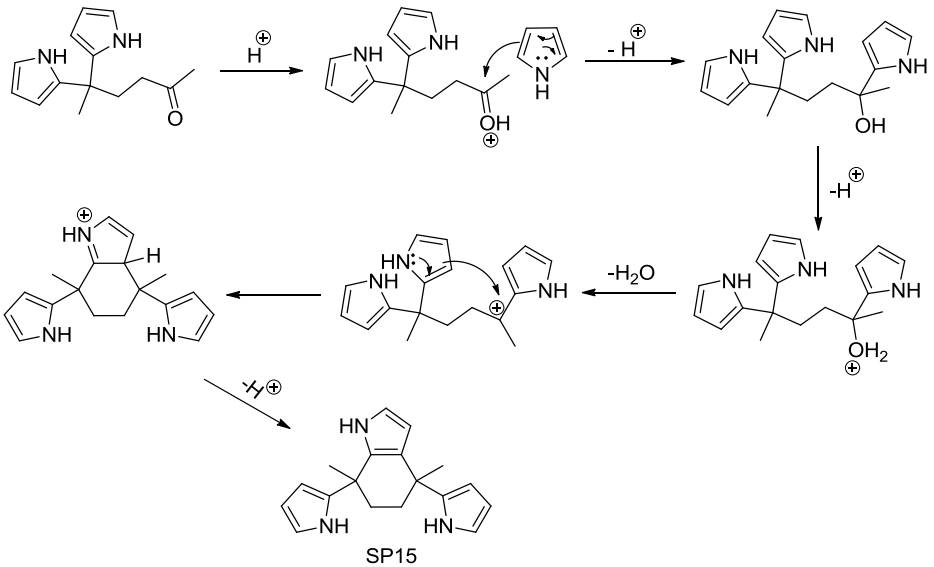

Scheme 3.11 Plausible mechanism for the formation of **SP15**.

Moreover, tetrahydroindole derivatives display a wide spectrum of biological activities: anti-implantation, hypoglycemic, anti-inflammatory, and analgesic, potent neuroleptic (*e.g.* molindone), and antitumor.[34] Tetrahydroindoles are also valuable intermediates in the synthesis of natural alkaloids such as goniomitine, arcyriacyanin A, 6,7-secoagroclavine, and chuangxinmycin, as well as synthetic drugs pindolol and highly functionalized indoles.[35] Because of their properties, synthesis of 4,5,6,7-tetrahydroindoles and their derivatives with different substitution patterns, is an exciting challenge for many chemists.[36] In our case, the selective formation of **SP15**, and the asymmetric nature of the three pyrrole units in the molecule make it an attractive building block for porphyrinoid as well as synthetic chemist.[37]

The reaction of 2,6-heptanedione with pyrrole, finally produced the desired divergent bisDPM **SP8c** via method A, in 30% yield. The reaction mixture was purified on a silica gel column to obtain the desired product as the first major fraction (the first moving minor fraction, a brown viscous oil was unstable and hence could not be characterized) and was followed by a small amount of mono-condensed product. However, method B produced many close lying spots in TLC along with little amount of product where separation becomes very difficult. **SP8c** was characterized by ^{1}H and ^{13}C NMR (shows the symmetric nature of the bisDPM) and mass spectral data and the final confirmation came from the solid state structure, obtained from a single crystal grown by slow evaporation of a chloroform solution

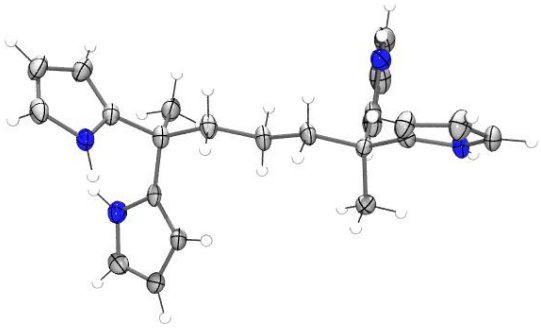

Figure 3.9 ORTEP diagram of **SP8c**. Thermal ellipsoids are scaled upto 35% probability level.

via X-ray diffraction (Figure 3.9). The divergent nature of the **SP8c** could be observed from the structure which shows that both the DPM units reside away from each other, linked via the propylene bridge and they are almost orthogonal to each other. Again, higher concentration of pyrrole (100 equiv.) resulted in slight increase in yield (34%), however the presence of a very minor quantity of mono condensed product still observed (only detected in

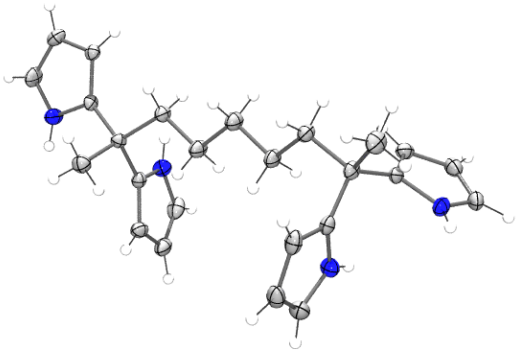

Figure 3.10 ORTEP diagram of **SP8d**. Thermal ellipsoids are scaled upto 35% probability level.

mass spectrum of the crude compound). Further, we carried out the reactions of 2,8-nonanedione and 2,10-undecanedione with pyrrole under the similar conditions and obtained the desired bisDPMs **SP8d** and **SP8e** in 57% (Table 3.1, entry 5) and 55% (Table 3.1, entry 6) respectively, following method A. The products were easily purified from the reaction mixtures by column chromatography over silica gel, which also contained a trace amount of mono condensed DPM derivative (from mass spectra). Both the compounds were characterized by ^{1}H and ^{13}C NMR and mass spectral data. Also solid state structure of **SP8d** could be obtained by single crystal XRD by growing crystals by slow evaporation of dichloromethane solution (Figure 3.10), which again confirmed the divergent nature of the dipyrromethane units in this type of bisDPMs like **SP8c**. Again higher concentration of pyrrole (100 equiv.) had very marginal effect on the yield of the products (**SP8d**: 59% and

Table 3.1 Products of reaction of different aliphatic acyclic diketones with pyrrole.

Entry	Diketones	Product	Yield	
			Method A	Method B
1	2,3-Butandione	**SP12**	65	67
2	2,4-Pentanedione	**SP14**	33	25
3	2,5-Hexanedione	**SP15**	44	42
4	2,6-Heptanedione	**SP8c**	30	-
5	2,8-Nonanedione	**SP8d**	57	-
6	2,10-Undecadione	**SP8e**	55	-

Condition A: Pyrrole (50 equiv.), TFA (0.25 equiv.), r.t., 12 h.; condition B: pyrrole (4 equiv.), conc. HCl (0.2 equiv.), H_2O, 90°C, 45 min.

SP8e: 54%) and still the presence of very minor quantity of mono condensed product could not be eradicated. Method B, once again did not result in the formation of any isolable products in either cases. These results, showed that in spite of being an environmentally benign pathway, method B is not as versatile as the Lindsey's method (method A), which could be easily modulated by changing the quantity of acid catalyst, time and quantity of pyrrole to obtain the desired product. Moreover, in case of ketones, owing to their lesser reactivity, very large excess of pyrrole is not warranted.

3.3.2 Reaction of cyclic diketones (*i.e.* cyclohexanediones) with pyrrole

The above observation increased our curiosity to study other alkyl-bridged diketones, in particular the cyclic ones. In this regard, cyclohexanediones appeared very attractive as it has three positional isomers viz., 1,2-, 1,3- and 1,4-cyclohexanedione, where the two carbonyls are present in a rigid (compared to acyclic diketones) cyclohexane scaffold. Our target was to see if we can get the desired bisDPMs (**SP9-11**) in these cases owing to the imposed steric constraint of the cyclohexane ring (Scheme 3.6). Further, we were also interested to see if ring annulation products form in these cases, similar to their acyclic congeners.

The reaction of 1,4-cyclohexanedione with pyrrole was reported by Lee and coworkers and they have successfully synthesized the bisDPM *i.e.* 1,4-bis(*α,α′*-dipyrrylmethyl)cyclohexane, **SP11** using BF_3-OEt_2 as the acid catalyst with 53% yield and additionally confirmed its structural integrity by single crystal X-ray diffraction analysis.[29a] However the solubility of **SP11** reported to be very low (soluble in DMSO only), probably limiting its utility as a building block towards synthesis of biscalixpyrrole **SP6**. We have also independently checked the reaction (also to find if any other product than the desired one forms) with TFA as the acid catalyst, which led to a slightly improved yield of the desired product **SP11** (60%). As expected the product came out as a precipitate from the reaction mixture and subsequent TLC analysis shows formation of only one product. The product was purified as reported and the analytical data matched with that of Lee's. This clearly indicates that owing to the imposed steric constraints, the cyclic diketone (*i.e.*1,4-cyclohexanedione) behaves differently than the analogous acyclic 2,5-hexanedione.

However, the reaction of 1,3-cyclohexanedione with pyrrole using our modified Lindsey method revealed the formation of four products in TLC analysis. After regular work up and isolation of the products by column chromatography (5% ethyl acetate in hexane as eluent), and subsequent detailed spectroscopic analysis revealed formation of the desired bisDPM

SP10 along with the mono-condensed product (second and third most nonpolar compound on TLC, Figure 3.11b and 3.11c respectively). The formation of both 1,3-bis(*α*,*α*'-dipyrrylmethyl)-cyclohexane **SP10** and 3-(*α*,*α*'-dipyrrylmethyl)cyclohexanone **SP16** (Scheme 3.12), clearly indicated that 1,3-cyclohexanedione is less reactive compared to its 1,4-isomer. On the other hand, the first and the fourth fractions could not be characterized on the basis of

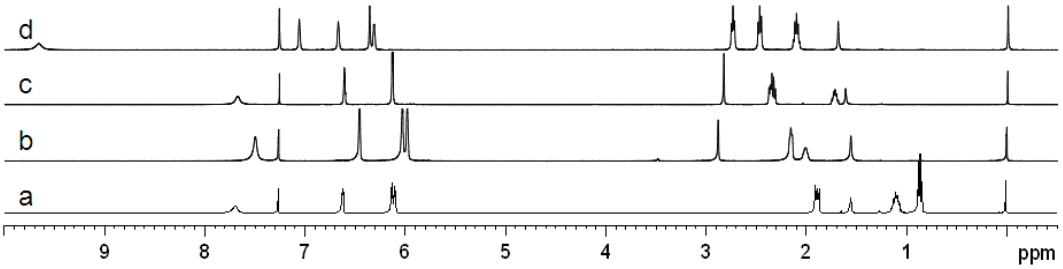

Figure 3.11 ^{1}H NMR spectra of the column purified fractions of reaction of 1,3-cyclohexanedione and pyrrole: (a) first, (b) second, (c) third and (d) fourth fraction in increasing order of polarity obtained during the condensation of 1,3-cyclohexanedione with pyrrole.

their ^{1}H NMR (Figure 3.11) and mass data (m/z = 230 and 161 respectively), although the formation of ring annulated products could be ruled out owing to the relatively simple nature of the proton NMR spectra. For example, the compound obtained as the first fraction (least polar), does not possess the characteristic bridging methylene signal (between the two dipyrromethane units) about 2.6 ppm in ^{1}H NMR, with concomitant upfield shift of all the aliphatic signals, indicating clearly the loss of cyclohexane integrity (Figure 3.11a). On the other hand, for the fourth fraction (most polar), the appearance of a new peak at ~7.1 ppm with concomitant large downfield shift of the NH signal to 10.55 ppm (Figure 3.11d) and ^{13}C signals at 200.08 and 151.11 ppm along with five more signals between 130.07 to 110.87

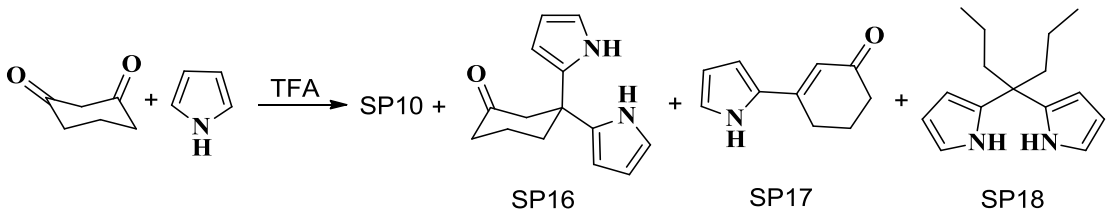

Scheme 3.12 Reaction of 1,3-cyclohexanedione with pyrrole.

ppm led us to infer at least presence of a carbonyl group and possibly some extended conjugation. Subsequent IR analysis showed the presence of two stretching frequencies at 1589 and 1643 cm^{-1}, confirming the presence of carbonyl group along with conjugation. From literature, we found Marinelli *et al.* reported the formation of 2-alkenylpyrroles upon reaction of 1,3-dicarbonyl compounds with pyrroles, using $AuBr_3$-AgOTf as a catalyst (rather expensive).[38] Our data matched with compound **SP17** (Scheme 3.12) as the probable product. To resolve the exact structure of the compounds, single crystals were grown for all the

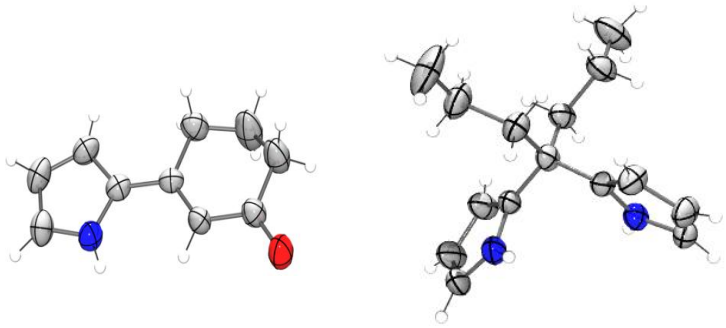

Figure 3.13 ORTEP diagram left: **SP17**, right: **SP18**. Thermal ellipsoids are scaled to the 25% probability level.

compounds and their structures were elucidated by XRD analysis. Solid state structures (obtained from ethyl acetate and hexane mixture) revealed the formation of 2-alkenylpyrrole derivative **SP17**, namely 3-(1H-pyrrol-2-yl)cyclohex-2-enone as the most polar fraction and accompanied with unexpected formation of 5,5-dipropyldipyrromethane **SP18** as the most nonpolar fraction, albeit as a very minor product (Figure 3.13). Subsequently the NMR, IR and mass data could be assigned appropriately for compound **SP17** and **SP18**. Since many biologically active compounds and natural products possess pyrrole as an important constituent, therefore this type of transition metal free and cost effective direct C-C bond formation reaction will be quite interesting for future investigations.[39] The highly unexpected formation of **SP18**, where ring opening of the cyclohexyl group takes place with concomitant addition of a sp^3-C, led us to check the purity of the starting material (obtained from Sigma Aldrich, USA). We subjected the starting material for further purification by recrystallization from hot benzene and separately by sublimation and then carried out the reactions. However, in both cases formation of compound **SP18** was still observed. This led us to conclude that during the course of the reaction, ring opening of 1,3-cyclohexanedione with concomitant addition of a sp^3-carbon takes place whose source and the mechanism of formation is beyond

Table 3.2 Yield of the products from the condensation of 1,3-cyclohexanedione with pyrrole (equiv. w.r.t. diketone) under different reaction conditions.

Entry	Pyrrole	Catalyst	Condition	% Yield			
				SP10	**SP16**	**SP17**	**SP18**
1	40	TFA, 0.025	rt, overnight	9	16.6	23.4	2
2	100	TFA, 0.25	rt, overnight	13	17.8	15	1.8
3	100	TFA, 1	rt, overnight	14.5	19.8	33	2.2
4	100	TFA, 1	rt, 50 h	17.3	26.7	27	1.4
5	100	TFA, 1	60°C, 6 h	39.8	22.2	10	2.2

our comprehension at this stage. We tried to modulate the reaction conditions in order to optimize the yield for compound **SP10**. All our attempts using TFA as catalyst, under various conditions resulted in the formation of all the four products (Table 3.2). On the other hand, we could enhance the yield of **SP10** up to 40% by slightly varying the reaction condition (Table 3.2, entry 5). Use of further excess of pyrrole did not led to any appreciable change in yield. On the other hand, use of $BF_3.OEt_2$ (pyrrole as a solvent) and conc. HCl (H_2O as a solvent)[10] as catalysts resulted in drastically decreased yield of **SP10** (6 and 5% respectively).

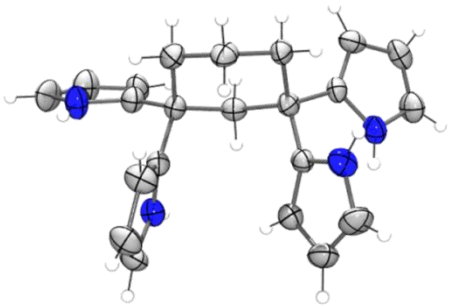

Figure 3.14 ORTEP diagram of compound **SP10**. Thermal ellipsoids are scaled upto 35% probability level.

The solid state structure of compound **SP10** displayed the existence of the cyclohexyl ring in chair conformation, with the two pyrrole units of each dipyrromethane residing in alternate conformation (Figure 3.14). Therefore, we could conclude that the cyclohexyl ring imposes sufficient steric restriction to rule out any intramolecular ring annulation as observed

in case of the acyclic analogue, acetylacetone and hence could favour the formation of bisDPM. Again this also confirmed that the ring annulation obtained in case of acetylacetone, is not a general phenomenon. While trying to grow single crystals for compound **SP16**, we obtained two polymorphic structures in Pbca (polymorph 1 by fast solidification of the dense liquid obtained from column chromatography) and Pbcn (polymorph 2 by slow evaporation of ethyl acetate solution) space group. In both the structures the two pyrrole units adopt alternate orientation (Figure 3.15).

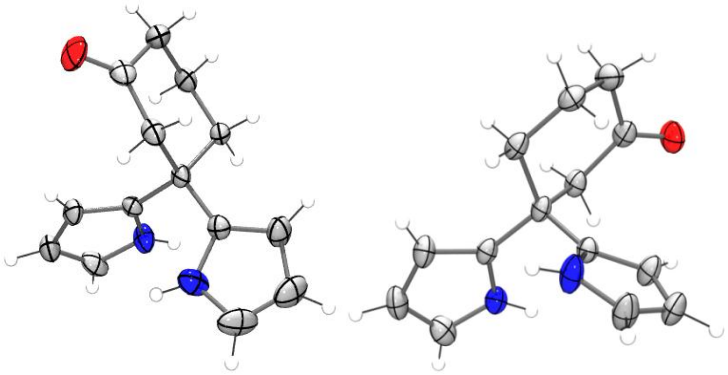

Figure 3.15 ORTEP diagram of compound **SP16** (Left: Polymorph-1, Right: Polymorph-2). Thermal ellipsoids are scaled upto 25% probability level.

The crystal structure revealed, polymorph 1 contains two molecules in the asymmetric unit (z′=2), where one of the molecule in the asymmetric unit formed a 1D linear chain along [100] axis via intermolecular N-H···O hydrogen bond between the pyrrole NH and cyclohexanone O atom (Figure 3.16, top). The second pyrrole NH group remained independent of any weak bond interactions owing to its inward orientation with torsion angle of 37.61° w.r.t. the other pyrrole moiety. On the other hand, the second molecule present in the asymmetric unit adopted a more open conformation (Figure 3.16, bottom), where the two pyrrole rings are exposed outward. The resultant steric flexibility led to the formation of N-H···O dimeric motif between the cyclohexanone O and pyrrolic NH of two adjacent molecules and vice versa. Moreover, the O atom of the cyclohexanone molecule is bifurcated, connecting another neighbouring dimer. Thus it formed a dimer layer parallel to (001) plane. In the three dimensional structure of polymorph 1, the two different type of hydrogen bonded packing patterns of the two molecules in the asymmetric unit (layers and the 1D chain), packed in alternate fashion forming ABAB stacks connected to each other via weak van der Waal forces (Figure 3.17).

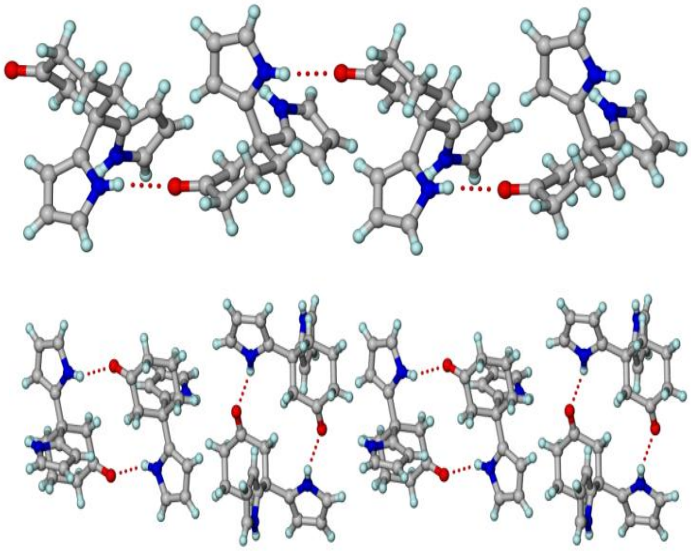

Figure 3.16 Crystal packing diagram of polymorph 1 of compound **SP16** showing two independent hydrogen bonding motifs by the molecule in the asymmetric unit. Top: Linear chain along [100] axis; bottom: dimer layer parallel to (001) plane. Colour code: red: O, Blue: N, Grey: C, Aqua: H.

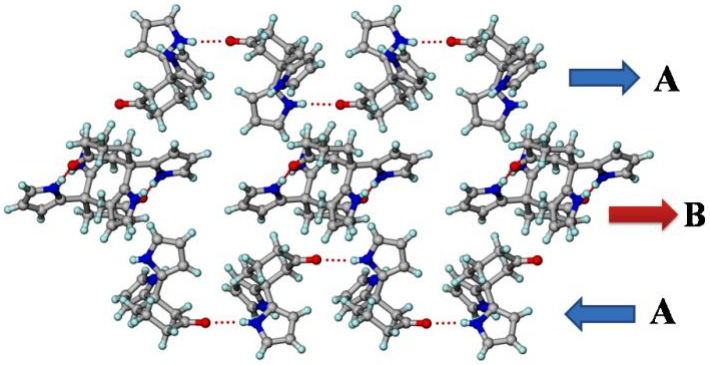

Figure 3.17 Crystal packing diagram of polymorph 1 of compound **SP16** in three dimension showing ABAB pattern.

In polymorph 2, only one molecule is there in the asymmetric unit and formed a dimeric motif via N-H···O hydrogen bonds, somewhat like that observed in case of polymorph **1**. However, the NH group of the second pyrrole ring, through N-H···π interaction with the pyrrole ring of adjacent molecule results in a herringbone type motif (Figure 3.18). This results showed that the desired bisDPM **SP10** could be obtained up to 40% yield in case of 1,3-cyclohexanedione, which is contradictory to the linear diketones and this consequently inferred that either the formation of bisDPM or the ring annulation, could not be justified as a

general phenomenon and depends on the structural disposition of the carbonyl groups.

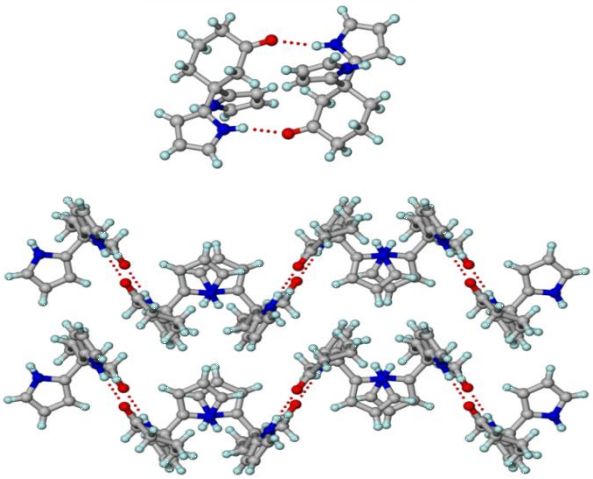

Figure 3.18 Crystal packing diagram of polymorph 2 of compound **SP16** showing dimeric H-bonding motif (top) and herringbone motif in 3D (bottom).

The above observations provoked us to explore the reactivity of 1,2-cyclohexanedione with pyrrole under similar condition, in anticipation to see if bisDPM **SP9** is formed, which are yet to be realized in case of the acyclic analogue (2,3-butandione). The reaction of 1,2-cyclohexanedione with pyrrole using TFA as catalyst, revealed the formation of three close lying products (by TLC). The products were isolated by column chromatography using 5% ethyl acetate in hexane. Initial ^{1}H NMR spectral analysis (Figure 3.19), excludes the formation of bisDPM, while indicating the formation of some unusual products. The ^{1}H NMR of the second fraction was quite simple to analyse and it resembled with 2-(*α*,*α*'-dipyrrylmethyl)cyclohexanone **SP19** (Scheme 3.13). This was also supported by LCMS data (m/z 228). Subsequent solid state structure obtained by XRD analysis, unequivocally

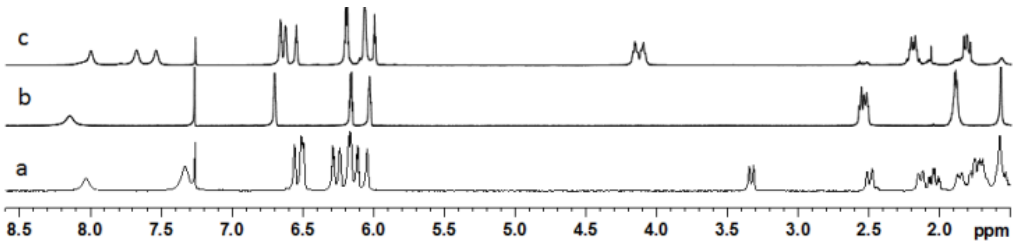

Figure 3.19 ^{1}H NMR spectra of the column purified fractions obtained during the reaction between 1,2-cyclohexanedione and pyrrole: (a) first, (b) second, and (c) third fraction in increasing order of polarity.

ascertained the mono-condensed product **SP19**, which showed similar alternate orientation of the pyrrole units, like other dipyrromethanes (Figure 3.20). On the other hand the ^{1}H NMR spectrum of the first fraction (least polar one) was quite complicated (Figure 3.19) and the mass spectrum showed a peak at m/z 279. The ^{1}H NMR spectrum exhibited two broad NH resonances at 8.03 and 7.32 ppm with 1:2 ratio respectively, along with seven multiplets between 6.6 and 6.0 ppm with intensity ratio of 1:2:1:1:2:1:1. The presence of three NHs and

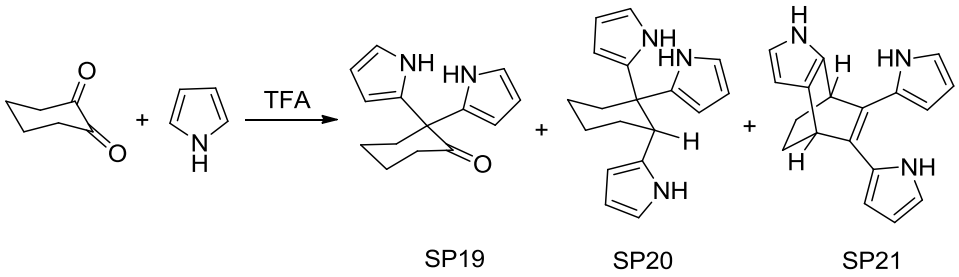

Scheme 3.13 Reaction of 1,2-cyclohexanedione with pyrrole.

nine *β*-CHs, excluded any possibility of ring annulation. Besides, a multiplet (*dd*) at 3.34 ppm corresponding to one proton signal and five multiplets between 2.50-1.73 ppm with intensity ratio of 1:1:1:1:4 were observed. Subsequent DEPT-135 experiments indicated that among the eighteen chemically different carbons, there are three quaternary carbons in the aromatic region (again excludes any possibility of annulation) and one in the aliphatic region. In addition, it showed four negative and one positive polarized peak in the aliphatic region indicating the presence of four CH_2, where the protons are diastereomeric in nature and a CH proton. The above observation prompted us to propose the structure as a tripyrrole derivative,

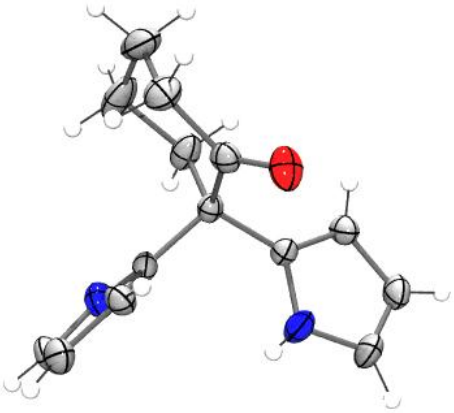

Figure 3.20 ORTEP diagram of compound **SP19**. Thermal ellipsoids are scaled upto 35% probability level.

α,*α*',*α*''-(cyclohexane-1,1,2-triyl)tris(1H-pyrrole) **SP20** (Scheme 3.13). In order to ascertain the exact structure, single crystal was grown from slow evaporation of the chloroform solution and the solid state structure obtained via XRD, unequivocally confirmed the presumed structure (Figure 3.21).

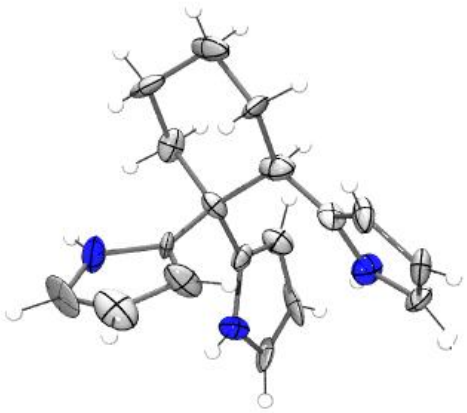

Figure 3.21 ORTEP diagram of compound **SP20**. Thermal ellipsoids are scaled upto 35% probability level.

On the other hand, the ^{1}H NMR spectrum of the third major fraction (most polar one), showed three different NH peaks at 7.99, 7.80 and 7.68 ppm with intensity ratio of 1:1:1 along with five peaks corresponding to eight pyrrole CH protons between 6.66-5.99 ppm with intensity ratio of 2:1:2:2:1 (Figure 3.19). The absence of one *β*-CH signal and the presence of three NHs led us to presume the probable presence of ring annulation occurring via *α*/*β*-CH as observed in case of acyclic diketones. Moreover, there are three multiplets at

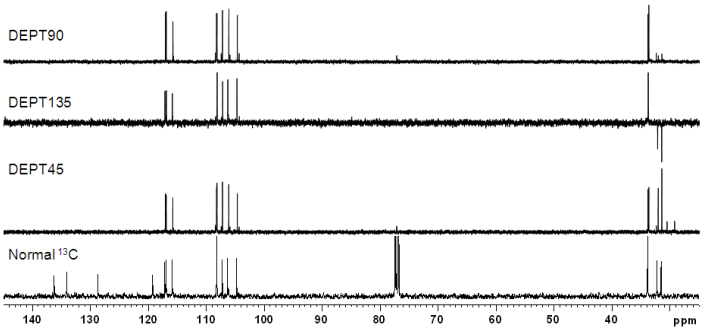

Figure 3.22 DEPT spectra of **SP21** in $CDCl_3$.

4.13, 2.20 and 1.82 ppm corresponding to two protons each. Interestingly, the DEPT study revealed the presence of two CH_2 and two CH groups (Figure 3.22). These experiments led

us to two probable structures for this compound (Scheme 3.14). Subsequent elemental analysis indicated the molecular formula as $C_{18}H_{17}N_3$. Unfortunately mass spectroscopy did

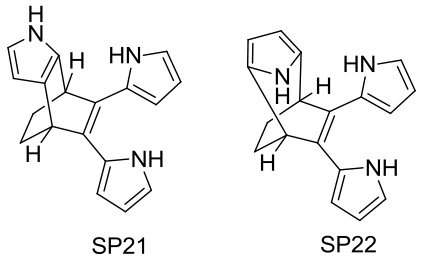

SP21 SP22

Scheme 3.14 The two probable structures for the third fraction obtained during the reaction of 1,2-cyclohexanedione with pyrrole.

not give any conclusive data (m/z value calculated 275, found 250) and this may be resulted owing to the possible instability of the ring annulated compound in the LCMS and HRMS operating conditions. All attempts to obtain single crystal for this compound remain unsuccessful so far. Therefore, to ascertain the final confirmation about the structure, 2D NMR experiments were performed. ^{1}H-^{1}H COSY shows that the protons at 4.13 ppm are coupled with the 2.20 and 1.82 ppm peaks. In addition the two peaks at 2.20 and 1.82 ppm are also coupled. Subsequent NOESY experiment showed strong NOE between the proton at 4.13, 2.20 and 1.82 ppm (Figure 3.23). These observations led us to conclude that these protons are adjacent to each other and the peak at 2.20 and 1.82 ppm may be an ensemble of two diastereomeric protons. This assumption was further confirmed by ^{1}H-^{13}C COSY which shows two cross peaks for each carbon at 2.20 and 1.82 ppm. The presence of the two diastereomeric protons rules out the possibility of **SP22** and confirmed the structure as pyrrole substituted bicyclic dihydroindole **SP21**. IR spectroscopy lends further credence to our structure by showing a weak stretching frequency at 1707 cm^{-1}, which may be assigned to the *endo* double bond. This clearly indicated that unlike 2,3-butandione, the reaction of 1,2-cyclohexanedione with pyrrole resulted in two unusual (including one ring annulated product), however interesting products (Scheme 3.13) whose mechanism of formation so far not understood by us. Further, the reaction at milder condition (*i.e.* at room temperature with 0.25 equiv. of TFA), displayed the formation of all the three products at different time interval (TLC analysis) and hence ruled out their possible formation, under only harsh condition.

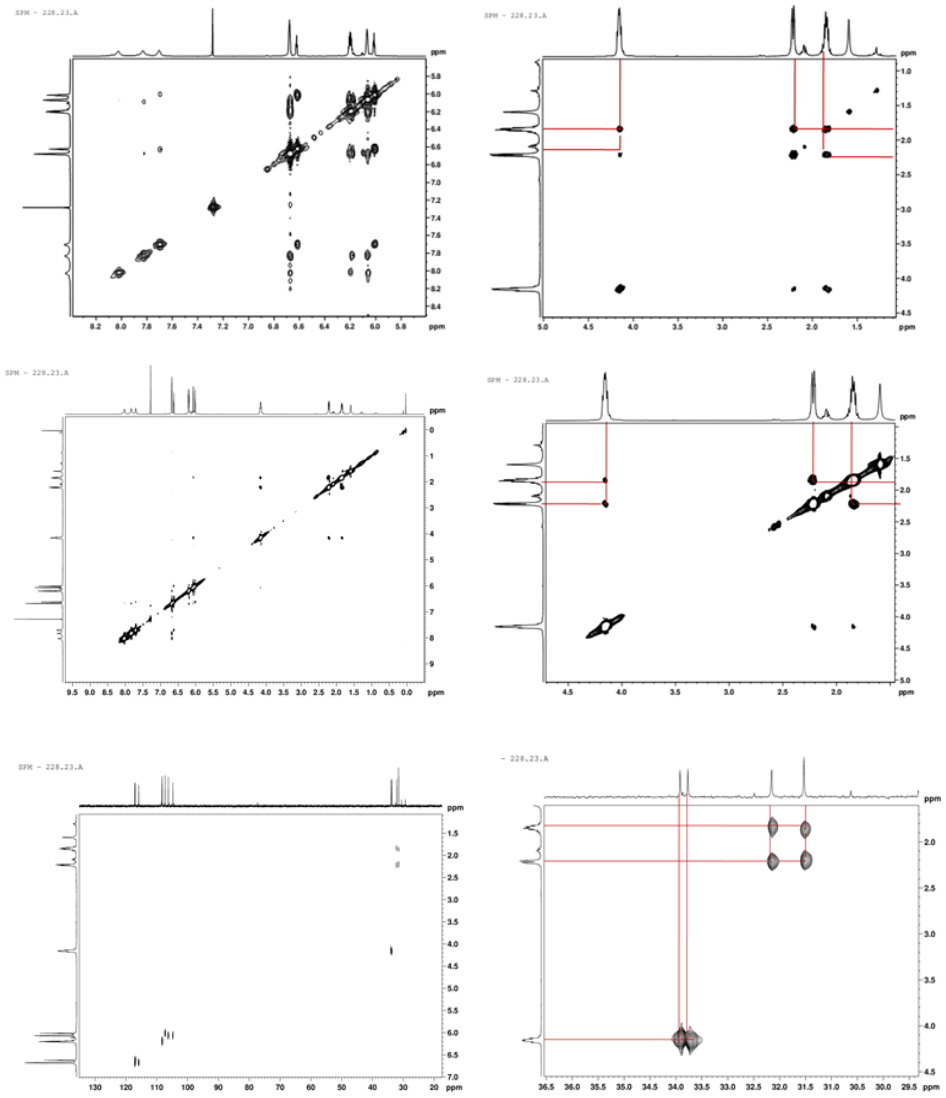

Figure 3.23 Different 2D NMR spectra of **SP21** in $CDCl_3$ top: ^1H-^1H COSY; middle: ^1H-^1H NOESY and bottom: ^1H-^{13}C COSY.

3.3.3 Reaction of Bisdipyrromethanes

The bisDPMs obtained from acyclic diketones (**SP8c-e**) were subjected to self-condensation in presence of acetone using various catalysts like $BF_3.OEt_2$, TFA, MSA, along with template type acid catalyst like terephthalic acid and so far remain unsuccessful in providing the desired biscalix[4]pyrroles. Similarly, the cyclohexane based bisDPM **SP10-11** when subjected to either self-condensation or with other dipyrromethanes (2 equiv.) in acetone using the abovementioned acid catalysts, so far did not yield any desired biscalix[4]pyrroles. However, still efforts are underway in this direction, in our laboratory to achieve the goal.

3.4 Conclusion

In conclusion, we have demonstrated the reactivity of different types of aliphatic diketones (acyclic and cyclic) with pyrrole under acidic conditions. In case of acyclic diketones, bisDPM could be achieved when the two carbonyl groups are apart with a minimum propylene unit. While among the cyclic diketones the 1,4-isomer appears to be most reactive, the 1,2-isomer displays least reactivity (absence of the formation of bisDPM). Moreover, several interesting and unusual products were isolated and characterized mostly by XRD analysis. The outcome of the reactions is shown below (Figure 3.24 and 3.25).

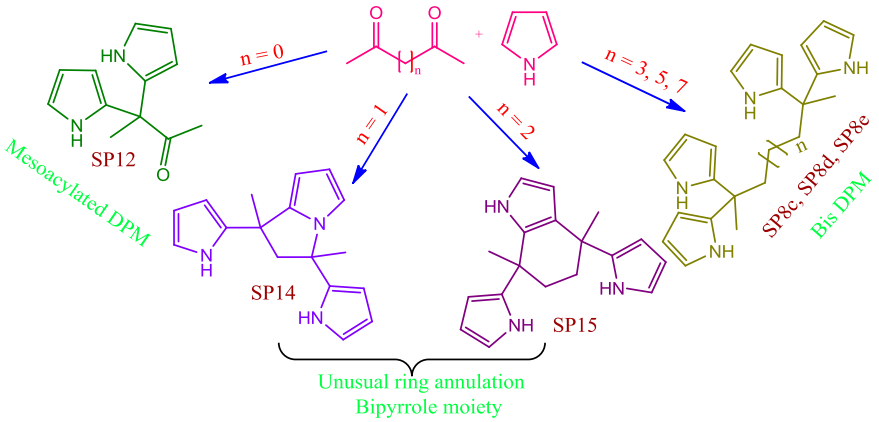

Figure 3.24 Pictorial representation of the outcome of the reaction of acyclic diketones with pyrrole under acidic condition.

Shorter linear aliphatic diketones viz. 2,4-pentanedione and 2,5-hexanedione yield ring annulated products, whereas smallest one (2,3-butandione) results in monocondensed product. The selective formation of **SP14** and **SP15** and the asymmetric nature of the three pyrrole units in the molecule may find its use as an interesting building block in porphyrinoid chemistry. On the other hand **SP8c-e** can be used as building block towards the synthesis of biscalixpyrroles and other related macrocycles. The use of **SP12** and **SP13** as a building blocks towards functionalized calix[4]pyrrole is described later in the fourth chapter.

Further, we could find a simple strategy to obtain 3-(1H-pyrrol-2-yl)cyclohex-2-enone **SP17**, which may provide a new route towards the transition metal free C-C bond formation

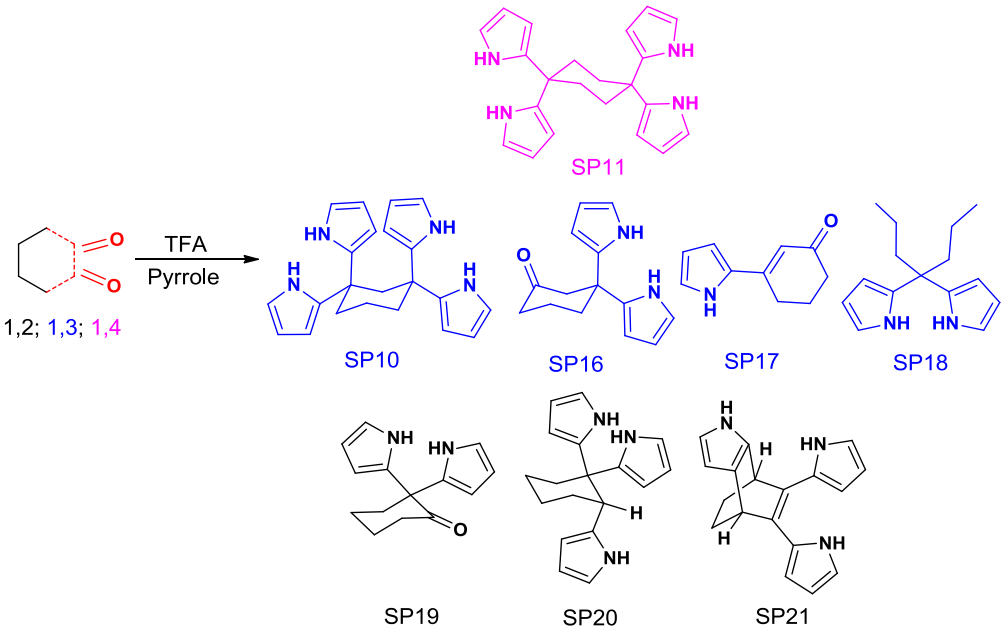

Figure 3.25 Pictorial representation of the outcome of the reaction of different isomers of cyclohexanedione with pyrrole under acidic condition.

reaction. The surprising formation of 5,5-dipropyldipyrromethane **SP18** (from 1,3-cyclohexanedione), the tripyrrole derivative **SP20** and the pyrrole substituted bicyclic dihydroindole **SP21** (from 1,2-cyclohexanedione) will be of greater interest in order to understand their mechanism. In addition we have reported two polymorphic structures of compound **SP16** and to the best of our knowledge this is the first report in literature regarding the different form of dipyrromethane derivatives in the solid state.

In summary, the reaction of pyrrole with ketone (in particular diketones) cannot be generalized. Recently Thompson *et al.* reported the reaction of substituted pyrroles with acetone and they found several annulated bispyrrole derivatives.[40] This led us to the conclusion that the reaction is dependent on the nature of the ketone as well as the pyrrole. Again the conversion of bisDPMs towards the targeted biscalix[4]pyrroles emerged as a more challenging job than anticipated.

3.5 Experimental Details

2,6-heptanedione and 2,8-nonanedione were prepared by reported method described in chapter 2.[32,33]

3.5.1 Synthesis of 2,10-undecanedione

1.6 M *n*-BuLi (32 mL, 58 mmol, 2.2 equiv.) was added to a solution of N,N-dimethyl hydrazone (7.2 mL, 52 mmol, 2 equiv.) in THF (200 mL) at -5 °C, under N_2 atmosphere and the mixture was stirred for 1 h. 1,5-Dibromopentane (3.6 ml, 26 mmol, 1 equiv.) was added at -5 °C and the reaction mixture was stirred for 15 h at room temperature, then 2M HCl (200 mL) was added and left standing for 15 h. The reaction mixture was diluted with water and extracted with ethyl acetate. The compound was purified over a silica gel column, using ethyl acetate:hexane (30:70) as the eluent. Evaporation of the eluent afforded the desired product as white oil (2.8 g) which solidifies on keeping at low temperature.

Yield: 52 %; Melting point: < 40 °C; ^{1}H NMR (400 MHz, $CDCl_3$): δ in ppm δ 2.41 (m, 4H, CH_2), 2.13 (s, 6H, CH_3), 1.55 (m, 4H, CH_2), 1.28 (s, 6H, CH_2); ^{13}C NMR (100 MHz, $CDCl_3$): δ in ppm 209.16, 43.64, 29.80, 29.08, 28.88, 23.65; LCMS m/z calcd. for $C_{11}H_{20}O_2$ (M+H) 185, found 185; Elemental analysis calcd. for $C_{11}H_{20}O_2$ C: 71.70; H: 10.94; found C: 71.45; H: 11.02.

3.5.2 General procedure for reaction of acyclic diketones with pyrrole

Method A:

Pyrrole (50 equiv.), diketone (1 equiv.) and TFA (0.25 equiv.) was stirred for 12 h under N_2 atmosphere. The reaction mixture was quenched by adding excess triethylamine. The excess pyrrole was removed by heating the mixture at ~70-80 ^{o}C under reduced pressure. The product was purified by column chromatography over silica gel.

Method B:

To a solution of diketone (1 equiv.) in boiling water, conc. HCl (1 equiv.) were added, followed by dropwise addition of pyrrole (4 equiv.). After refluxing for 45 min, the suspension was left to cool and then neutralized with 10 % aq. $NaHCO_3$. The compound was extracted with ethyl acetate, dried with anhyd. Na_2SO_4 and concentrated under reduced pressure. The crude product was purified by column chromatography using silica gel.

3,3-Di(1H-pyrrol-2-yl)butan-2-one (SP12)

The product was purified by distillation under reduced pressure (temperature ~ 150 ^{o}C) followed by column chromatography using ethyl acetate in hexane (20:80).

Yield: 43% (method A), 67% (method B); Melting point: 72-74 °C; FTIR Data (KBr) - 3362, 1705 cm^{-1}; ^{1}H NMR (in $CDCl_3$, 400MHz): δ in ppm 8.45 (br s, 2H, NH), 6.74 (s, 2H, α-CH), 6.18 (s, 2H, β-CH), 6.06 (s , 2H, β-CH), 2.13 (s, 3H, CH_3), 1.85 (s, 3H, CH_3); ^{13}C

NMR (in $CDCl_3$, 100MHz): δ in ppm 210.04, 132.34, 118.07, 108.35, 106.82, 52.75, 26.60, 25.10; LCMS m/z calcd. for $C_{12}H_{14}N_2O$ (M+H) 203, found 203; Elemental analysis for $C_{12}H_{14}N_2O$ calcd. C: 71.26, H: 6.98, N: 13.85; found C: 71.42, H: 6.93, N: 13.96.

3,3'-(1H-pyrrole-2,5-diyl)bis(3-(1H-pyrrol-2-yl)butan-2-one) (SP13)

Melting point: 126-128 °C; FTIR Data (KBr) - 3736.7, 3392.1, 1703.6 cm^{-1}; ^1H NMR (in $CDCl_3$, 400 MHz): δ in ppm 8.49-8.69 (br m, 3H, NH), 6.74 (s, 2H, α-CH), 6.16 (m, 2H, β-CH), 5.95-6.01 (m, 4H, β-CH), 2.10 (s, 3H, CH_3), 1.81 (s, 3H, CH_3); ^{13}C NMR spectrum (in $CDCl_3$, 100 MHz): δ in ppm 209.67, 132.81, 132.08, 118.05, 108.46, 106.83, 106.76, 52.66, 26.53, 25.00; LCMS m/z calcd. for $C_{20}H_{23}N_3O_2$ (M-H) 336, found 336; Elemental analysis for $C_{20}H_{23}N_3O_2$ calcd. C 71.19, H 6.87, N 12.45; found C 71.28, H 6.76, N 12.56.

1,3-Dimethyl-1,3-di(1H-pyrrol-2-yl)-2,3-dihydro-1H-pyrrolizine (SP14)

The product was purified by column chromatography using ethyl acetate in hexane (10:90) as eluent and further recrystallized from ethyl acetate and hexane mixture (10:90).

Yield: 33% (method A), 25% (method B); Melting point: 156-158 °C; ^1H NMR (in $CDCl_3$, 400MHz): δ in ppm 7.95 (br s, 1H), 7.32 (br s, 1H), 6.53 (m, 2H), 6.34 (m, 1H), 6.29 (m, 1H), 6.14 (m, 1H), 6.07 (m, 1H), 6.04 (m, 1H), 6.00 (m, 1H), 5.95 (m, 1H), 3.18 (d, 1H, J= 3.3 Hz), 2.83 (d, 1H, J= 3.3 Hz), 1.92 (s, 3H), 1.76 (s, 3H); ^{13}C NMR (in $CDCl_3$, 100MHz): δ in ppm 140.66, 138.35, 135.74, 117.81, 116.22, 113.14, 111.73, 109.16, 107.82, 104.82, 103.77, 98.48, 60.97, 60.86, 41.65, 30.32, 28.70; LCMS m/z calcd. for $C_{17}H_{20}N_3$ (M+H) 266, found 266; Elemental analysis for $C_{17}H_{20}N_3$ C: 76.95, H: 7.22, N: 15.84; found C: 76.99, H: 7.17, N: 15.84.

4,7-Dimethyl-4,7-di(1H-pyrrol-2-yl)-4,5,6,7-tetrahydro-1H-indole (SP15)

The product was purified by column chromatography using ethyl acetate in hexane (30:70) as eluent and further recrystallized from chloroform and hexane mixture (50:50).

Yield: 44% (method A), 42 % (method B); Melting point: 206-208 °C; ^1H NMR (in $CDCl_3$, 400MHz): δ in ppm 7.88 (s, 1H, NH), 7.79 (s, 1H , NH) , 7.62 (s, 1H , NH), 6.75 (t, 1H, J = 2.8 Hz), 6.60 (d, 1H, J = 1.6 Hz), 6.55 (d, 1H, J = 1.6 Hz), 6.15 (m, 3H), 5.94 (m, 2H), 1.91-1.75 (m, 4H, CH_2), 1.62 (s, 6H, CH_3); ^{13}C NMR (in $CDCl_3$, 100MHz): δ in ppm 141.0, 139.3, 131.6, 123.5, 117.6, 116.0, 114.8, 108.4, 108.2, 105.9, 103.7, 102.7, 38.1, 37.9, 36.0, 35.7, 30.4, 28.0; LCMS m/z calcd. for $C_{18}H_{22}N_3$ (M+H) 280, found 280; Elemental analysis calcd. for $C_{18}H_{22}N_3$ C: 77.38, H: 7.58, N: 15.04; found C: 77.31, H: 7.62, N: 15.12.

2,2',2'',2'''-(Heptane-2,2,6,6-tetrayl)tetrakis(1H-pyrrole) (SP8c)

The product was purified by column chromatography using dichloromethane and further recrystallized from methanol.

Yield: 30%; Melting point: 148-150 °C; ^{1}H NMR (in $CDCl_3$, 400MHz): δ in ppm 7.69 (br s, 4H, NH), 6.60 (s, 4H, α-CH), 6.12 (s, 4H, β-CH), 6.00 (s , 4H, β-CH), 1.88 (t, 4H, J = 8 Hz, CH_2), 1.49 (s, 6H, CH_3), 1.17 (m, 2H, CH_2); ^{13}C NMR (in $CDCl_3$, 100MHz): δ in ppm 138.23, 116.96, 107.65, 104.52, 41.45, 39.03, 26.40, 19.40; LCMS m/z Calcd. for $C_{23}H_{28}N_4$ (M+H) 360, found 360; Elemental analysis calcd. for $C_{23}H_{28}N_4$ C: 76.63, H: 7.83, N: 15.54; found C: 76.63, H: 7.84, N: 15.87.

2,2',2'',2'''-(Nonane-2,2,8,8-tetrayl)tetrakis(1H-pyrrole) (SP8d)

The product was purified by column chromatography using dichloromethane and further recrystallized from methanol.

Yield: 57%; Melting point: 168-170 °C; ^{1}H NMR (in $CDCl_3$, 400MHz): δ in ppm 7.72 (s, 4H, NH), 6.60 (s, 4H, α-CH), 6.12 (m, 4H, β-CH), 6.04 (t, 4H, β-CH, J = 8Hz), 1.87 (m, 4H, CH_2), 1.55 (s, 6H, CH_3), 1.33-1.20 (m, 6H, CH_2); ^{13}C NMR (in $CDCl_3$, 100MHz): δ in ppm 138.18, 116.86, 107.69, 104.46, 41.22, 39.05, 30.50, 26.23, 24.38; LCMS m/z Calcd. for $C_{25}H_{33}N_4$ (M+H) 389, found 389; Elemental analysis calcd. for $C_{25}H_{33}N_4$ C: 77.28, H: 8.30, N: 14.42; found C: 77.45, H: 8.28, N: 14.29.

2,2',2'',2'''-(Undecane-2,2,10,10-tetrayl)tetrakis(1H-pyrrole) (SP8e)

The product was purified by column chromatography using dichloromethane and further recrystallized from methanol.

Yield: 55%; Melting point: 140-142 °C; ^{1}H NMR (400 MHz, $CDCl_3$): δ 7.73 (s, 4H, NH), 6.63 (m, 4H, α-CH), 6.15 (m, 4H, β-CH), 6.09 (m, 4H, β-CH), 1.93 (m, 4H, CH_2), 1.57 (m, 8H, CH_2), 1.36-1.23 (m, 2H, CH_2), 1.20 (s, 6H, CH_3); ^{13}C NMR (100 MHz, $CDCl_3$): δ 138.24, 116.84, 107.64, 104.42, 41.27, 39.05, 30.06, 29.69, 26.55, 26.29, 26.21, 24.40; LCMS m/z Calcd. for $C_{27}H_{37}N_4$ (M+H) 417, Found 417; Elemental analysis calcd. for $C_{27}H_{37}N_4$ C: 77.84, H: 8.71, N: 13.45; found C: 77.89, H: 8.65, N: 13.68.

3.5.3 General procedure for reaction of cyclohexanediones with pyrrole

The solution of cyclohexanedione (1 equiv.) and pyrrole (100 equiv.) was stirred at room temperature in a round bottom flask under N_2 atmosphere. After the reaction mixture

becomes homogeneous, TFA (1 equiv.) was added and the reaction mixture was heated at 60 °C for 6 h and then allowed to cool and quenched with excess Et_3N. Excess pyrrole was removed in vacuum and the compounds were efficiently isolated by column chromatography using silica gel (eluent: 5-30% ethyl acetate in hexane).

1,3-Bis(*α,α′*-dipyrryl-methyl)cyclohexane (SP10)

Yield: 40%; Melting point: 199-201 °C; FTIR Data (KBr) – 3381.52 cm^{-1}. ^1H NMR (400 MHz, $CDCl_3$): δ in ppm 7.49 (s, 4H, NH), 6.45 (s, 4H, β-CH), 6.02 (m, 8H, β-CH), 2.87 (s, 2H, CH_2), 2.15 (m, 4H, CH_2), 2.01 (m, 2H, CH_2); ^{13}C NMR (100 MHz, $CDCl_3$): δ in ppm 137.96, 117.07, 107.78, 103.96, 44.67, 39.18, 37.84, 20.98; LCMS m/z calcd. for $C_{22}H_{24}N_4$ (M-H) 343, found 343; Elemental analysis calcd. for $C_{22}H_{24}N_4$ C: 76.71; H: 7.02; N: 16.27; found C: 76.37; H: 7.12; N: 16.18.

3-(*α,α*'-Dipyrroylmethyl)cyclohexanone (SP16)

Yield: 27%; Melting point: 138-140 °C; FTIR Data (KBr)-3454.82, 3377.66, 1693.65 cm^{-1}. ^1H NMR (400 MHz, $CDCl_3$): δ in ppm 7.67 (s, 2H, NH), 6.61 (m, 2H, β-CH), 6.13 (t, 4H, β-CH, J = 2.3Hz), 2.83 (s, 2H, CH_2), 2.35 (m, 4H, CH_2), 1.72 (m, 2H, CH_2); ^{13}C NMR (100 MHz, $CDCl_3$): δ in ppm 209.66, 135.30, 117.87, 108.10, 105.37, 52.91, 43.25, 40.67, 35.32, 21.40; LCMS m/z calcd. for $C_{14}H_{16}N_2O$ (M+H) 229, found 229; Elemental analysis for $C_{14}H_{16}N_2O$ calcd. C: 73.66, H: 7.06, N: 12.27; found C: 73.56, H: 7.12, N: 12.18.

3-(1H-pyrrol-2-yl)cyclohex-2-enone (SP17)

Yield: 33%; Melting point: 141-143 °C; FTIR Data (KBr) - 3315.93, 1643.5, 1589.49 cm^{-1}; ^1H NMR (400 MHz, $CDCl_3$): δ in ppm 10.55 (s, 1H, NH), 7.09 (m, 1H, β-CH), 6.68 (m, 1H, β-CH), 6.54 (s, 1H, CH), 6.30 (m, 1H, β-CH), 2.74 (t, 2H, CH_2, J = 6.2Hz), 2.47 (t, 2H, CH_2 J = 6.9Hz), 2.09 (m, 2H, CH_2); ^{13}C NMR (100 MHz, $CDCl_3$): δ in ppm 200.08, 151.11, 130.07, 123.69, 117.29, 113.23, 110.87, 37.37, 26.50, 22.44; LCMS m/z calcd. for $C_{10}H_{11}NO$ (M+H) 162, found 162; Elemental analysis for $C_{10}H_{11}NO$ calcd. C: 74.51, H: 6.81, N: 8.69, found C: 74.65, H: 6.81, N: 8.59.

5,5-Dipropyldipyrromethane (SP18)

Yield: 2%; Melting point: 106-108 °C; FTIR Data (KBr) - 3379.5 cm^{-1}; ^1H NMR (400 MHz, $CDCl_3$): δ in ppm 7.68 (s, 2H, NH), 6.61 (m, 2H, β-CH), 6.11 (m, 4H, β-CH), 1.88 (m,

4H, CH_2), 1.09 (m, 4H, CH_2), 0.85 (t, J = 7.28 Hz, 6H, CH_3); ^{13}C NMR (400 MHz, $CDCl_3$): δ in ppm 137.239, 116.785, 107.35, 105.45, 42.79, 39.94, 17.16, 14.53; LCMS m/z calcd. for $C_{15}H_{22}N_2$ (M+H) 231, found 231; Elemental analysis calcd. for $C_{15}H_{22}N_2$ C: 78.21, H: 9.63, N: 12.16; found C: 78.11, H: 9.56, N: 12.06.

2-(*α,α′*-dipyrroylmethyl)cyclohexanone (SP19)

Yield: 9%; Melting point: 134-136 °C; FTIR Data (KBr) – 3375.21, 1704.05 cm^{-1}; ^{1}H NMR (400 MHz, $CDCl_3$): δ in ppm 8.13 (s, 2H, NH), 6.69 (m, 2H, β-CH), 6.16 (q, 2H, β-CH, J= 2.8 Hz), 6.02 (m, 2H, β-CH), 2.55 (m, 4H, CH_2), 1.88 (m, 4H, CH_2); ^{13}C NMR (100 MHz, $CDCl_3$): δ in ppm 210.95, 131.77, 117.84, 108.04, 106.03, 54.17, 39.60, 37.65, 26.25, 21.40; LCMS m/z calcd. for $C_{18}H_{21}N_3$ (M+H) 229, found 229; Elemental analysis for $C_{18}H_{21}N_3$ calcd. C: 73.66, H: 7.06, N: 12.27, found C: 73.52, H: 7.12, N: 12.36.

***α,α′,α′′*-(cyclohexane-1,1,2-triyl)tris(1H-pyrrole) (SP20)**

Yield: 5%; Melting point: 178-180 °C; FTIR Data (KBr) – 3397.5 cm^{-1}; ^{1}H NMR (400 MHz, $CDCl_3$): δ in ppm 8.03 (s, 1H, NH), 7.33 (s, 2H, NH), 6.56 (s, 1H, β-CH), 6.50 (m, 2H, β-CH), 6.28 (m, 1H, β-CH), 6.24 (br s, 1H, β-CH), 6.17 (m, 2H, β-CH), 6.12 (m, 1H, β-CH), 6.05 (br s, 1H, β-CH), 3.34 (dd, 1H, CH), 2.50 (d, J = 12.4 Hz, 1H, CH), 2.14 (m, 1H, CH), 2.04 (m, 1H, CH), 1.86 (m, 1H, CH), 1.73 (m, 4H, CH); ^{13}C NMR (100 MHz, $CDCl_3$): δ in ppm 141.17, 135.35, 131.90, 117.70, 117.10, 115.20, 109.12, 108.40, 107.67, 107.56, 105.37, 102.49, 46.56, 45.32, 40.33, 27.37, 26.30, 22.61; LCMS m/z calcd. for $C_{18}H_{21}N_3$ (M+H) 280, found 280; Elemental analysis for $C_{18}H_{21}N_3$ calcd. C: 77.38, H: 7.58, N: 15.04; found C: 77.26, H: 7.51, N: 15.12.

(4R,7R)-5,6-di(1H-pyrrol-2-yl)-4,7-dihydro-1H-4,7-ethanoindole (SP21)

Yield: 27%; Melting point: 49-51°C; FTIR Data (KBr) – 3399.7, 1707.6 cm^{-1}; ^{1}H NMR (400 MHz, $CDCl_3$): δ in ppm 8.01 (s, 1H, NH), 7.82 (s, 1H, NH), 7.70 (s, 1H, NH), 6.66 (br s, 2H, β-CH), 6.60 (t, J = 4 Hz, 1H, β-CH), 6.17 (m, 2H, β-CH), 6.05 (br s, 2H, β-CH), 5.99 (m, 1H, β-CH), 4.13 (m, 2H, CH), 2.20 (m, 2H, CH), 1.822 (m, 2H, CH); ^{13}C NMR (100 MHz, $CDCl_3$): δ in ppm 136.27, 134.017, 128.56, 119.18, 117.09, 116.96, 115.81, 108.26, 108.19, 107.27, 106.19, 104.72, 104.39, 33.91, 33.76, 32.15, 31.53; LCMS m/z calcd. for $C_{18}H_{17}N_3$ (M+H) 276, found 251; Elemental analysis for $C_{18}H_{17}N_3$ calcd. C: 78.52, H: 6.22, N: 15.26; found C: 78.46, H: 6.26, N: 15.12.

3.6 Crystallographic details

Crystallographic data for **SP8c**, **SP8d, SP10, SP12**, **SP14** and **SP15** were collected on BRUKER SMART-APEX CCD diffractometer. Crystallographic data for **SP16** (polymorph-1 and polymorph-2), **SP17**, **SP18**, **SP19** and **SP20** were collected on Oxford Gemini A Ultra diffractometer with dual source.

Pertinent crystallographic data collection and refinement parameter are shown in the following tables:

Table 3.3 Crystallographic parameters of crystals of **SP8c**, **SP8d**, **SP11** and **SP13**

Crystal data	**SP8c**	**SP8d**	**SP10**	**SP12**
CCDC No	748779	748780	903470	804966
Formula unit	$C_{23}H_{28}N_4$	$C_{25}H_{32}N_4$	$C_{22}H_{24}N_4$	$C_{12}H_{14}N_2O$
Formula wt.	360.49	388.55	344.45	202.25
Crystal system	Monoclinic	Monoclinic	Monoclinic	Monoclinic
T [K]	298 (2)	298 (2)	298 (2)	298 (2)
a [Å]	10.558 (3)	8.874 (2)	8.531 (3)	7.0771 (7)
b [Å]	14.448 (5)	28.503 (6)	18.801 (7)	19.1132 (19)
c [Å]	13.595 (4)	8.7620 (19)	11.864 (5)	8.2747 (8)
α [°]	90.00	90.00	90.00	90.00
β [°]	97.920 (7)	98.879 (4)	108.015 (6)	103.131 (2)
γ [°]	90.00	90.00	90.00	90.00
volume [$Å^3$]	2053.9 (11)	2189.8 (8)	1809.6 (12)	1090.02 (19)
Space group	P2(1)/n	P2(1)/c	P2(1)/n	P2(1)/c
Z′	1	1	1	1
Z	4	4	4	4
D_{calc} [$g.cm^{-3}$]	1.166	1.179	1.264	1.232
μ/mm^{-1}	0.070	0.070	0.077	0.080
Reflns collected	14275	25607	18206	10215
Unique reflns	3641	5285	3561	2137
Observed reflns	1657	2590	886	1825

Crystal data	**SP8c**	**SP8d**	**SP10**	**SP12**
R(int)	0.1116	0.0301	0.3971	0.0249
R_1 [I > 2σ(I)],	0.0997,	0.1100,	0.0777,	0.0468,
wR_2	0.1884	0.1737	0.1658	0.1188
GOF	1.089	1.096	0.856	1.047

Table 3.4 Crystallographic parameters of crystals of **SP14**, **SP15** and **SP16** (polymorph 1 and 2)

Crystal data	**SP14**	**SP15**	**SP16** (polymorph **1**)	**SP16** (polymorph **2**)
Formula unit	$C_{17}H_{19}N_3$	$C_{18}H_{21}N_3$	$C_{14}H_{16}N_2O$	$C_{14}H_{16}N_2O$
CCDC No	703494	748778	903471	903472
Formula wt.	265.35	279.38	228.29	228.29
Crystal system	Triclinic	Monoclinic	Orthorhombic	Orthorhombic
T [K]	298 (2)	298 (2)	298 (2)	298 (2)
a [Å]	9.490 (3)	6.303 (3)	12.9488 (7)	16.4455 (8)
b [Å]	9.615 (3)	21.098 (11)	14.6721 (12)	7.7792 (3)
c [Å]	9.869 (3)	11.306(6)	25.565 (2)	18.8199 (9)
α [°]	80.171 (5)	90.00	90.00	90.00
β [°]	62.662 (4)	100.824 (9)	90.00	90.00
γ [°]	64.498 (4)	90.00	90.00	90.00
volume [$Å^3$]	721.6 (4)	1476.7 (13)	4857.0 (6)	2407.68 (19)
Space group	P-1	P2(1)/n	Pbca	Pbcn
Z′	1	1	2	1
Z	2	4	16	8
D_{calc} [$g.cm^{-3}$]	1.221	1.257	1.249	1.260
μ/mm^{-1}	0.074	0.076	0.080	0.081
Reflns collected	7428	12759	12737	6605
Unique reflns	2834	2888	4929	2766
Observed reflns	2350	1447	1358	2766

Cryatal data	**SP14**	**SP15**	**SP16** (polymorph 1)	**SP16** (polymorph 1)
R(int)	0.0207	0.1701	0.1793	0.0351
R_1 [I > 2σ(I)],	0.0496,	0.0773,	0.0539,	0.0587,
wR_2	0.1476	0.1367	0.0597	0.1060
GOF	1.221	1.257	1.249	1.260

Table 3.5 Crystallographic parameters of crystals of **SP18**, **SP19**, **SP20** and **SP21**

Crystal data	**SP18**	**SP19**	**SP20**	**SP21**
Formula unit	$C_{10}H_{11}NO$	$C_{15}H_{22}N_2$	$C_{18}H_{21}N_3$	$C_{14}H_{16}N_2O$
CCDC No	903472	903469	914173	914174
Formula wt.	161.20	230.35	279.38	228.29
Crystal system	monoclinic	Orthorhombic	Monoclinic	Monoclinic
T [K]	298 (2)	298 (2)	298 (2)	298 (2)
a [Å]	10.0240 (10)	10.0647 (7)	17.324 (3)	15.4220 (12)
b [Å]	5.3217 (5)	13.9863 (12)	9.7036 (13)	9.7194 (6)
c [Å]	16.2081 (16)	20.4134 (15)	18.044 (3)	17.4527 (16)
α [°]	90.00	90.00	90.00	90.00
β [°]	94.059(9)	90.00	91.045 (19)	110.396 (10)
γ [°]	90.00	90.00	90.00	90.00
volume [$Å^3$]	862.45 (15)	2873.6 (4)	3032.8 (8)	2452.0 (3)
Space group	P2(1)/n	P 2(1) 2(1) 2(1)	P2(1)/n	P21/c
Z′	1	2	2	2
Z	4	8	8	8
D_{calc} [g.cm-3]	1.241	1.065	1.224	1.237
μ/mm^{-1}	0.081	0.063	0.074	0.079
Reflns collected	3434	8892	9081	10629
Unique reflns	1942	5847	5382	5547
Observed reflns	1059	2600	883	1846
R(int)	0.0200	0.032	0.1008	0.0635
R_1 [I > 2σ(I)],	0.0682,	0.0813,	0.0848,	0.0748,
wR_2	0.1538	0.1213	0.1207	0.1758
GOF	1.016	1.017	0.771	0.851

3.7 References

1. (a) In *The Porphyrin Handbook*, Eds. Kadish, K. M.; Smith; K. M.; Guilard, R. Academic Press, New York, 2000, vol. 1–10.
2. (a) Pandey, R. K.; Jagerovic, N.; Ryan, M. J.; Dougherty, T. J.; Smith, K. M. *Tetrahedron* **1996**, *52*, 5349. (b) Sessler, J. L.; Anzenbacher Jr., P.; Jursíková, K.; Miyaji, H.; Genge, J. W.; Tvermoes, N. A.; Allen, W. E.; Shriver, J. A.; Gale, P. A.; Král, V. *Pure App. Chem.* **1998**, *70*, 2401. (c) Benech, J. M.; Bonomo, L.; Solari, E.; Scopelliti, R.; Floriani, C. *Angew. Chem. Int. Ed.* **1999**, *38*, 1957. (d) Král, V.; Sessler, J. L.; Zimmerman, R. S.; Seidel, D.; Lynch, V.; Andrioletti, B. *Angew. Chem. Int. Ed.* **2000**, *39*, 1055. (e) Dolensky, B.; Kroulik, J.; Král, V.; Sessler, J. L.; Dvorykova, H.; Boury, P.; Bernatkova, M.; Bucher, C.; Lynch, V. *J. Am. Chem. Soc.* **2004**, *126*, 13714. (f) Bernatkova, M.; Andrioletti, B.; Král, V.; Rose, E.; Vaissermann, J. *J. Org. Chem.* **2004**, *69*, 8140. (g) Jha, S. C.; Lorch, M.; Lewis, R. A.; Archibald, S. J.; Boyle, R. W. *Org. Biomol. Chem.* **2007**, *5*, 1970.
3. (a) Gale, P. A.; Sessler. P. A.; Král, V. *Chem. Commun.* **1998**, 1. (b) Gale, P. A.; Anzenbacher Jr., P.; Sessler, J. L. *Coord. Chem. Rev.* **2001**, *222*, 57. (c) Sessler, J. L.; Gale, P. A. In *The Porphyrin Handbook*; Kadish, K. M., Smith, K. M., Guilard, R., Eds.; Academic Press: New York, **2000**, *6*, 257.
4. (a) Floriani, C., Floriani-Moro, R. In *The Porphyrin Handbook*; Kadish, K. M., Smith, K. M., Guilard, R., Eds.; Academic Press: New York, **2000**, *3*, 385. (b) Floriani, C., Floriani-Moro, R. In *The Porphyrin Handbook*; Kadish, K. M., Smith, K. M., Guilard, R., Eds.; Academic Press: New York, **2000**, *3*, 405.
5. (a) Smith, G. F. *Adv. Heterocycl. Chem.* **1963**, 2, 287. (b) Gryko, D. T.; Gryko, D.; Lee, C. -H. *Chem. Soc. Rev*. **2012**, *41*, *3780.*
6. (a) Nagarkatti, J. P.; Ashley, K. R. *Synthesis* **1974**, 186. (b) Hammel, D.; Erk, P.; Schuler, B.; Heinze J.; Müllen, K. *Adv. Mater*. **1992**, *4*, 737. (c) Vigmond, S. J.; Chang, M. C.; Kallury, K. M. R.; Thompson, M. *Tetrahedron Lett.* **1994**, *35*, 2455. (d) Boyle, R. W.; Karunaratne,V.; Jasat, A.; Mar, E. K.; Dolphin, D. *Syn.lett*. **1994**, 939. (e) Boyle, R. W.; Xie L. Y., Dolphin, D. *Tetrahedron Lett.* **1994**, *35*, 5377. (f) Staab, H. A.; Carell, T.; Dóhling, A.; *Chem. Ber.* **1994**, *127*, 223. (g) Shipps, Jr. G.; Rebek, Jr., J. *Tetrahedron Lett.* **1994**, *35*, 6823.
7. Lee, C. -H.; Lindsey, J. S. *Tetrahedron* **1994**, *50*, 11427.

8. (a) Littler, B. J.; Miller, M. A.; Hung, C. -H.; Wagner, R. W.; O'Shea, D. F.; Boyle, P. D.; Lindsey, J. S. *J. Org. Chem.***1999**, *64*, 1391. (b) Carcel, C. M.; Laha, J. K.; Loewe, R. S.; Thamyongkit, P.; Schweikart, K. -H.; Misra, V.; Bocian, D. F.; Lindsey, J. S. *J. Org. Chem.* **2004**, *69*, 6739. (c) Gryko, D.; Lindsey, J. S. *J. Org. Chem.* **2000**, *65*, 2249.
9. Dudič, M.; Lhoták, P.; Král, V.; Lang, K.; Stibor, I. *Tetrahedron Lett.* **1999**, *40*, 5949.
10. (a) Sobral, A. J. F. N.; Rebanda, N. G. C. L.; Silva, M. D.; Lampreia, S. H.; Silva, M. R.; Beja, A. M.; Paixao, J. A.; Gonsalves, A. M. D. *Tetrahedron Lett.* **2003**, *44*, 3971. (b) Sobral, A. J. F. N. *J. Chem. Edu.* **2006**, *83*, 1665.
11. Casiraghi, G.; Cornia, M.; Rassu, G.; Del Sante, C.; Spanu, P. *Tetrahedron* **1992**, *48*, 5619.
12. Mizutani, T.; Ema, T.; Tomita, T.; Kuroda, Y.; Ogoshi, H. *J. Am. Chem. Soc.* **1994**, *116*, 4240.
13. Casiraghi, G.; Cornia, M.; Zanardi, F.; Rassu, G.; Ragg, E.; Bortolini, R. *J. Org. Chem.* **1994**, *59*, 1801.
14. Laha, J. K.; Dhanalekshmi, S.; Taniguchi, M.; Ambroise, A.; Lindsey, J. S. *Org. Process Res. Dev.* **2003**, *7*, 799.
15. Lindsey, J. S.; Taniguchi, M.; Balakumar, A.; Fan, D. US2007/27312.55.
16. Baeyer, A. *Ber. Dtsch. Chem. Ges.* **1886**, *19*, 2184.
17. (a) Gale, P. A.; Sessler, J. L.; Král, V.; Lynch, V. *J. Am. Chem. Soc.* **1996**, *118*, 5140. (b) Allen, W. E.; Gale, P. A.; Brown, C. T.; Lynch, V. M.; Sessler J. L. *J. Am. Chem. Soc.* **1996,** *118*, 12471.
18. (a) Gale, P. A.; Sessler, J. L.; Allen, W. E.; Tvermoes, N. A.; Lynch,V. M. *Chem. Commun.* **1997**, 665. (b) Miyaji, H.; Sato, W.; Sessler, J. L. *Angew. Chem. Int. Ed.* **2000**, *39*, 1777. (c) Lee, C.-H.; Miyaji, H.; Yoon, D. -W.; Sessler, J. L. *Chem. Commun.* **2008**, 24. (d) Sessler, J. L.; Anzenbacher, Jr., P.; Shriver, J. A.; Jursı´kova´, K.; Lynch, V. M.; Marquez, M.; *J. Am. Chem. Soc.* **2000**, *122*, 12061. (e) Sessler, J. L.; An, D.; Cho, W. –S.; Lynch, V. M. *Angew. Chem. Int. Ed.* **2003**, *42*, 2278. (f) Král, V.; Gale, P. A.; Anzenbacher Jr., P.; Jursı´kova´, K.; Lynch, V.; Sessler, J. L. *Chem. Commun.* **1998**, 9. (g) Sessler, J. L.; An, D.; Cho, W. -S.; Lynch, V. M.; Marquez, M. *Chem. Eur. J.* **2005**, *11*, 2001.

19. Park, J. S.; Yoon, K. Y.; Kim, D. S.; Lynch, V. M.; Bielwaski, C. W.; Johnston K. P.; Sessler, J. L. *Proc. Natl. Acad. Sci. USA.*, **2011**, *108*, 20913.
20. (a) Adrian, J. C., Wilcox, C. S. *J. Am. Chem. Soc.* **1989**, *111*, 8055. (b) Goswami, S.; Hamilton, A. D.; Van Engen, D. *J. Am. Chem. Soc.* **1989**, *111*, 1090. (c) Rebek Jr., J. *Acc. Chem. Res.* **1990**, *23*, 399. (d) Scherder, J.; Engbersen, J. F. J.; Casnati, A.; Ungaro, R.; Reinhoudt, D. N. *J.Org.Chem.* **1995**, *60*, 6448. (e) In *Comprehensive Supramolecular Chemistry* Eds. Atwood, J. L.; Davies, J. E. D.; MacNicol, D. D.; Vögtle, F. *Elsevier*, 1996. (f) Haino, T.; Yanase, M.; Fukazawa, Y. *Angew. Chem. Int. Ed.* **1998**, *37*, 997. (g) Beer, P. D.; Hopkins P. K.; McKinney, J. D. *Chem. Commun.*, **1999**, 1253. (h) Abouderbala, L. O.; Belcher, W. J.; Boutelle, M. G.; Cragg, P. J.; Steed, J.W.; Turner, D. R.; Wallace K. J. *Proc. Natl. Acad. Sci. USA.* **2002**, *99*, 5001. (i) Deutmana, A. B. C.; Monnereaua, C.; Moalina, M.; Coumansa, R. G. E.; Velinga, N.; Coenena,M.; Smitsa, J. M. M.; Geldera, R.; Elemansa, J. A. A.; Ercolanib, W. G.; Noltea, R. J. M.; Rowana, A. E. *Proc. Natl. Acad. Sci. USA.* **2009**, *106*, 10371. (j) Li, C.; Han, K.; Li, J.; Zhang, H.; Ma, J.; Shu, X.; Chen, Z.; Weng, L.; Jia, X. *Org. Letts.* **2012**, *14*, 42.
21. (a) Král, V.; Andrievsky, A.; Sessler, J. L. *Chem. Commun.* **1995**, 2349. (b) Sessler, J. L.; Andrievsky, A.; Král, V.; Lynch, V. *J. Am. Chem. Soc.* **1997**, *119*, 9385.
22. (a) Sato, W.; Miyaji, H.; Sessler, J. L., *Tetrahedron Lett.* **2000**, *41*, 6731. (b) Valderrey, V.; Escudero-Adán, E. C.; Ballester, P. *J. Am. Chem. Soc.* **2012**, *134*, 10733.
23. (a) Kurreck, H.; Huber, M. *Angew. Chem. Int. Ed.* **1995**, *34*, 849. (b) Sanders, J. K. M. In *The Porphyrin Handbook*; Kadish, K. M., Smith, K. M., Guilard, R., Eds.; Academic Press: New York, **2000**, *3*, 347. (c) Ambroise, A.; Wagner, R. W.; Rao, P. D.; Riggs, J. A.; Hascoat, P.; Diers, J. R.; Seth, J.; Lammi, R. K.; Bocian, D. F.; Holten D.; Lindsey, J. S. *Chem. Mater.* **2001**, *13*, 1023. (d) Aratani, N.; Osuka, A. *Org. Lett*. **2001**, *3*, 4213. (e) Burrell, A. K.; Officer, D. L.; Plieger, P. G.; Reid, D. C.W. *Chem. Rev.* **2001**, *101*, 2751. (f) Speckbaacher, M.; Yu, L.; Lindsey, J. S. *Inorg. Chem.* **2003**, *42*, 4322. (g) Park, M.; Cho, S.; Yook, Z. S.; Aratani, N.; Osuka, A.; Kim, D. *J. Am. Chem. Soc.* **2005**, *127*, 15201. (h) Sankar, J.; Rath, H.; Prabhuraja, V.; Gokulnath, S.; Chandrashekar, T. K.; Purohit, C.; Verma, S. *Chem. Eur. J.* **2007**, *13*, 105. (i) Punidha, S.; Ravikanth, M. *Tetrahedron* **2008**, *64*, 8016.

24. (a) Král, V.; Sessler, J. L.; Zimmerman, R. S.; Seidel, D.; Lynch, V.; Andrioleetti, B.; *Angew. Chem. Int. Ed.* **2000**, *39*, 1055. (b) Dolenský, B.; Kroulík, J.; Král, V.; Sessler, J. L.; Dvořáková, H.; Bouř, P.; Bernátková, M.; Bucher, C.; Lynch, V. *J. Am. Chem. Soc.* **2004**, *126*, 13714. (c) Mahanta, S. P.; Kumar, B. S.; Panda, P. K. *Chem. Commun.* **2011**, 4496.

25. (a) Jang, Y.-S.; Kim H.-J.; Lee, P.-H.; Lee, C.-H. *Tetrahedron Lett.* **2000**, *41*, 2919. (b) Arumugam, N.; Jang, Y. -S.; Lee, C. -H. *Org. Lett.* **2000**, *2*, 3115. (c) Nagarajan, A.; Ka, J. -W.; Lee, C. -H. *Tetrahedron* **2001**, *57*, 7323. (d) Lee, E. -C.; Park, Y. -K.; Kim, J. -H.; Hwang, H.; Kim, Y. -R.; Lee, C. -H. *Tetrahedron Lett.* **2002**, *43*, 9493. (e) Song, M. -Y.; Na, H. -K.; Kim, E. -Y.; Lee, S. -J.; Kim, K. I.; Baek, E. -M.; Kim, H. -S.; An, D. K.; Lee, C. -H. *Tetrahedron Lett.* **2004**, *45*, 299. (f) Sessler, J. L.; An, D.; Cho, W. S.; Lynch, V. *J. Am. Chem. Soc.* **2003**, *125*, 13646. (g) Sessler, J. L.; An, D.; Cho, W. -S.; Lynch ,V.; Yoon , D. -W.; Hong , S. -J.; Lee. C. -H. *J. Org. Chem.*, **2005**, *70*, 1511.

26. Thamyongkit, P.; Lindsey, J. S. *J. Org. Chem.* **2004**, *69*, 5796.

27. (a) Yoon, D. W., Hwang, H.; Lee, C. H. *Angew. Chem. Int. Ed.* **2002**, *41*, 1757. (b) Lee, C. H.; Na, H. K.; Yoon, D. W.; Won, D. H.; Cho, W. S.; Lynch, V. M.; Shevchuk, S. V.; Sessler, J. L. *J. Am. Chem. Soc.* **2003**, *125*, 7301. (c) Panda, P. K.; Lee, C. H. *Org. Lett.* **2004**, *6*, 671. (d) Panda, P. K.; Lee, C. H. *J. Org. Chem.* **2005**, *70*, 3148. (e) Miyaji, H.; Kim, H. K.; Sim, E. K.; Lee, C. K.; Cho, W. S.; Sessler, J. L.; Lee, C. H. *J. Am. Chem. Soc.* **2005**, *127*, 12510. (f) Lee, C. H.; Lee, J. S.; Na, H. K.; Yoon, D. W.; Miyaji, H.; Cho, W. S.; Sessler, J. L. *J. Org. Chem.* **2005**, *70*, 2067. (g) Samanta, R.; Mahanta, S. P.; Chaudhuri, S.; Panda, P. K.; Narahari, A. *Inorganica Chim. Acta* **2011**, *372*, 281.

28. (a) Chang,C. K.; Abdalmuhdi, I. *J. Org. Chem.* **1983**, *48*, 5388. (b) Sessler, J. L.; Hugdahl, J.; Johnson, M. R. *J. Org. Chem.* **1986**, *51*, 2838. (c) Heiler, D.; McLendon, G.; Rogalskyj, P. *J. Am. Chem. Soc.* **1987**, *109*, 604. (d) Osuka, A.; Maruyama, K.; Yamazaki, I.; Tamai, N. *J. Chem. Soc. Chem. Commun.* **1988**, 1243. (e) Khoury, R. G.; Jaquinod, L.; Smith, K. M. *Chem. Commun.* **1997**, 1057.

29. (a) Arumugam, N.; Chung, W. Y.; Lee, S. W.; Lee, C. H. *Bull. Korean Chem. Soc.* **2001**, *22***,** 932. (b) Renic, M.; Basaric, N.; Mlinaric-Majerski, K. *Tetrahedron Lett.* **2007, *48,*** 7873.

30. Overberger, C. G.; Thomas Jr., B. G.; Chibnik, S.; Huang, P.; Monagle, J. J. *J. Am.Chem. Soc.* **1952**, *74*, 3290.

31. (a) Hatt, H. H. *Org. Synth.* **1936,** *16*, 22. (b) Yamashita, M.; Matsumiya, K.; Morimoto, H.; Seumitsu, R. *Bull. Chem. Soc. Jpn.* **1989**, *62*, 1668. (c) Bai, X.; Eliel, L. E. *J. Org. Chem.* **1991**, *56,* 2087.

32. (a) Pagani, G.; Berlin, A.; Canavesi, A.; Schiavon, G.; Zecchin, S.; Zotti, G. *Adv. Mater.* **1996**, *8*, 819. (b) Harmjanz, M.; Gill, H. S.; Scott, M. J. *J. Org. Chem.* **2001**, *66*, 5374.

33. (a) Hall, G.; Sugden, J. K.; Waghela, M. B. *Synthesis*, **1987**, 10. (b) Kojima, H.; Ozaki, K.; Matsumura, N.; Inoue, H. *Chem. Lett.* **1989**, 1499. (c) Minyan, T.; Stephen, G. P. *J. Org. Chem.* **2003**, *68*, 7818. (d) Qingsu. X.; Ming, W. C.; Ge, L.; Peter, P. F. *Chem. Res. Toxicol.* **2004**, *17*, 702. (e) Haiyu, P.; Shaojie, W.; Zhijuan, Y.; Zhengang, W. *Disi Junyi Daxue Xuebao* **2006**, *27*, 1339. (f) Canan, U.; Sertan, A.; Baris, T. *Heterocycles* **2007**, *71*, 2427. (g) Canan, U.; Arife, Y. *Tetrahedron* **2007**, *63*, 5608. (h) Stanislav, R.; Josef, C.; Ondrej, K.; Jan, S.; Lukas, P.; Zuzana, M. *Tetrahedron Lett.* **2008**, *49*, 5316.

34. (a) Wipf, P.; Spencer, S. R. *J. Am. Chem. Soc.* **2005**, *127*, 225. (b) Pilli, R. A.; Rosso, G. B.; Ferreira de Oliveira, M. C. *Nat. Prod. Rep.* **2010**, *27*, 1908. (c) Nagarajan, K. *J. Chem. Sci.* **2006**, *118*, 291. (d) Nagarajan, K.; Talwalker, P. K.; Shah, R. K.; Mehta, S. R.; Nayak, G. V. *Ind. J. Chem. Sect. B: Org. Chem. Incl. Med. Chem.* **1985**, *24*, 98. (e) Rubin, A. A.; Yen, H. C.; Pfeffer, M. *Nature* **1967**, *216*, 578. (f) Martínez, R.; Clara-Sosa, A.; Ramírez Apan, M. T. *Bioorg. Med. Chem.* **2007**, *15*, 3912.

35. (a) Morales, C. L.; Pagenkopf, B. L. *Org. Lett.* **2008**, *10*, 157. (b) Ishibashi, H.; Akamatsu, S.; Iriyama, H.; Hanaoka, K.; Tabata, T.; Ikeda, M. *Chem. Pharm. Bull.* **1994**, *42*, 271. (c) Hatanaka, N.; Watanabe, N.; Matsumoto, M. *Heterocycles* **1986**, *24*, 3157. (d) Remers, W. A.; Roth, R. H.; Gibs, G. J.; Weiss, M. J. *J. Org. Chem.* **1971**, *36*, 1232.

36. (a) Stetter, H.; Dierichs, W.; *Chem. Ber.* **1955**, *271*, 88. (b) O'Brien, S.; Smith, D. C. C. *J. Chem. Soc.*, **1960**, 4609. (c) Young, D. V.; Snyder H. R. *J. Am. Chem. Soc.* **1961**, *83*, 3160. (d) Hershenson, F. M. *J. Org. Chem*, **1975**, *40*, 1260. (d) Greenhouse, R.; Ramirez, C.; Muchowski, J. M. *J. Org. Chem.* **1985**, *50*, 2962. (e) Dhanak, D.; Reese, C. B.; Romana, S.; Zappia, G. *J. Chem. Soc, Chem. Comm.* **1986**, *12*, 903. (f) Chelucci, G.; Gladiali, S.; Marchetti, M. *J. Het. Chem.* **1988**, *25*, 1761. (g)

Masaguer, C.F.; Ravina, E. *Tetrahedron Lett.* **1996**, *37*, 5171. (h) McComas, C. C.; Van Vranken D. L. *Tetrahedron Lett.* **1999**, *40*, 8039. (i) Mori, M.; Akashi, M.; Nishida, M. *Chem. Lett.* **1999**, 465.

37. Miyaji, H.; Hong, S. J.; Jeong, S. D.; Yoon, D. W.; Na, H. K.; Hong, J.; Ham, S.; Sessler, J. L.; Lee, C. H. *Angew. Chem. Int. Ed.* **2007**, *46*, 2508.
38. Arcadi, A.; Alfonsi, M.; Bianchi, G.; Anniballe, G. D.; Marinelli, F. *Adv. Synth. Catal.* **2006**, *348*, 331.
39. (a) Baran, P. S.; Guerrero, C. A.; Ambhaikar, N. B.; Hafensteiner, B. *Angew. Chem. Int. Ed.* **2005**, *44*, 606. (b) Baran, P. S.; Richter, J. M.; Lin, D. W. *Angew. Chem. Int. Ed.* **2005**, *44*, 609. (c) Gupton, J. T. *Top. Heter. Chem.* **2006**, *2*, 53. (d) Forte, B.; Malgesini, B.; Piutti, C.; Quartieri, F.; Scolaro, A.; Papeo, G. *Mar. Drugs* **2009**, *7*,705.
40. Smithen, D. A.; Cameron,T. S.; Thompson, A. *Org. Lett.* **2011**, *13*, 5846.

CHAPTER 4

Meso-diacylated calix[4]pyrroles

4.1 Introduction

4.1.1 General background

Meso-octamethylporphyrinogen **L48** was first achieved by Baeyer in 1886 by acid catalyzed condensation of pyrrole with acetone.[1] Thirty years later in 1916, Chelintzev and Tronov proposed correctly a cyclic tetrameric structure as *α*,*β*,*γ*,*δ*-octamethylporphyrinigen,[2] which was followed by some researchers involved in the synthesis and functionalization of this macrocycle.[3] This macrocycle **L48** contains four NH groups and is a conformationally flexible neutral nonaromatic molecule. In 1991, Floriani employed it as a ligand for metal coordination, through deprotonation under very harsh condition.[4] They found that **L97** forms complexes with alkali metals, transition metals, lanthanides and actinides via a combination of direct pyrrole-N-metal and pyrrole-*π*-metal interactions.[5] In contrary to Floriani's findings,

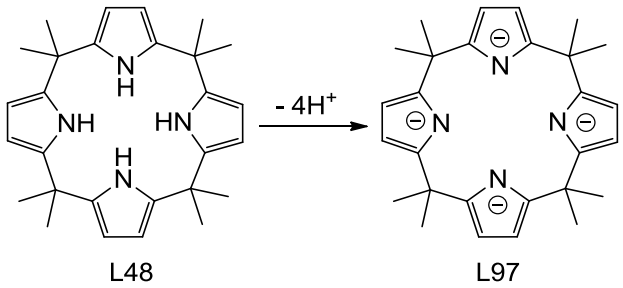

in 1996 Sessler and coworkers presented it as a neutral anion binding host, especially for halides and neutral guest and renamed it as calix[4]pyrrole due to its structural resemblance with calix[4]arene.[6] In analogy to the calix[4]arene, which has received extensive attention for years,[7] calix[4]pyrrole is also a macrocyclic system that can adopt a range of limiting conformations.[8] However, the latter contains four pyrroles, instead of the four phenol units in

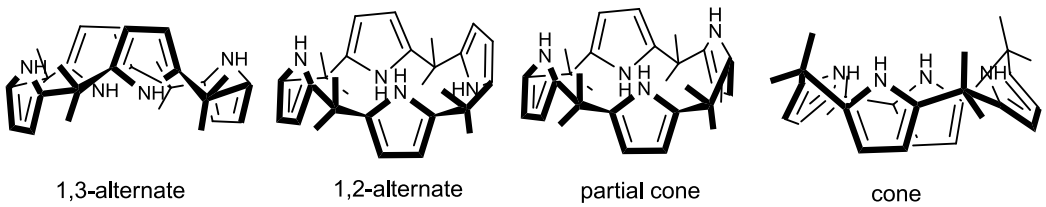

Figure 4.1 Depiction of the four limiting possible conformations conceivable for calix[4]pyrrole.

the former macrocycle. The theoretical conformational preference of calix[4]pyrrole and its anion complex was studied independently by Jorgensen and Sessler and they found that **L48**

can adopt four limiting conformations: 1,3-alternate, 1,2-alternate, partial cone and cone. In gas phase and in dichloromethane solution the stability sequence is 1,3-alternate > partial cone > 1,2-alternate > cone.[8,9]

The solid state study of this family of macrocycle also reveals that in general in guest free form it adopts 1,3-alternate conformation except *β*-octabromo-*meso*-octamethylcalix[4]-pyrrole, which adopts a 1,2-alternate conformation.[10] However, in the resulting anion complexes the four pyrrolic NH units act as hydrogen bond donors and the macrocycle generally adopts a cone like conformation, whereas in neutral guest complexes it can adopt conformation depending on the strength of the interaction, such as **L48**.2(MeOH) adopts 1,3-alternate conformation while **L48**.2(DMF) possesses 1,2-alternate conformation.[6b]

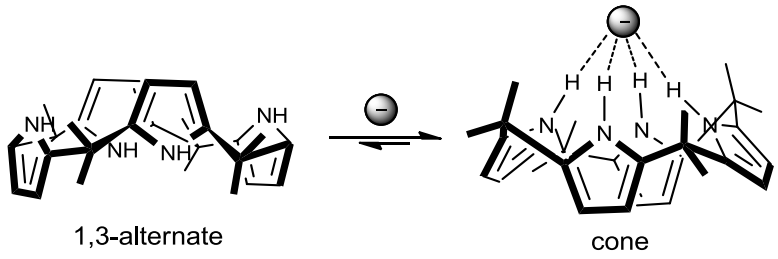

Figure 4.2 Conformational preference of **L48** without anion and with anion.

In Sessler's first report, the solution binding properties of **L48** was studied using ^{1}H NMR titration techniques and revealed that it displays high selectivity for fluoride ion in dichloromethane relative to the other tested anions (Table 4.1).[6a] Subsequently, they have studied the binding affinity of **L48** with neutral guest in benzene-d_6 solution using ^{1}H NMR technique.[6b]

Table 4.1 Summary of anion binding constants for calix[4]pyrrole **L48** as determined by ^{1}H NMR studies carried out in CD_2Cl_2. The counter cations were tetrabutylammonium in all cases.[6a]

Anion	F^-	Cl^-	Br^-	I^-	$H_2PO_4^-$	HSO_4^-
K_a (M^{-1})	17170	350	10	< 10	97	< 10

In 2002, in a short communication Schmidtchen reported the anion affinity of **L48** with the help of isothermal titration calorimetry (ITC) and revealed that the binding affinity

depends on the counter cation also.[11b] This was the first report of use of ITC to determine the absolute affinity constant in this type of macrocycle and showed that this technique includes an increased dynamic range, higher detection limits and greater reproducibility. Table 4.2 summarizes the affinity constants of **L48** measured by ITC as well as its thermodynamic parameters (*i.e.* ΔH°, ΔG°, TΔS°). In case of fluoride ion, the association constant was obtained with crpytand-222 and KF, instead of tetraalkylammonium salt due to the unreliable titration curve observed in case of the latter, owing to the presence of the residual water molecules.[11b]

Table 4.2 Energetics of binding of various anions to calix[4]pyrrole **L48** in dry acetonitrile **(**<10 ppm H_2O) at 30 °C as determined by ITC.[11b]

Anion		F^-	Cl^-		$H_2PO_4^-$	
Cation	Mode[a]	K-cryptand222$^+$	K-cryptand222$^+$	NEt_4^+	K-cryptand222$^+$	NBu_4^+
ΔH	A	-8.25	-10.60	-8.81	-10.94	-11.60
	B	-10.35	-9.80	-8.87		
ΔG°	A	-7.18	-7.30	-6.90	-5.85	-5.79
	B	-7.08	-7.00	-6.68		
TΔS°	A	-1.05	-3.30	-1.90	-5.07	-5.81
	B	-3.26	-2.80	-2.18		
K_a	A	153 000	185 000	95 400	16 800	15 100
	B	129 000	111 000	66 700		

[a] A = titration of guest into host solution; B = titration of host into guest solution.

These developments drew wide attention of researchers toward this area and till date more than 300 literatures appeared on this macrocycle, which prove its potential as a supramolecular host. This has led to a number of analyses carried out in different solvents using different techniques to compare their affinities. These studies revealed that the binding affinity and selectivity with competing guests is not a function of host structure alone but is heavily dependent on the nature of the solvents used in the measurements and the methods of measurement. Table 4.3 and 4.4 summarizes some of this findings.[11]

Table 4.3 Association constants of different anions with **L48** in different solvents determined by NMR titration.

Anion	DCM-d_2	acetonitrile-d_3 +0.5% v/v D_2O	acetonitrile-d_3 + $CDCl_3$ (1:9 v/v)	DMSO-d_6
F^-	17 170	>10 000	23 800	1060
Cl^-	350	5 000	6 800	1025
Br^-	10	ND	270	17
I^-	< 10	17	ND	ND
$H_2PO_4^-$	97	1300	ND	ND

Table 4.4 Association constants of different anions with **L48** in different solvents determined by isothermal titration calorimetry (ITC).

Anion	1,2-DCE	acetonitrile	DMSO	DMF
F^-	ND	ND	ND	6 310 000
Cl^-	35 000	14 0000	1 300	16 000
Br^-	< 1000	3 400	ND	2500
I^-	ND	ND	ND	35
$H_2PO_4^-$	ND	15 100	ND	ND

ND: Not determined.

4.1.2 Synthesis of calix[4]pyrrole

The design of any synthetic host relies on the attractive interactions between the host and the guest to drive complexation.[12] The development of novel receptors for enhanced selectivity towards targeted guest requires fine tuning of interaction sites, which in turn requires proper functionalization, such that the complementarity of size and shape between the receptor and guest is achieved. Due to this, many transformations and modifications has been carried out on macrocycle **L48**, including, *meso*-sustitution(s), *β*-substitution(s), single side strapping and core modification.[10,11,13-16] The core modification strategy will be discussed in greater detail in chapter 5. In this chapter we will deal with *meso*- and C-rim functionalization strategy in order to increase the selectivity and/or affinity of calix[4]-pyrrole macrocycle towards various anions.

There are four general methods for the synthesis of calix[4]pyrrole: a one pot [1+1+1+1], [2+2], [2+1+1], and [3+1] condensations, where the numbers in the bracket refer to the number of pyrrolic subunits in the precursors involved.

4.1.2.1 One-pot condensation [1+1+1+1]

This protocol involves the condensation of pyrroles and ketones in a 1:1 ratio in the presence of an acid catalyst such as methanesulfonic acid (MSA), trifluoroacetic acid (TFA), BF_3-OEt_2 etc. Further, depending on the number of types of pyrroles and ketones involved in the condensation, one-pot condensation can be categorized as homo or mixed condensation.[6a, 11a, 17] The term 'homo' condensation is meant to define the reaction of condensation of a specific pyrrole with a particular ketone in 1:1 ratio.[6a] The condensation gives a single product when the ketone is symmetric (Scheme 4.1), whereas in case of asymmetric ketone

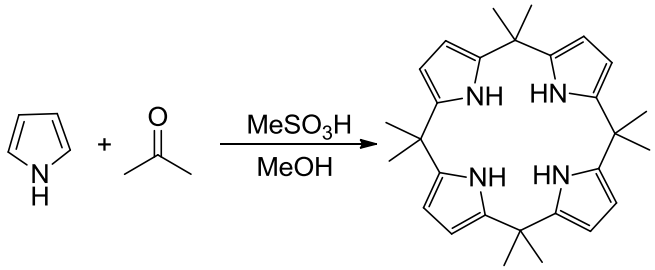

Scheme 4.1 [1+1+1+1] condensation leads to **L48**.[6a]

(Scheme 4.2) it gives a mixture of configurational isomers.[11a] Mixed condensation involves either the condensation of more than one ketone with a single pyrrole or more than one pyrrole with a single ketone.[18,19] In this case a mixture of products formed and hence yield is

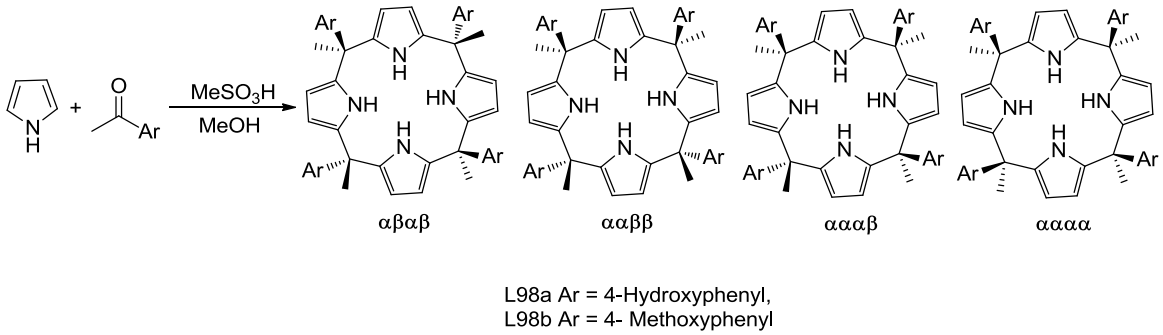

Scheme 4.2 Asymmetric homo condensation reaction.[11a]

less.[18] Here the reactants ratio must be carefully controlled so as to optimized the yield of the desired product. In spite of tedious chromatographic procedure involved in the isolation of the products this method can provide a good entry to functionalized calixpyrrole (Scheme 4.3).

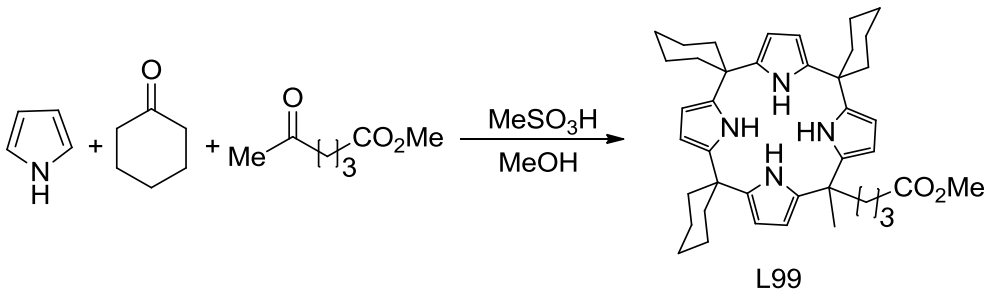

Scheme 4.3 Mixed condensation reaction leading to functionalized calixpyrrole.[18]

4.1.2.2 [2+2] condensation

It refers to acid catalyzed condensations of two dipyrromethane units with ketones. This approach is quite popular in porphyrin synthesis,[20] and provides an important means of formation of less symmetric *meso*-functionalized porphyrinogen, because it gives flexibility in modification at the two opposite *meso*-centres keeping the dipyrromethane units same (Scheme 4.4).[21]

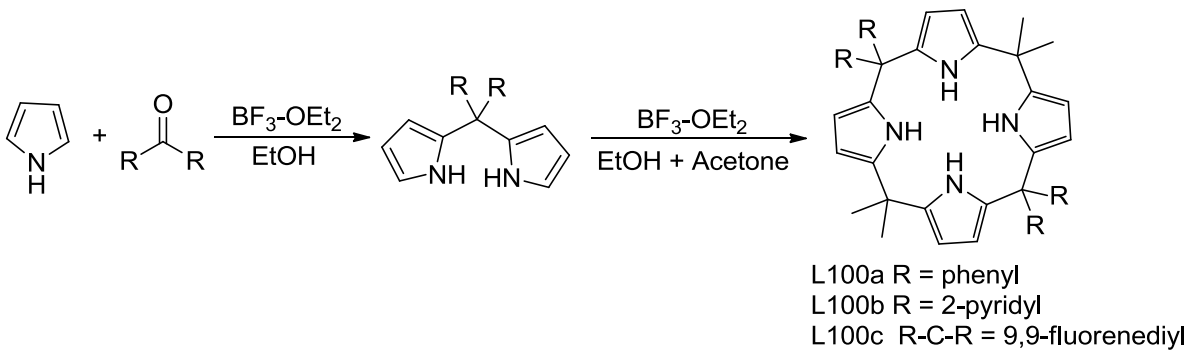

Scheme 4.4 [2+2] condensation reaction.

4.1.2.3 [2+1+1] condensation

It refers to the acid catalyzed condensation of one dipyrromethane unit with a pyrrole or pyrrole derivative in presence of a ketone (Scheme 4.5).[11g]

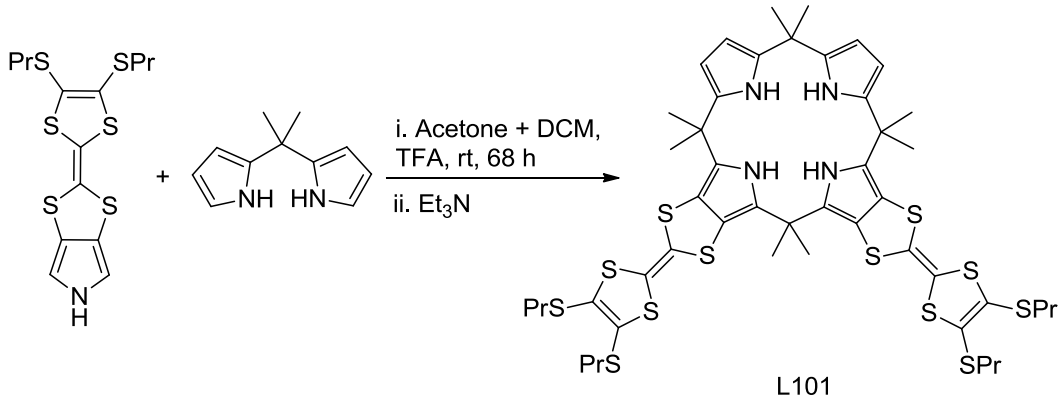

Scheme 4.5 [2+1+1] condensation reaction towards calixpyrrole.

4.1.2.4 [3 + 1] condensation

[3 + 1] condensation involves the reaction of a tripyrrane with a pyrrole in the presence of an acid catalyst (Scheme 4.6). The synthesis of tripyrrane was first optimized by Sessler in 2001 by using lower equivalent of pyrrole (2.5 equiv.) and TFA (0.025 equiv.) compared to the ratio involved in the dipyrromethane synthesis.[22]

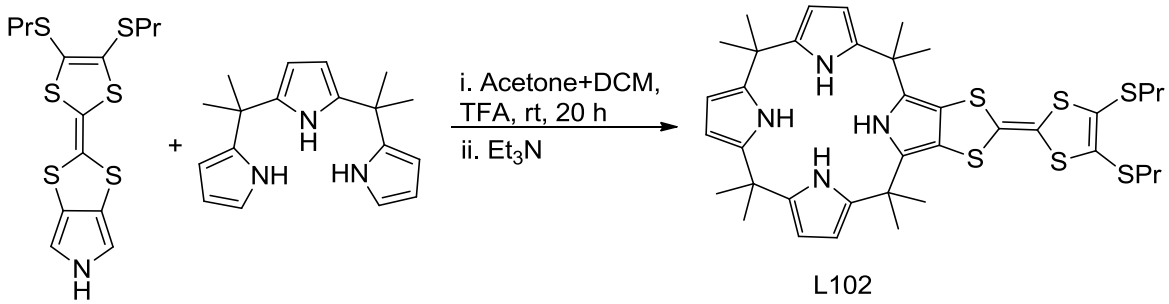

Scheme 4.6 [3+1] condensation reaction towards calixpyrrole.

4.1.3 Modulation of anion binding properties of calix[4]pyrroles: Functionalization of calix[4]pyrrole

Calix[4]pyrrole can be functionalized at either *β*-positions (C-rim) or *meso* positions to tune its anion binding affinity. Such substitutions not only affect the anion binding properties of calix[4]pyrrole but also produce precursors useful for the synthesis of calix[4]pyrrole based anion sensors, transporting agents and solid phase anion separation.[3c,23] The functionalization can be achieved either by pre-modification of the ketone and the pyrrole unit before subjecting them to condensation as shown above in the various schemes or post-modification where the calix[4]pyrrole moiety is subjected to different functionalization.

4.1.3.1 *Meso*-modifications

Extension of the H-bonding domain of receptor **L48** may confer new binding properties onto the macrocycle for guest binding. In this regard, introduction of aryl or other rigid groups onto the *meso* positions of **L48** skeleton resulted in calixpyrroles possessing a deep cavity (Scheme 4.2). Calix[4]pyrrole **L98** consists of four configurational isomers *αααα*, *αβαβ*, *ααββ* and *αααβ* according to the relative disposition of the bulky substituted phenyl groups (Scheme 4.2).[11a] Anion binding study revealed that these systems show lower affinities for small anions, especially chloride and dihydrogenphosphate ions, in acetonitrile-water (99.5:0.5) than **L48** (Table 4.5). On the other hand, their increased selectivities and other binding effects may be ascribed to the presence of rigid walls at the macrocycle periphery, which controls the access of guest molecules. Combinedly, these results served to illustrate just how important slight deviations in structure can be in terms of fine-tuning the anion binding properties of a given calix[4]pyrrole type receptor system. Further, Namor and

Table 4.5 Stability Constants for Compounds **L98a-b** with different anions in acetonitrile-d_3 (0.5% v/v D_2O).

	L48	**L98a**			**L98b**		
		ααββ	*αααβ*	*αααα*	*ααββ*	*αααβ*	*αααα*
F^-	> 10 000	> 10 000	5 000	> 10 000	4 600	1 100	> 10 000
Cl^-	> 5 000	1 400	260	320	100	220	300
$H_2PO_4^-$	1 300	520	230	500	<100	<80	<100

coworkers reported two isomers of *meso*-tetramethyltetrakis(3-hydroxyphenyl)calix[4]-pyrrole **L103** (*ααββ* and *αβαβ*). Their interaction with anions was investigated by ^{1}H NMR titration analysis in CD_3CN, while the complex composition was accessed through conductance measurement and showed that *ααββ* isomer prefers $H_2PO_4^-$ in acetonitrile, whereas *αβαβ* isomer is selective towards the fluoride ion. Again the stoichiometry is altered for the complexation of the fluoride ion with *ααββ* (1:1 complex) relative to *αβαβ* isomer (1:2 complex) in acetonitrile. Further investigation carried out in N,N-dimethylformamide shows no evidence of complex formation with dihydrogenphosphate or other spherical anions except fluoride ion, with which the formation of a 1:2 complex is observed again.[24] On the other hand, Ballester and coworkers reported a series of deep cavity *meso*-tetraaryl calix[4]pyrroles **L104** and their *αααα* isomer used as a model system to quantify chloride-*π*

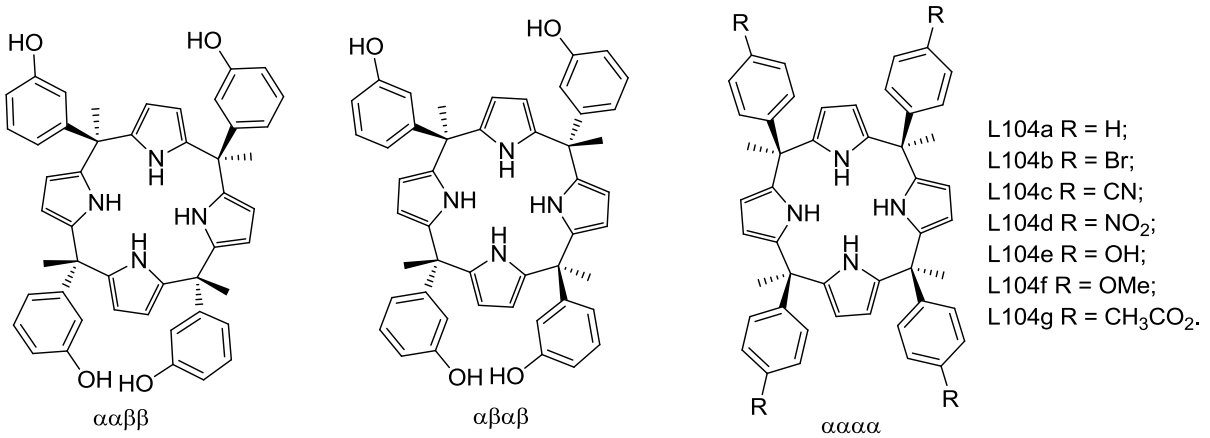

L103

interactions in solution. With the help of ^{1}H NMR and X-ray crystallographic studies they have demonstrated that the chloride-arene interactions observed in those complexes were established exclusively with the π-aromatic system.[25]

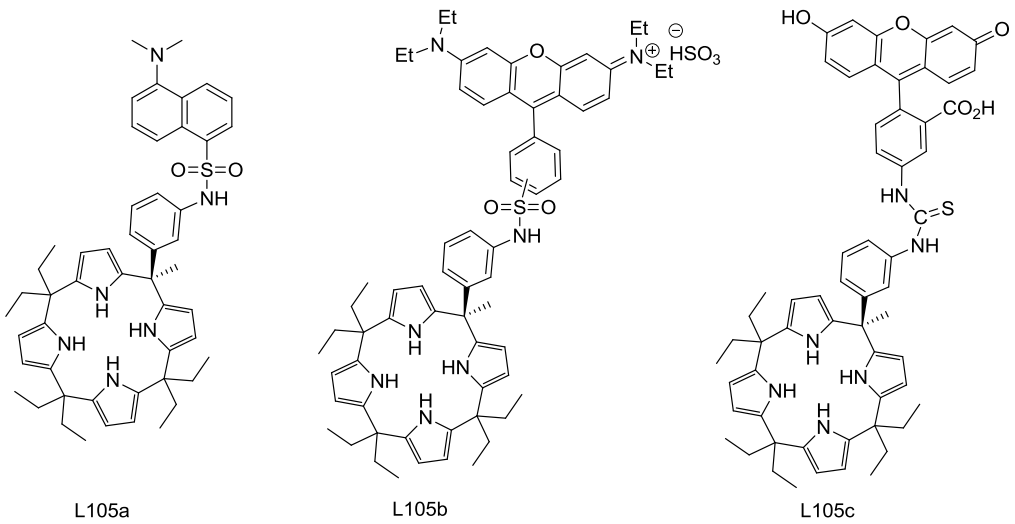

L105a L105b L105c

In addition to the modification noted above, Sessler *et al.* explored another new type of functionalization and synthesized mono-*meso*-functionalized calix[4]pyrroles **L105** with additional H-bonding site and reporter unit which binds anions with greater affinity than **L48**, while displaying an effective fluorometric response and named it as second generation anion sensors. They were also the first to show high phosphate/chloride selectivity (2 orders of magnitude) for these receptors (Table 4.6).[19] This selectivity can be attributed to the presence of the additional NH moiety at the macrocycle periphery which could provide ancillary hydrogen bonding interaction with the non-spherical anions (Figure 4.3).

Table 4.6 Affinity constants of sensors **L105** towards anionic substrates determined by fluorescence spectroscopy [Sensors **L105a** and **L105b** in acetonitrile (0.01% v/v water) and Sensor **L105c** in acetonitrile (4% water)].[19]

Anion	Association constant (M^{-1})		
	L105a	**L105b**	**L105c**
F^-	222 500	> 1 000 000	> 2000 000
I^-	10 500	18 200	< 10 000
$H_2PO_4^-$	168 300	446 000	682 000
$HP_2O_7^{3-}$	131 000	170 000	> 2 000 000

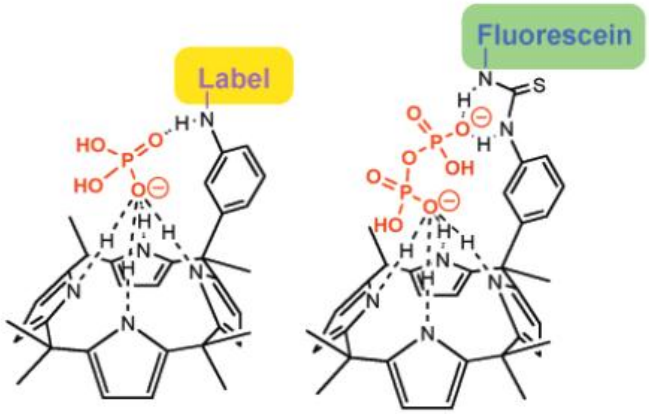

Figure 4.3 Schematic representation of the multiple hydrogen bonding interactions that are believed to account for the high phosphate and pyrophosphate affinities observed for **L105a-c.**[19]

4.1.3.2 C-rim modification

C-rim modification remains one of the most attractive means for improving the anion binding properties of calixpyrrole. The main motif behind this is to modulate the acidity of

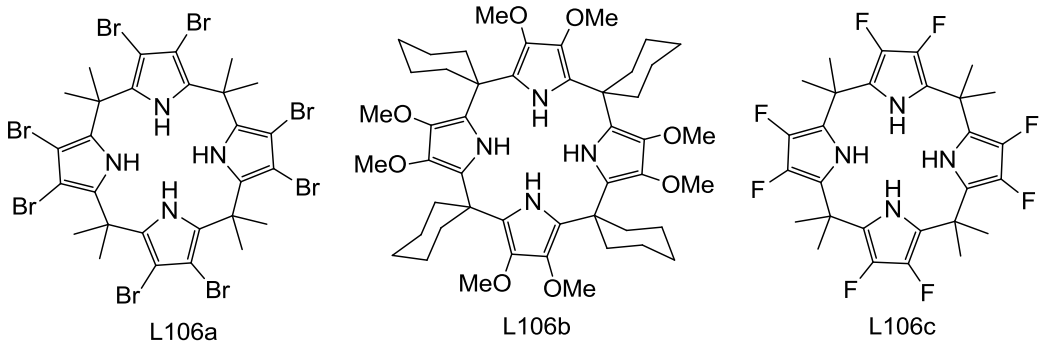

the NHs of the pyrroles, by introducing different substituents. In 1997 Gale *et al.* first reported the *β*-octa substituted calix[4]pyrroles **L106a-b** and later Anzenbacher Jr. *et al.* reported **L106c**.[10,26] Anion coordination studies revealed that **L106a** and **L106c** shows enhanced affinities relative to **L48** while **L106b** shows relatively decreased affinity compared to the parent cyclohexylcalix[4]pyrrole. The above observation can be attributed to the increase or decrease of acidity of pyrrolic NHs owing to the presence of electron withdrawing or donating substituents at their *β*- positions respectively.

In another report on C-rim modification of **L48**, only one *β*-position was functionalized by linking anthracene reporter unit with **L48** through both conjugated and unconjugated spacers to obtain **L107**.[27] Their anion binding affinity was determined by fluorescence quenching study in two solvent systems viz. dichloromethane and acetonitrile. This study revealed that the quenching of fluorescence of the anthracene guoup depends on its distance from the anion binding site (Table 4.7).

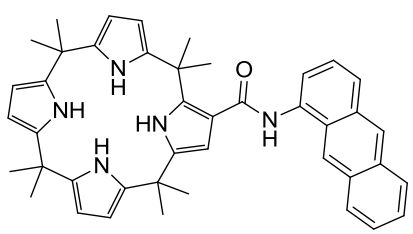

L107a

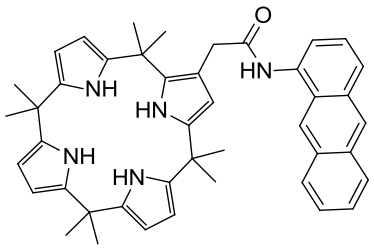

L107b

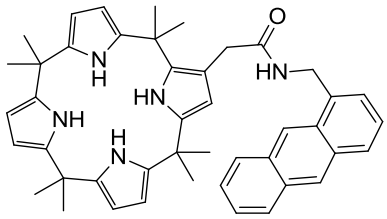

L107c

Table 4.7 Affinity constants for sensors **L107** towards anionic substrates as determined in acetonitrile and dichloromethane by fluorescence spectroscopy.

Anion	log*K* (CH_2Cl_2)			log*K* (CH_3CN)		
	L107a	**L107b**	**L107c**	**L107a**	**L107b**	**L107c**
F^-	4.94	4.52	4.49	5.17	4.69	4.69
Cl^-	3.69	2.96	2.79	4.87	3.81	3.71
Br^-	3.01	a	a	3.98	2.86	a
$H_2PO_4^-$	4.02	3.56	a	4.96	3.90	a

a: insufficient quenching to provide an accurate stability constant value.

Further, in a subsequent communication Sessler *et al.* reported a new set of *β*-substituted calix[4]pyrroles **L108a-c**, where a chromophore is appended in conjugation with one of the pyrrole unit and these systems act as naked eye chemosensors, which can discriminate

different anionic substrates as the results of disparate changes in color occurring via anion induced charge transfer from the bound anion to the anthraquinone moiety.[28]

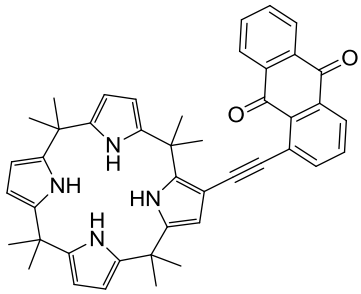

L108a

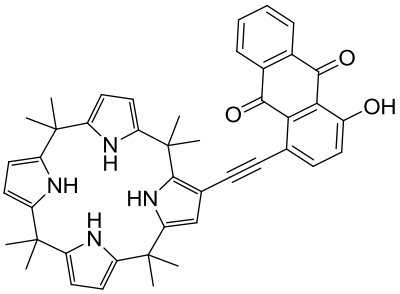

L108b

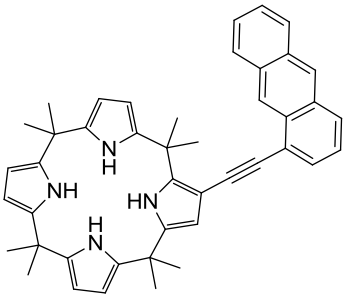

L108c

4.2 Research goal

The above discussion highlights the importance of calix[4]pyrrole as a promising anion receptor. However, owing to its small cavity size, calix[4]pyrrole only binds small anions such as fluoride and chloride effectively in aprotic solvents. However, the introduction of various rigid structural motif at its periphery resulted in a deep cavity, that display selectivity towards anions with reduced affinity owing to steric constraints, while resulting in the formation of four configurational isomers, which need elaborate chromatographic

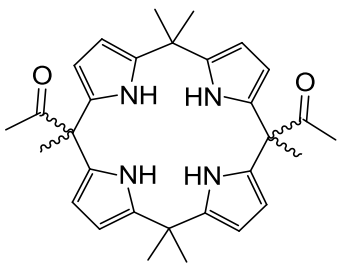

SP23

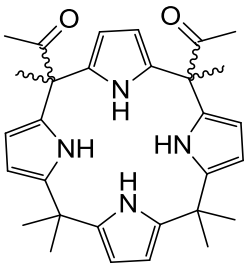

SP24

purification. Further, the presence of additional hydrogen bonding moieties at the macrocycle periphery could provide additional interactions with the anions to increase their binding affinity towards nonspherical anions. Therefore, we presumed that the presence of two functionalized units as flexible anchors at the *meso*-positions will not only help in enhancing the anion binding properties owing to better access, but also will reduce the total number of configurational isomers to only two and make the purification relatively easy.

As discussed in the introductory chapter, phosphate played an important role in biology, health, environment and hence selective binding of phosphates is of great importance to researchers and in this regard a variety of receptors has been put forward in literature.[29] In this chapter, we tried to modulate the dihydrogenphosphate affinity of calix[4]pyrrole by

incorporating complementary hydrogen bonding functionality *i.e.* acyl group at the periphery of the macrocycle. In this context, we intend to synthesize two positional isomers of *meso*-diacylated calixpyrrole *i.e.* 5,15- (**SP23**) and 5,10- diacylcalix[4]pyrrole (**SP24**). Both the isomers are expected to form as a mixture of two configurational isomers. Here the two acyl group can act as ancillary H-bond acceptor which can increase its affinity towards anions with H-bond donor sites such as dihydrogenphosphate due to enforced complementarity (Figure 4.4).

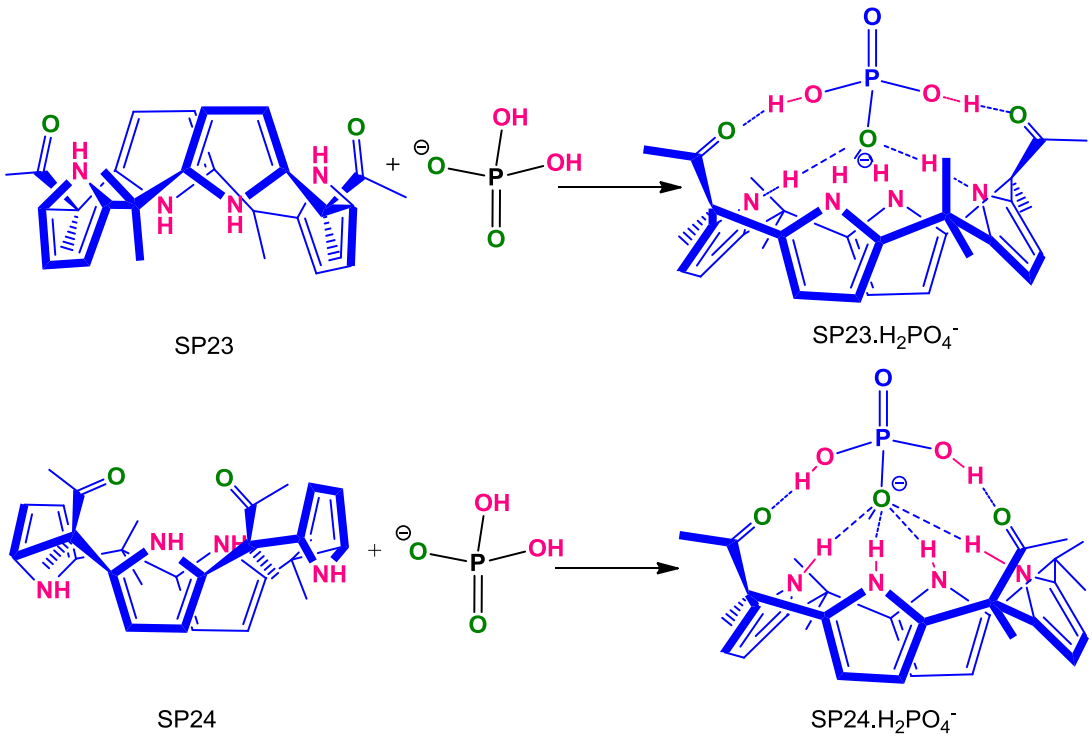

Figure 4.4 Schematic representation of the binding mode of **SP23** and **SP24** with dihydrogenphosphate.

4.3 Results and discussion

4.3.1 Synthesis and structural characterization of 5,15-*meso*-diacylcalix[4]pyrrole SP23

The synthesis of 5,15-diacylcalix[4]pyrrole was achieved via two simple steps. The motivation for this work came from the unexpected synthesis of **SP12** from 2,3-butandione while attempting to synthesize the *meso-meso* directly linked bisdipyrromethane **SP7**. Our attempts to convert the diketone to bisdipyrromethane only resulted in the exclusive formation of **SP12** along with minor amount of **SP13** (Scheme 4.7). This reaction was described in brief earlier in chapter 3. To our knowledge, this is the second instance in

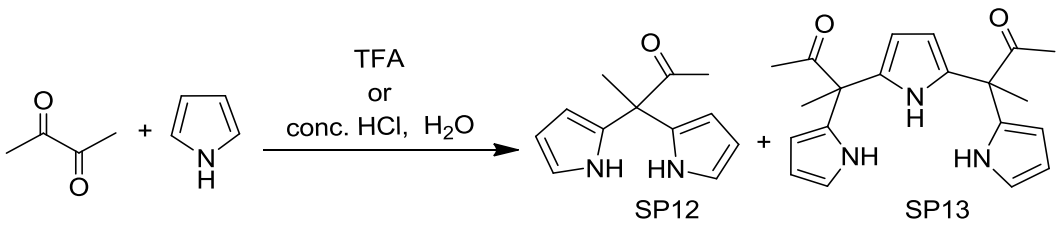

Scheme 4.7 Reaction of 2,3-butandione with pyrrole.

literature, where only one of the carbonyl moiety of a dicarbonyl compound could be selectively converted to dipyrromethane without using any protecting group, the earlier being conversion of a sterically rigid and congested acenaphthenequinone to its corresponding monodipyrromethane.[30] The selective formation of dipyrromethane **SP12** may be attributed to the steric hindrance imposed by the two pyrrole moieties towards the third incoming pyrrole.

The desired calix[4]pyrrole derivatives **SP23** were synthesized using [2+2] condensation method (Scheme 4.8). The self-condensation of **SP12** with acetone in dichloromethane using $BF_3.OEt_2$ as catalyst resulted two clear close spots in TLC. On the basis of literature, our presumption is that, either they are the two configurational isomers of **SP23** resulting from [2+2] condensation or a mixture of [2+2] and [2+2+2] condensation product *i.e.* calix[6]pyrrole. After the regular work up, the compounds were isolated by column chromatography with 20% EtOAc in hexane as eluent. ^{1}H NMR spectral analysis in $CDCl_3$ displayed almost similar spectra for both compounds, with one NH peak at ~7.4 ppm and two

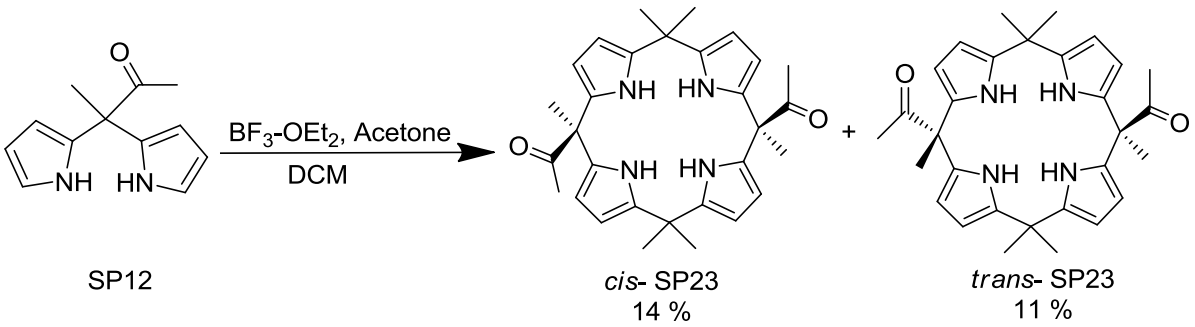

Scheme 4.8 Syntheses of **SP23**.

β-pyrrole CH peaks with equal intensity (1:1:1). The absence of *α*-^{1}Hs indicated the formation of macrocycle. In the aliphatic region as expected three different types of -CH_3 protons were observed with intensity ratio (1:1:2). But in CD_3CN the more polar fraction showed four -CH_3 signals with intensity 1:1:1:1. Further, ^{13}C NMR analysis showed one more signal for this fraction at ~ 29 ppm. However, ^{13}C NMR spectrum of the first compound

(nonpolar one) could not be recorded in CD_3CN owing to its poor solubility. Remarkably, the LCMS analysis showed m/z value 484 for both the compounds, indicating the formation of diacylated calix[4]pyrroles excluding the possible formation of any hexapyrrolic or higher macrocycles. From the above spectroscopic studies, we could infer that both the compounds are the configurational isomers of diacylcalix[4]pyrrole **SP23,** which can be designated as *cis* ($\alpha\alpha$) or *trans* ($\alpha\beta$) depending upon the disposition of the acyl groups with regard to the calix[4]pyrrole moiety (scheme 4.8). Further, their structural integrity could be unequivocally assigned in the solid state via X-ray diffraction analysis. The solid state structure clearly revealed the *cis* and *trans* orientation of the *meso*-acyl substituents with respect to the calix[4]pyrrole moiety in the first and second fraction respectively.

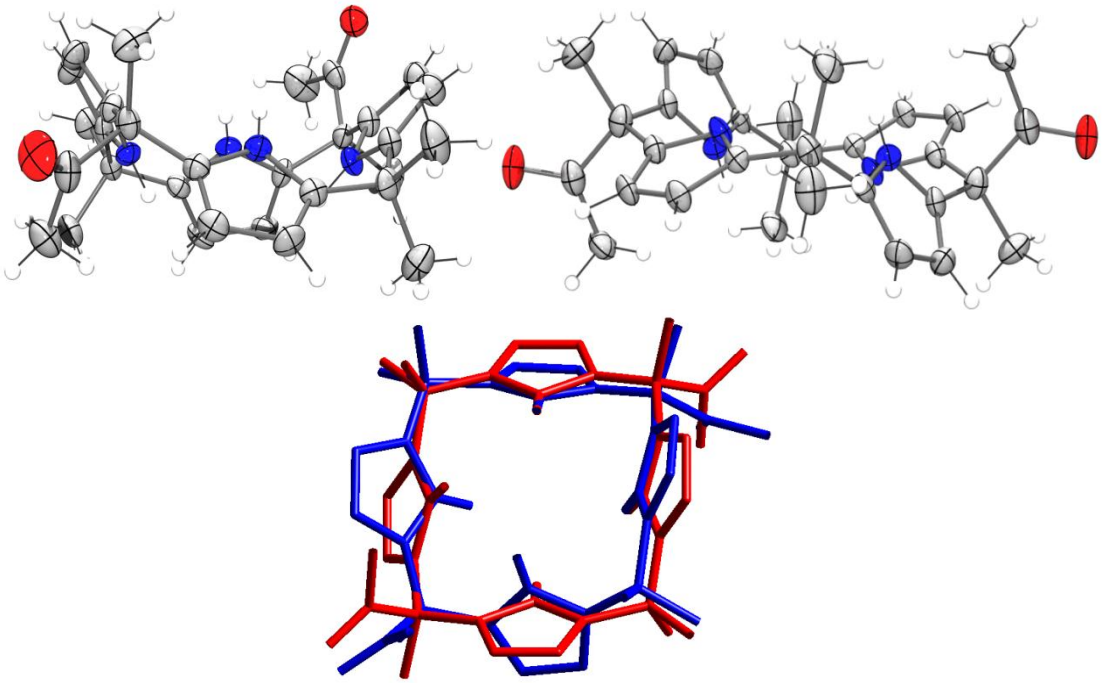

Figure 4.5 Top: ORTEP diagram of *trans*-**SP23** in 1,3-alternate (left) and 1,2-alternate conformation (right). The displacement ellipsoids were drawn at the 35% probability level. Bottom: Overlay diagram of the two polymorphic structure red: 1,2-alternate conformation, blue: 1,3-alternate conformation.

While trying to grow single crystals for compound *trans*-**SP23,** we obtained two polymorphic structures (Figure 4.5). The single crystal, grown by slow evaporation of acetonitrile solution, displayed pyrroles in regular 1,3-alternate conformation (Pbca space group), whereas the crystal obtained by slow evaporation of ethyl acetate solution exhibited

1,2-alternate conformation (I4(1)/a space group) of pyrroles. The overlay diagram showing the different orientation of the pyrrole rings in the two forms of the *trans*-**SP23** isomer is shown in Figure 4.5. Lattice energies of the two polymorphs of *trans*-**SP23** (1,3- and 1,2-alternate) were computed using the Dreiding force fields in the Cerius2 program package. The calculations yielded an overall energy of -474.159 kcal.mol^{-1} for 1,3-alternate (Pbca) form and -466.228 kcal.mol^{-1} for 1,2-alternate (I4(1)/a) form, indicating the thermodynamically higher stability of the former. The crystal packing study of the Pbca polymorph, where the pyrroles adopted 1,3-alternate conformation, displayed intermolecular H-bonding between one of the acyl oxygens with the NH of another macrocycle and vice versa to form a dimeric structural motif which were again interconnected via N-H…O hydrogen bonding with another dimer (Figure 4.6). On the other hand, the single crystal structure of I4(1)/a polymorph of *trans* isomer revealed that each acyl groups involved in

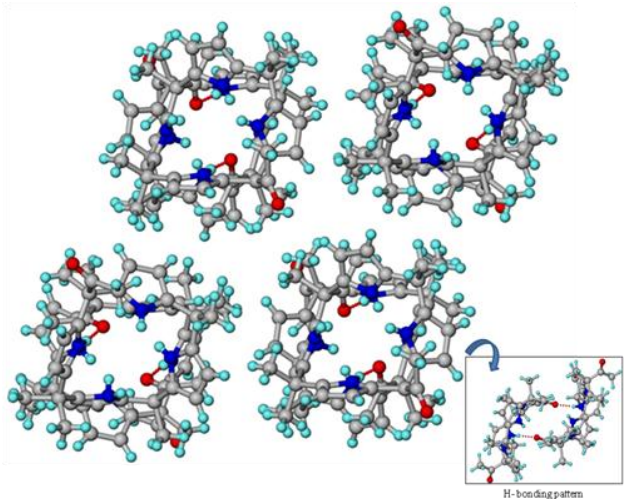

Figure 4.6 POV-Ray picture of hydrogen bonding pattern in Pbca form of *trans*-**SP23**.

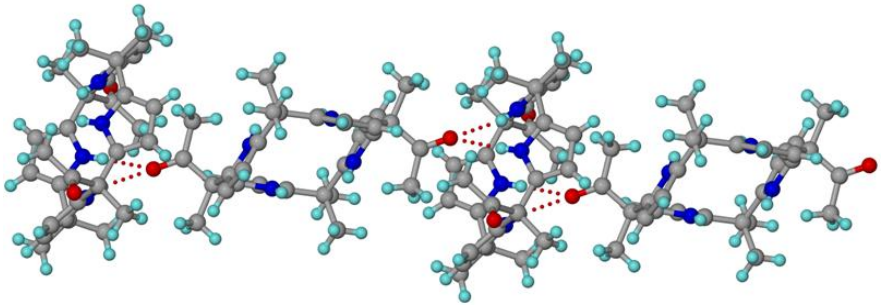

Figure 4.7 POV-Ray picture of Hydrogen bonding pattern in I4(1)/a form of *trans*-**SP23**.

bifurcated N-H···O hydrogen bonding with two adjacent NH of a neighbouring macrocycle and C-H···O hydrogen bonding with the meso methyl group between the two pyrrole units

involved in the bifurcation (Figure 4.7). These weak interactions may be the reason behind the stabilization of the otherwise less favorable 1,2-alternate conformation in the solid state to get the kinetically stable I4(1)/a form.

However, the comparison of the powder X-ray diffraction patterns of *trans*-**SP23** isomer (obtained after column chromatography) with the simulated ones of the two polymorphs (Figure 4.8) revealed its predominant existence in the 1,2-alternate conformation, although the lattice energy calculation indicated 1,3-alternate conformation as the thermodynamically more stable conformation. Further differential scanning calorimetry (DSC) analysis of the

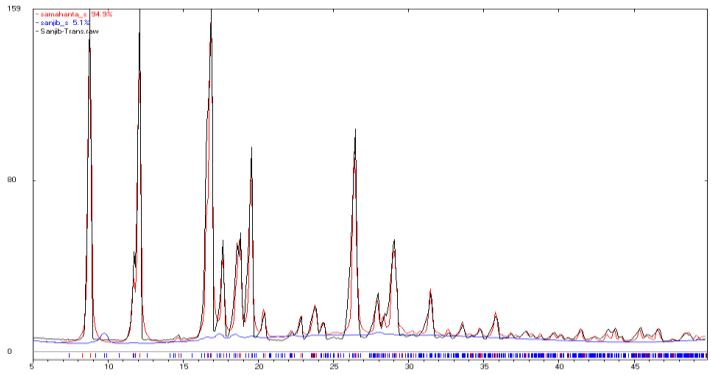

Figure 4.8 Comparison of the powder XRD pattern of the column purified *trans*-**SP23** (black) with the simulated pattern of the I4(1)/a (red) and Pbca (blue) crystals. The powder cell refinement shows I4(1)/a one resembles ~95% and the Pbca one ~5% with the column purified one.

trans-**SP23** showed the phase transition during heat-cool-heat experiment indicating the conversion of the 1,2-alternate form to the thermodynamically stable 1,3-form. To our knowledge, this is the second report in calix[4]pyrrole literature where the macrocycle exists in 1,2-alternate conformation in guest free form in the solid state.[10] However, there is no report on the existence of polymorphic structure in this type of macrocycles. This study indicated that by fine tuning the H-bonding functionality on the periphery of the macrocycle could lead to the other kinetically favorable conformers of calixpyrrole in the solid state.

In contrast, *cis*-**SP23** isomer always crystalized as a solvate. We have crystallized it as dichloromethane, water and methanol solvate (Figure 4.10). The macrocycle when crystallized as water and dichloromethane solvates adopted 1,3-alternate conformation, whereas that in the methanol solvate, adopted 1,2-alternate conformation. For instance,

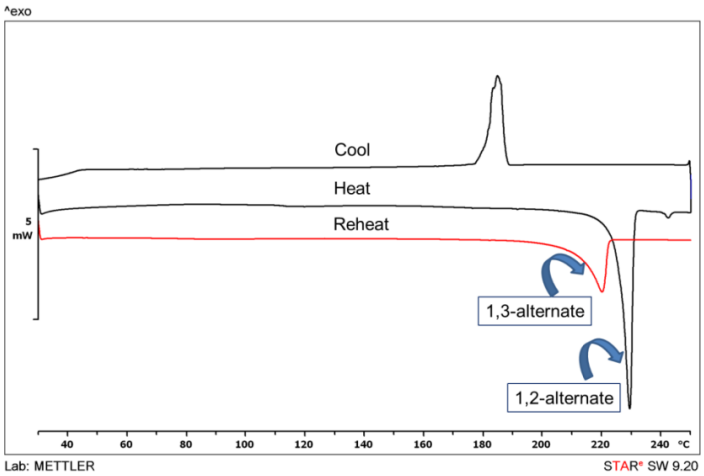

Figure 4.9 DSC pattern of the *trans*-**SP23** showing polymorphic transition.

the crystals obtained by slow evaporation of dichloromethane solution had the macrocycle with one dichloromethane molecule in the asymmetric unit. Here one of the acyl oxygen of one molecule, hydrogen bonded to the pyrrolic-NH of another macrocycle, resulting in the formation of a helical network, where the dichloromethane molecule sits in the helical twist (Figure 4.11). On the other hand, the crystals grown from slow evaporation of the acetonitrile

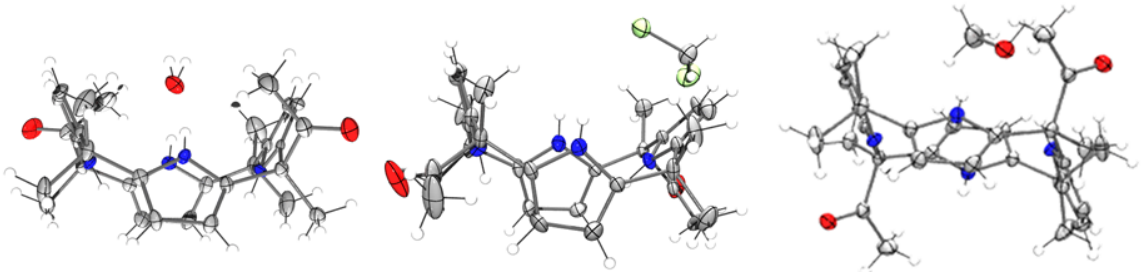

Figure 4.10 ORTEP diagram of *cis*-**SP23**.(H_2O) (left); *cis*-**SP23**.(CH_2Cl_2) in 1,3-alternate conformation (middle) and *cis*-**SP23**.(CH_3OH) 1,2-alternate conformation (right). Displacements ellipsoids were drawn at the 35% probability level.

solution was found to pick up one residual water molecule per asymmetric unit to form a hydrate. The water molecule in the hydrate connected to one of the calixpyrrole moieties via H- bonding to the oxygen of the other acyl substituent. Furthermore, the oxygen atom of the water was found to H-bonded to alternate NHs of another calixpyrrole moiety in the neighboring helical strand and resulted in a chiral helical network in solid state (Figure 4.12). In case of methanol solvate, two molecules of macrocycle and two methanol molecules are present in the asymmetric unit where each methanol molecule form one bifurcated N-H···O

H-bonding with two adjacent pyrrole moieties of one macrocycle and O-H···O H-bonding with acyl group of another macrocycle in opposite side. Here formation of the bifurcated H-bonding favors the 1,2-alternate conformation in the solid state (Figure 4.13).

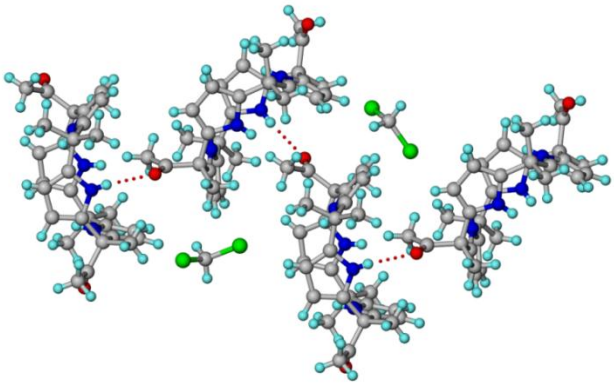

Figure 4.11 POV-Ray picture of the packing pattern in the crystal structure of *cis*-**SP23**.CH_2Cl_2.

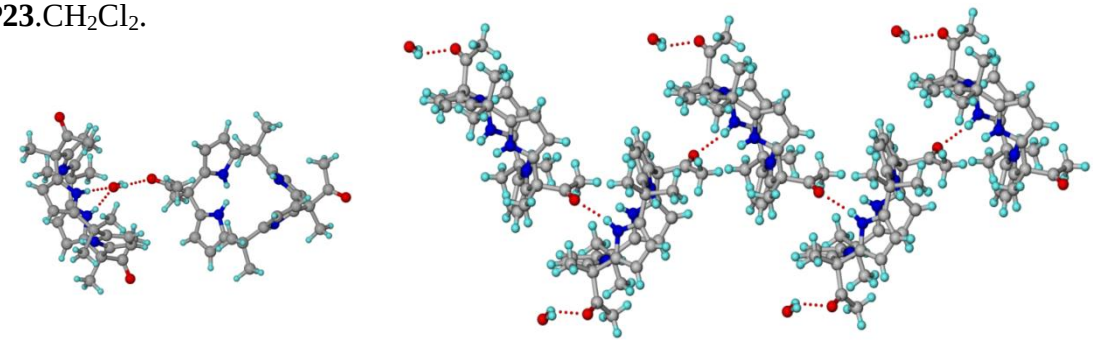

Figure 4.12 POV-Ray picture showing hydrogen bonding pattern (left) and packing pattern in the crystal structure of *cis*-**SP23**.H_2O.

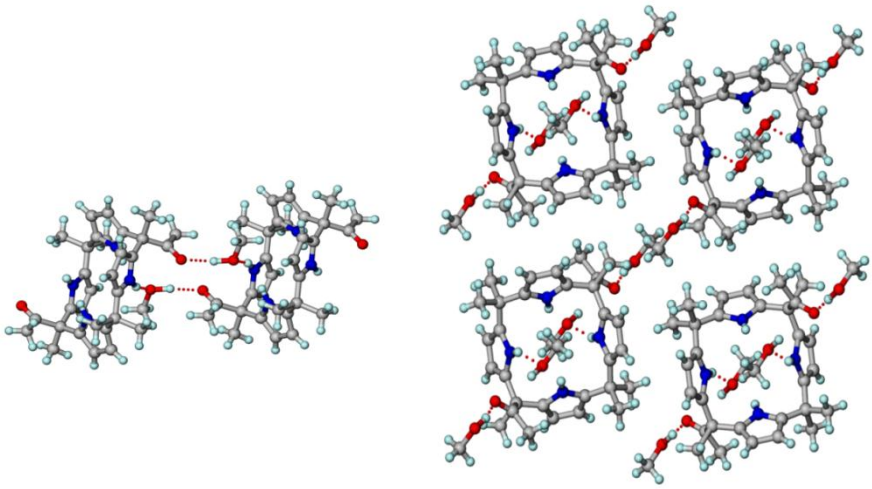

Figure 4.13 POV-Ray picture showing hydrogen bonding pattern (left) and the packing pattern in the crystal structure of *cis*-**SP23**.CH_3OH.

4.3.2 Synthesis and structural characterization of 5,10-*meso*-diacylcalix[4]pyrrole SP24

Compound **SP24** was synthesized by following a two-step protocol where the first step involved the synthesis of tripyrrane **SP13**, followed by its acid catalyzed [3+1] condensation with pyrrole in presence of acetone. This work resulted owing to the accidental detection of trace amount of **SP13**, while trying to synthesize *meso-meso* linked bisdipyrromethane **SP7**. In order to optimize the formation of **SP13**, initially we followed Sessler's protocol.[22] However, this only resulted in the formation of dipyrromethane **SP12** (31%) along with a colorless liquid compound. ^{1}H NMR spectroscopic analysis of the latter compound displayed a similar spectrum like dipyrromethane **SP12**, however an additional broad singlet appeared

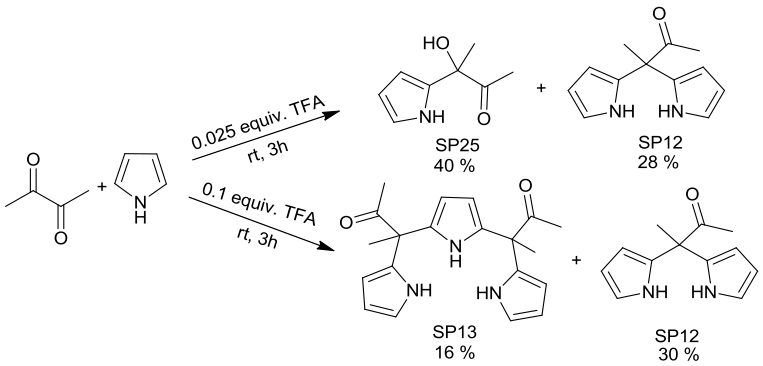

Scheme 4.9 Synthesis of tripyrrane **SP13**.

at 4.59 ppm. Furthermore, the intensity ratio of α and β-pyrrolic protons, NH and *meso*-methyl and acyl-methyl protons along with the new signal appeared as 1:2:1:3:3:1 (that in case of the **SP12** is 2:4:2:3:3 without the new signal). On the other hand, the corresponding ^{13}C NMR spectrum showed disappearance of the peak at 52.74 ppm (as observed in **SP12**), with concomitant evolution of a new peak at 77.45 ppm. Deuterium exchange study revealed the exchangeable nature of the peak at 4.59 ppm and hence led us to tentatively presume the structure as a pyrrole-2-carbinol **SP25** (Scheme 4.9). LCMS didn't provide any consistent data (m/z + 1 = 136 and m/z + 1 = 154), may be owing to its instability during the operating

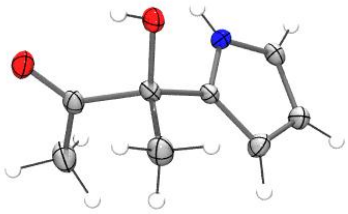

Figure 4.14 ORTEP diagram of **SP25**, with the displacement ellipsoids drawn at the 35% probability level.

condition. In order to understand its structure unequivocally, we tried to grow single crystals at low temperature. Fortunately, crystals were found at keeping the compounds at -20 °C and the solid state structure obtained via single crystal X-ray diffraction analysis at 100 K confirmed our presumption (Figure 4.14). To our knowledge, this is the first stable, structurally characterized pyrrole-2-carbinol with alkyl substituents. Even though mono alkyl and/or aryl pyrrole-2-carbinol are well known in porphyrinogen chemistry[31] but the diaryl or alkyl-functional group substituted pyrrole-2-carbinols are quite rare in literature.[32] Subsequently, we optimized the reaction condition, in order to obtain the desired tripyrrane **SP13**, which involved addition of higher equivalent of TFA (0.1 instead of 0.025 equiv.) to a

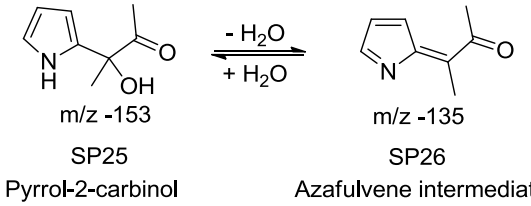

Scheme 4.10 Conversion of pyrrol-2-carbinol to azafulvene intermediate.

mixture of pyrrole and 2,3-butandione (molar ratio 3:1) and stirring it for 3h followed by quenching with excess triethylamine. The column chromatographic isolation yielded tripyrrane **SP13** (16 %) along with dipyrromethane **SP12** (Scheme 4.19). This observation led us to conclude that at higher acid concentration, the pyrrole-2-carbinol to azafulvene intermediate conversion (Scheme 4.10) is more facile, resulting in the formation of the desired tripyrrane.[33] The unexpected stability of compound **SP25** may be attributed to the

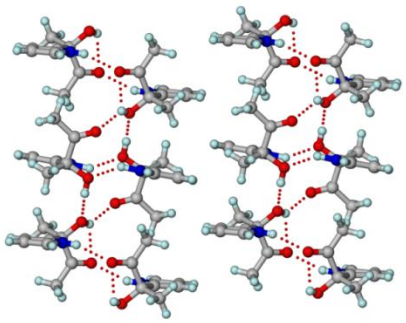

Figure 4.15 Packing diagram of **SP25**.

presence of strong O-H···O and N-H···O hydrogen bonds (Figure 4.15). In order to check the fate of the reaction, we monitored the acid catalyzed homo-condensation reaction of the pyrrole-2-carbinol using mass spectroscopy, which clearly provided mass of some azafulvene

intermediates indicating the formation of azafulvene intermediate during the course of the reaction and led us to infer that at low acid concentration (with 0.05 equiv. of TFA), the pyrrole-2-carbinol **SP25** to azafulvene **SP26** conversion is not efficient. The self-condensation study further indicated that the stability of these intermediates depends on the amount of acid used. The mass and the structure of the azafulvenes observed upon the study are shown in table 4.8.

Table 4.8 Probable structure of the compounds corresponding to the m/z values found in the HRMS analysis of homocondensation reaction.

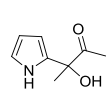 m/z (M+Na) = 176.0687	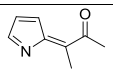 m/z (M+H) = 136.0762	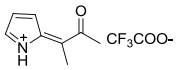 m/z = 249.0613	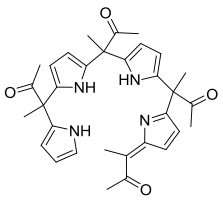 m/z (M+H) = 541.2815
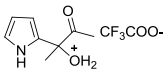 m/z = 267.0718	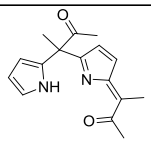 m/z (M+H) = 271.1447	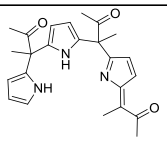 m/z (M+H) = 406.2131	

The plausible mechanisms for the formation of the above azafulvene intermediates are shown below:

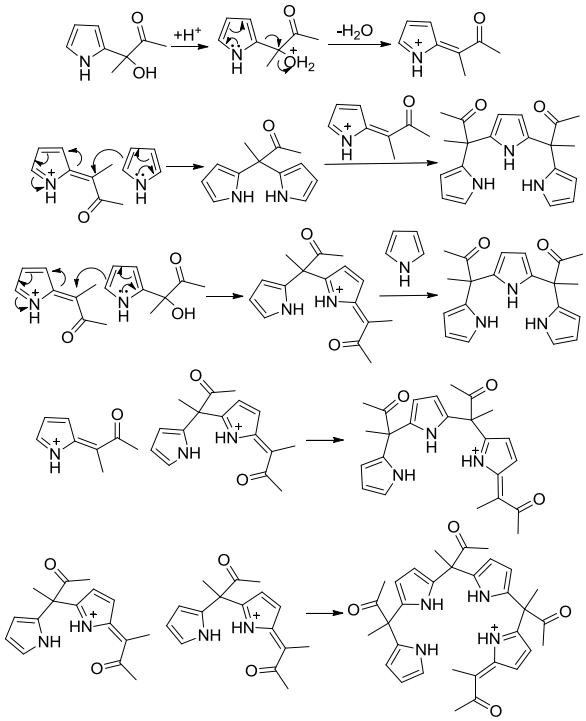

Scheme 4.11 Plausible mechanism for the formation of **SP12**, **SP13** and different azafulvenium intermediates observed during the HRMS analysis.

Further the structure and orientation of the two acyl groups in **SP13** was unequivocally established form the single crystal grown by crystallizing the oily material at low temperature (Figure 4.16). The solid state structure showed the *cis* disposition of the two acyl groups w.r.t. the tripyrrane skeleton with the two oxygens residing away from each other.

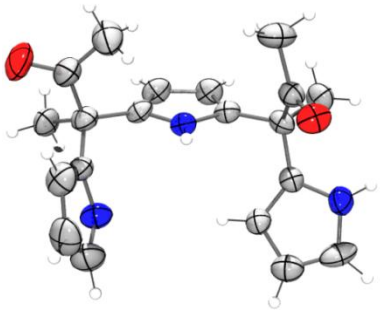

Figure 4.16 ORTEP of **SP13**, with the displacement ellipsoids drawn at the 35% probability level.

With the desired precursor in hand, finally we could successfully carried out the condensation of the tripyrrane **SP13** with pyrrole and acetone using $BF_3.OEt_2$ as a catalyst in dichloromethane solvent, at room temperature to obtain the desired macrocycle 5,10-diacylcalix[4]pyrrole **SP24**, as a mixture of five compounds (Scheme 4.12). In this case we did the reaction for longer time (12 h), such that sufficient acidolysis occur to form the *trans*-isomer in reasonable quantity. Subsequent purification by silica gel column chromatography

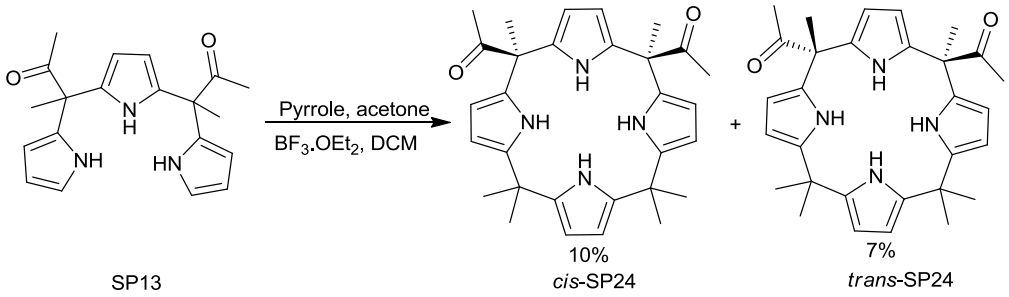

Scheme 4.12 Syntheses of **SP24**.

of the reaction mixture resulted in the isolation of *trans*-**SP24** (7 %) followed by the *cis*-**SP24** (10%) as white solids as the more polar fractions, along with the first three fractions as *meso*-octamethyl calix[4]pyrrole **L48** and two configurational isomers of 5,15-diacylcalix[4]pyrrole **SP23** (forms due to acidolysis) as the unwanted product. Both the isomers of **SP24** were characterized by ^1H and ^{13}C NMR, mass, IR and elemental analysis. ^1H NMR spectra of both isomers revealed the presence of three types of NH protons with

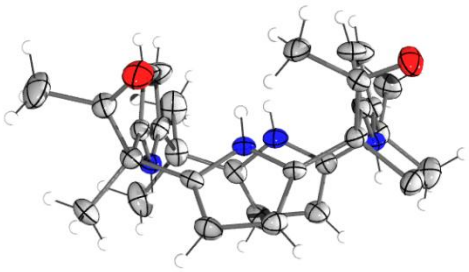

Figure 4.17 ORTEP diagram of *cis*-**SP24**, with the displacement ellipsoids drawn at the 35% probability level.

intensity ratio 1:2:1 and 1:1:2 for the *cis* and *trans* isomers respectively thereby indicating the asymmetric nature of their hydrogen bonding cavity. Further, the structural integrity of the *cis*-isomer (crystals grown by slow evaporation of an ethyl acetate solution) could be unequivocally assigned in the solid state via X-ray diffraction analysis (Figure 4.17). The structure clearly reveals the *cis*-orientation of the *meso*-acyl substituents with respect to the

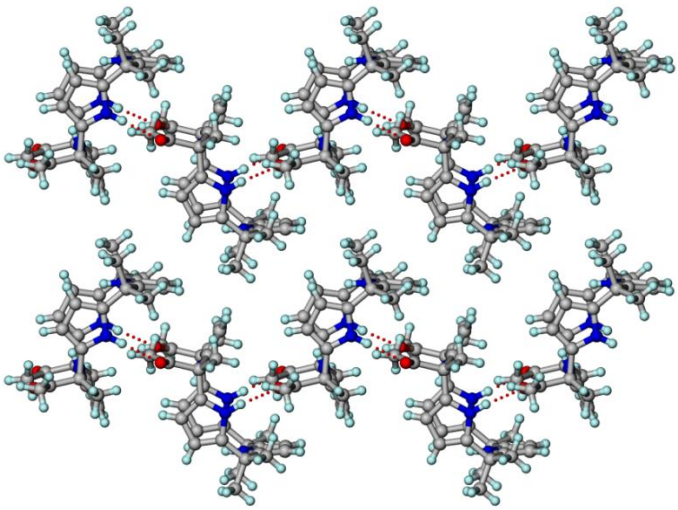

Figure 4.18 Packing diagram of *cis*-**SP24**.

calix[4]pyrrole moiety, along with the regular 1,3-alternate conformation of the pyrrole units. Interestingly, one acyl moiety orient towards the binding domain of the calix[4]pyrrole, while the other one resides away, probably to minimize the nonbonding repulsive interaction between them. Further, the crystal packing displays intermolecular hydrogen bonding between the two acyl oxygens with the NHs of adjacent macrocycle, while its two NHs (directed away from the acyl groups) form H-bonding with the two acyl oxygens of another calixpyrrole moiety, to form a two-dimensional helical network (Figure 4.18). Unfortunately our efforts to obtain good quality single crystals of *trans*-**SP24** could not be realized so far.

4.3.3 Anion binding study

Preliminary solution phase anion binding behavior of the four isomers were carried out by ^{1}H NMR titration studies in $CDCl_3$ with various anions viz. F^-, Cl^-, Br^-, I^-, $H_2PO_4^-$, HSO_4^-, ClO_4^- and NO_3^- as their tetrabutylammonium (TBA) salts. Due to the poor solubility of *trans*-isomers in acetonitrile NMR experiments could not be performed. However, the binding affinities could be evaluated in acetonitrile using isothermal titration calorimetry (ITC). It is observed that all isomers show a general affinity toward halides and dihydrogenphosphate

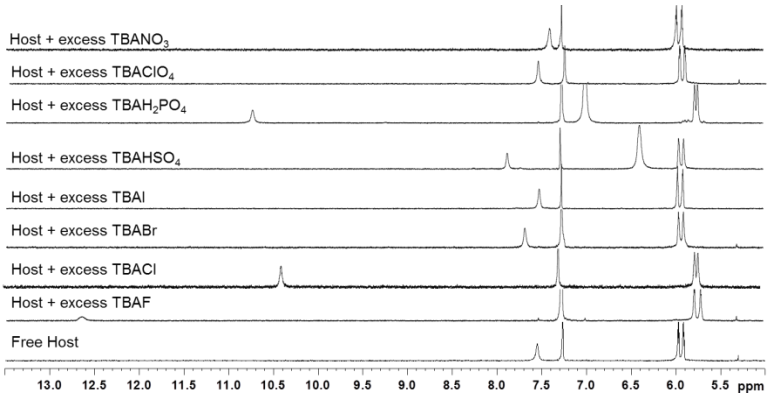

Figure 4.19 Anion screening of *cis*-**SP23** in $CDCl_3$ by ^{1}H NMR technique.

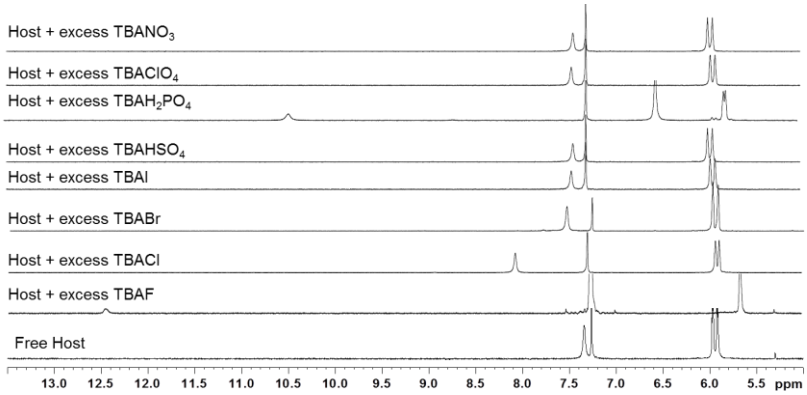

Figure 4.20 Anion screening of *trans*-**SP23** in $CDCl_3$ by ^{1}H NMR technique.

ion, among the studied oxoanions and none bind to I^-, HSO_4^-, ClO_4^- and NO_3^-. The anion screening experiment of the two isomers of **SP23** revealed that *cis*-**SP23** display comparatively higher affinity for anions than the *trans*-isomer (Figure 19-20). The quantitative ^{1}H NMR titration revealed that with gradual addition of anions in the $CDCl_3$ solution, like **L48** the NH resonance shifts towards downfield, indicating the occurrence of NH…anion H-bonding, while upfield shift was observed for the *β*-CH resonances indicating the increase in the electron density in the pyrrole rings due to the formation of NH…anion H-

bonding. Both in case of *cis*- and *trans*-**SP23**, the order of shift of the NH signal, for different anions is F^- > $H_2PO_4^-$ > Cl^- >Br^-, whereas other anions did not show any reasonable change. Upon complexation, the NMR spectra of the **SP23** isomers displayed a single peak for NH signal indicating the symmetric nature of the binding domain before and after complexation. Competitive NMR experiment between $H_2PO_4^-$ and Cl^- ions revealed that in case of *cis*-isomer, $H_2PO_4^-$ can displace Cl^- ion immediately, whereas in case of its *trans*-counterpart the displacement process is rather slow (Figure 4.21-4.24). Job's plot analysis indicated formation of 1:1 stoichiometric complexes for both the isomers of **SP23** with fluoride and dihydrogenphosphate ions (Figure 4.25-4.26).

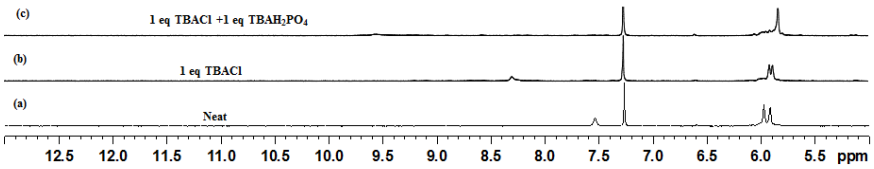

Figure 4.21 ^{1}H NMR spectra (in $CDCl_3$) of (a) *cis*-**SP23**, (b) addition of 1 equiv. of TBACl, and (c) after addition of 1equiv. of $TBAH_2PO_4$ to (b).

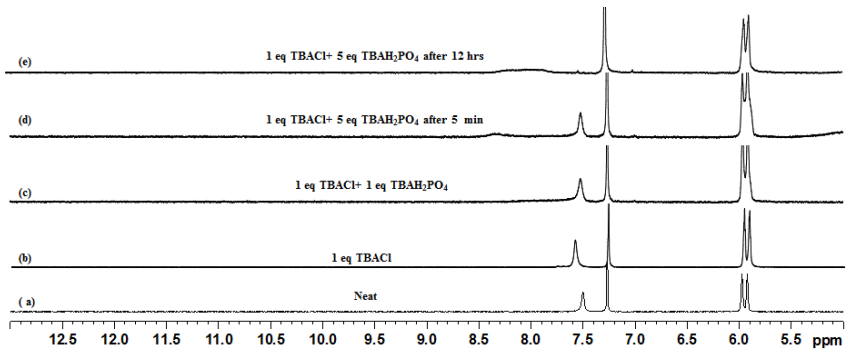

Figure 4.22 ^{1}H NMR spectra (in $CDCl_3$) of (a) *trans*-**SP23**, (b) addition of 1 equiv. of TBACl, (c) after addition of 1equiv. of $TBAH_2PO_4$ to (b), (d) 5 min after addition of 5 equiv. of $TBAH_2PO_4$, and (e) after 12 h.

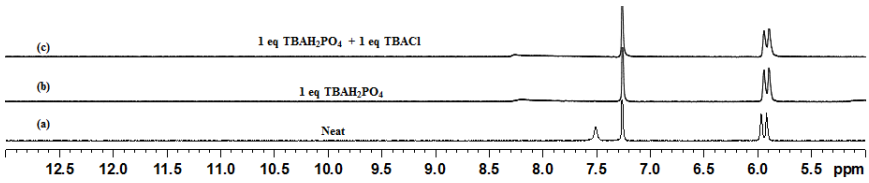

Figure 4.23 ^{1}H NMR spectra (in $CDCl_3$) of (a) *cis*-**SP23**, (b) addition of 1 equiv. of $TBAH_2PO_4$, and (c) after addition of 1equiv. of TBACl to (b).

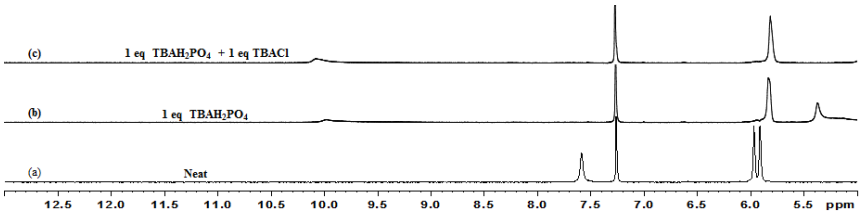

Figure 4.24 ^{1}H NMR spectra (in $CDCl_3$) of a) *trans*-**SP23**, b) after adding 1 equiv. of $TBAH_2PO_4$, and c) after adding 1 equiv. of TBACl to (b).

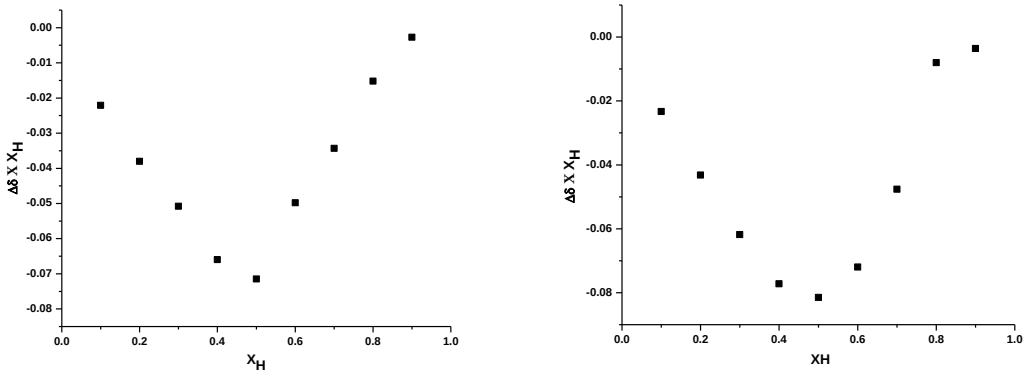

Figure 4.25 Job's plot in $CDCl_3$. left: *cis*-**SP23** vs F^-, right: *trans*-**SP23** vs F^-.

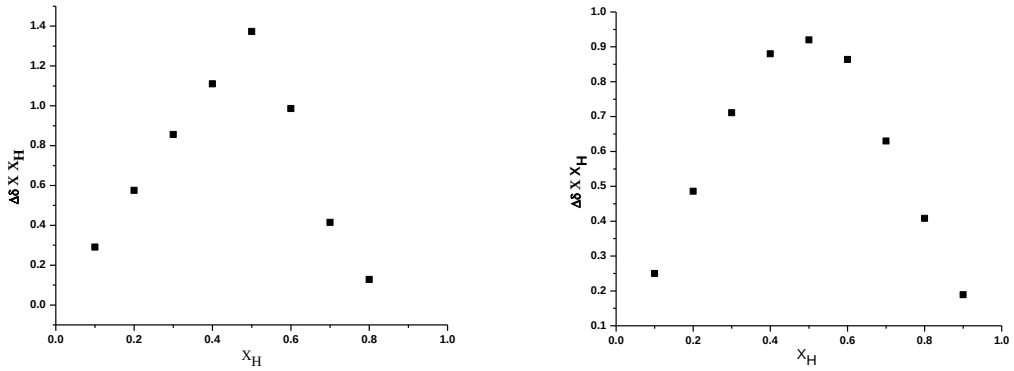

Figure 4.26 Job's plot in $CDCl_3$. left: *cis*-**SP23** vs $H_2PO_4^-$ and right: *trans*-**SP23** vs $H_2PO_4^-$

On the other hand, ^{1}H NMR spectra of both isomers of **SP24** revealed the presence of three types of NH protons, thereby indicating the asymmetric nature of their H-bonding cavity. Preliminary anion binding studies carried out on both the isomers using ^{1}H NMR titration studies in $CDCl_3$ displayed a general affinity towards halides and $H_2PO_4^-$ ion among the studied oxoanions by both isomers and neither bind to I^-, NO_3^-, HSO_4^- and ClO_4^-, a trend earlier noticed in case of **SP23** (Figures 4.27-4.28).

Quantitative binding studies showed the general trend of distinct down field shift for NH and upfield shift for *β*-CH proton signals with gradual addition of anion indicating the formation of N-H…anion hydrogen bonds. Further, ^{1}H NMR titration analyses revealed the onset of a very fast complexation-decomplexation equilibria in case of *cis*-**SP24**.F^-, *trans*-**SP24**.F^- and *cis*-**SP24**.$H_2PO_4^-$ complexes, since addition of approximately 0.2 equiv. of the

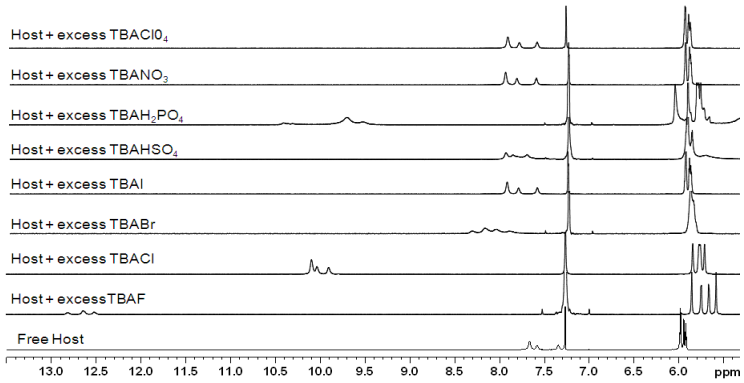

Figure 4.27 ^{1}H NMR titration plot of *cis*-**SP24** vs. tetrabutylammonium salt of different anions in $CDCl_3$.

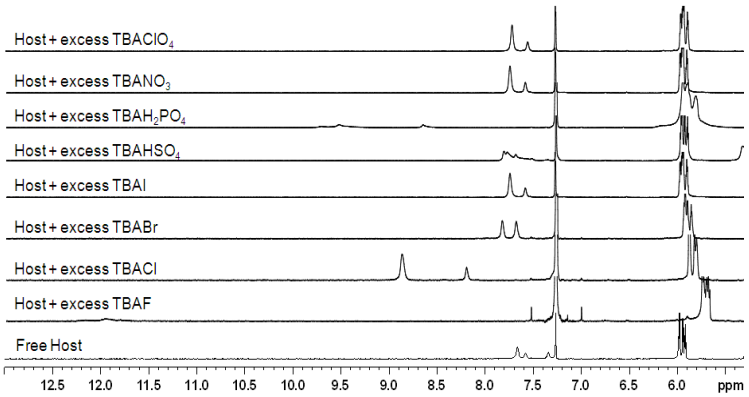

Figure 4.28 ^{1}H NMR titration plot of *trans*-**SP24** vs. tetrabutylammonium salt of different anions in $CDCl_3$.

corresponding salts resulted in the broadening of the pyrrole NH signals and their subsequent disappearance until addition of ~1 equiv. of these salts (Figures 4.29-4.32). On the other hand, in case of *cis*-**SP24.**Cl^- and *cis*-**SP24.**Br^- and *trans*-**SP24.**$H_2PO_4^-$ complexes the NH signals remained intact, indicating the occurrence of a rather slow complexation-decomplexation equilibria in NMR time scale (Figures 4.29-4.32). The formation of more than one singlet corresponding to the NH resonances, both in case of *cis*-**SP24** and *trans*-**SP24** upon complexation with anions, reflects about the retention of the asymmetric nature of their H-bonding core in the resultant complexes. Moreover, the ^{1}H NMR study revealed that the observed anisochronicity of the binding domain is more in case of *trans*-isomer than

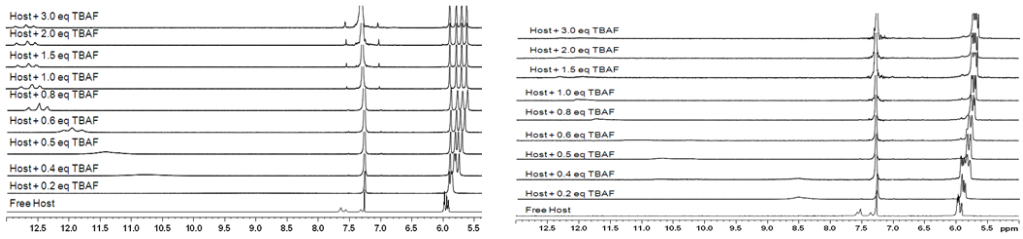

Figure 4.29 ^{1}H NMR titration plot of *cis*-**SP24** (left) and *trans*-**SP24** (right) vs. TBAF in $CDCl_3$.

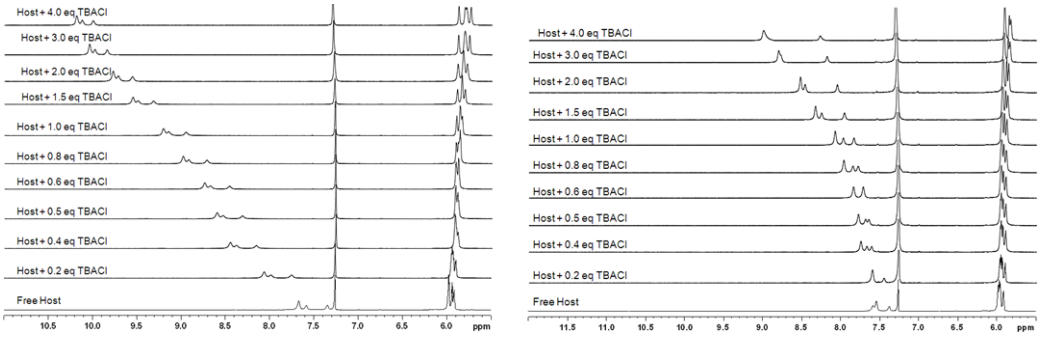

Figure 4.30 ^{1}H NMR titration plot of *cis*-**SP24** (left) and *trans*-**SP24** (right) vs. TBACl in $CDCl_3$.

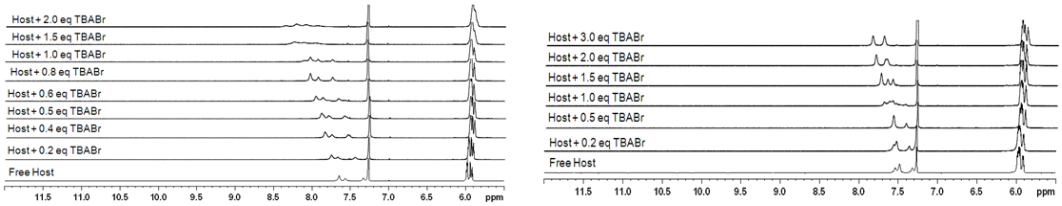

Figure 4.31 ^{1}H NMR titration plot of *cis*-**SP24** (left) and *trans*-**SP24** (right) vs. TBABr in $CDCl_3$.

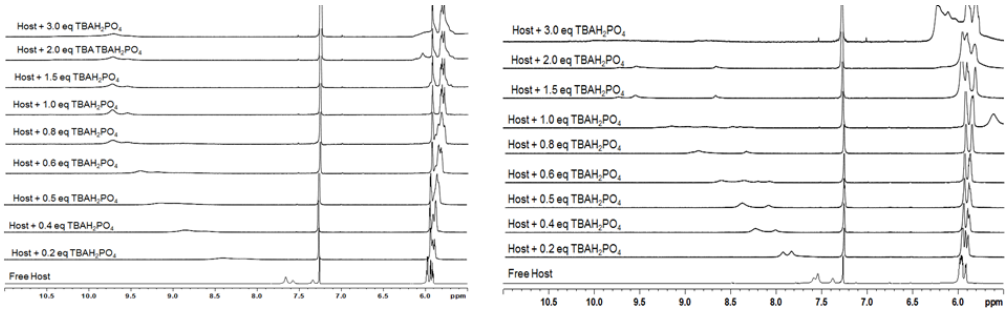

Figure 4.32 ^{1}H NMR titration plot of *cis*-**SP24** (left) and *trans*-**SP24** (right) vs. TBA(H_2PO_4) in $CDCl_3$.

its *cis*- analogue. For example, in case of *trans*-**SP24**, addition of $H_2PO_4^-$ separated the NH peaks by almost 1 ppm (~8.5 ppm and ~9.5ppm), on the other hand, in case of the *cis*-isomer the difference between them is negligible (Figure 4.29-4.32). In addition, in case of *cis*-**SP24**, the *β*-pyrrolic protons, which resonated at 5.90-6.00 ppm appeared as asymmetric multiplet, however addition of 1 equiv. of TBAF, split them into four equivalent singlets, which is not visualized in case of its *trans*-counterpart, supporting our abovementioned observation. A closer inspection revealed that in case of both isomers the affinity order towards anions is F^- > Cl^- ≈$H_2PO_4^-$ > Br^- (shift in NH resonances). However, competitive NMR experiment studies between $H_2PO_4^-$ and Cl^- anions exhibited complete displacement of the Cl^- by the $H_2PO_4^-$ ion

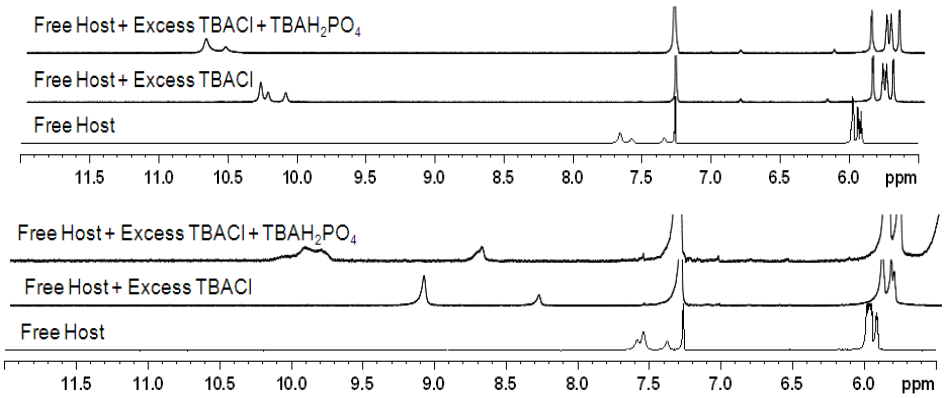

Figure 4.33 ^{1}H NMR competition study of top: *cis*- **SP24**, bottom: *trans*-**SP24** with chloride and dihydrogenphosphate ions in $CDCl_3$.

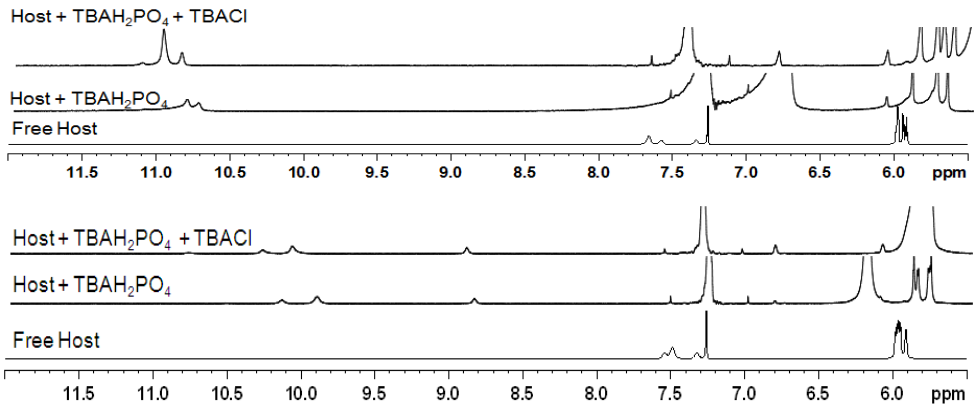

Figure 4.34 ^{1}H NMR competition study of top: *cis*-**SP24**, bottom: *trans*-**SP24** with dihydrogenphosphate and chloride ions in $CDCl_3$.

from the **SP24**.Cl^- complex of both the isomers, indicating comparatively stronger affinity of **SP24** for $H_2PO_4^-$ in chloroform (Figure 4.33-4.34).

Further detailed studies to determine the affinity constants were performed by isothermal titration calorimetry (ITC) in acetonitrile (Figures 4.35-4.42). In contrast to NMR spectroscopic methods, ITC analysis allows one to study the overall heat change of the system including solvent contribution. Thus, it provides direct access to the energetics of the binding event without retreating to a structural probe that may or may not reflect the entirety of the associative processes.[34] A glance at the binding constants obtained (Table 4.9), showed a marginal difference in overall affinity constant between the receptors S**P23** and **SP24**, which is on the expected line owing to their inherent similarity. However, as a significant general trend, it was observed that *cis*-**SP24** possesses relatively higher binding ability than *cis*-**SP23** in case of complexation with F^-, Cl^- and Br^- ions, whereas in case of $H_2PO_4^-$ ion the opposite trend is noticed, which are otherwise higher than that reported for receptor **L48**. In all cases, good fit to 1:1 receptor-anion stoichiometry were obtained. On the other hand, the *trans*-isomers displayed a relatively lower affinity towards anions than **L48**.

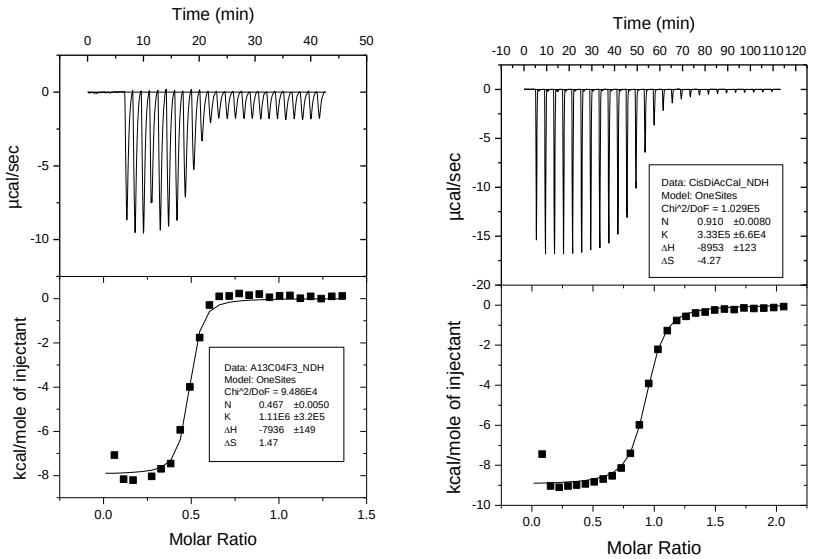

Figure 4.35 ITC in acetonitrile at 303 K of *cis*-**SP23** at 0.4 mM with left: TBAF, right: TBACl. The curve shows the fit of the experimental data to a 1:1 binding profile.

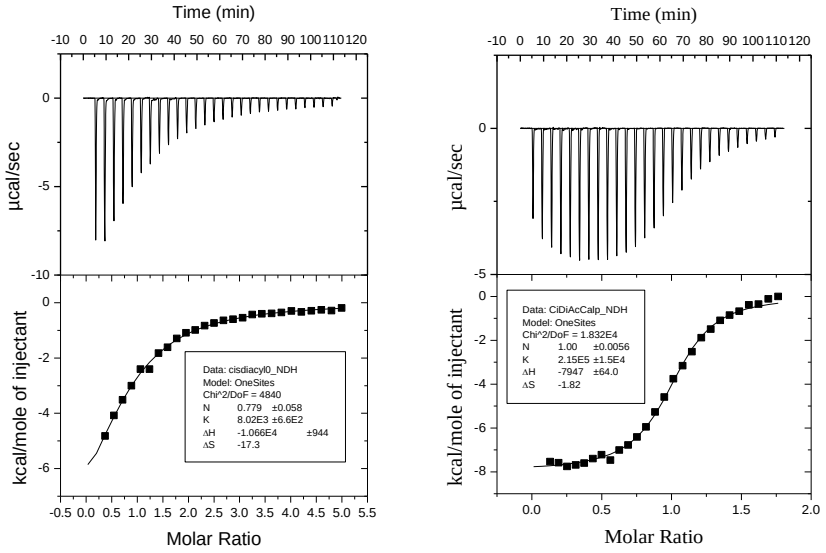

Figure 4.36 ITC in acetonitrile at 303 K of *cis*-**SP23** at 0.4 mM with left: TBABr, right: $TBAH_2PO_4$. The curve shows the fit of the experimental data to a 1:1 binding profile.

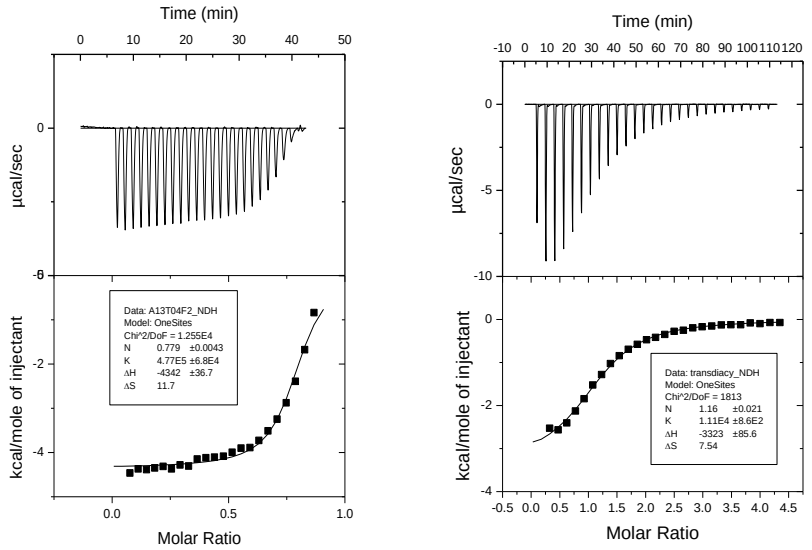

Figure 4.37 ITC in acetonitrile at 303 K of *trans*-**SP23** at 0.4 mM with left: TBAF, right: TBACl. The curve shows the fit of the experimental data to a 1:1 binding profile.

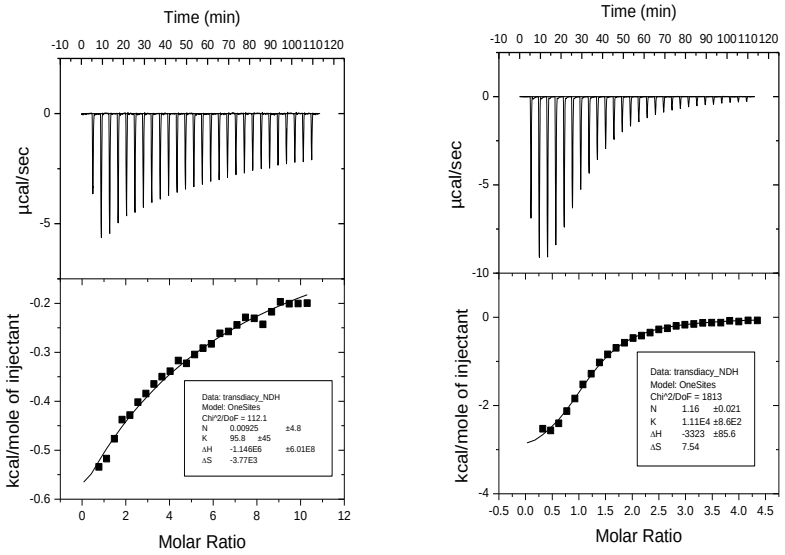

Figure 4.38 ITC in acetonitrile at 303 K of *trans*-**SP23** at 0.4 mM with left: TBABr, right: TBA(H_2P0_4). The curve shows the fit of the experimental data to a 1:1 binding profile.

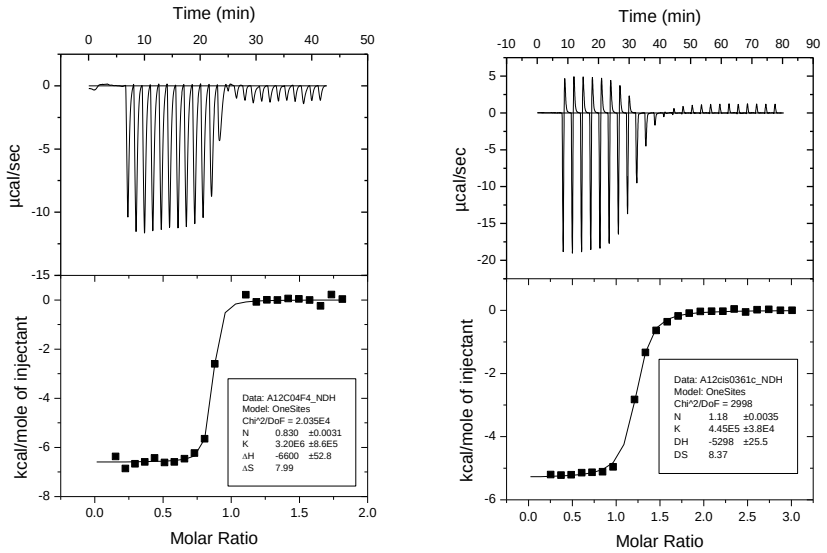

Figure 4.39 ITC in acetonitrile at 303 K of *cis*-**SP24** at 0.4 mM with left: TBAF; right: TBACl. The curve shows the fit of the experimental data to a 1:1 binding profile.

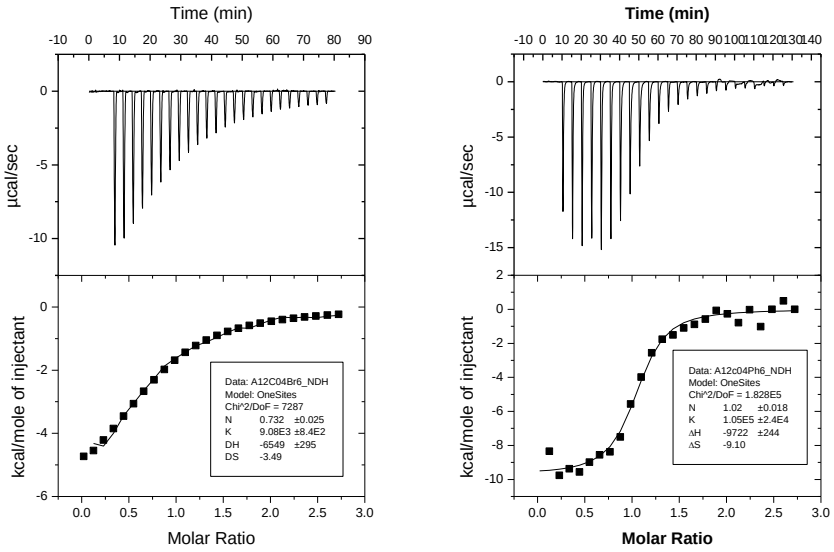

Figure 4.40 ITC in acetonitrile at 303 K of *cis*-**SP24** at 0.4 mM with left: TBABr; right: $TBAH_2PO_4$. The curve shows the fit of the experimental data to a 1:1 binding profile.

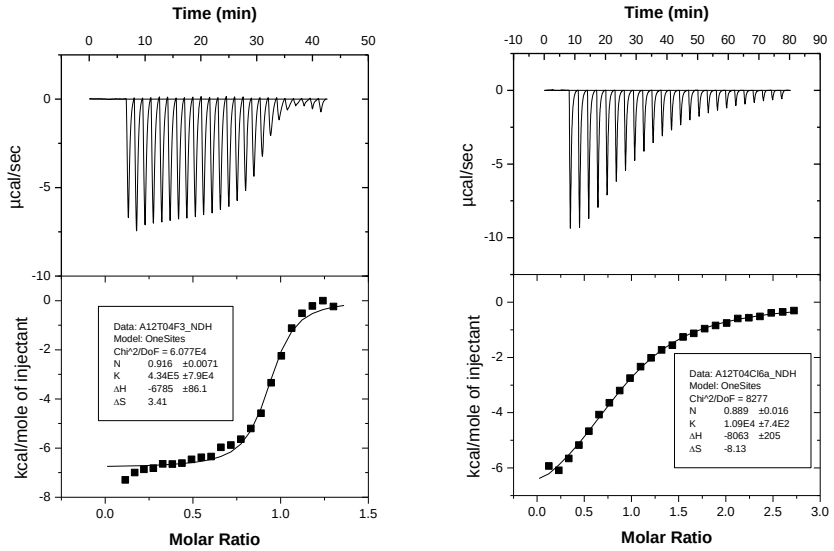

Figure 4.41 ITC in acetonitrile at 303 K of *trans*-**SP24** isomer at 0.4 mM with left: TBAF; right: TBACl. The curve shows the fit of the experimental data to a 1:1 binding profile.

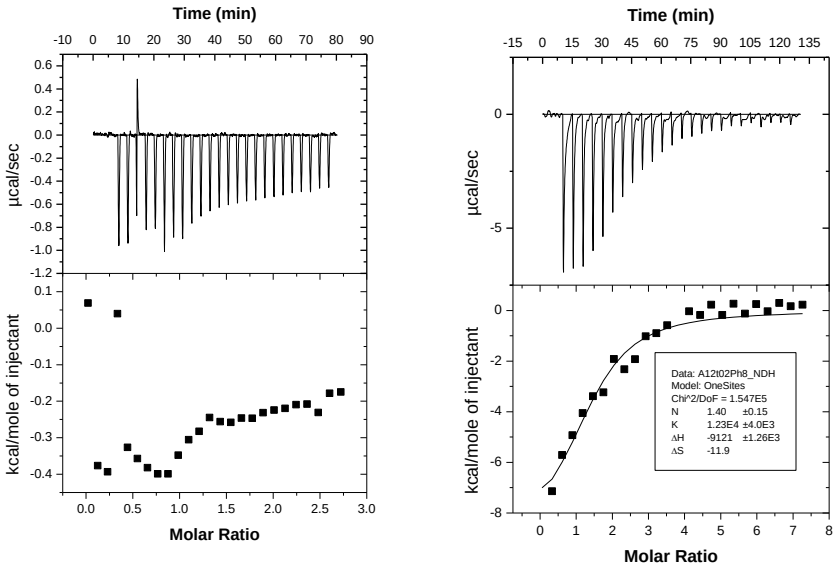

Figure 4.42 ITC in acetonitrile at 303 K of *trans*-**SP24** isomer at 0.4 mM with left: TBABr; right: $TBAH_2PO_4$. The curve shows the fit of the experimental data to a 1:1 binding profile.

A closer look at the thermodynamic parameters obtained from the ITC experiments (Table 4.9) revealed that fluoride complexation is both enthalpically and entropically favoured, although the former contribution is relatively more. On the other hand, in case of other anions the complexation is entropically not favorable (except *cis*-**SP24**.Cl^- and *trans*-**SP23**.$H_2PO_4^-$). The favorable entropy observed upon complexation with fluoride ion, may be attributed to the release of the three water molecules from the hydrated tetrabutylammonium fluoride salt to the bulk solution. Further, the overall enthalpy-entropy compensation in case of dihydrogenphosphate ion is more than that of chloride complexation and hence resulted in the lower value of affinity of the receptors towards dihydrogenphosphate than chloride ion, although NMR experiments in $CDCl_3$ shows the opposite trend. The difference between the observation obtained from ITC in acetonitrile and NMR in chloroform can be ascribed to the fact that the anion binding properties varies depending on properties of the solvent media. The plausible factors that could account for this are differences in ion pairing efficiency in different solvents and these two methods probe different chemistries (*e.g.*, interactions with pyrrolic NHs vs system thermodynamics). Although the data obtained from NMR cannot be directly compared with that from ITC, still qualitatively the reversal of affinity may be assigned to the formation of ion pairs in less polar solvent in NMR ($CDCl_3$). On the other

hand the overall enthalpy-entropy penalty is lower in case of *cis*-**SP23** and *cis*-**SP24** than **L48**, resulting in their higher affinity constants towards dihydrogenphosphate ion.

Table 4.9 Energetics of host-guest binding of the two isomers of **SP23** and **SP24** with tetrabutylammonium salts in acetonitrile at 303 K as determined by isothermal titration calorimetry (ITC).

Anion	Host	TΔS (kcal. mol^{-1})	ΔH (kcal. mol^{-1})	ΔG (kcal. mol^{-1})	K_a (ITC) (M^{-1})
F^-	*cis*-**SP23**	0.44	-7.93	-8.37	1.11×10^6
	cis-**SP24**	2.42	-6.6	-9.02	3.2×10^6
	trans-**SP23**	3.54	-4.34	-7.88	4.77×10^5
	trans-**SP24**	1.03	-6.78	-7.81	4.34×10^5
	L48	ND	ND	ND	ND
Cl^-	*cis*-**SP23**	-1.29	-8.95	-7.66	3.3×10^5
	cis-**SP24**	2.53	-5.29	-7.82	4.45×10^5
	trans-**SP23**	-1.75	-7.06	-5.31	6.77×10^3
	trans-**SP24**	-2.46	-8.06	-5.60	1.09×10^4
	L48[a]	-2.91	-10.16	-7.29	2.2×10^5
Br^-	*cis*-**SP23**	-1.24	-6.84	-5.6	1.1×10^4
	cis-**SP24**	-1.05	-6.54	-5.49	9.08×10^3
	trans-**SP23**	BDL	BDL	BDL	BDL
	trans-**SP24**	BDL	BDL	BDL	BDL
	L48[b]	-3.56	-8.34	-4.77	2.7×10^3
$H_2PO_4^-$	*cis*-**SP23**	-0.546	-7.94	-7.40	2.15×10^5
	cis-**SP24**	-2.75	-9.72	-6.97	1.05×10^5
	trans-**SP23**	2.262	-3.32	-5.58	1.16×10^4
	trans-**SP24**	-3.60	-9.12	-5.52	1.23×10^4
	L48	-3.27	-9.774	-6.504	4.5×10^4

ND: Not determined by ITC. BDL: Below detection limit of ITC. (a) from reference 11d, (b) from reference 11b.

Although the exact nature of the host-guest interaction could not be ascertained owing to lack of good quality diffraction grade crystals, however, the DFT optimized structure of the

complexes in gas phase confirmed the above presumption (Figure 4.43-4.48). The enhanced affinity of both the *cis*-isomers towards dihydrogenphosphate ion (compared to **L48**) may be attributed to the additional C=O···H-O hydrogen bonds between the carbonyl oxygen and

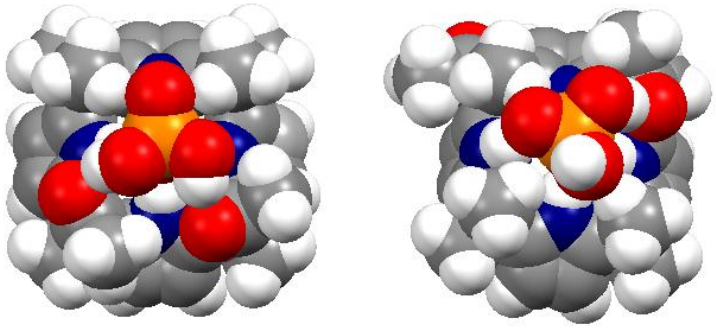

Figure 4.43 Space filling model of DFT-optimized structure of [*cis*-**SP23.**H_2PO_4]$^-$ (left) and [*trans*-**SP23.**H_2PO_4]$^-$ (right). Color code: red: O, blue: N, orange: P, grey: C and white: H.

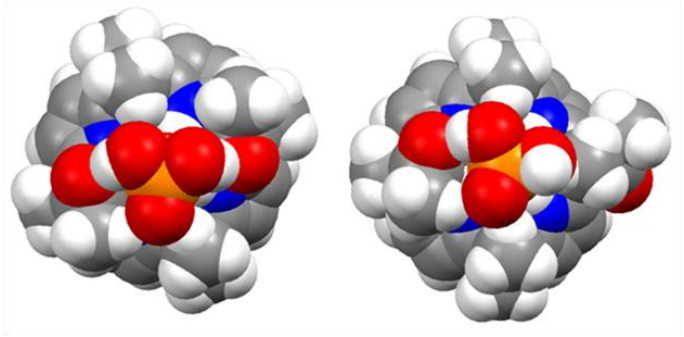

Figure 4.44 Space filling model of DFT-optimized structure of [*cis*-**SP24**.H_2PO_4]$^-$ (left) and [*trans*-**SP24**.H_2PO_4]$^-$ (right). Color code: red: O, blue: N, orange: P, grey: C and white: H.

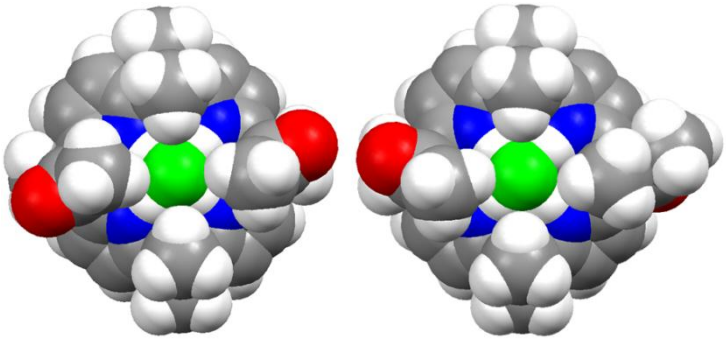

Figure 4.45 Space filling model of DFT-optimized structure of [*cis*-**SP23**.F]$^-$ (left) and [*trans*-**SP23**.F]$^-$. Color code: red: O, blue: N, green: F, grey: C and white: H.

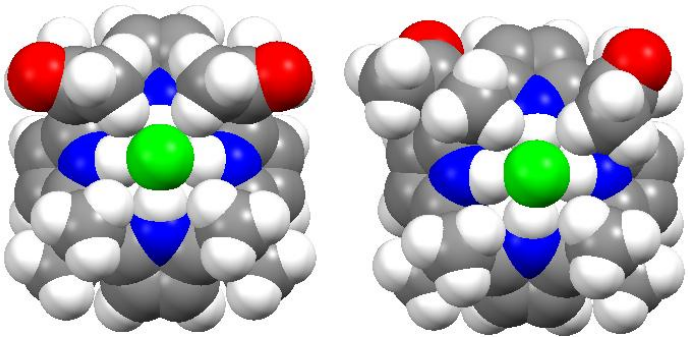

Figure 4.46 Space filling model of DFT-optimized structure of [*cis*-**SP24**.F]$^-$ (left) and [*trans*-**SP24**.F]$^-$ (right). Color code: red: O, blue: N, green: F, grey: C and white: H.

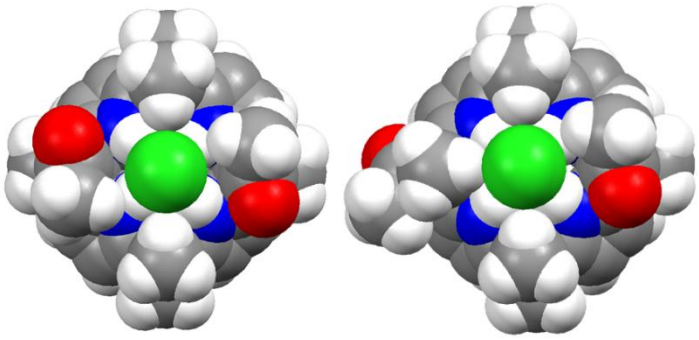

Figure 4.47 Space filling model of DFT-optimized structure of [*cis*-**SP23**.Cl]$^-$ (left) and [*trans*-**SP23**.Cl]$^-$ (right). Color code: red: O, blue: N, green: Cl, grey: C and white: H.

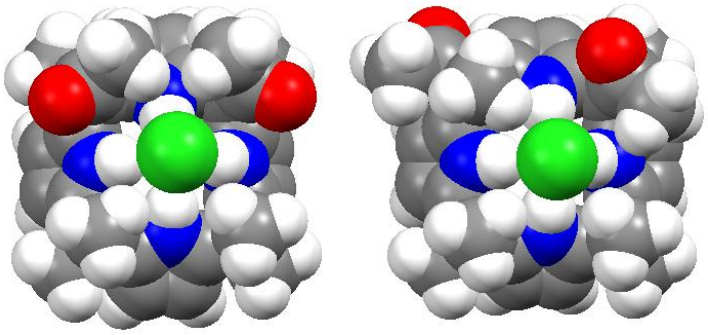

Figure 4.48 Space filling model of DFT-optimized structure of [*cis*-**SP24**.Cl]$^-$ (left) and [*trans*-**SP24**.Cl]$^-$ (right). Color code: red: O, blue: N, green: Cl, grey: C and white: H.

hydrogens of the anion (Figure 4.43). Furthermore, the relatively higher affinity of *cis*-**SP23** and *cis*-**SP24** towards halides than **L48** (Table 4.9) may be attributed to the weak C-H$^{\cdots}$X$^-$ interaction between the methyl groups of the acyl substituents to the anion due to the enforced proximity.[16] This is again reflected in the magnitude of their observed K_a, where the difference in affinity constants of the two isomers drastically reduced as the size of the halide

ion increases (Table 4.9). On the other hand, the relatively lower affinity of *cis*-**SP24** towards dihydrogenphosphate than *cis*-**SP23** may be attributed to the steric mismatch of the hydrogen bonding sites of the host and the anion (tetrahedral disposition between the two OHs of anion, compared to almost right angled orientation of the two *meso*-acyl groups). Receptors *trans*-**SP23** and **SP24** displayed lower affinity towards anions compared to their *cis*-analogues and **L48**, probably due to the competition by the acyl group (directed away from the core) with the incoming anions of a neighboring macrocycle. Whereas, the marginally higher binding affinity of *trans*-**SP24** than *trans*-**SP23** towards chloride and dihydrogenphosphate ion may be ascribed to the additional weak interaction between the methyl hydrogens with anion, apart from the relatively strong interaction between anchoring acyl group directed towards the core with the anion.

4.4 Conclusion

In conclusion, we have demonstrated two simple two-step methods of synthesis of the two positional isomers of the *meso*-diacylcalix[4]pyrroles **SP23** and **SP24** (viz. 5,10- and 5, 15-). The present study illustrates that suitably chosen substituents at the opposite *meso*-positions of calix[4]pyrrole, can lead to designer macrocycles having preferential binding ability towards desired anionic guest. When the two acyl groups are placed at the 5,10-positions of the calix[4]pyrrole periphery, their preference towards halides increases (fluoride displays largest enhancement), on the other hand, their placement at the 5,15-positions leads to higher affinity towards dihydrogenphosphate ion.

Moreover, we could also demonstrate that presence of flexible substituents at calix[4]pyrrole periphery, can lead to kinetically stable other conformers (1,2-conformation of *trans*-**SP23**), along with interesting solid state structures, which, can expand the domain of host-guest chemistry of calix[4]pyrroles in solid state. Further, the synthesis and structure of a stable pyrrole-2-carbinol **SP25** (the first derivative containing alkyl and a functionalized group) and its subsequent *in-situ* conversion to tripyrrane **SP13** is also demonstrated. Ours is also the first example of a one-pot synthesis of functionalized tripyrrane. This may spur the development of new functionalized building blocks leading to interesting porphyrinoids.

4.5 Experimental details

4.5.1 Preparation of 3-hydroxy-3-(1H-pyrrol-2-yl)butan-2-one (SP25)

Pyrrole (2.3 mL, 33 mmol, 3 equiv.), 2,3-butandione (1 mL, 11 mmol, 1 equiv.) were mixed in a 10 mL round bottom flask. The flask was immersed in a salt-ice water bath and

TFA (0.021 mL, 0.27 mmol, 0.025 equiv.) was slowly added and the reaction mixture was stirred at room temperature for 3 h under N_2 atmosphere. The reaction mixture was quenched by adding triethylamine. The excess pyrrole was removed by vacuum distillation at ~70-80 °C. The product was purified by column chromatography (20% EtOAc in hexane). The first fraction, obtained as white oil (650 mg), solidified at low temperature or under high vacuum corresponds to compound *meso*-acyldipyrromethane **SP12**. The second (720 mg) fraction which is obtained as colorless liquid (at room temperature) corresponds to compound **SP25**. Compound **SP24** crystallized upon storing in freezer at -20 °C.

Yield: 40%; FTIR Data (KBr): 3398, 1709 cm^{-1}; ^1H NMR (in $CDCl_3$, 400 MHz): δ in ppm 8.39 (br s, 1H, NH), 6.73 (d, 1H, pyrrole CH, J = 1.6Hz), 6.22 (m, 2H, pyrrole CH), 4.59 (s, 1H, OH), 2.21 (s, 3H, CH_3), 1.72 (s, 3H, CH_3); ^{13}C NMR (in $CDCl_3$, 100 MHz): δ in ppm 209.50, 131.33, 118.42, 108.79, 106.65, 77.45, 24.44, 23.01; LCMS m/z calcd. for $C_8H_{11}NO_2$ (M+H) 154, found 154; Elemental analysis for $C_8H_{11}NO_2$ calcd. C: 62.73, H: 7.24, N: 9.14; found C: 62.86, H: 7.13, N: 9.21.

4.5.2 Synthesis of 5,15-*meso*-diacylcalix[4]pyrrole (SP23)

Meso-acylated dipyrromethane **SP12** (2 g, 9.9 mmol, 1 equiv.) was dissolved in a mixture of dry acetone (70 mL) and dry dichloromethane (400 mL) at room temperature under nitrogen atmosphere and then $BF_3.OEt_2$ (0.122 mL, 0.9 mmol, 0.1 equiv.) was added. The reaction mixture was stirred at room temperature for 30 min. The reaction was quenched with 1M sodium hydroxide. The organic layer was separated and the aqueous layer was extracted with dichloromethane (30 mL × 3), and the combined organic layer was dried over anhyd. sodium sulfate. The solution was evaporated under reduced pressure, and the residue was purified by column chromatography over silica gel (eluent: 20% ethyl acetate in hexane) to afford the required *meso*-diacylated calixpyrrole **SP23** with *trans* (263 mg) and *cis* (350 mg) isomers as white solids.

Trans-SP23 isomer

Yield: 11%; Melting point: 228-230 ^oC; FTIR Data (KBr): 1684 cm^{-1}; ^1H NMR (in $CDCl_3$, 400 MHz): δ in ppm 7.41(br s, 4H, NH), 5.92-5.97 (m, 8H, pyrrole CH), 2.17 (d, 6H, CH_3), 1.76 (s, 6H, CH_3), 1.54(s, 12H, CH_3); ^1H NMR (in CD_3CN, 100 MHz): δ in ppm 8.38 (br s, 4H, NH), 5.83-5.89 (m, 8H, pyrrole CH), 2.01 (s, 6H, CH_3), 1.71 (s, 6H, CH_3), 1.53 (s, 12H, CH_3); ^{13}C NMR (in $CDCl_3$, 400 MHz): δ in ppm 207.84, 139.06, 131.68, 105.71,

104.08, 52.41, 35.45, 29.58, 27.15, 24.48; LCMS m/z calcd. for $C_{30}H_{36}N_4O_2$ (M+H) 485.63, found 485.55; Elemental analysis for $C_{30}H_{36}N_4O_2$ calcd. C: 74.35, H: 7.49, N: 11.56; found C: 74.25, H: 7.51, N: 11.68.

***Cis*-SP23 isomer**

Yield: 14%; Melting point: 208-210 ^oC; FTIR Data (KBr): 1699.44 cm^{-1}; ^1H NMR (in $CDCl_3$, 400 MHz): δ in ppm 7.44 (br s, 4H, NH), 5.90-5.97 (m, 8H, pyrrole CH), 2.15 (d, 6H, CH_3), 1.74 (d, 6H, CH_3), 1.52 (s, 12H, CH_3); ^1H NMR (in CD_3CN, 400 MHz): δ in ppm 8.29 (br, s, 4H, NH), 5.80-5.88 (m, 8H, pyrrole CH), 2.02 (s, 6H, CH_3), 1.67 (s, 6H, CH_3), 1.53 (s, 6H, CH_3), 1.57 (s, 6H, CH_3); ^{13}C NMR (in $CDCl_3$, 100 MHz): δ in ppm 207.39, 139.22, 131.70, 105.74, 103.98, 52.47, 35.45, 29.92, 29.10, 27.12, 24.08; LCMS m/z calcd. for $C_{30}H_{36}N_4O_2$ (M+H) 485.63, found 485.50; Elemental analysis for $C_{30}H_{36}N_4O_2$ calcd. C: 74.35, H: 7.49, N: 11.56; found C: 74.41, H: 7.55, N: 11.45.

4.5.3 Synthesis of 5,10-*meso*-diacylcalix[4]pyrrole (SP24)

Tripyrrane **SP14** (900 mg, 2.7 mmol, 1 equiv.) was dissolved in a mixture of freshly distilled pyrrole (2 mL, 27 mmol, 10 equiv.), dry acetone (10 mL) and dry dichloromethane (200 mL) at room temperature under nitrogen atmosphere and then $BF_3.OEt_2$ (0.083 mL, 0.7 mmol, 0.25 equiv.) was added. The reaction mixture was stirred at room temperature for overnight. The reaction was quenched with 1M solution of NaOH. The organic layer was separated and the aqueous layer was extracted with CH_2Cl_2 (30 mL × 3) and the combined organic layer was dried over anhyd. sodium sulfate. The solution was evaporated under reduced pressure and the residue was purified by column chromatography over silica gel (eluent: 15% EtOAc in hexane) to afford the required 5,10-diacylcalix[4]pyrrole **SP24** with *trans*-**SP24** (100 mg) and *cis*-**SP24** (125 mg) isomers as white solids.

***Trans*-SP24 isomer**

Yield: 7%; Melting point: 210-212 °C; FTIR Data (KBr): 3369.73, 3298.5, 1704.05 cm^{-1}; ^1H NMR (in $CDCl_3$, 400 MHz): δ in ppm 7.58 (br s, 1H, NH), 7.54 (br s, 2H, NH), 7.36 (br s, 1H, NH), 5.95 (m, 6H, pyrrole CH), 5.91 (m, 2H, pyrrole CH), 2.11 (s, 6H, CH_3), 1.71 (s, 6H, CH_3), 1.52 (s, 12H, CH_3); ^{13}C NMR (in $CDCl_3$, 100 MHz): δ in ppm 207.20, 140.07, 138.20, 132.55, 130.66, 106.77, 106.25, 103.66, 103.42, 52.69, 35.34, 29.41, 28.97, 26.76, 25.10;

LCMS m/z calcd. for $C_{30}H_{36}N_4O_2$ (M+H) 485.63, found 485.25; Elemental analysis for $C_{30}H_{36}N_4O_2$ calcd. C: 74.35, H: 7.49, N: 11.56. found C: 74.28, H: 7.58, N: 11.66.

***Cis*-SP24 isomer**

Yield: 10%; Melting point: >220 °C (with decomposition); FTIR Data (KBr): 3408.22, 3364.38, 3287.67, 1693.15 cm^{-1}; ^1H NMR (in $CDCl_3$, 400 MHz): δ in ppm 7.65 (br s, 2H, NH), 7.57 (br s, 1H, NH), 7.33 (br s, 1H, NH), 5.97 (m, 4H, pyrrole CH), 5.94 (d, 2H, pyrrole CH, J = 2.4 Hz), 5.91 (t, 2H, pyrrole CH, J = 2.8Hz), 2.14 (s, 6H, CH_3), 1.73 (s, 6H, CH_3), 1.53 (s, 12H, CH_3); ^{13}C NMR (in $CDCl_3$, 100 MHz): δ in ppm 207.36, 140.10, 138.29, 132.714, 130.64, 106.48, 106.28, 103.69, 103.43, 52.58, 35.37, 29.61, 28.85, 26.73, 24.40; LCMS m/z calcd. for $C_{30}H_{36}N_4O_2$ (M+H) 485.63, found 485.15; Elemental analysis for $C_{30}H_{36}N_4O_2$ calcd. C: 74.35, H: 7.49, N: 11.56; found C: 74.51, H: 7.41, N: 11.48.

4.6 Crystallographic details

Crystallographic data for *cis*-**SP23** (water and methanol solvate) and *trans*-**SP23** (both 1,2- and 1,3- alternate) were collected at 298 K and **SP25** were collected at 100 K on BRUKER SMART-APEX CCD diffractometer.

Crystallographic data for *cis*-**SP23** (dichloromethane solvate), *cis*-**SP24** and **SP13** were collected on Oxford Gemini A Ultra diffractometer with dual source.

Pertinent crystallographic data collection and refinement parameter are shown in the following tables:

Table 4.10 Crystallographic parameters of crystals of *cis*-**SP23**.(CH_2Cl_2), *cis*-**SP23**.(H_2O), *cis*-**SP23**.(CH_3OH) and *trans*-**SP23** (I4).

Crystal data	*cis*-**SP23**.(CH_2Cl_2)	*cis*-**SP23**.(H_2O)	*cis*-**SP23**.(CH_3OH)	*trans*-**SP23** (I4/a)
CCDC No.	804419	804420	-	804421
Formula unit	$C_{31}H_{38}Cl_2N_4O_2$	$C_{30}H_{38}N_4O_3$	$C_{31}H_{40}N_4O_3$	$C_{30}H_{36}N_4O_2$
Formula wt.	569.55	502.64	516.65	484.63
Crystal system	Monoclinic	Monoclinic	Triclinic	Tetragonal
T [K]	298 (2)	298 (2)	298 (2)	298 (2)
a [Å]	10.2397 (12)	10.309 (7)	9.757 (4)	21.3560 (19)
b [Å]	12.4463 (13)	13.246 (9)	9.773 (4)	21.3560 (19)

Crystal data	*cis*-**SP23**.(CH_2Cl_2)	*cis*-**SP23**.(H_2O)	*cis*-**SP23**.(CH_3OH)	*trans*-**SP23** (I4/a)
c [Å]	24.466 (3)	11.386 (8)	15.744 (5)	11.329 (2)
α [°]	90.00	90.00	88.275(7)	90.00
β [°]	101.040 (13)	113.540 (11)	88.343 (8)	90.00
γ [°]	90.00	90.00	85.511 (10)	90.00
volume [$Å^3$]	3060.5 (6)	1425.6 (18)	1495.5 (10)	5167.0 (12)
Space group	P 21/n	P2(1)	P-1	I4(1)/a
Z´	1	1	2	1
Z	4	2	4	8
D_{calc} [$g.cm^{-3}$]	1.236	1.171	1.433	1.246
μ/mm^{-1}	0.246	0.076	0.129	0.079
Reflns collected	23447	13621	15749	17738
Unique reflns	5395	5030	5893	2203
Observed reflns	1444	4941	3516	1913
R(int)	0.2627	0.0356	0.0452	0.0768
R_1 [$I > 2\sigma(I)$], wR_2	0.0810, 0.1351	0.0807, 0.1624	0.0668, 0.1666	0.1076, 0.2051
GOF	0.817	1.302	1.023	1.234

Table 4.11 Crystallographic parameters of crystals of *trans*-**SP23** (Pbca), *cis*-**SP24**, **SP25** and **SP13**.

Crystal data	*trans*-**SP23** (Pbca)	*cis*-**SP24**	**SP25**	**SP13**
CCDC No.	804422	909035	909033	909034
Formula unit	$C_{30}H_{36}N_4O_2$	$C_{30}H_{33}N_4O_2$	$C_{16}H_{22}N_2O_4$	$C_{20}H_{23}N_3O_2$
Formula wt.	484.63	481.60	306.36	337.41
Crystal system	Orthorhombic	monoclinic	triclinic	Triclinic
T [K]	298 (2)	298 (2)	298 (2)	298 (2)
a [Å]	11.3085 (18)	10.3743 (16)	8.37 (2)	8.4855 (12)
b [Å]	19.412 (3)	12.098 (2)	10.24 (3)	10.2487 (12)

Crystal data	*trans*-**SP23** (Pbca)	*cis*-**SP24**	**SP25**	**SP13**
c [Å]	23.713 (4)	11.1576 (18)	10.52 (3)	11.0122 (13)
α [°]	90.00	90.00	95.85 (5)	87.534 (10)
β [°]	90.00	105.030 (17)	110.15 (4)	76.273 (11)
γ [°]	90.00	90.00	112.75 (4)	85.501 (11)
volume [$Å^3$]	5205.4 (14)	1352.5 (4)	752 (4)	927.2 (2)
Space group	Pbca	P2(1)	P-1	P-1
Z′	1	1	1	1
Z	8	2	2	2
D_{calc} [$g.cm^{-3}$]	1.237	1.183	1.353	1.209
μ/mm^{-1}	0.079	0.075	0.098	0.079
Reflns collected	49734	5326	4625	7211
Unique reflns	5141	3833	2670	4200
Observed reflns	1572	2339	1631	1071
R(int)	0.5031	0.0843	0.0432	0.0970
R_1 [$I > 2\sigma(I)$], wR_2	0.0887, 0.1303	0.0480, 0.0954	0.1007, 0.2831	0.0899, 0.1314
GOF	0.945	0.894	1.271	0.941

4.7 References

1. (a) Baeyer, A. *Ber. Dtsch. Chem. Ges.* **1886**, *19*, 2184. (b) Baeyer, A. *Ber.* **1872**, *5*, 1094.
2. (a) Chelintzev, V. V.; Tronov, B. V. *J. Russ. Phys. Chem. Soc.* **1916**, *48*, 105. (b) Chelintzev, V. V.; Tronov, B. V. *J. Russ. Phys. Chem. Soc.* **1916**, *48*, 1197.
3. (a) Rothenmund, P.; Gage, C. L. *J. Am. Chem. Soc.* **1955**, *77*, 3340. (b) Brown, W. H.; Hutchinson, B. J.; MacKinnon, M. H. *Can. J. Chem.* **1971**, *49*, 4017. (c) Sessler, J. L.; Gale, P. A. In *The Porphyrin Handbook*; Kadish, K. M., Smith, K. M., Guilard, R., Eds.; Academic Press: New York, **2000**, *6*, 257.
4. Jubb, J.; Jacoby, D.; Floriani, C.; Cheisi-Villa, A.; Rizzoli, C. *J. Chem. Soc. Chem. Commun.* **1991**, 220.

5. (a) Floriani, C.; Floriani-Moro, R. In *The Porphyrin Handbook*; Kadish, K. M., Smith, K. M., Guilard, R., Eds.; Academic Press: New York, **2000**, *3*, 385. (b) Floriani, C.; Floriani-Moro, R. In *The Porphyrin Handbook*; Kadish, K. M., Smith, K. M., Guilard, R., Eds.; Academic Press: New York, **2000**, *3*, 405.
6. (a) Gale, P. A.; Sessler, J. L.; Kra´l, V.; Lynch, V. *J. Am. Chem. Soc.* **1996**, *118*, 5140. (b) Allen, W. E.; Gale, P. A.; Brown, C. T.; Lynch, V. M.; Sessler J. L. *J. Am. Chem. Soc.* **1996,** *118*, 12471.
7. Bohmer, V. *Angew. Chem. Int. Ed.* **1995**, *34*, 713.
8. Van Hoorn, W. P.; Jorgensen, W. L. *J. Org. Chem*. **1999**, *64*, 7439.
9. Wu, Y.-D.; Wang, D. –F.; Sessler, J. L. *J. Org. Chem.* **2001,** *66*, 3739.
10. Gale, P. A.; Sessler, J. L.; Allen, W. E.; Tvermoes, N. A.; Lynch V. M. *Chem. Commun*. **1997**, 665.
11. (a) Anzenbacher Jr., P.; Jursíková, K.; Lynch, V. M.; Gale, P. A.; Sessler, J. L. *J. Am. Chem. Soc.* **1999**, *121*, 11020. (b) Schmidtchen, F. P. *Org. Lett.* **2002**, *4*, 431. (c) Namor, A. F.; Shehab, M. *J. Phys. Chem. B* **2003**, *107*, 6462. (d) Sessler, J. L.; An, D.; Cho, W.-S.; Lynch, V. *Angew. Chem. Int. Ed.* **2003**, *42*, 2278. (e) Sessler, J. L.; An, D.; Cho, W. -S.; Lynch, V. *J. Am. Chem. Soc.* **2003**, *125*, 13646. (f) Sessler, J. L.; An, D.; Cho, W. -S.; Lynch, V.; Marquez, M. *Chem. Eur. J.* **2005**, *11*, 2001. (g) Nielsen, A. K.; Cho, W. -S.; Lyskawa, J.; Levillain, E.; Lynch, V. M.; Sessler, J. L.; Jeppesen, J. O. *J. Am. Chem. Soc.* **2006**, *128*, 2444.
12. (a) Schmidtchen, F. P.; Berger, M. *Chem. Rev.* **1997**, *97*, 1609. (b) Beer, P. D.; Bayly, S. R. *Top. Curr. Chem.* **2005**, *255*, 373. (c) Bowman-James, K. *Acc. Chem. Res.* **2005**, *38*, 671. (d) Metrangolo, P.; Neukrich, H.; Pilati, T.; Resnati, G. *Acc. Chem. Res*. **2005**, *38*, 386. (e) Schottel, B. L.; Chifotides, H. T.; Dunbar, K. R. *Chem. Soc. Rev.* **2008**, *37*, 68. (f) Guha, S.; Saha, S. *J. Am. Chem. Soc.* **2010**, *132*, 17674. (g) Frontera, A.; Gamez, P.; Mascal, M.; Mooibroek, T. J.; Reddijk, J. *Angew. Chem. Int. Ed.* **2011**, *50*, 9564.
13. (a) Sessler, J. L.; Anzenbacher Jr., P.; Jursíková, K.; Miyaji, H.; Genge; J. W.; Tvermoes, N. A.; Allen, W. E.; Shiver, J. A. *Pure Appl. Chem.* **1998**, *70*, 2401. (b) Anzenbacher, Jr. P.; Jursíková, K.; Lynch, V. M.; Gale, P. A.; Sessler J. L. *J. Am. Chem. Soc.* **1999,** *121*, 11020. (c) Anzenbacher Jr., P.; Jursíková, K.; Sessler J. L. *J. Am. Chem. Soc.* **2000,** *122*, 9350. (d) Gil-Ramírez, G.; Escudero-Adán, E. C.; Benet-Buchholz, J.; Ballester, P. *Angew. Chem. Int. Ed.* **2008**, *47*, 4114.

14. Anzenbacher Jr., P.; Try, A. C.; Miyaji, H.; Jursíková, K.; Lynch, V. M.; Marquez, M.; Sessler J. L. *J. Am. Chem. Soc.* **2000**, *122*, 10268.
15. (a) Yoon, D. W.; Hwang, H.; Lee, C. -H. *Angew. Chem. Int. Ed.* **2002**, *41*, 1757. (b) Lee, C. -H.; Na, H. K.; Yoon, D. W.; Won, D. H.; Cho, W. S.; Lynch, V. M.; Shevchuk, S. V.; Sessler, J. L. *J. Am. Chem. Soc.* **2003,** *125*, 7301. (c) Panda, P. K.; Lee, C. -H. *Org. Lett.* **2004**, *6*, 671. (d) Panda, P. K.; Lee, C. -H. *J. Org. Chem.* **2005,** *70*, 3148. (e) Miyaji, H.; Kim, H. K.; Sim, E. K.; Lee, C. K.; Cho, W. S.; Sessler, J. L.; Lee, C. -H. *J. Am. Chem. Soc.* **2005**, *127*, 12510. (f) Lee, C. -H.; Lee, J. S.; Na, H. K.; Yoon, D. W.; Miyaji, H.; Cho, W. S.; Sessler, J. L. *J. Org. Chem.* **2005**, *70*, 2067. (g) Samanta, R.; Mahanta, S. P.; Chaudhuri, S.; Panda, P. K.; Narahari, A. *Inorg. Chim. Acta* **2011**, *372*, 281. (h) Samanta, R.; Mahanta, S. P.; Ghanta, S.; Panda, P.K. *RSC Adv.* **2012**, *2*, 7974.
16. (a) Král, V.; Gale, P. A.; Anzenbacher Jr., P.; Jursíková, K.; Lynch, V.; Sessler, J. L. *Chem. Commun.* **1998**, 9. (b) Arumugam, N.; Jang, Y.-S.; Lee, C.-H. *Org. Lett.* **2000**, *2*, 3115. (c) Sessler, J. L.; An, D.; Cho, W. -S.; Lynch, V.; Yoon, D. -W.; Hong, S. -J.; Lee, C.-H. *J. Org. Chem.* **2005**, *70*, 1511. (d) Sessler, J. L.; An, D.; Cho, W. -S.; Lynch, V. M. *J. Am. Chem. Soc.* **2003**, *125*, 13646.
17. Sessler, J. L.; Anzenbacher Jr. P.; Jursíková, K.; Miyaji, H.; Genge, J. W.; Tvermoes, N. A.; Allen, W. E.; Shiver, J. A. *Pure Appl. Chem.* **1998**, *70*, 2401.
18. Sessler, J. L.; Andrievsky, A.; Gale, P. A.; Lynch, V. *Angew. Chem. Int. Ed.* **1996**, *35*, 2782.
19. Anzenbacher Jr., P.; Jursíková, K.; Sessler, J. L. *J. Am. Chem. Soc.* **2000**, *122*, 9350.
20. (a) Král, V.; Sessler, J. L.; Zimmerman, R. S.; Seidel, D.; Lynch, V.; Andrioleetti, B. *Angew. Chem. Int. Ed.* **2000**, *39*, 1055. (b) Jang, Y. -S.; Kim H. -J.; Lee, P. -H.; Lee, C. -H. *Tetrahedron Lett.* **2000**, *41*, 2919. (c) Arumugam, N.; Jang, Y. -S.; Lee, C. -H. *Org. Lett.* **2000**, *2*, 3115. (d) Nagarajan, A.; Ka, J. -W.; Lee, C. -H. *Tetrahedron* **2001**, *57*, 7323. (e) Lee, E. -C.; Park, Y. -K.; Kim, J. -H.; Hwang, H.; Kim, Y. -R.; Lee, C. -H. *Tetrahedron Lett.* **2002**, *43*, 9493. (f) Sessler, J. L.; An, D.; Cho, W. S.; Lynch, V. *J. Am. Chem. Soc.* **2003**, *125*, 13646. (g) Dolenský, B.; Kroulík, J.; Král, V.; Sessler, J. L.; Dvořáková, H.; Bouř, P.; Bernátková, M.; Bucher, C.; Lynch, V. *J. Am. Chem. Soc.* **2004**, *126*, 13714. (h) Balakumar, A.; Muthukumaran, K.; Lindsey J. S. *J. Org. Chem.* **2004**, *69*, 5112. (i) Thamyongkit, P.; Speckbacher, M.; Diers, J. R.; Kee, H. L.; Kirmaier, C.; Holten, D.; Bocian, D. F.; Lindsey, J. S. *J. Org. Chem.* **2004**, *69*, 3700.

(j) Song, M. -Y.; Na, H. -K.; Kim, E. -Y.; Lee, S. -J.; Kim, K. I.; Baek, E. -M.; Kim, H. -S.; An, D. K.; Lee, C. -H. *Tetrahedron Lett.* **2004**, *45*, 299. (k) Sessler, J. L.; An, D.; Cho, W. -S.; Lynch,V.; Yoon, D. -W.; Hong, S. -J.; Lee, C. -H. *J. Org. Chem.*, **2005**, *70*, 1511. (l) Mahanta, S. P.; Kumar, B. S.; Panda, P. K. *Chem. Commun.* **2011**, 4496.

21. Turner, B.; Botoshansky, M.; Eichen, Y. *Angew. Chem. Int. Ed.* **1998**, *37*, 2475.
22. Bucher, C.; Zimmerman, R. S.; Lynch, V.; Král, V.; Sessler J. L. *J. Am. Chem. Soc.* **2001,** *123*, 2099.
23. (a) Gale, P. A.; Anzenbacher Jr., P.; Sessler, J. L. *Coord. Chem. Rev.* **2001**, *222*, 57. (b) Sessler, J. L.; Gale, P. A.; Genge, J. W. *Chem. Eur. J.* **1998**, *4*, 1095. (c) Gale, P. A.; Tong, C. C.; Haynes, C. J. E.; Adeosun, O.; Gross, D. E.; Karnas, E.; Sedenberg, E. M.; Quesada, R.; Sessler, J. L. *J. Am. Chem. Soc.* **2010**, *132*, 3240.
24. (a) Namor, A. D.; Shehab, M.; Abbas, I.; Withams, M. V.; Zvietcovich-Guerra, J. *J. Phys. Chem. B*, **2006**, *110*, 12653. b) Namor, A. D.; Shehab, M.; Khalife, R.; Abbas, I. *J. Phys. Chem. B*, **2007**, *111*, 12177.
25. Gil-Ramírez, G.; Escudero-Adán, E. C.; Benet-Buchholz, J.; Ballester, P. *Angew. Chem. Int. Ed.* **2008**, *47*, 4114.
26. Anzenbacher Jr., P.; Try, A. C.; Miyaji, H.; Jursíková, K.; Lynch, V. M.; Marquez, M.; Sessler, J. L. *J. Am. Chem. Soc.* **2000,** *122*, 10268.
27. Miyaji, H.; Anzenbacher Jr., P.; Sessler, J. L.; Bleasdale, E. R.; Gale, P. A. *Chem. Commun.* **1999**, 1723.
28. Miyaji, H.; Sato, W., Sessler, J. L. *Angew. Chem. Int. Ed.* **2000**, *39*, 1777.
29. Hargrove, A. E.; Nieto, S.; Zhang, T.; Sessler, J. L.; Anslyn, E. V. *Chem. Rev.* **2011**, *111*, 6603.
30. (a) Pagani, G.; Berlin, A.; Canavesi, A.; Schiavon, G.; Zecchin, S.; Zotti, G. *Adv. Mater.* **1996**, *8*, 819. (b) Harmjanz, M.; Gill, H. S.; Scott, M. J. *J. Org. Chem.* **2001**, *66*, 5374.
31. (a) Lee, C. -H.; Li, F.; Iwamoto, K.; Dadok, J.; Bothner-By, A. A.; Lindsey, J. S. *Tetrahedron* **1995**, *51*, 11645. (b) Zaidi, S. H. H.; Fico Jr., R. M.; Lindsey, J. S. *Org. Proc. Res. Dev.* **2006**, *10*, 118.
32. (a) Blay, G.; Fernández, I. ; Munoz, M. C.; Pedro, J. R.; Recuenco, A.; Vila, C. *J. Org. Chem.* **2011**, *76*, 6286. (b) Blay, G.; Fernández, I.; Monleón, A.; Pedro, J. R.; Recuenco, A.; Vila, C. *Org. Lett.* **2009**, *11*, 441. (c) Hafner, K.; Pfeiffer, K.;

Tetrahedron Lett. **1968**, *40*, 4311. (d) Toganoh, M.; Harada, N.; Furuta, H. *J. Organometallic Chem.* **2008**, *693*, 3141. (e) Sreedevi, K. C. G.; Thomas, A. P.; Salini, P. S.; Ramakrishnan, S.; Anju, K. S.; Holaday, M. G. D.; Reddy, M. L. P.; Suresh, C. H.; Srinivasan, A. *Tetrahedron Lett.* **2011**, *52*, 5995.

33. (a) Battersby, A. R.; Leeper, F. J. *Chem. Rev.* **1990**, *90*, 1261. (b) Barcock, R. A.; Moorcroft, N. A.; Storr, R. C.; Young, J. H.; Fuller, L. S. *Tetrahedron Lett.* **1993**, *34*, 1187. c) Wallace, D. M.; Leung, S. H.; Senge, M. O.; Smith, K. M. *J. Org. Chem*. **1993**, *58*, 7245. d) Abell, A. D.; Nabbs, B. K.; Battersby, A. R. *J. Am. Chem. Soc*. **1998**, *120*, 1741.
34. Sessler, J. L.; Gross, D. E.; Cho, W. -S.; Lynch, V. M.; Schmidtchen, F. P.; Bates, G. W.; Light, M. E.; Gale, P. A. *J. Am. Chem. Soc.* **2006**, *128*, 12281.

CHAPTER 5

Calix[2]bispyrrolylalkenes: Smallest expanded calix[4]pyrroles

5.1 Introduction

In order to modulate the anion binding ability of calix[4]pyrroles **L48** several approaches has been reported.[1] Enhanced binding strength and selectivity was achieved by increasing the acceptor ability of the macrocycle by incorporation of electron withdrawing substituents at the β-position and single side strapping with suitable spacer units. We have discussed about some of them in the previous chapters. Another approach envisaged towards binding of larger anions, is core expansion, which is one of the most attractive modification strategies, being highly explored in the last two decades. Replacement of one or more pyrrole moieties with some other heterocyclic subunit, for example, furan or thiophene[2] **L49**, pyridine[3] **L109**, and benzene[4] **L110** changes the H-bonding domain of the macrocycle. This type of core modified calixpyrrole is known as hybrid calixpyrroles. But, the number of heterocycles and/or carbacycles in the macrocycle remains four. This type of hybrid calixpyrroles, proved to be

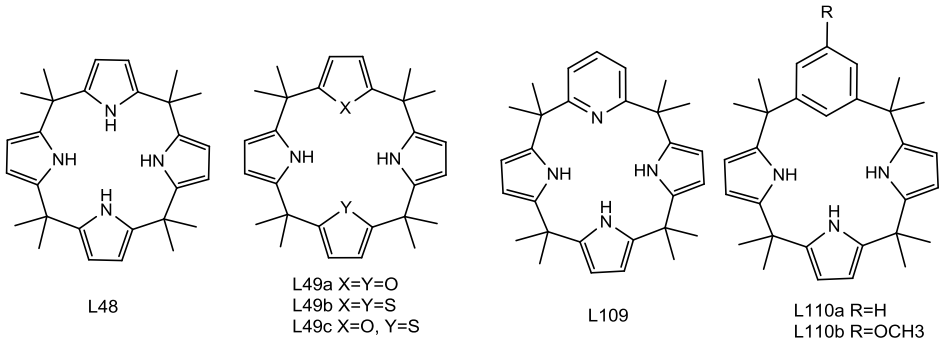

less effective ligand for anions, due to the reduced number of anion binding subunits *i.e.* H-bond donor group compared to the parent calix[4]pyrroles, although they did show varied selectivities.

Due to the small size of calix[4]pyrrole cavity, it only binds small anions such as fluoride and chloride ions and the solid state structure of the complex reveals that the anion sit above the macrocycle planes but not within the cavity. Further, the energy needed to adopt the cone conformation from 1,3-alternate conformation, upon complexation, could reduce the anion affinities. Therefore, it is envisaged that by increasing the size of the cavity, the macrocycle will be more flexible and hence need lesser energy to adopt desirable conformation. Further, the affinity of the macrocycle towards larger anions may increase due to the increased core size and possible geometry match. Core expansion can be achieved by two ways (Figure 5.1) - either by increasing the number of pyrrole or heterocyclic units in the core *i.e.* by making higher order calix[n]pyrrole and its hybrids where n > 4 (n = number of heteroarene unit), or by putting some spacer units between the two dipyrromethane residues such that the size of

the macrocyclic core increases without increasing the number of the pyrrolic (or heteroarene) units.

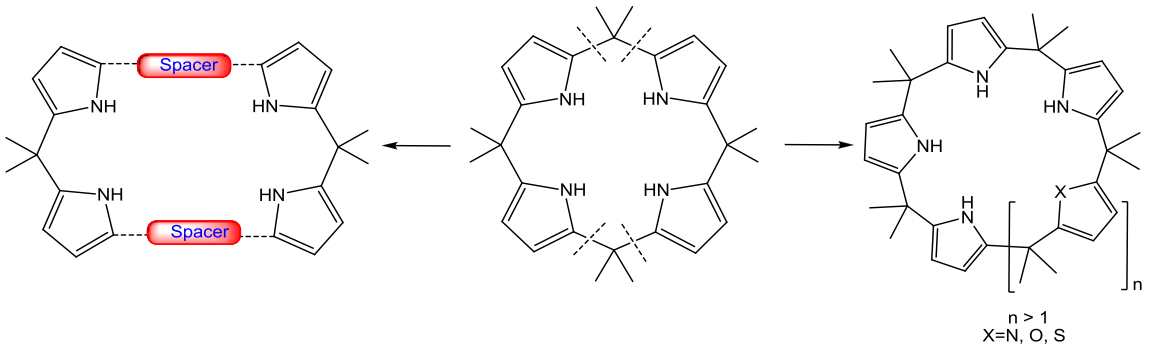

Figure 5.1 Schematic diagram showing the two plausible ways of expansion of calix[4]pyrrole core.

5.1.1 Calix[n]pyrroles (n > 4; n: number of heteroarenes)

The first expanded calixpyrrole was reported by Sessler and coworker as a calix[5]pyrrole-calix[5]arene pseudo dimer **L111** using a calixarene moiety as the synthetic template (Scheme 5.1).[5] The prime motive behind this modification is that by increasing the number of pyrrole or other heteroaromatics in the core, the size of the central core as well as the number of H-bonding units can increase, which in due course improve the affinity and selectivity of the core towards larger anions. Unfortunately, the pseudo dimer did not show

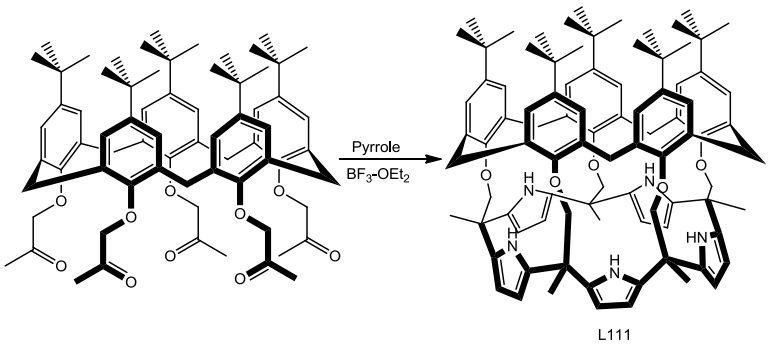

Scheme 5. 1 Synthesis of compound **L111**.

any affinity towards fluoride ion, due to the presence of strong intramolecular N-H···O H-bond. The cleavage of the free calix[5]pyrrole could not be achieved, which became the main setback of this approach. The first synthesis of higher order calix[n]pyrrole was achieved by Eichen and coworkers by acid catalyzed condensation of sterically encumbered *meso* aryldipyrromethane with acetone in reasonably good yields.[6] Interestingly, in this reaction

TFA yields the targeted calix[6]pyrrole while Lewis acid catalyst $BF_3.OEt_2$ results in calix[4]pyrrole. Preliminary, ^{1}H NMR titration studies shows that compound **L113a** has

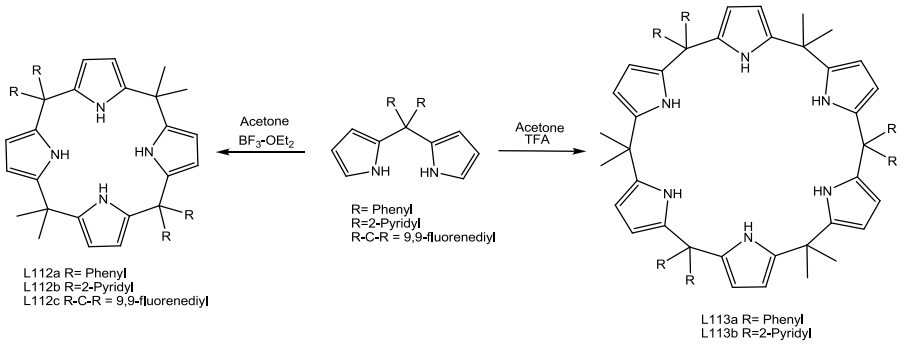

Scheme 5.2 Synthesis of calix[6]pyrrole (**L113**) and calix[4]pyrrole (**L112**).

moderate preference for iodide and BF_4^- ions, with halide affinities in the order $I^- > F^- >> Cl^- > Br^-$, whereas its lower congener **L112a** displays anion affinity like parent octamethyl-calix[4]pyrrole **L48**. As seen in cation selectivities in crown ether, here also the expansion of the cavity, with concomitant increase in the number of H-bond donor entities, enhances I^- binding affinity, on the other hand, fluoride is presumably unable to benefit from the full complement of such multiple interactions.[7]

In a subsequent report, by following a completely different strategy, Kohnke and coworkers synthesized calix[n]pyrrole from calix[n]furan (n = 5, 6). The key intermediate of

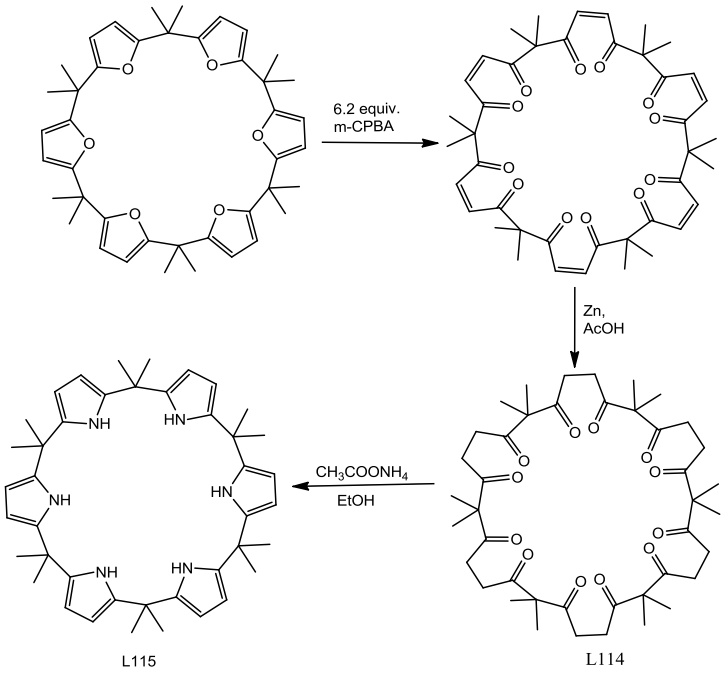

Scheme 5.3 Synthesis of calix[6]pyrrole **L115**.

this reaction is a ketone **L114**, which they have confirmed by single crystal X-ray diffraction analysis.[8] The key step in this protocol is the ring opening of the furan rings (Scheme 5.3), which depends on the stoichiometry of the *m*-CPBA used and hence by varying the stoichiometry they had successfully synthesized a variety of expanded hybrid calixpyrroles calix[n]furan[m]pyrrole (**L116**: n=1, m=5; **L117**: n=3, m=3; **L118**: n=2, m=4).[8] They have studied the anion binding behavior of these compounds by following NMR titration and Cram's extraction method in CD_2Cl_2 and in some cases CD_2Cl_2 saturated with D_2O. Therefore comparison of the data obtained with the screened anions is not possible since K_a values determined were neither under identical condition nor by the same method.

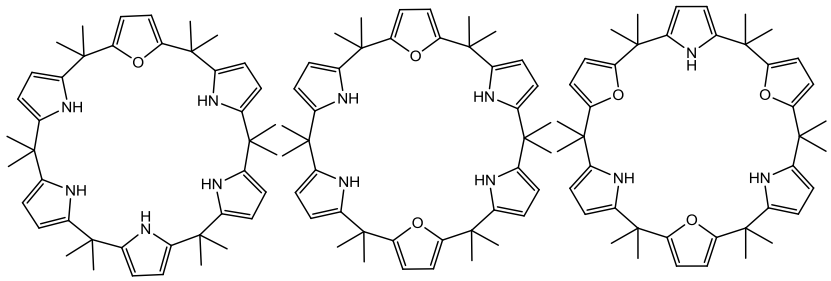

Sessler and coworkers found that the direct acid catalyzed condensation of acetone and pyrrole *i.e.* the Baeyer condition does not give good yield of higher order calix[n]pyrrole (n > 4), as they are present as very minor components in the reaction mixture and the difficulty involved in their isolation. This failure has been ascribed further to the fact that higher calixpyrroles undergoes mitosis reaction, even under very mild acidic conditions to generate the tetramer. They found that when pyrrole unit bear fluorine substituents at their *β*-positions, the mitosis reaction becomes slow. By exploring this observation they were able to isolate the *β*-fluoro substituted calix[5]pyrrole and a larger homologue calix[8]pyrrole (Scheme 5.4).[9] They found that the yield of the higher calixpyrrole depends on the concentration of the

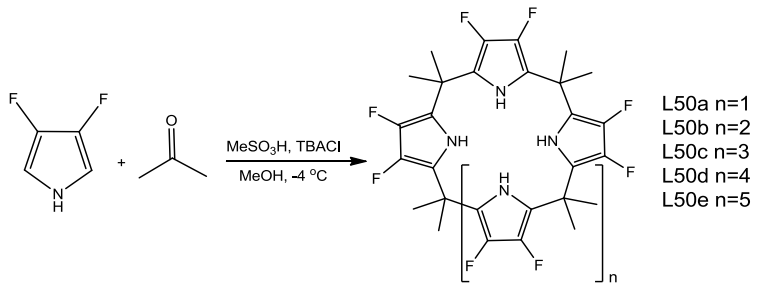

Scheme 5.4 Syntheses of fluoro substituted calix[n]pyrroles **L50a-e**.

starting materials, reaction time and temperature. In a later communication, they reported that the intermediate analogue calix[6]pyrrole and calix[7]pyrrole are thermodynamically unstable under the room temperature reaction conditions and finally, they could achieve the synthesis of dodecalfluorocalix[6]pyrrole and tetradecafluorocalix[7]pyrrole along with n=2 and n=5 analogue at -4 °C, in the presence of tetrabutylammonium chloride template.[10] Anion binding studies, using several test anions and three different solvent systems (CH_3CN; CH_3CN+2% H_2O; DMSO), revealed that the higher order fluorinated calixpyrroles show comparatively weaker binding affinity relative to the octafluorocalix[4]pyrrole **L50a** and relatively, these species showed a preference for larger anions. Further, an increase in the relative affinity for bromide over chloride with increasing macrocycle size was observed, as manifested in a corresponding decrease in the binding ratio $K_a(Cl^-)/K_a(Br^-)$ with increasing size of the macrocycle.[10]

Surprisingly, several of these reported higher calix[n]pyrrole systems did not show improved binding affinity and selectivity for anions. These findings, of interest in their own

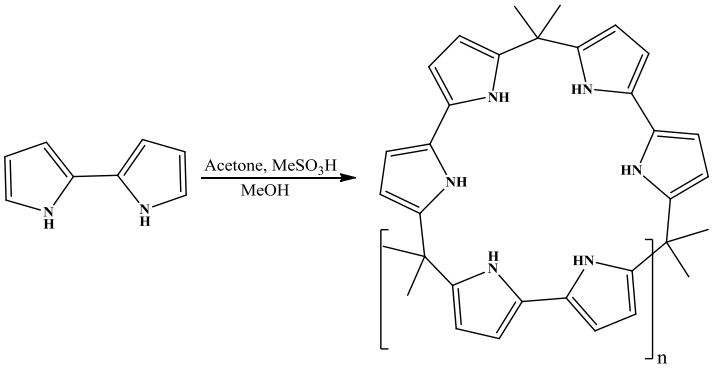

L51a n=1
L51b n=2

Scheme 5.5 Syntheses of bipyrrole based calixpyrroles **L51a-b**.

right, also provide a stimulus to generate other kinds of expanded calixpyrrole analogues. This raises the question, if other kinds of "expanded" calixpyrroles could be made that would indeed display enhanced selectivities for larger anions and search began for new building blocks. One set of compounds where efficacy for anion binding has been established, consists of the bipyrrole as the building blocks instead of pyrrole, *i.e.*calix[3]bipyrrole and calix[4]bipyrrole (Scheme 5.5).[11] It was anticipated that these receptors, to the extent they bound anions, would favor larger species. Anion binding studies of calix[3]bipyrrole in acetonitrile and DMSO, displays enhanced bromide and iodide ion binding, compared to **L48**. In the case of higher analogue **L51b**, the receptor containing eight potential pyrrolic NH

donor groups, the binding constant for chloride was observed to be much higher than that of bromide. This unexpected trend is attributed to its ability to form V-shaped "nesting" complexes, confirmed by single crystal X-ray diffraction that are very different from those seen for **L48** and **L51a**.

In order to make more efficient receptors for larger anions, several groups especially Lee and coworkers have synthesized new expanded hybrid calixpyrrole type systems that are based on various combinations of furan, thiophene and pyrrole, by following a different approach than Kohnke's approach.[3a-c] However, all of those systems were not able to display efficient anion binding ability. Later, Sessler and coworkers reported two hybrid calixpyrrole calix[2]bipyrrole[2]furan **L52a** and calix[2]bipyrrole[2]thiophene **L52b** (Scheme 5.6) and their anion binding studies in acetonitrile reveal that these compounds display good affinities for Y-shaped anions, such as benzoate and acetate, whereas spherical anions such as chloride and bromide, bind only weakly due to the size mismatch between the anion and receptor binding domain.[12]

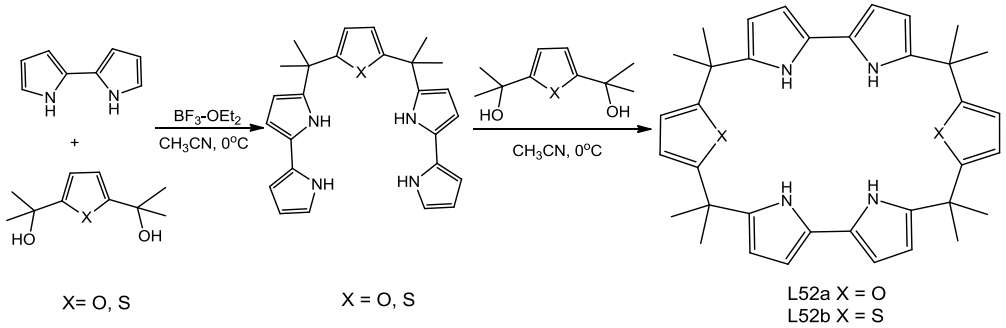

Scheme 5.6 Syntheses of **L52a-b**.

This finding is noteworthy because it shows that fine tuning of the cavity size and overall shape of calixpyrrole type receptors, can lead to systems whose selectivities are optimized for certain classes of anions. Moreover, this illustrates how changes in calix[n]pyrrole core design as opposed to external ring functionalization, may be used to generate receptors for species that are relatively weak hydrogen bond acceptors.

5.1.2 Expanded Calix[4]pyrroles

The central core size of the calix[4]pyrrole can also be increased by putting some spacer in between the two dipyrromethane moieties where the spacer unit may or may not directly take part in the binding event. The main motive behind this was to increase the size and shape

of the hydrogen bond binding domain, such that larger anions can bind effectively and with better selectivity.

In 2004, Sessler and coworkers highlighted this approach by synthesizing a new type of expanded calix[4]pyrrole *i.e.* calix[4]pyrrole[2]carbazzole **L119** containing carbazole subunit in place of two alternate *meso* carbons (Scheme 5.7).[13] The advantage of incorporation of the carbazole moiety within the macrocycle framework was that it could provide a system that not only bind anions but also signal its presence directly via optical means. Anion binding studies of **L119** in dichloromethane and acetonitrile, by fluorescence quenching experiment, displayed slight preference for acetate relative to other carboxylate ions (viz. benzoate, oxalate, succinate), as well as to chloride and dihydrogenphosphate ions. In the solid state, the macrocycle adopts a wing like conformation as evident from the single crystal X-ray diffraction analyses of both free system and the corresponding benzoate ion complex. The

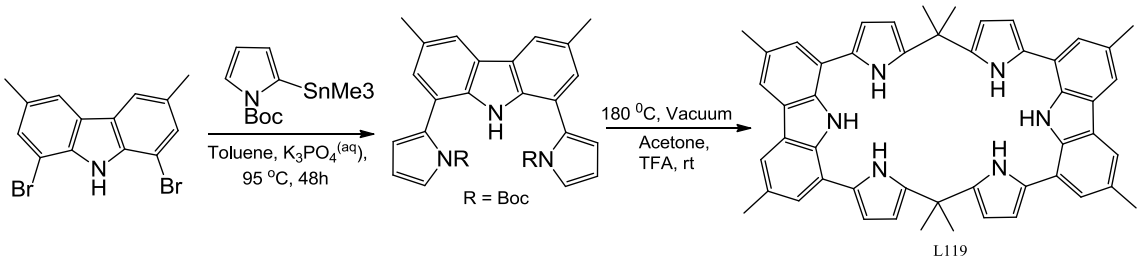

Scheme 5.7 Synthesis of **L119**.

solid state structure of the benzoate complex revealed that the anion reside deep within the saddle formed by the wings of the macrocycle with one of the oxygen of benzoate being close to pyrrole NH entities and the other within hydrogen bonding distance of the other two pyrrole NHs, and possibly the carbazole NH as well. However the presence of additional NHs in the carbazole moieties made it appear more like a hexapyrrolic macrocycle.

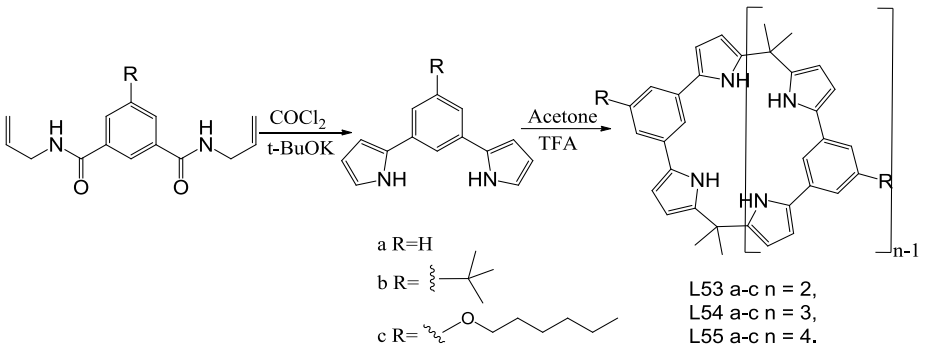

Scheme 5.8 Syntheses of **L53-55**.

One year later, Sessler and coworkers reported bispyrrolylbenzenes as an alternative building block of terpyrrole, since the condensation reaction with the later did not work and used them in the synthesis of expanded calix[4]pyrroles, calix[n]1,3-bis(pyrrol-2-yl)benzenes **L53-55** (n = 2,3,4) where some of the *meso* bridges are replaced by benzene rings (Scheme 5.8).[14] The single crystal X-ray diffraction study showed that **L53a** binds chloride and nitrate via four H-bonding interactions and adopts cone conformation. While the four pyrrolic NH protons were involved in binding with a single chloride anion, only two of the oxygen atoms from the nitrate anion were involved in hydrogen bonds with the four pyrrolic NH protons. The corresponding X-ray analysis of the PF_6^- and NO_3^- complexes of calix[3]bispyrrolylbenzene **L54a** displayed a V-shape conformation. Further, all three oxygens of the nitrate interacts with the receptor via H-bonds involving four of the six pyrrolic NHs.[15] Anion binding of calix[2]-bispyrrolylbenzene displayed selectivity for Cl^- over Br^-, HSO_4^-, and NO_3^- as determined by ITC in 1,2-dichloroethane. The anion binding affinities of these macrocycles were in the order **L53a**> **L53b** > **L53c**.

In 2007, Cafeo *et al.* reported two isomeric calix[2]pyrrolylbenzene **L120-121** where the pyrroles of the dipyrromethane units were connected via *m*- and *p*- phenylenes through additional carbon atoms (Scheme 5.9).[15] The X-ray structure of **L120** *i.e. m*-isomer adopts a centrosymmetric rectangular box conformation, where the pyrrole units adopt 1,2-alternate conformation while in **L121** *i.e. p*-isomer adopts a conformation resembling a twisted tennis ball seam. Although chemically very similar, these two macrocycles have considerably different anion binding properties. In dichloromethane *m*-isomer is found to act as a better host than *p*-isomer toward anions. In fact, **L121** binds F^- and CH_3COO^- ion to appreciable extent while **L120** binds Br^-, Cl^-, I^- and $H_2PO_4^-$ ions among the tested anions.

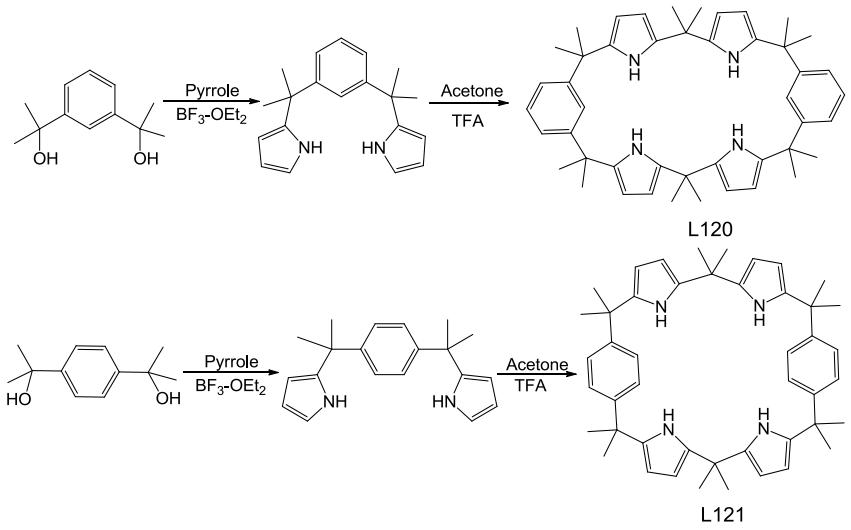

Scheme 5.9 Synthesis of **L120** and **L121**.

5.2 Research goal

After the intial reports by Sessler *et al.* [13,14] and Cafeo *et al.*[15] on spacer induced expanded calix[4]pyrroles this approach remain unexplored which may be attributed to the absence of suitable building blocks. In light of the previous three reports, it is clear that slight modification of the spacer unit can lead to different structure of the core and improved binding affinities as well as selectivities with regard to anions. Aware of this fact and in an effort to investigate the effect of the size of the spacer on anion binding affinity and selectivity, we designed a set of new expanded calixpyrroles namely calix[2]bispyrrolylethenes (**SP27-29**) where the two dialkyldipyrromethane units are linked via ethene bridges, the smallest spacer units employed so far. Compared to calix[2]bispyrrolylbenzene **L53**, these new receptors possess a relatively smaller core size, which in turn is bigger than that of *meso*-octamethylcalix[4]pyrrole, **L48**. This may facilitate

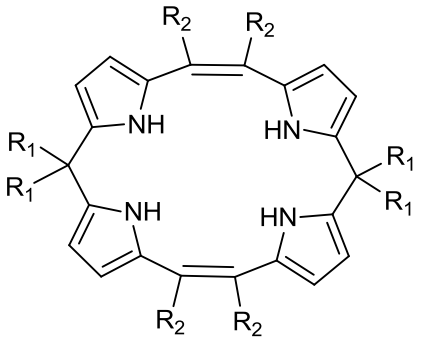

SP27 R_1,R_2 = Me
SP28 R_1 = Cy, R_2 = Me
SP29 R_1 = Me, R_2 = H

better binding affinity and selectivity towards bigger halide ions. Further, the presence of two double bonds in the macrocyclic core is expected to influence their anion binding ability through possible anion-π interactions.

5.3 Results and discussion

5.3.1 Synthesis and characterization

The synthesis of the targeted macrocycles **SP27-29** is summarized in scheme 5.10. These macrocycles are conveniently synthesized in two steps from dialkyldipyrromethane via Vilsmeir-Haack method,[16] followed by McMurry coupling.[17] Although both the reactions are very familiar in porphyrinogen chemistry, since Vogel employed towards the synthesis of porphycenes (an isomer of porphyrin), nobody has implemented it in calixpyrrole chemistry.[18]

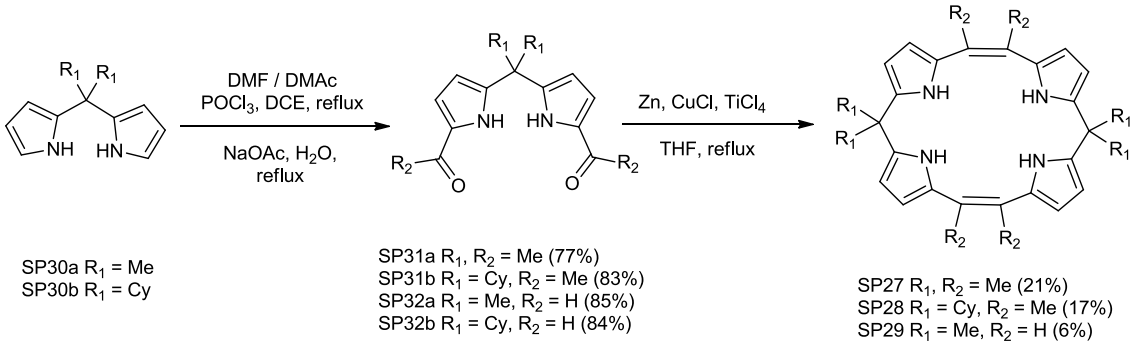

Scheme 5.10 Synthetic scheme of calix[2]bispyrrolylalkenes **SP27-29**.

The starting materials, dialkyldipyrromethane **SP30a-b** can be easily synthesized in gram scale by condensation of pyrrole with acetone and cyclohexanone separately following Lindsey's protocol which were discussed in chapter 2.[19] The dipyrromethanes **SP30a-b** were separately acylated and formylated to obtain **SP31a-b** (77 and 83%) and **SP32a-b** (85 and 84%) respectively via Vilsmeir-Haack method.[16] Subsequent reductive coupling, following McMurry strategy, using Zn-CuCl/$TiCl_4$ adduct led to the formation of the desired expanded calix[4]pyrroles **SP27** (21%), **SP28** (17%) and **SP29** (6%) as white solids.[19c] In spite of many modulation of reaction conditions *i.e.* by varying addition rate of the substrate, reaction time we were unable to improve the yield of **SP29**. McMurry coupling with **SP32b** did not yield the desired product. While the yields of the final compounds proved low (in particular **SP29**), it is important to note that the synthesis of the starting material for cyclization *i.e.* **SP31a-b** and **SP32a-b** is very facile and can be easily carried out in gram scale.

All compounds were characterized by ^{1}H NMR, ^{13}C NMR spectroscopy, mass and elemental analysis. Further, some of their solid state structures were unequivocally characterized by single crystal X-Ray diffraction analysis. Diffraction grade crystals for

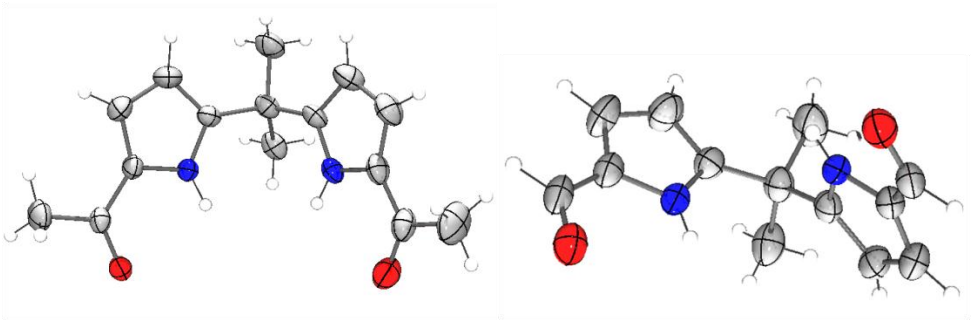

Figure 5.2 ORTEP diagrams of **SP31a** (left) and **SP32a** (right). Thermal ellipsoids are scaled upto 35% probability level.

SP31a and **SP32a** were grown by slow evaporation of their chloroform solutions and their structures were elucidated by single crystal XRD analysis. As illustrated in figure 5.2, **SP31a** adopts a configuration where all the pyrroles and acyl groups orient in the same direction. Whereas, in case of its diformyl homologue **SP32a**, each pyrrole unit and the attached formyl group orient in the same direction, however they reside away from each other by forming a torsion angle of 37.6 °C between the two pyrrole units. The ^{1}H NMR spectra of all the calix[2]bispyrrolylethene systems **SP27-29**, indicated the symmetric nature of the central core with a single NH peak and a doublet for the *β*-CH protons. Crystals of **SP27** suitable for X-ray structural analysis were grown by slow evaporation of dicholomethane and dimethylsulfoxide solution. The solid state structure reveals that crystals obtained from dimethylsulfoxide contain one molecule of dimethylsulfoxide trapped in the lattice. The

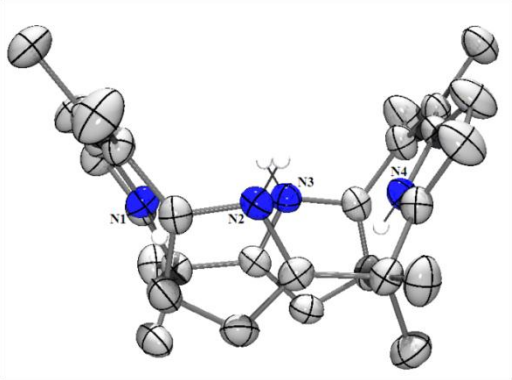

Figure 5.3 ORTEP diagram of **SP27**. Thermal ellipsoids are scaled upto 35% probability level. All the methyl and pyrrole *β*-CH are removed for clarity.

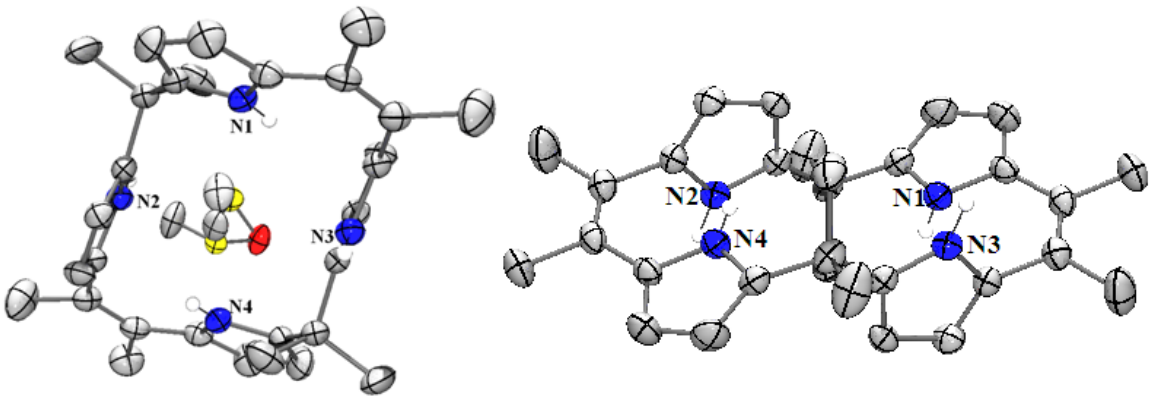

Figure 5.4 ORTEP diagram showing two different view of **SP27.**DMSO. Left: with solvent, Right:solvent was removed for clarity. Thermal ellipsoids are scaled upto 35% probability level. All the methyl and pyrrole *β*-CH are removed for clarity.

structural analysis of the guest free form of **SP27**, obtained from dichloromethane, revealed the 1,3-alternate conformation of the molecule, wherein adjacent pyrrole rings and NHs are oriented in opposite directions (Figure 5.3). The nitrogen-nitrogen cross ring distances are N1-N4 4.71 Å and N2-N3 4.31 Å. In this compound, all the nitrogens are almost coplanar where the distance between the r.m.s. plane defined by the four nitrogens and each nitrogen is ~0.02 Å. Here two alternate pyrrole units reside in the plane of the *meso* like C-C double bonds (dihedral angles 3.37 and 4.36°) with their NHs towards the core, while the remaining

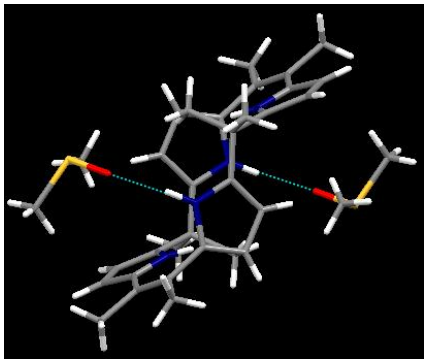

Figure 5.5 Mercury View of the H-bonding pattern of NHs and DMSO molecule in **SP27**.**$(CH_3)_2SO$**.

two pyrrole units adopt almost orthogonal geometry w.r.t. the double bonds (dihedral angles 93.78 and 97.54°) and their NHs are directed in opposite direction w.r.t. each other unlike octamethylcalix[4]pyrrole. On the other hand, **SP27**.**$(CH_3)_2SO$** *i.e.* DMSO solvate adopts a slightly distorted 1,2-alternate conformation (Figure 5.4) which may be attributed to the interaction of **SP27** with the solvent molecule. In this compound all the nitrogens are coplanar with the nitrogen-nitrogen cross ring distances N1-N4 5.53 Å and N2-N3 5.32 Å.

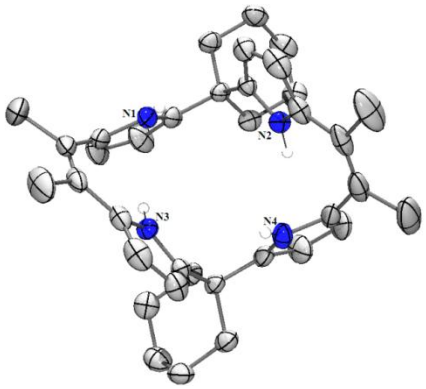

Figure 5.6 ORTEP diagram of **SP28**. Thermal ellipsoids are scaled upto 35% probability level. All the methyl hydrogens and pyrrole *β*-CH are removed for clarity.

Here, two alternate pyrrole units orient towards the core while the other two orients away from the core interacting with two dimethylsulphoxide molecule through two symmetry equivalent N-H…O H-bonds with N…O distance of 2.972 Å (Figure 5.5). The single crystal X-ray analysis of **SP27** crystals obtained by slow evaporation of its dichlormethane solution, reflected the 1,3-alternate conformation of the pyrrole units where the two cyclohexyl rings resides on the same side (Figure 5.6). Here the nitrogen-nitrogen cross ring distances are N1-N4 4.47 Å and N2-N4 4.82 Å and all the nitrogen are almost coplanar where the distance between the r.m.s. plane defined by the four N atoms and each nitrogen is ~0.033 Å. The presence of cyclohexyl groups at the alternate *meso* positions creates more steric congestion in **SP28** and as a result, pyrrole units are more distorted (dihedral angles 13.67 and 68.3° w.r.t. C-C duble bond) compared to **SP27**. Single crystal of **SP29** was obtained by slow evaporation of its ethyl acetate solution. Solid state structures obtained by XRD confirms 1,3-alternate conformation of the pyrrole residues (Figure 5.7). However, owing to the greater steric flexibility, the two opposite pyrrole units are found to align slightly away from the cavity (dihedral angles 150.83 and 151.84° w.r.t. the C-C double bonds) with their NHs are directed in opposite direction, whereas the other two pyrrole entities are oriented towards the core (dihedral angles 11.76 and 13.47° w.r.t. the C-C double bonds) and reside almost in the same plane. In this case nitrogen-nitrogen cross ring distances are N1-N4 5.49 and N2-N4 5.53 Å. Further all the four nitrogen are almost coplanar and the distance between the r.m.s. plane defined by the four N atoms and each nitrogen is ~0.075 Å.

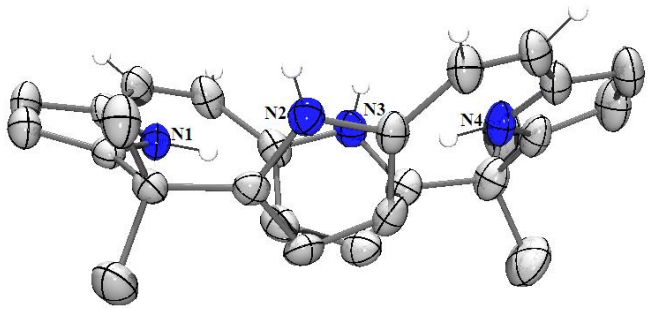

Figure 5.7 ORTEP diagram of **SP29**. Thermal ellipsoids are scaled upto 35% probability level. All the methyl hydrogens and pyrrole *β*-CH are removed for clarity.

5.3.2 Anion binding study

Tetrabutylammonium salts of fluoride, chloride, bromide, iodide, dihydrogenphosphate, bisulphate, perchlorate, acetate, nitrate, cyanide and hexafluorophosphate were used during anion binding study.

Preliminary anion binding studies of compound **SP27** and **SP29** were carried out in acetonitrile-d_3, via ^{1}H NMR spectroscopic titration method, using the above mentioned anions. Due to poor solubility of compound **SP28** in acetonitrile, its binding studies could not be performed with NMR. The qualitative anion screening experiment of **SP27**, with the respective anions indicated that compound **SP27** exhibits highest affinity towards fluoride ion, somewhat lesser extent towards acetate anion and little to none toward other anions (Figure 5.8). Further to get an insight into the binding affinity quantitative titration of fluoride, chloride, acetate, dihydrogen phosphate were performed, where the receptor solutions were titrated by adding known quantities (10 equiv.) of concentrated solution of the anions in question. The anion solutions used to effect the titrations contained the receptor at the same concentration as the receptor solutions into which they were being titrated so as to nullify the dilution effect. The data were fitted to a 1:1 binding profile in MATLAB 7.0

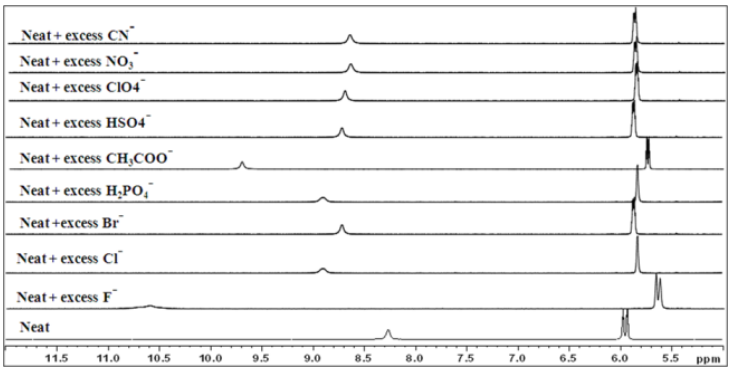

Figure 5.8 ^{1}H NMR spectroscopic titration study of **SP27** at 10 mM concentration in CD_3CN with addition of different anions as their tetrabutylammonium salts.

package according to the method of Wilcox[20] using the changes in the β-pyrrolic CH resonances in the ^{1}H NMR spectra.

Quantitative addition of TBAF, to 1mM solution of **SP27** displayed a significant downfield shift of the pyrrolic NHs from 8.25 to 10.8 ppm with concomitant upfield shift of the β-pyrrolic CH signals. Moreover a new sharp peak appeared at 7.63 ppm, which is relatively ~0.6 ppm upfield relative to the unbound host NH signals. The intensity of this new signal increases with increased addition of TBAF, whereas its position and sharpness remain unchanged (Figure 5.9). We have performed the titration experiments at different concentration of host **SP27** viz. 5mM and 10 mM concentration. Surprisingly it showed that at higher

concentration of **SP27** *i.e.* 10 mM, the new peak is not generating and the compound behaves almost like octamethylcalixpyrrole **L48** during the titration event. To explore the identity of,

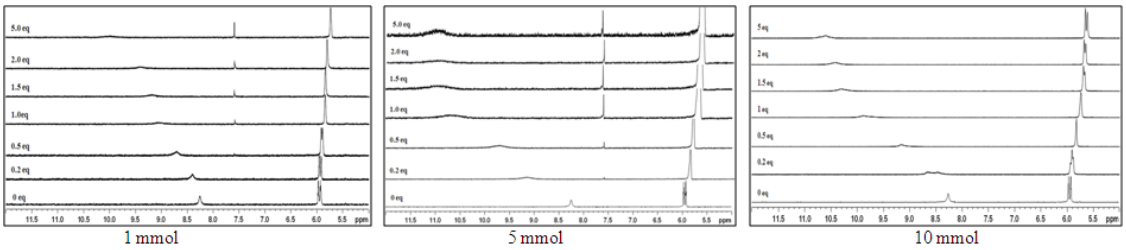

Figure 5.9 ^{1}H NMR spectroscopic titration spectra of **SP27** with addition of TBAF at different concentration (1, 5 and 10 mM) in CD_3CN

this new peak we performed D_2O exchange studies which displayed neither exchange nor broadening of this signal even after 24 h, indicating its nonpyrrolic NH nature (Figure 5.10). This indicated the occcurence of some secondary event during fluoride addition. Further the downfield shift of the β-CH resonances upon addition of D_2O indicates the release of F^- ion. This infers that the **SP27**.F^- complex is unstable in aqueous environment.

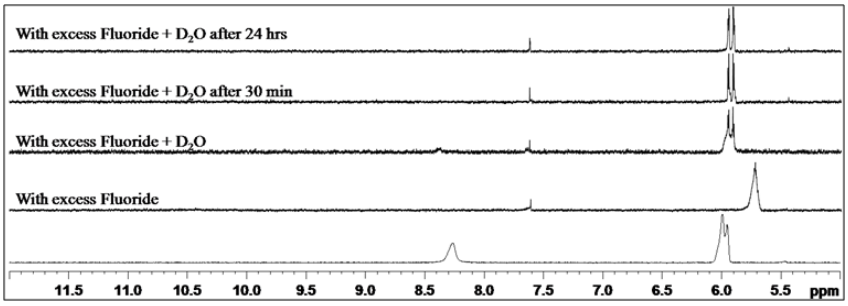

Figure 5.10 Deuterium exchange study of [**SP27**.F]$^-$ complex in CD_3CN. Here concentration of **SP26** is 1 mM.

Further we have carried out the quantitative titration experiments with chloride, acetate and dihydrogenphosphate ions at 1mM and 10 mM concentration of **SP27**. While addition of acetate anion, the NH peak shifts from 8.2 to ~9 ppm with concomitant upfield shift of the β-CH peak (Figure 5.11). But unlike fluoride, in this cases no new peak emerges. This is indicative of the presence of some additional events in case of fluoride binding. Further chloride and dihydrogen phosphate ions show a minor shift in NH resonances at higher concentration of **SP27** *i.e.* at 10 mM, while no appreciable change with 1mM solution noticed (Figure 5.12 and 5.13).

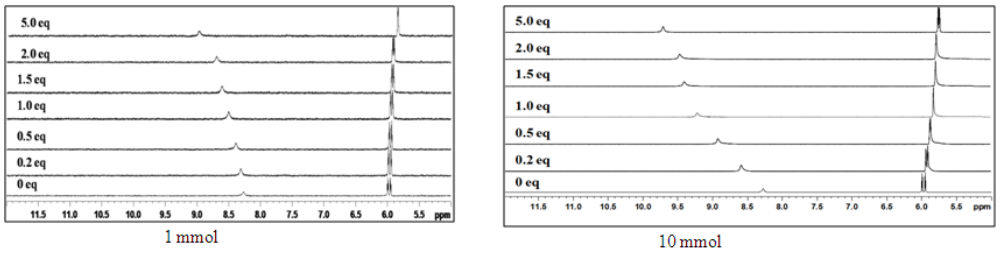

Figure 5.11 ^{1}H NMR titration spectra of **SP27** at different concentration in CD_3CN with TBA(CH_3COO).

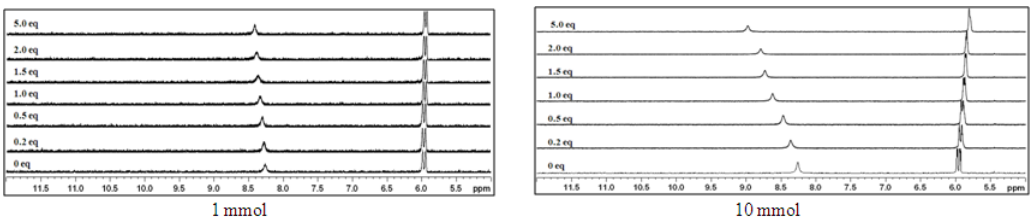

Figure 5.12 ^{1}H NMR titration spectra of **SP27** at different concentration (1 and 10 mM) in CD_3CN with TBACl.

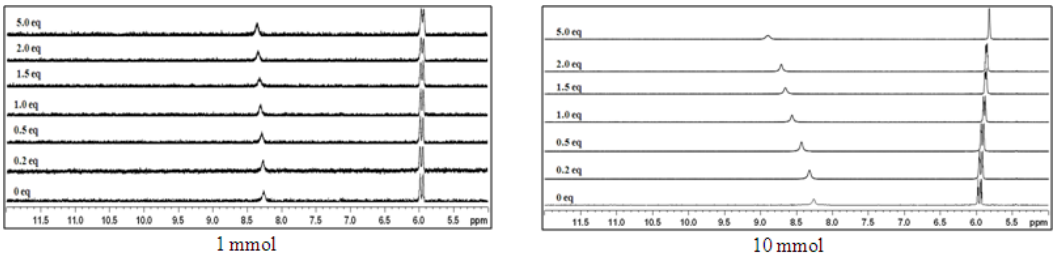

Figure 5.13 ^{1}H NMR titration spectra of **SP27** at different concentration (1 and 10 mM) in CD_3CN with $TBAH_2PO_4$.

The stoichiometry of the **SP27**.anion complexes were determined by continuous variation method *i.e.* Job's plot in CD_3CN. Here, 1 mM of compound **SP27** and 1 mM of the tetrabutylammonium salt was mixed in ratios from 1:10 to 10:1. In these experiments, in case

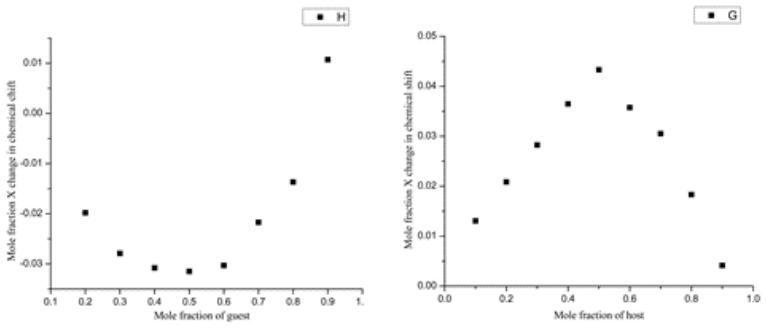

Figure 5.14 Job plot of **SP27** for Left: TBAF; Right: TBA(CH_3COO).

of fluoride complexation, pyrrole β-CH proton resonance were considered, since in this case the pyrrole NH signal became broad due to the fast complexation-decomplexation equilibrium, whereas for acetate complexation, pyrrole NH resonances were considered. Nonlinear curve fitting analysis of the titration data with Wilcox equation of the upfield shift of the β-CHs shows a good fit with 1:1 binding stoichiometry.[21]

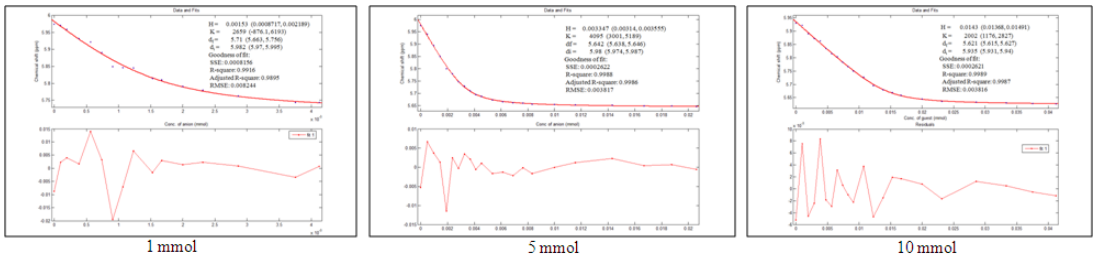

Figure 5.15 ^{1}H NMR titration fitting curve for compound **SP27** and TBAF in different concentration (1, 5 and 10 mM) of **SP27**. Left: [**SP27**] = 1×10^{-3} M, [TBAF] = 10×10^{-3} M, Middle: [**SP27**] = 5×10^{-3} M, [TBAF] = 50×10^{-3} M, Right: [**SP27**] = 10×10^{-3} M, [TBAF] = 100×10^{-3} M.

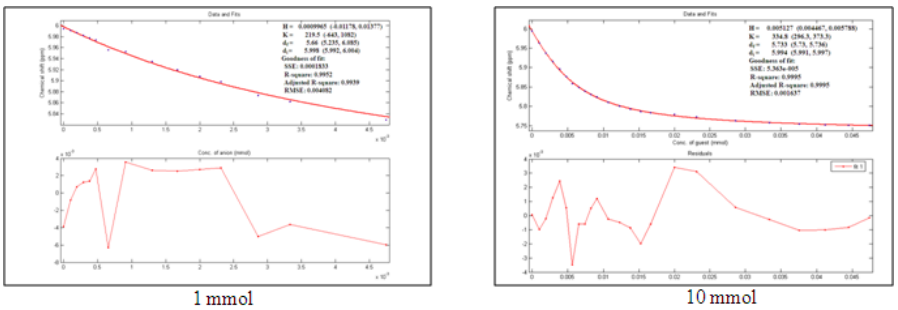

Figure 5.16 ^{1}H NMR titration fitting curve for compound **SP27** with TBA(CH_3COO) in different concentration (1 and 10 mM) of **SP27**. Left: [**SP27**] = 1×10^{-3} M, [TBA(CH_3COO)] = 10×10^{-3} M, Right : [**SP27**] = 10×10^{-3} M, [TBA(CH_3COO)] = 100×10^{-3} M.

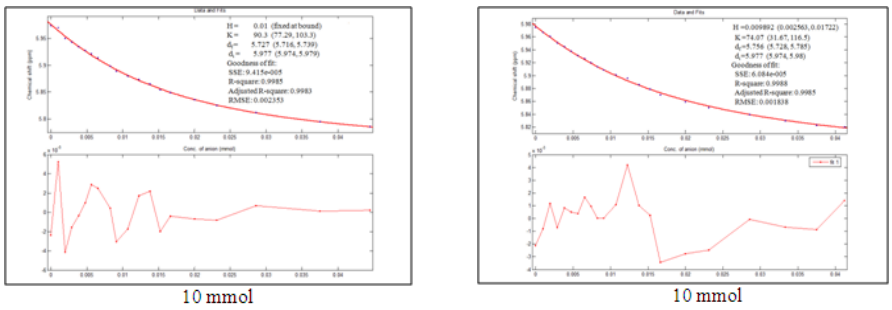

Figure 5.17 ^{1}H NMR titration fitting curve for compound **SP27** with TBACl and $TBAH_2PO_4$ in different concentration (1 and 10 mM) of **SP27**. Left: [**SP27**] = 10×10^{-3} M, [TBACl] = 100×10^{-3} M, Right : [**SP27**] = 10×10^{-3} M, [$TBAH_2PO_4$] = 100×10^{-3} M.

Table 5.1 Binding affinity constants of **SP27** for different anions measured by NMR titration study in CD_3CN.

Anion	K_a (M^{-1})		
	SP27 (1 mM)	**SP27** (5 mM)	**SP27** (10 mM)
F^-	2.6×10^3	4.09×10^3	2.0×10^3
Cl^-	-	-	90.3
CH_3COO^-	2.89×10^2	-	3.34×10^2
$H_2PO_4^-$	-	-	74.07

The affinity constant K_a of **SP27** for the measured anions shows relatively selective binding towards fluoride ion (Table 5.1). However, the discrepancy of the affinity constant of **SP27** towards fluoride at different **SP27** concentration is quite unusual and indicates the presence of some concentration dependent secondary events.

Further, quantitative thermodynamic insight into the proposed anion binding behavior came from ITC studies, carried out in acetonitrile at 303K, using tetrabutylammonium salts of anions as the anion source. Both **SP27** and **SP28** display acetate ion affinities in NMR that were too low to be determined by ITC (in acetonitrile), however both showed substantial

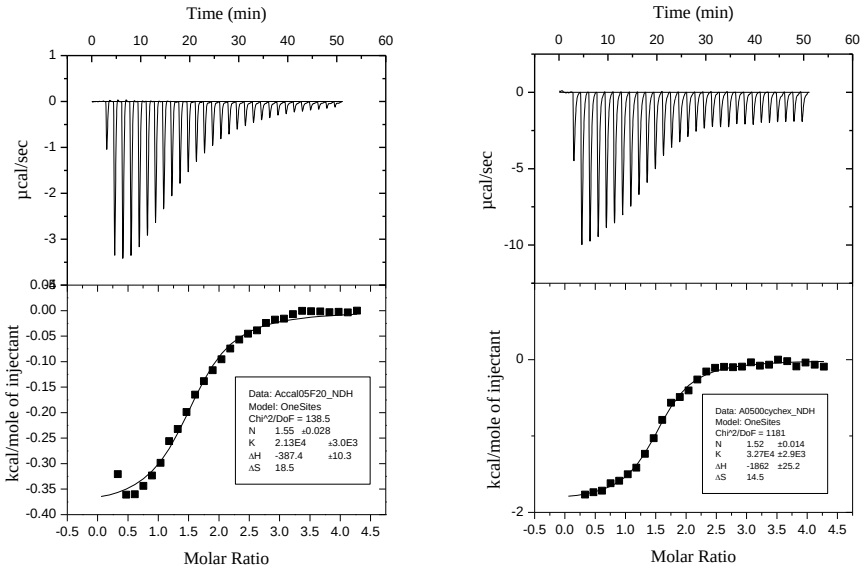

Figure 5.18 ITC curves produced from the titration of compound **SP27** (Left) and **SP28** (Right) (0.5 mM) with TBAF (20 mM) in CH_3CN at 303K.

fluoride affinities (Figure 5.18 and table 5.2). ITC studies showed the fit of the experimental data to a 1:1 binding profile. Table 5.2 shows **SP28** possess a slightly higher affinity (K_a) than **SP27** towards fluoride ion. The fluoride ion complexations were driven by both favorable enthalpy and entropy contribution. In particular, the entropy factor was found to be a major determinant in driving the fluoride ion recognition event. The large positive entropy of complexation may be attributed to the release of the three water molecules of the tetrabutylammonium fluoride to the bulk solvent, upon complexation. Further, The ITC profile shows almost eight times more strong binding affinity for **SP27** than that measured by ^{1}H NMR titration method and this discrepancy may be attributed to the different concentrations at which both experiments are carried out, in addition to the presence of other simultaneous event which could not be accounted for by NMR experiments.

Table 5.2 Energetics of host-guest binding of **SP27** and **SP28** with tetrabutylammonium fluoride in acetonitrile at 303 K as determined by ITC.

Host	TΔS (kCal.mol^{-1})	ΔH (kCal.mol^{-1})	ΔG (kCal.mol^{-1})	K_a (M^{-1})
SP27	5.605	-0.387	-5.992	2.13 ×10^4
SP28	4.493	-1.862	-6.255	3.27 ×10^4

Preliminary anion binding studies of compound **SP29**, carried out out in CD_3CN, via the ^{1}H NMR spectroscoic titration method, using tetrabutylammonium salts of the above mentioned anions, display relatively small shift *i.e.* ~0.8 ppm shift of NH resonances, indicating relatively weak interaction with fluoride ion only, among the tested anions (Figure 5.19). Surprisingly, during the NMR screening experiment with the tested anions, strong

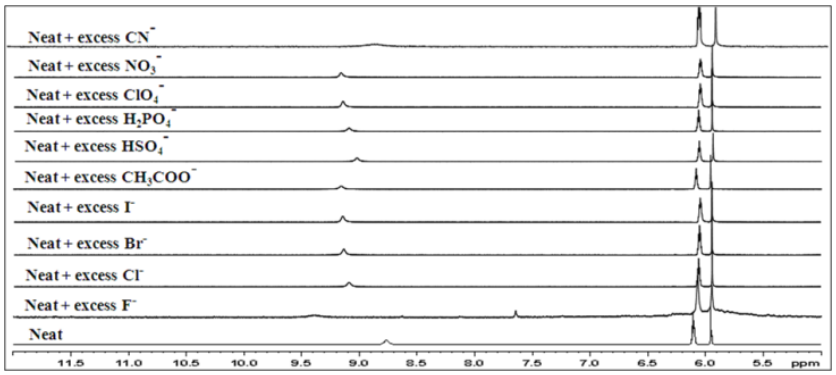

Figure 5.19 ^{1}H NMR titration of **SP29** at 10 mM concentration in CD_3CN with addition of different anions as their tetrabutylammonium salts.

colorimetric response for fluoride ion is observed. A sharp change in color from colorless to dark red resulted immediately with the addition of fluoride ion, which could be clearly observed by naked eye (Figure 5.20). The quantitative ^{1}H NMR titration of **SP29** with TBAF did not show any significant shift in NH resonances at 1mM conc. of host, while a minor shift is observed at 10 mM concentration. But, like **SP27** a new sharp peak appears at 7.58 ppm, which is 1.2 ppm upfield shifted compared to that of the unbound host NH signal. The

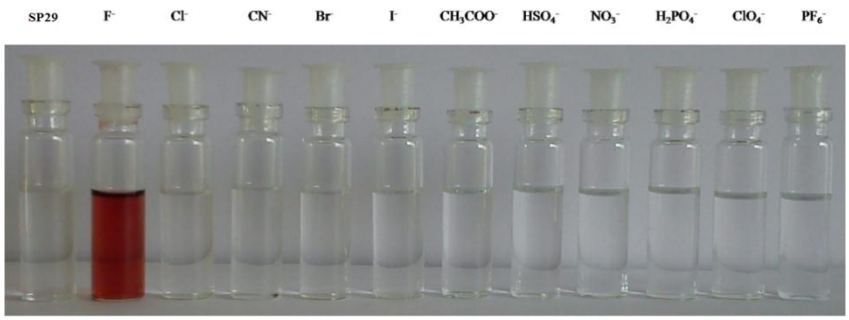

Figure 5.20 Naked eye view of the color change while addition of different anions as their tetrabutylammonium salts to the solution of **SP29** in CH_3CN.

position of this peak remain unchanged, however its intensity increased, with increase in fluoride concentration (Figure 5.21). Interestingly, no shift of the *β*-CH resonances also noticed. This precludes any major change in the conformation of the macrocycle upon anion binding. The absence of HF_2^- also ruled out the NH deprotonation mechanism. The quantitative titration experiments for other anions neither show any NH shift nor emergence of any new peak, indicating **SP29**'s inertness towards other anions (Figure 5.22).

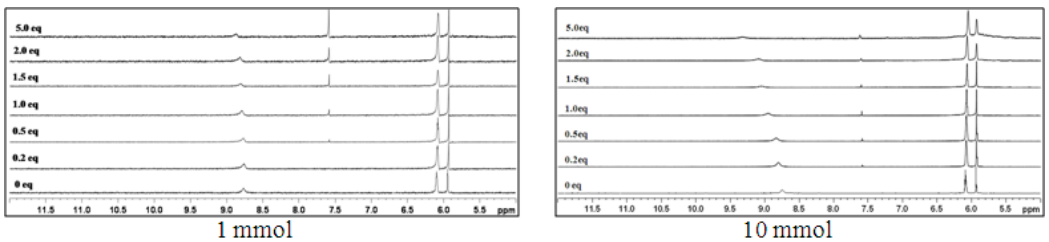

Figure 5.21 ^{1}H NMR titration spectra of **SP29** at different concentration in CD_3CN with TBAF.

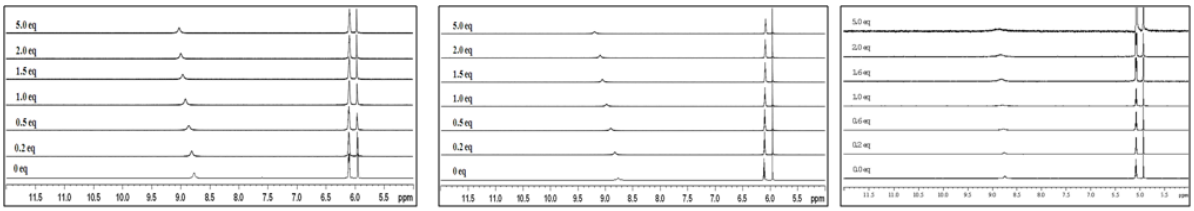

Figure 5.22 ^{1}H NMR titration spectra of **SP29** at 10 mM concentration in CD_3CN with Left: TBACl, Middle: TBA(CH_3COO), Right: TBACN

We performed ITC study, to get some thermodynamic insight into the binding event, however after repeated attempts; we could not get a suitable enthalpy change profile to fit into the binding isotherm (Figure 5.23). This may be attributed to the occurrence of very weak interaction event, with thermodynamic parameters below the detection limit of ITC.

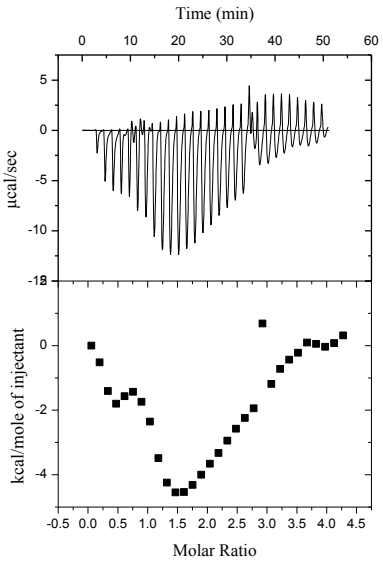

Figure 5.23 ITC titration curves produced from the titration of compound **SP29** (0.5 mM) with TBAF (20 mM) in CH_3CN at 303 K.

To get further insight into the interaction of anions, the absorption profile of **SP29** upon addition of excess of the tested anions were recorded. The host concentration considered for this experiment is 20µM. The study revealed, after addition of fluoride ion, the absorption peaks of free **SP29** at 316 nm disappears and two new peaks at 337 and 515 nm appears, inducing the color change to dark red, whereas in cases of other anions the absorption profile of **SP29** remain almost unchanged (Figure 5.24). The quantitative titration of **SP29** with TBAF was performed, where the receptor solutions were titrated by adding known quantities of fluoride ion (Figure 5.25). It reveals that the absorption band centered at 316 nm decreased

gradually up to addition of ~1 mM of fluoride anion with two isobestic points at 295 and 337 nm. Further addition of TBAF resulted in the red shift of the spectra with the emergence of two new peaks at 337 and 515 nm and hence imparted the resultant colorimetric response. In addition, Job's plot analysis displays the formation of 1:1 stoichiometric complex of **SP29** and fluoride ion. Competition experiments also confirmed the fluoride induced color change,

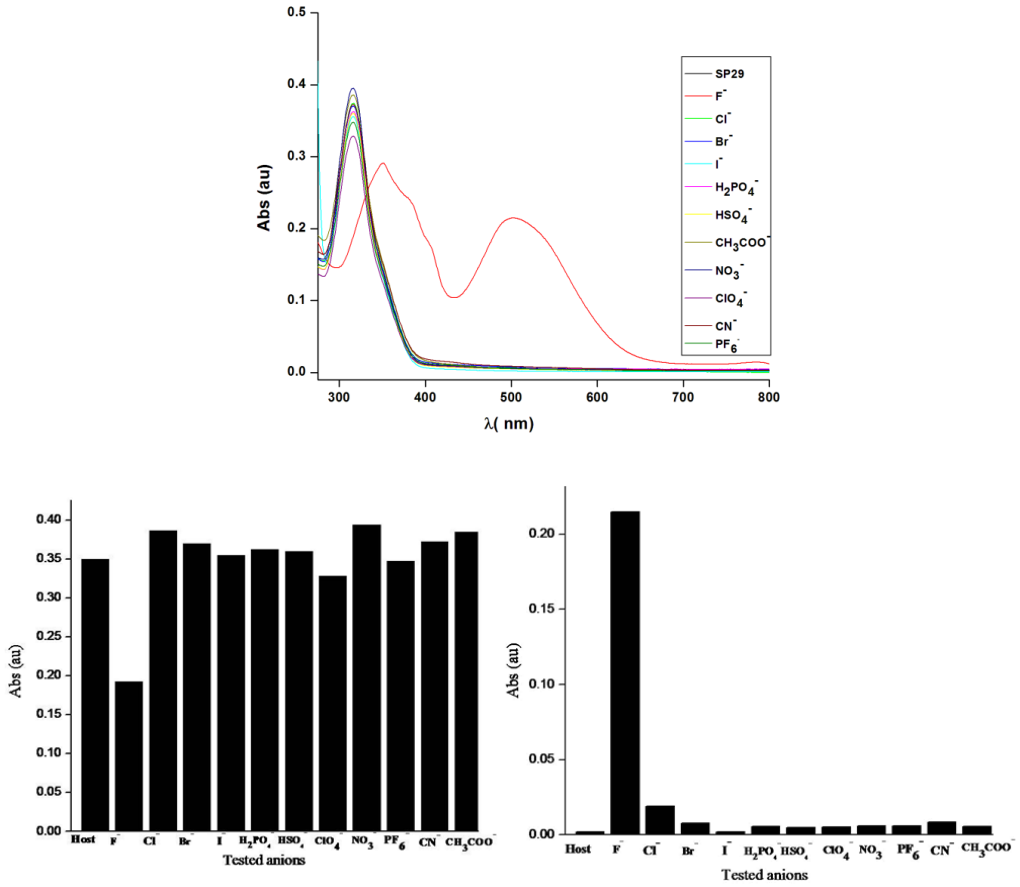

Figure 5.24 Top: electronic spectra of **SP29** in the absence and presence of the TBA salt of different anions (F^-, Cl^-, Br^-, I^-, $H_2PO_4^-$, HSO_4^-, ClO_4^-, CH_3COO^-, NO_3^-, CN^- and PF_6^-) in CH_3CN. Bottom : UV-Visible absorbance response of **SP29** (20×10^{-6} M) at λ=316 nm (left) and 515 nm (right) in the absence and presence of the TBA salt of different anions.

in the presence of other tested anions. Further addition of water to the fluoride complex of **SP29** led to a change of color from red to yellow (Figure 5.26). This observation indicated the occurrence of some irreversible process during fluoride complexation. To check the versatility of the colorimetric response of **SP29** towards fluoride we have performed solvent screening experiment, which display colorimetric response with varying intensity in polar aprotic solvents like DMSO, DMF, benzonitrile, tetrahydrofuran, acetone and ethylacetate

but not in dichloromethane, chloroform, methanol, isopropanol and *n*-butanol (Figure 5.27).This indicates the charge transfer nature of the host-guest complexation.

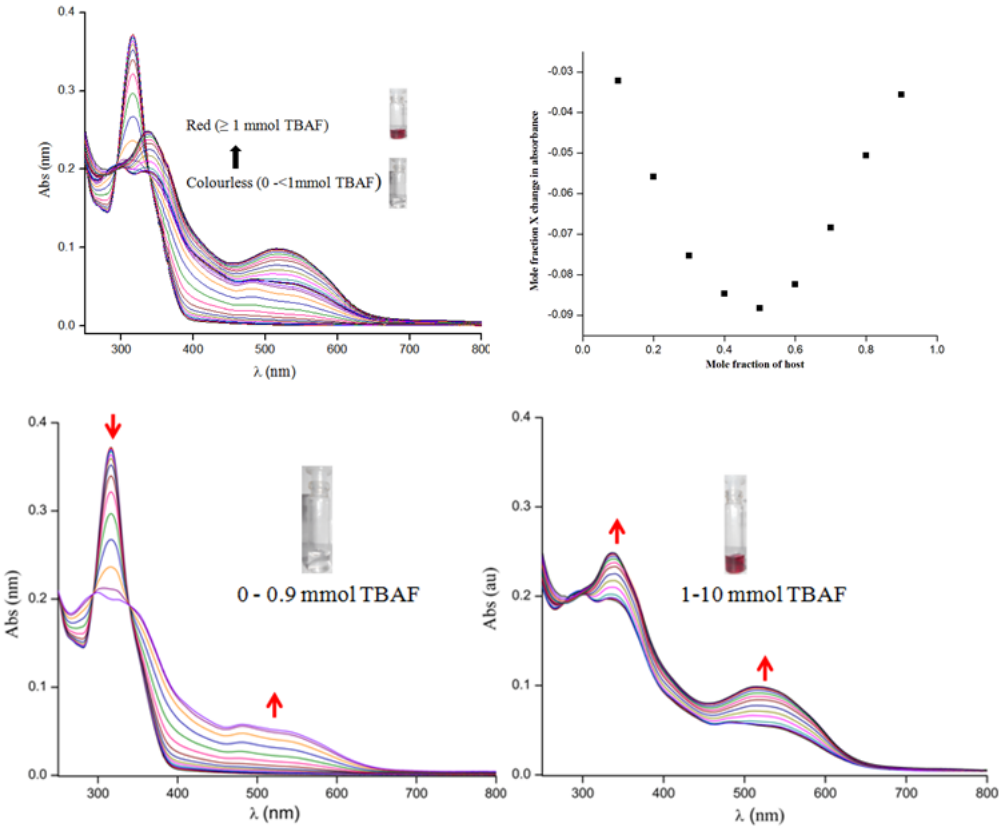

Figure 5.25 Top left**:** UV-Vis absorption spectra of **SP29** upon addition of TBAF; top right: Job's plot; bottom: UV-Vis absorption spectra of **SP29** upon addition of TBAF in acetonitrile. left: up to addition of 0.9 mM; right: after addition of 1mM.

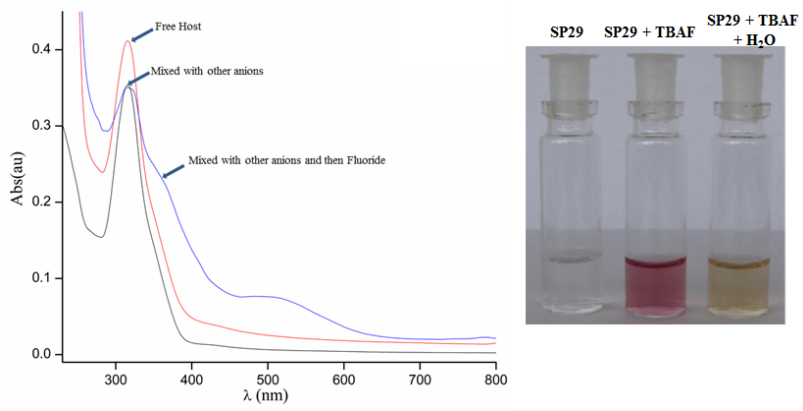

Figure 5.26 Left: UV-Visible spectra: red: **SP29**, gray: **SP29** and TBA salts of other anions and blue: addition F^- in **SP29** combined with other anions; right: naked eye view of the colour change while addition of tetrabutyl ammonium fluoride to the solution of **SP29** in CH_3CN and then water.

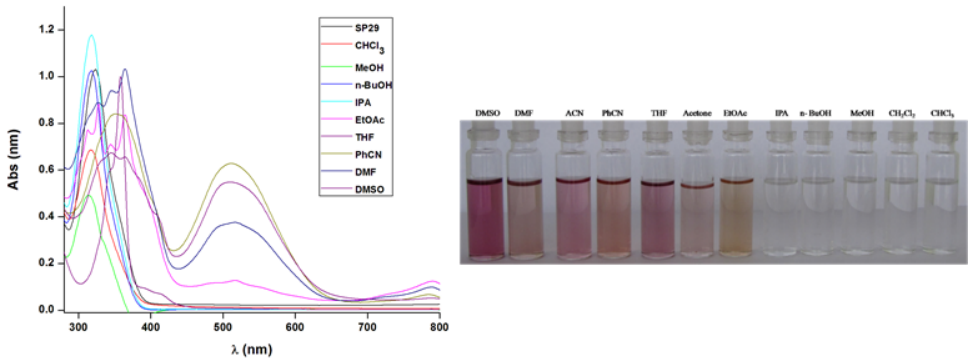

Figure 5.27 Left: Electronic spectra of **SP29** in presence of TBAF in different solvent medium**;** Right: naked eye view of the color change while addition of tetrabutylammonium fluoride to the solution of **SP29** in different solvents.

In light of the colorimetric response of **SP29** with fluoride, analogous titration were performed with **SP27** and **SP28** to check if there is any change in the UV-Vis spectra in presence of anions (Figure 5.28). However, these compounds did not show any appreciable change even in UV region.

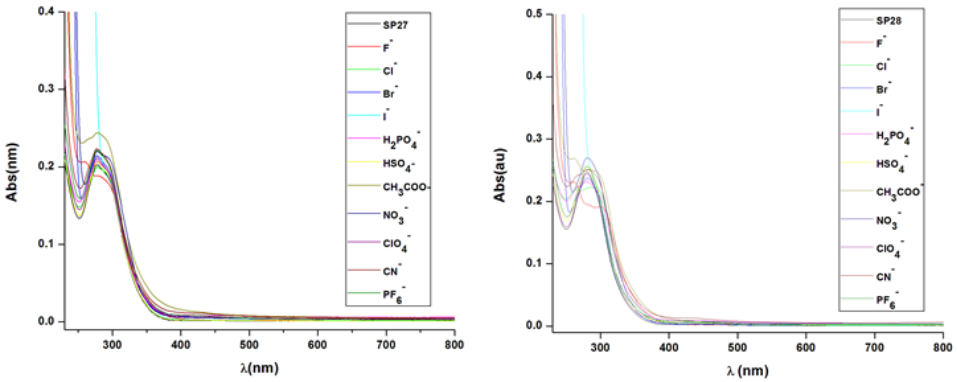

Figure 5.28 Electronic spectra of **SP27** and **SP28** (20×10^{-6} M) in the absence and presence of the TBA salt of different anions in CH_3CN medium.

In order to investigate the source of the colorimetric response, electron paramagnetic resonance (EPR) studies were performed for both **SP27**.F^- and **SP29**.F^- complexes which did not show any signal at room temperature. Subsequent lowering of temperature resulted in the appearance of a strong signal at 30 K for both the complexes. The *g*-values are 2.0023 and 2.0021 for **SP27**.F^- and **SP29**.F^- respectively. This indicates the presence of an unpaired electron or formation of anion radical and thereby confirms the charge transfer nature of the complexes. We presume, in case of **SP29** the charge transfer may be more facile than the

other two and that may be the plausible cause behind the colorimetric response in presence of fluoride ion.

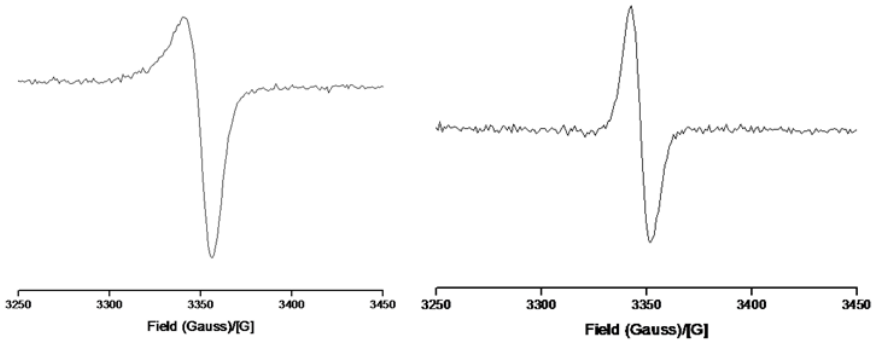

Figure 5.29 The EPR spectra of **SP27.F**$^-$ (left) and **SP29.F**$^-$ (right) in presence of TBAF in acetonitrile at 30 K.

To get better insight into the binding behavior of the macrocycles, we tried to grow XRD quality single crystals of **SP27-29** in presence of fluoride ion by various methods of crystallization. Unfortunately all our efforts met with failure. Therefore, we carried out density functional theory (DFT) optimization for fluoride complexes of **SP27** and **SP29** to gain further understandings about the binding mechanism. The optimized structure obtained for the **SP27**.F$^-$ and **SP29**.F$^-$ complexes indicate a more planar type of conformation along with better encapsulation of anion by **SP29** than **SP27** (Figure 5.30). Further, HOMO-LUMO

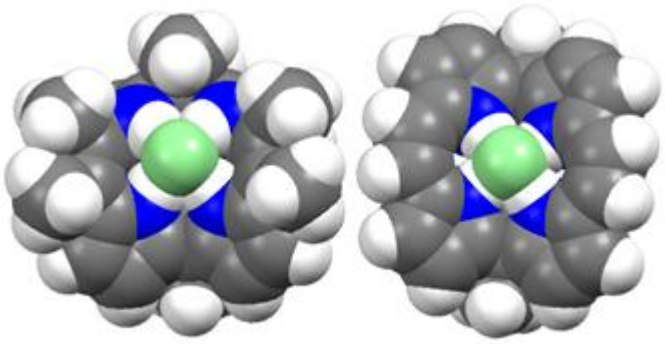

Figure 5.30 Space filling model of DFT-optimized structure of the fluoride complexes: [**SP27**.F]$^-$ (left) and [**SP29**.F]$^-$ (right) showing clearly the binding pattern. Color code: green: F, red: blue: N, grey: C and white: H.

energies were calculated both for free host and fluoride complexes of **SP27** and **SP29** in the gas phase, chloroform and acetonitrile. A glance at the HOMO-LUMO energies indicates

while formation of complex raises the energy difference between HOMO and LUMO in **SP27** (for example 4.35 to 4.77 eV in acetonitrile), that in case of **SP29** decreases from 4.02 to 3.71 eV (Figure 5.31), accompanied by stabilization of both HOMO and LUMO in more polar solvent (viz. acetonitrile) than in gas phase or less polar solvent and hence explains its colorimetric response towards fluoride ion. As the LUMO of the macrocycle resides on the C–C double bond, therefore we can conclude that during the complex formation, charge transfer occurs from the fluoride ion to the ethene bonds through anion-π interactions.

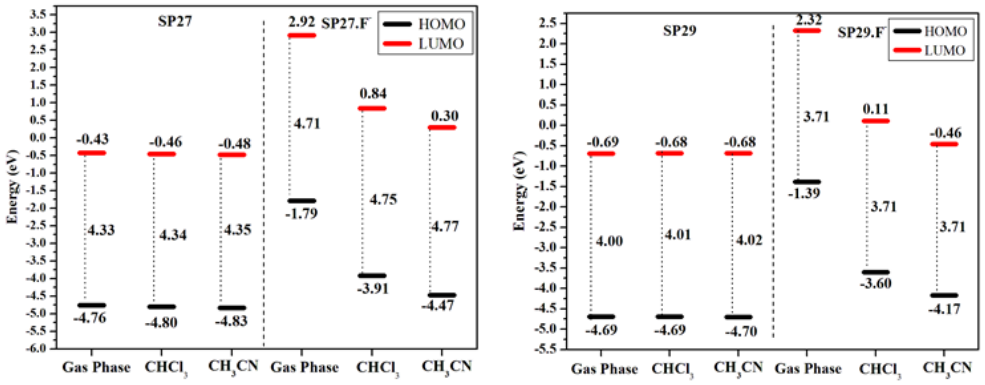

Figure 5.31 HOMO-LUMO energies in gas phase, chloroform and acetonitrile for Left: **SP27** and **SP27.F**$^-$.Right: **SP29** and **SP29.F**$^-$.

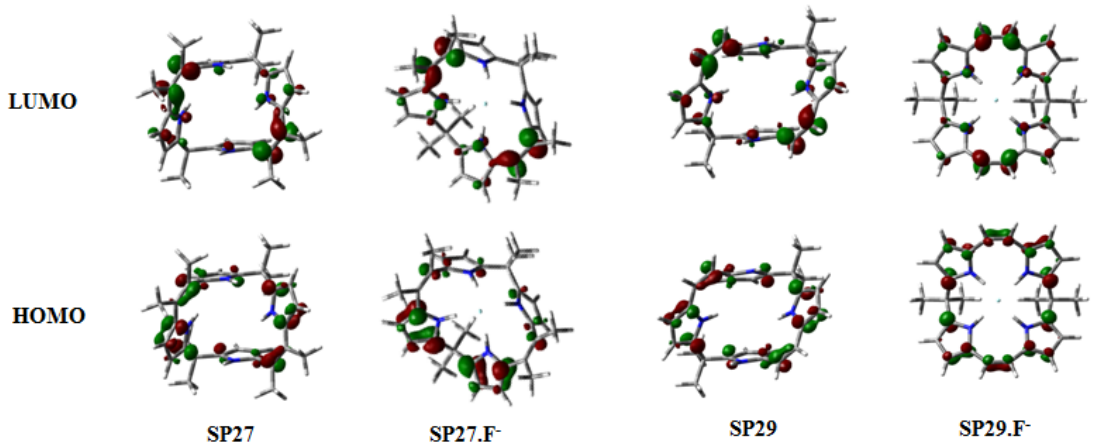

Figure 5.32 pictorial views of the HOMOs and LUMOs of the optimized structures of the free host and their fluoride complexes.

On the basis of computational outcome, it is important to appreciate that owing to this putative charge transfer, the electron density on the fluoride ion is depleted; thereby it could not interact favourably with the pyrrolic NHs. Probably, owing to this reason, no shift in the NH resonances in ^{1}H NMR of **SP29** was observed, upon addition of fluoride ion. The charge

transfer process becomes more facile in relatively planar **SP29**.F^- complex (hence no shift in NH resonances) than **SP27**.F^- (NH resonance shifts from 8.25 to 10.8 ppm). Moreover, in case of **SP27** the presence of electron donating methyl groups on the bridging double bonds, relatively increases the electron density on the double bonds, as a consequence disfavours the charge transfer from fluoride to the host.

5.4 Conclusion

In conclusion, we have designed and synthesized three new *meso*-expanded calix[4]pyrrole receptors following the McMurry strategy for the first time. Among them, calix[2]bispyrrolylethene **SP29** displays easy to observe colorimetric sensing of fluoride ion (colorless to dark red) in polar aprotic solvents through anion-π interaction. Supramolecular interactions promote an unprecedented electron transfer process from the F^- ion to the receptors. The synthesized molecules are highly selective towards fluoride over other anions because of better encapsulation or preorganization.

As discussed in chapter 1 fluoride malfunctioning creates serious health risk so the low level of F^- tolerance demands for a selective and sensitive F^- sensor. Owing to its importance a large number of synthetic receptors containing H-bond donor motif, with Lewis acidic sites and with electron deficient organic π-system have been designed.[21] Because of the nonchromogenic nature of most Y-H…X^- interactions, H-bonded receptors rely on either adjacent chromophore units or deprotonation followed by electron delocalization to display a colorimetric response. Our study clearly revealed how a small change in the periphery of the receptor led to complete change in the supramolecular interaction, from H-bonding to the charge transfer type. In addition, the molecule **SP29** shows a clear colorimetric response for fluoride although it does not contain any chromophore.

These macrocycles represent a new class of the smallest expanded calix[4]pyrrole reported so far. This study also highlights that it is not always true that increasing the core size will increase the affinity towards the larger anions. Presently, further study is going on to modulate this system, in order to enhance its host-guest response.

5.5. Experimental Details

5.5.1 Synthesis of compound SP30a and SP30b

Compound **SP30a** and **SP30b** were synthesized by following Lindsey's[19] method as described in chapter 2.

5.5.2 Synthesis of compound SP31a

In a three necked flask, equipped with a stirrer, a dropping funnel and a reflux condenser, N,N-dimethylacetamide (3 mL, 34 mmol, 6 equiv.) was placed. The flask was immersed in an ice bath and internal temperature was maintained below 5 °C, while phosphorous oxychloride (2.6 mL, 28 mmol, 5 equiv.) was added slowly through the dropping funnel. An exothermic reaction occurs with the formation of phosphorousoxychloride-DMAc complex. The ice bath was removed and the mixture was stirred for another 15 min at room temperature. 1,2-Dichloroethane (10 mL) was added and the ice bath was replaced. When the internal temperature is lowered to 5 °C, 5,5´-dimethyldipyrromethane **SP30a** (1 g, 5.7 mmol, 1 equiv.) dissolved in 1,2-dichloroethane (10 mL) slowly added to it. After the addition was completed, the ice bath was removed and the mixture was refluxed for 1 h, and then cooled to room temperature and a sat. solution of sodium acetate (12 g, 143 mmol) was added slowly to the reaction mixture. The reaction mixture was again refluxed for 3 h, during which copious evolution of hydrogen chloride noticed. Vigorous stirring was maintained during the above process. The cooled reaction mixture was extracted three times with dichloromethane. The combined organic layer was washed with sat. aq. Na_2CO_3 solution and dried over anhyd. sodium carbonate. The crude product was purified by column chromatography with 30% EtOAc in hexane as eluent. Evaporation of the eluent resulted in the desired product as white crystalline solid (1.14 g).

Yield: 77 %; Melting point: 199-201 °C; FTIR Data (KBr): 3323, 1649 cm^{-1}; ^1H NMR (400 MHz, $CDCl_3$): δ in ppm 9.862 (s, 2H, NH), 6.77 (m, 2H, β-CH), 6.1 (m, 2H, β-CH), 2.33 (s, 6H, CH), 1.67 (s, 6H, CH); ^{13}C NMR (100 MHz, $CDCl_3$): δ in ppm 188.00, 146.06, 131.96, 117.60, 107.32, 36.25, 28.83, 25.31; LCMS m/z calcd. for $C_{15}H_{18}N_2O_2$ (M+H) 259, found 259; Elemental analysis for $C_{15}H_{18}N_2O_2$ calcd. C: 69.74, H: 7.02, N: 10.84; found C: 69.85, H: 7.12, N: 10.64.

5.5.3 Synthesis of compound SP31b

In a three necked flask, equipped with a stirrer, a dropping funnel and a reflux condenser, N,N-dimethylacetamide (5.5 mL, 58.4 mmol, 5 equiv.) was placed. The flask was immersed in an ice bath and internal temperature was maintained below 5 °C, while phosphorous oxychloride (5.4 mL, 58.4 mmol, 5 equiv.) was added slowly through dropping funnel. An exothermic reaction occurs with the formation of phosphorousoxychloride-DMAc complex. The ice bath was removed and the mixture was stirred for another 15 min in room temperature. 1,2-Dichloroethane (10 mL) was added and the ice bath was replaced. When the

internal temperature is lowered to 5 °C, 5,5´-cyclohexyldipyrromethane **SP30b** (2.5 g, 11.6 mmol) dissolved in 1,2-dichlloroethane (25 mL) slowly added to it. After the addition was completed, the ice bath was removed and the mixture was refluxed for 1 h, the mixture was then cooled to room temperature and a sat. solution of sodium acetate (25 g) was added slowly to the reaction mixture. The reaction mixture is again refluxed for 3 h, during which copious evolution of hydrogen chloride noticed. Vigorous stirring was maintained during the above process. The cooled reaction mixture is extracted three times with dichloromethane. The combined organic layer was washed with sat. aq. Na_2CO_3 solution and dried over anhyd. sodium carbonate. The crude product was purified by column chromatography with 30% EtOAc in hexane as eluent. Evaporation of the eluent resulted in the desired product as white crystalline solid (2.9 g).

Yield: 83 %; Melting point: 228-231 °C; FTIR Data (KBr): 3321, 1643 cm^{-1}. ^1H NMR (400 MHz, $CDCl_3$): δ in ppm 10.38 (s, 2H, NH), 6.85 (m, 2H, β-CH), 6.11 (m, 2H, β-CH), 2.37 (s, 6H, CH), 2.27 (s, 4H, CH), 1.50 (m, 6H, CH).^{13}C NMR (100 MHz, $CDCl_3$): δ in ppm 187.92, 144.87, 131.77, 118.07, 107.71, 39.95, 35.23, 25.62, 25.13, 22.49. LCMS m/z calcd. for $C_{18}H_{22}N_2O_2$ (M-H) 297, found 297; Elemental analysis for $C_{18}H_{22}N_2O_2$ calcd. C: 72.46, H: 7.43, N: 9.39; found C: 72.55, H: 7.36, N: 9.25.

5.5.4 Synthesis of compound SP32a

In a three necked flask, fitted with a dropping funnel and a reflux condenser, N,N-dimethylformamide (2.1 mL, 28 mmol, 5 equiv.) was placed. The flask was immersed in an ice bath and internal temperature was maintained below 5 °C, while phosphorousoxychloride (2.6 mL, 28 mmol, 5 equiv.) was added slowly through dropping funnel. An exothermic reaction occurs with the formation of phosphorousoxychloride-DMF complex. The ice bath was removed and the mixture was stirred for another 15 min in room temperature. 1,2-Dichloroethane (10 mL) was added and the ice bath was replaced. When the internal temperature is lowered to 5 °C, 5,5´-dimethyldipyrromethane **SP30a** (1 g, 5.7 mmol, 1 equiv.) dissolved in 1,2-dichloroethane (10 mL) slowly added to it. After the addition was completed, the ice bath was removed and the mixture was refluxed for 1 h. The mixture was then cooled to room temperature and a sat. solution of sodium acetate (12 g, 143 mmol) was added slowly to the reaction mixture. The reaction mixture is again refluxed for 2 h, during which copious evolution of hydrogen chloride noticed. Vigorous stirring was maintained during the above process. The cooled mixture is extracted three times with dichloromethane. The combined organic layer was washed with sat. aq. Na_2CO_3 solution and dried over anhyd.

sodium carbonate. The crude product was purified by column chromatography with 30% EtOAc in hexane as eluent. Evaporation of the eluent resulted in the desired product as white crystalline solid (1.12 g).

Yield: 85 %; Melting point: 183-185 °C; FTIR Data (KBr): 3362, 1645 cm^{-1}. ^{1}H NMR (400 MHz, $CDCl_3$): δ in ppm 10.91 (s, 2H, NH), 9.27 (s, 2H, CH), 6.86 (m, 2H, β-CH), 6.22 (m, 2H, β-CH), 1.76 (s, 6H, CH).^{13}C NMR (100 MHz, $CDCl_3$): δ in ppm 179.37, 148.01, 132.57, 122.62, 108.33, 36.30, 28.22. LCMS m/z calcd. for $C_{13}H_{14}N_2O_2$ (M+H) 231, found 231; Elemental analysis for $C_{13}H_{14}N_2O_2$ calcd. C: 67.81, H: 6.13, N: 12.17; found C: 67.93, H: 6.30, N: 12.30.

5.5.5 Synthesis of compound SP32b

In a three necked flask, fitted with a dropping funnel and a reflux condenser, N,N-dimethylformamide (5 mL, 58.4 mmol, 5 equiv.) was placed. The flask was immersed in an ice bath and internal temperature was maintained below 5 °C, while phosphorousoxychloride (5.4 mL, 58.4 mmol, 5 equiv.) was added slowly through dropping funnel. An exothermic reaction occurs with the formation of phosphorousoxychloride-DMF complex. The ice bath was removed and the mixture was stirred for another 15 min in room temperature. 1,2-Dichloroethane (10 mL) was added and the ice bath was replaced. When the internal temperature is lowered to 5 ^{0}C, 5,5´-cyclohexyldipyrromethane **SP30b** (2.5 g, 11.6 mmol) dissolved in 1,2-dichloroethane (25 mL) slowly added to it. After the addition was completed, the ice bath was removed and the mixture was refluxed for 1 h, the mixture was then cooled to 25-30 ^{0}C and a sat. solution of sodium acetate (25 g) was added slowly to the reaction mixture. The reaction mixture is again refluxed for 2 h, during which copious evolution of hydrogen chloride noticed. Vigorous stirring was maintained during the above process. The cooled reaction mixture is extracted three times with dichloromethane. The combined organic layer was washed with sat. aq. Na_2CO_3 solution and dried over anhyd. sodium carbonate. The crude product was purified by column chromatography with 30% EtOAc in hexane as eluent. Evaporation of the eluent resulted in the desired product as white crystalline solid (2.6 g).

Yield: 84 %; Melting point: 210-212 °C; FTIR Data (KBr): 3279, 1639 cm^{-1}; ^{1}H NMR (400 MHz, $CDCl_3$): δ in ppm 10.34 (s, 2H, NH), 9.44 (s, 2H, CH), 6.92 (d, 2H, β-CH), 6.21 (m, 2H, β-CH), 2.29 (br s, 4H, CH), 1.62 (br s, 4H, CH), 1.48 (br s, 2H, CH); ^{13}C NMR (100 MHz, $CDCl_3$) : δ in ppm 179.47, 146.71, 132.58, 123.22, 108.7, 39.95, 34.95, 25.60, 22.51; LCMS m/z calcd. for $C_{18}H_{22}N_2O_2$ (M+H) 271, found 271; Elemental analysis for $C_{18}H_{22}N_2O_2$ calcd. C: 71.09, H: 6.71, N: 10.36; found C: 71.23, H: 6.78, N 10.45.

5.5.6 Synthesis of compound SP27

To a dry nitrogen filled flask, zinc (4 g, 62.4 mmol, 40 equiv.), CuCl (0.61 g, 6.2 mmol, 40 equiv.) and dry THF (180 mL) were added. Then $TiCl_4$ (3.5 mL, 31.2 mmol, 20 equiv.) was added dropwise, under constant stirring via a syringe. The resulting mixture was refluxed for 4 h under an atmosphere of nitrogen to yield black slurry. 2,2´-Diacetyldipyrromethane **SP31a** (400 mg, 1.56 mmol, 1 equiv.) in boiling THF (150 mL) was added with the help of a cannula and the mixture was left under reflux for 30 min. After being quenched in a cold bath at -10 ^{0}C, the mixture was slowly neutralized by 10% aq. Na_2CO_3. The solution was filtered through celite and washed with CH_2Cl_2. The organic phase was washed with water, dried over anhyd. Na_2SO_4, filtered and evaporated to dryness. The crude product was purified by silica gel column chromatography with 5% EtOAc in hexane. Evaporation of the eluent and recrystallization from dichloromethane resulted in the desired product as white crystalline solid (75 mg).

Yield: 21 %; Melting point: 212-214 °C; ^{1}H NMR (400 MHz, $CDCl_3$): δ in ppm 7.47 (s, 4H, NH), 5.99 (m, 8H, β-CH), 2.00 (s, 12H, CH), 1.25 (s, 12H, CH);^{13}C NMR (100 MHz, $CDCl_3$): δ in ppm 139.21, 132.50, 122.32, 106.95, 103.82, 35.53, 29.43, 19.49; LCMS m/z calcd. for $C_{30}H_{36}N_4$ (M+H) 453, found 453; Elemental analysis for $C_{30}H_{36}N_4$ calcd. C: 79.61, H: 8.02, N: 12.38; found C: 79.68, H: 7.96, N: 12.45.

5.5.7 Synthesis of compound SP28

To a dry nitrogen filled flask, zinc (2.63 g, 40 mmol, 40 equiv.), CuCl (0.4 g, 4 mmol, 4 equiv.) and dry THF (120 mL) were added. Then $TiCl_4$ (2.2 mL, 20 mmol, 20 equiv.) was added dropwise under constant stirring via a syringe. The resulting mixture was refluxed for 2 h under an atmosphere of nitrogen to yield a black slurry. 2,2´-Diacetylcyclohexyldipyrromethane **SP31b** (300 mg, 1 mmol) in boiling THF (100 mL) was added with the help of a cannula and the mixture was left under reflux for 30 min. After being quenched in a cold bath at -10 ^{0}C, the mixture was slowly neutralized by 10% aq. Na_2CO_3. The solution was filtered through celite and washed with CH_2Cl_2 .The organic phase was washed with water, dried over anhyd. Na_2SO_4, filtered and evaporated to dryness. The crude product was purified by silica gel column chromatography with 5% EtOAc in hexane. Evaporation of the eluent and recrystallization from dichloromethane resulted in the desired product as white crystalline solid (45 mg).

Yield: 17 %; Melting point: 252-254 °C; ^{1}H NMR (400 MHz, $CDCl_3$): δ in ppm 7.11 (s, 4H, NH), 6.04 (m, 8H, β-CH), 2.01 (s, 12H, CH), 1.85 (br s, 8H, CH), 1.37 (s, 12H, CH);^{13}C

NMR (100 MHz, $CDCl_3$): δ in ppm 137.49, 131.71, 122.52, 107.02, 104.74, 40.46, 37.97, 29.70, 25.64, 22.76, 19.86; LCMS m/z calcd. for $C_{36}H_{44}N_4$ (M+H) 533, found 533; Elemental analysis for $C_{36}H_{44}N_4$ calcd. C: 81.16, H: 8.32, N: 10.52; found C: 81.32, H: 8.23, N: 10.41.

5.5.8 Synthesis of compound SP29

To a dry nitrogen filled flask, zinc (11.3 g, 173 mmol, 40 eqiuv.), CuCl (1.72 g, 17.3 mmol, 4 eqiuv.) and dry THF (300 mL) were added. Then $TiCl_4$ (9.5 mL, 86.9 mmol, 20 equiv.) was added dropwise under constant stirring via a syringe. The resulting mixture was refluxed for 2 h under an atmosphere of nitrogen to yield a black slurry. 2,2´-Diformyldipyrromethane **SP32a** (1 g, 4.3 mmol, 1 equiv.) in boiling THF (150 mL) was added with the help of a cannula and the mixture was left under reflux for 30 min. After being quenched in a cold bath at -10 ^{0}C, the mixture was slowly neutralized by 10% aq. Na_2CO_3. The solution was filtered through celite and washed through with CH_2Cl_2 .The organic phase was washed with water, dried over anhyd. Na_2SO_4, filtered and evaporated to dryness. The crude product was purified by silica gel column chromatography with 30% $CHCl_3$ in hexane. Evaporation of the eluent resulted in the desired product as white crystalline solid (52 mg).

Yield: 6 %; Melting point: 262-264 °C; ^{1}H NMR (400 MHz, $CDCl_3$): δ in ppm 8.14 (s, 4H, NH), 6.08 (m, 8H, β-CH), 5.96 (s, 4H, olefin CH), 1.63 (s, 12H, CH); ^{13}C NMR (100 MHz, $CDCl_3$): δ in ppm 139.74, 129.62, 115.97, 109.32, 104.56, 35.57, 28.92; LCMS m/z calcd. for $C_{30}H_{36}N_4$ (M+H) 397, found 397; Elemental analysis for $C_{30}H_{36}N_4$ (M+H) calcd. C: 78.75, H: 7.12, N: 14.13; found C: 78.61, H: 7.21, N: 14.25.

5.6 Crystallographic details

Crystallographic data for **SP27**, **SP29**, **SP31a** and **SP32a** were collected on BRUKER SMART-APEX CCD diffractometer. Mo−Kα (λ = 0.71073 Å) radiation was used to collect X-ray reflections on the single crystal. Crystallographic data for **SP27.$(CH_3)_2$SO** and **SP28** were collected on Oxford Gemini A Ultra diffractometer with dual source. Mo-K_α (λ = 0.71073 Å) radiation was used to collect the X-ray reflections of the crystal.

Pertinent crystallographic data collection and refinement parameter are shown in the following tables:

Table 5.3 Crystallographic parameters of crystals of **SP31a**, **SP31b** and **SP27**

Crystal data	**SP31a**	**SP31b**	**SP27**
CCDC No	850228	850229	850230
Formula unit	$C_{15}H_{18}N_2O_2$	$C_{13}H_{14}N_2O_2$	$C_{30}H_{36}N_4$
Formula wt.	258.31	230.26	452.63
Crystal system	Monoclinic	Orthorhombic	Triclinic
T [K]	298 (2)	298 (2)	298 (2)
a [Å]	5.6131(5)	16.7103 (15)	10.0710 (10)
b [Å]	25.331(2)	11.6052 (10)	11.9300 (12)
c [Å]	10.1079 (9)	12.5938 (11)	13.1405 (13)
α [°]	90.00	90.00	76.838 (2)
β [°]	91.766 (2)	90.00	83.588 (2)
γ [°]	90.00	90.00	71.284 (2)
volume [$Å^3$]	1436.5 (2)	2442.3 (4)	1454.7 (3)
Space group	P2(1)/c	Pca2(1)	P-1
Z′	1	2	1
Z	4	8	2
D_{calc} [g.cm-3]	1.194	1.252	1.033
μ/mm^{-1}	0.080	0.086	0.061
Reflns collected	12185	10363	11552
Unique reflns	2827	4389	5676
Observed reflns	1728	3430	3656
R(int)	0.0555	0.0263	0.0248
R_1 [$I > 2\sigma(I)$],	0.0648,	0.0445,	0.0673,
wR_2	0.1364	0.0918	0.1680
GOF	1.024	1.007	1.023

Table 5.4 Crystallographic parameters of crystals of **SP27.$(CH_3)_2SO$**, **SP28** and **SP29**

Crystal data	**SP27.$(CH_3)_2SO$**	**SP28**	**SP29**
CCDC No	850231	850232	850233
Formula unit	$C_{17}H_{24}N_2OS$	$C_{36}H_{44}N_4$	$C_{26}H_{28}N_4$
Formula wt.	304.44	532.75	396.52
Crystal system	Monoclinic	tetragonal	Triclinic
T [K]	298 (2)	298 (2)	298 (2)
a [Å]	8.627 (8)	13.9875 (18)	9.4161 (12)
b [Å]	21.841 (8)	13.9875 (18)	9.7498 (13)
c [Å]	9.936 (5)	31.440 (7)	13.4677 (17)
α [°]	90.00	90.00	110.833 (2)
β [°]	110.68 (9)	90.00	93.481(2)
γ [°]	90.00	90.00	102.570 (2)
volume [$Å^3$]	1751.5 (19)	6151.2 (17)	1114.9 (2)
Space group	P2(1)/c	I41/a	P-1
Z′	1	1	1
Z	4	16	2
D_{calc} [g.cm-3]	1.155	1.151	1.181
μ/mm^{-1}	0.186	0.068	0.071
Reflns collected	13580	13670	10826
Unique reflns	7053	3649	3916
Observed reflns	1582	1287	2826
R(int)	0.0907	0.1398	0.0393
R_1 [$I > 2\sigma(I)$],	0.0490,	0.0933,	0.0791,
wR_2	0.0850	0.1229	0.1416
GOF	0.698	1.013	1.170

5.7 References

1. (a) Baeyer, A. *Ber. Dtsch. Chem. Ges.* **1886**, *19*, 2184. (b) Gale, P. A.; Sessler, J. L.; Král, V.; Lynch, V. *J. Am. Chem. Soc.* **1996**, *118*, 5140. (c) Allen, W. E.; Gale, P. A.; Brown, C. T.; Lynch, V. M.; Sessler, J. L. *J. Am. Chem. Soc.* **1996**, *118*, 12471. (d) Gale, P. A.; Sessler, J. L.; Allen, W. E.; Tvermoes, N. A.; Lynch, V. M. *Chem.*

Commun. **1997**, 665. (e) Gale, P. A.; Sessler, J. L.; Gale, P. A.; Král, V. *Chem. Commun.* **1998**, 1. (f) Sessler, J. L.; Anzenbacher Jr., P.; Jursíková, K.; Miyaji, H.; Genge; J. W.; Tvermoes, N. A.; Allen, W. E.; Shiver, J. A. *Pure Appl. Chem.* **1998**, *70*, 2401. (g) Anzenbacher Jr., P.; Jursíková, K.; Lynch, V. M.; Gale, P. A.; Sessler, J. L. *J. Am. Chem. Soc.* **1999**, *121*, 11020. (h) Bonomo, L.; Solari, E.; Toraman, G.; Scopelliti, R.; Laatronico, M.; Floriani, C. *Chem. Commun.* **1999**, 2413. (i) Sessler, J. L.; Gale, P. A. In *The Porphyrin Handbook*; Kadish, K. M.; Smith, K. M.; Guilard, R.; Eds.; Academic Press: New York, **2000**, *6*, 257. (j) Anzenbacher Jr., P.; Jursíková, K.; Sessler, J. L. *J. Am. Chem. Soc.* **2000**, *122*, 9350. (k) Anzenbacher Jr., P.; Try, A. C.; Miyaji, H.; Jursíková, K.; Lynch, V. M.; Marquez, M.; Sessler, J. L. *J. Am. Chem. Soc.* **2000**, *122*, 10268. (l) Gale, P. A.; Anzenbacher Jr., P.; Sessler, J. L. *Coord. Chem. Rev.* **2001**, *222*, 57. (m) Yoon, D. W.; Hwang, H.; Lee, C. -H. *Angew. Chem. Int. Ed.* **2002**, *41*, 1757. (n) Lee, C. -H.; Na, H. K.; Yoon, D. W.; Won, D. H.; Cho, W. S.; Lynch, V. M.; Shevchuk, S. V.; Sessler, J. L. *J. Am. Chem. Soc.* **2003**, *125*, 7301. (o) Panda, P. K.; Lee, C. -H. *Org. Lett.* **2004**, *6*, 671. (p) Panda, P. K.; Lee, C. -H. *J. Org. Chem.* **2005**, *70*, 3148. (q) Lee, C. -H.; Lee, J. S.; Na, H. K.; Yoon, D. W.; Miyaji, H.; Cho, W. S.; Sessler, J. L. *J. Org. Chem.* **2005**, *70*, 2067. (r) Namor, A. D.; Shehab, M.; Abbas, I.; Withams, M. V.; Zvietcovich-Guerra, J. *J. Phys. Chem. B* **2006**, *110*, 12653. (s) Nielsen, K. A.; Cho, W. -S.; Lyskawa, J.; Levillain, E.; Lynch, V. M.; Sessler, J. L.; Jeppesen; J. O. *J. Am. Chem. Soc.* **2006**, *128*, 2444. (t) Gil-Ramírez, G.; Escudero-Adán, E. C.; Benet-Buchholz, J.; Ballester, P. *Angew. Chem. Int. Ed.* **2008**, *47*, 4114. (u) Miyaji, H.; Kim, H. K.; Sim, E. K.; Lee, C. K.; Cho, W. S.; Sessler, J. L.; Lee, C. -H. *J. Am. Chem. Soc.* **2005**, *127*, 12510. (v) Samanta, R.; Mahanta, S. P.; Chaudhuri, S.; Panda, P. K.; Narahari, A. *Inorg. Chim. Acta* **2011**, *372*, 281. (w) Samanta, R.; Mahanta, S. P.; Ghanta, S.; Panda, P.K. *RSC Adv.* **2012**, *2*, 7974. (x) Anzenbacher Jr., P.; Nishiyabu, R.; Palacios, M. A. *Coord. Chem. Rev.* **2006**, *250*, 2929.

2. Sessler, J. L.; Cho, W. -S.; Lynch, V.; Král, V. *Chem. Eur. J.* **2002**, *8*, 1134.
3. (a) Jang, Y. -S.; Kim, H. -J.; Lee, P. -H.; Lee, C. -H. *Tetrahedron Lett.* **2000**, *41*, 2919. (b) Arumugam, N.; Jang, Y. -S.; Lee, C. -H. *Org. Lett.* **2000**, *2*, 3115. (c) Nagarajan, A.; Ka, J. -W.; Lee, C. -H. *Tetrahedron* **2001**, *57*, 7323. (d) Lee, E. -C.; Park, Y. -K.; Kim, J. -H.; Hwang, H.; Kim, Y. -R.; Lee, C. -H. *Tetrahedron Lett.*

2002, *43*, 9493. (e) Song, M. -Y.; Na, H. -K.; Kim, E. -Y.; Lee, S. -J.; Kim, K. I.; Baek, E. -M.; Kim, H. -S.; An, D. K.; Lee, C. -H. *Tetrahedron Lett.* **2004**, *45*, 299.

4. Král, V.; Gale, P. A.; Anzenbacher Jr., P.; Jursíková, K.; Lynch V.; Sessler, J. L. *Chem. Commun*. **1998**, 9.
5. Gale, P.A.; Genge, J. W.; Král. V.; McKervey, M. A.; Sessler, J. L.; Walker, A. *Tetrahedron Lett.* **1997**, *38*, 8443.
6. Turner, B.; Botoshansky, M.; Eichen, Y. *Angew. Chem. Int. Ed., Eng*. **1998**, *37*, 2475.
7. Turner, B.; Shterenberg, A.; Kapon, M.; Suwinska, K.; Eichen, Y. *Chem. Commun*. **2001**, 13.
8. (a) Cafeo, G.; Kohnke, F. H.; La Torre, G. L.; White, A. J. P.; Williams, D. J. *Angew. Chem. Int. Ed.* **2000**, *39*, 1496. (b) Cafeo, G.; Kohnke, F. H.; Parisi, M. F.; Nascone, R. P.; La Torre, G.; Williams, D. J. *Org. Lett.* **2002**, *4*, 2695. (c) Cafeo, G.; Kohnke, F. H.; La Torre, G. L.; White, A. J. P.; Williams, D. J. *Chem. Commun*. **2000**, 1207.
9. Sessler, J. L.; Anzenbacher Jr., P.; Shriver, J. A.; Jursíková, K.; Lynch, V. M.; Marquez, M. *J. Am. Chem. Soc.* **2000**, *122*, 12061.
10. Sessler , J. L.; Cho , W. -S.; Gross , D. E.; Shriver , J. A.; Lynch , V. M.; Marquez M. *J. Org. Chem.* **2005**, *70*, 5982.
11. (a) Sessler, J. L.; An, D.; Cho, W.-S.; Lynch, V. *Angew. Chem. Int. Ed.* **2003**, *42*, 2278. (b) Sessler, J. L.; An, D.; Cho, W. -S.; Lynch, V.; Marquez, M. *Chem. Commun.* **2005**, 540.
12. (a) Sessler, J. L.; An, D.; Cho, W. -S.; Lynch, V. *J. Am. Chem. Soc.* **2003**, *125*, 13646. (b) Sessler, J. L.; An, D.; Cho, W. -S.; Lynch, V.; Yoon, D. -W.; Hong, S. -J.; Lee, C. -H. *J. Org. Chem.* **2005**, *70*, 1511.
13. Piatek, P.; Lynch, V. M.; Sessler, J. L. *J. Am. Chem. Soc.* **2004**, *126*, 16073.
14. Sessler, J. L.; An, D.; Cho, W. -S.; Lynch, V.; Marquez, M. *Chem. Eur. J.* **2005**, *11*, 2001.
15. Cafeo, G.; Kohnke, F. H.; White, A. J. P.; Garozzo, D.; Messina, A. *Chem. Eur. J.* **2007**, *13*, 649.
16. Silverstein, R. M.; Ryskiewicz, E. E.; Willard, C. *Org. Synth.* **1956**, *36*, 74.
17. (a) McMurry, J. E.; Fleming, M. P. *J. Am. Chem. Soc.* **1974**, *96*, 4708. (b) Mukaivama, T.; Sato. T.; Hanna, J. *Chem. Lett.* **1973**, 1041. (c)Tyrlik, S.; Wolochowicz, I. *Bull. Soc. Chim. Fr.* **1973**, 2147. (d) McMurry J. E. *Chem. Rev.* **1989**, *89*, 1513.

18. (a) Vogel, E.; Kocher, M.; Schmickler, H.; Lex, J. *Angew. Chem. Int. Ed.* **1986**, *25*, 257. (b) Vogel, E.; Balci, M.; Pramod, K.; Koch, P.; Lex, J.; Ermer, O. *Angew. Chem. Int. Ed.* **1987**, *26*, 928. (c) Vogel, E.; Kocher, M.; Lex, J.; Ermer, O. *Isr. J. Chem.* **1989**, *29*, 257. (d) Vogel, E.; Koch, P.; Hou, X. -L.; Lex, J.; Lausmann, M.; Kisters, M.; Aukauloo, M. A.; Richard, P.; Guilard, R. *Angew. Chem. Int. Ed.* **1993**, *32*, 1600.
19. Littler, B. J.; Miller, M. A.; Hung, C. -H.; Wagner, R. W.; O'Shea, D. F.; Boyle, P. D.; Lindsey, J. S. *J. Org. Chem.* **1999**, *64*, 1391.
20. Wilcox, C. S. In *Frontiers in Supramolecular Organic Chemistry and Photochemistry*; Eds. Schneider, H. J.; Dürr, H.; VCH: Weinheim, 1991.
21. Takeuchi, M.; Shioya, T.; Swager, T. M. *Angew. Chem. Int. Ed.* **2001**, *40*, 3372. (b) Mizuno, T.; Wei, W. -H; Eller, L. R.; Sessler, J. L. *J. Am. Chem. Soc.* **2002**, *124*, 1134. (c) Jose, D. A.; Kumar, D. K.; Ganguly, B.; Das, A. *Org. Lett.* **2004**, *6*, 3445. (d) Gomez, D. E.; Fabbrizzi, L.; Licchelli, M. *J. Org. Chem.* **2005**, *70*, 5717. (e) Cametti, M.; Rissanen, K. *Chem. Commun.* **2009**, 2809. (f) Jeong, S. -D.; Nowak-Krol, A.; Kim, Y., Kim, S. -J.; Gryko, D. T.; Lee, C. -H. *Chem. Commun.* **2010**, 8737. (g) Wade, C. R.; Broomsgrove, A. E. J.; Aldridge, S.; Gabbai, F. P. *Chem. Rev.* **2010**, *110*, 3958. (h) Zhao, H.; Gabbaï, F. P. *Nat. Chem.* **2010**, *2*, 984. (i) Bhalla, V.; Singh, H.; Kumar, M. *Org. Lett.* **2010**, *12*, 628. (j) Guha, S.; Saha S. *J. Am. Chem. Soc.* **2010**, *132*, 17674. (k) Tripier, R.; Platas-Iglesias, C.; Boos, A.; Morfin, J.-F.; Charbonnière, L. *Eur. J. Inorg. Chem.* **2010**, 2735. (l) Sokkolingam, P.; Lee, C. -H. *J. Org. Chem.* **2011**, *76*, 3820. (m) Bhalla, V.; Gupta, A.; Singh, H.; Kumar, M. *J. Org. Chem.* **2011**, *76*, 1578.

CHAPTER 6

Pyrrole-benzimidazole conjugates: a new class of anion receptors

6.1 Introduction

Considering the important roles of anions in biological, environmental and industrial processes, in the last three decades anion coordination chemistry has developed into an independent research area focused on the structure and binding modes of anions.[1,2] Over the years, manifold receptor architectures for anions have been synthesized and a considerable number have now been employed in structural and transport studies. The goal of these studies have been to understand specific binding behavior, to derive structure-function relationships and, last but not least, to find useful applications.[3]

In the last three decades, several neutral receptors containing different hydrogen bonding donor motifs and their conjugates, such as polyamines,[4] ureas and thioureas,[5] amides and thioamides,[6] sulfonamides,[7] pyrroles,[8] phenols,[9] indoles,[10] imidazoles and benzimidazoles[11] have been reported, which generally contain polarizable H-bond donor groups (Figure 6.1). Recently, Flood *et al.* reported triazole CH as a hydrogen bond donor for complexation of chloride ion owing to appropriate preorganization in triazolophane host.[12] In a recent report, Das and coworkers utilized active methylene groups as hydrogen bond donor in a naphthalene derived salt towards fluoride ion.[13]

In the case of hydrogen bond based receptors, the relative affinity of the receptors, towards different anions could be correlated to the geometry and complementarity of the H-bonding sites, the acidity of the H-bond donor sites and the basicity of the anions.

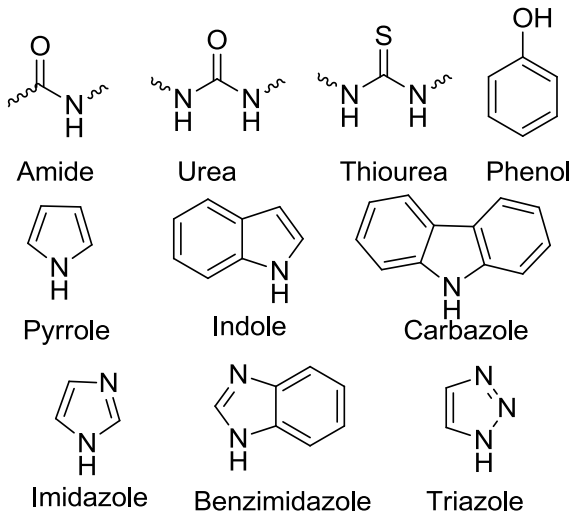

Figure 6.1 Structure of some H-bonding motif used in the design of anion host.

The discovery of prodigiosin, a pyrrolylopyrromethene, an open chain oligopyrrole derivative, as an antineoplastic and immunosuppressive agent and its protonation-counter anion binding mode of action, drew attention of researchers towards acyclic oligopyrroles as

a new class of anion binding receptors. In this context, Sessler and Gale explored several oligopyrroles and acyclic pyrrole conjugated with other H-bonding motifs as host for anions.[14]

The design and synthesis of receptors, capable of converting the anion binding event, into a naked eye readable signal output, have received considerable attention recently.[15] As discussed in chapter 1, colorimetric chemosensors generally consist of two parts: the anion binding unit and the signaling unit *i.e.* the chromophore which is responsible for the observed color change. Recently, there is a lot of emphasis on the development of chromogenic sensors, for convenient detection of anions. Towards this, most synthetic sensor molecules generally involve the covalent linking of an optical signaling unit to a neutral or cationic receptor, which provides one or more H-bond donor sites for selective binding and sensing of targeted anion.

6.2 Research Goal

Among the receptors reported so far, very few deals with benzimidazole based anion receptors.[16] While, this moiety contains one H-bond donor as well as an acceptor moiety, pyrrole contains only one H-bond donor site. Bordwell reported that the pK_a of benzimidazole is 16.4 in DMSO, which is quite lower than that of pyrrole (pK_a = 23.0), [17] suggesting, a relatively higher deprotonation tendency of NH of the former. So these two moieties may interact differently with anions resulting in interesting host-guest chemistry. Further, the benzimidazole is more flexible with regard to its H-bonding functionality due to the presence of aromatic CH groups, which may act as alternate/additional H-bond donor. Thus, we intend to couple these two moieties to produce a pyrrole-benzimidazole conjugate and subsequently, use this conjugate as H-bonding motif in different organic scaffolds towards anion recognition. Further, it should be possible to manipulate the H-bonding ability of the benzimidazole moiety w.r.t. the complementarity of binding sites of anions.

From the receptor perspective, the chemistry of **SP35a** is attractive owing to its ease of synthesis. Moreover, both moieties have already proven utility toward anions. In addition, the electronic distribution of the benzimidazole moiety can be further fine-tuned by inserting suitable substituent onto the benzene ring. By taking into account the above facts, we desired to introduce the nitro functionality at the benzimidazole periphery, so as to convert it into a built-in colorimetric probe in addition to its H-bonding sites.

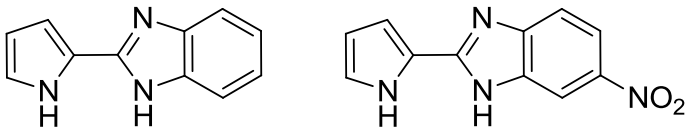

SP35a SP35b

The schematic representation of plausible charge transfer of **SP35b** in presence of anion is shown in the following figure.

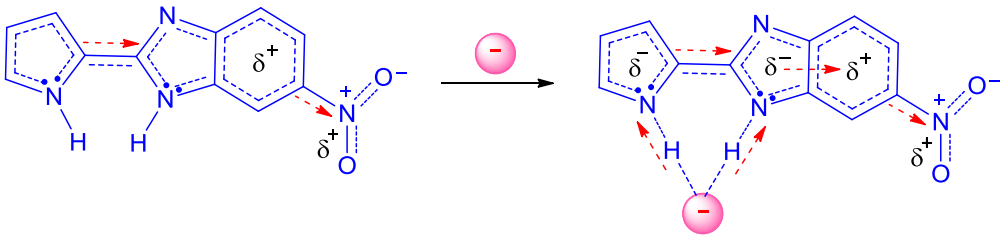

Figure 6.2 Pictorial representation of the anion induced charge polarization of **SP35b**.

Furthermore, these motifs represent larger and more extended H-bonding domain, once prepared, and should provide more space towards larger anions with varied selectivity and stoichiometry. In addition to the basic conjugates, herein, we have proposed two different sets of their dimers, where two units are bridged via two different spacer motifs- first, an electronically non-coupled sp^3-carbon and in the other case, they are coupled by a fluorescent quinoxaline moiety.

6.3 Results and discussion

6.3.1 Synthesis of the receptors

The pyrrole-benzimidazole conjugates were synthesized by one step condensation of pyrrole-2-carboxaldehyde and *o*-phenylenediamine or its nitro derivative by slightly modulating the strategies reported in literature as shown in scheme **6.1**.[16h]

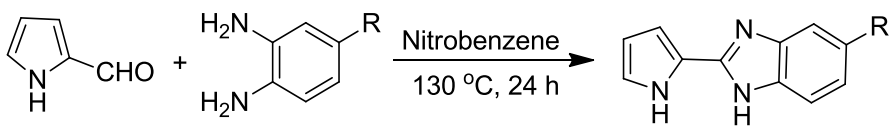

SP33

SP35a R = H (55%)
SP35b R = NO_2 (46%)

Scheme 6.1 Syntheses of pyrrole-benzimidazole conjugate **SP35a** and **SP35b**.

For example, the condensation of pyrrole-2-carboxaldehyde and *o*-phenylenediamine following literature procedure[16h] *i.e.* heating the reaction mixture at 80 °C for 8 h resulted in two close lying spots in TLC. Mass spectral analysis of the crude mixture showed the probable presence of the unoxidized condensed product, along with the targeted conjugate. Elevating the temperature and continuing the reaction for longer time, resulted in single spot in TLC, indicating complete oxidation. The optimized reaction condition needs stirring of the

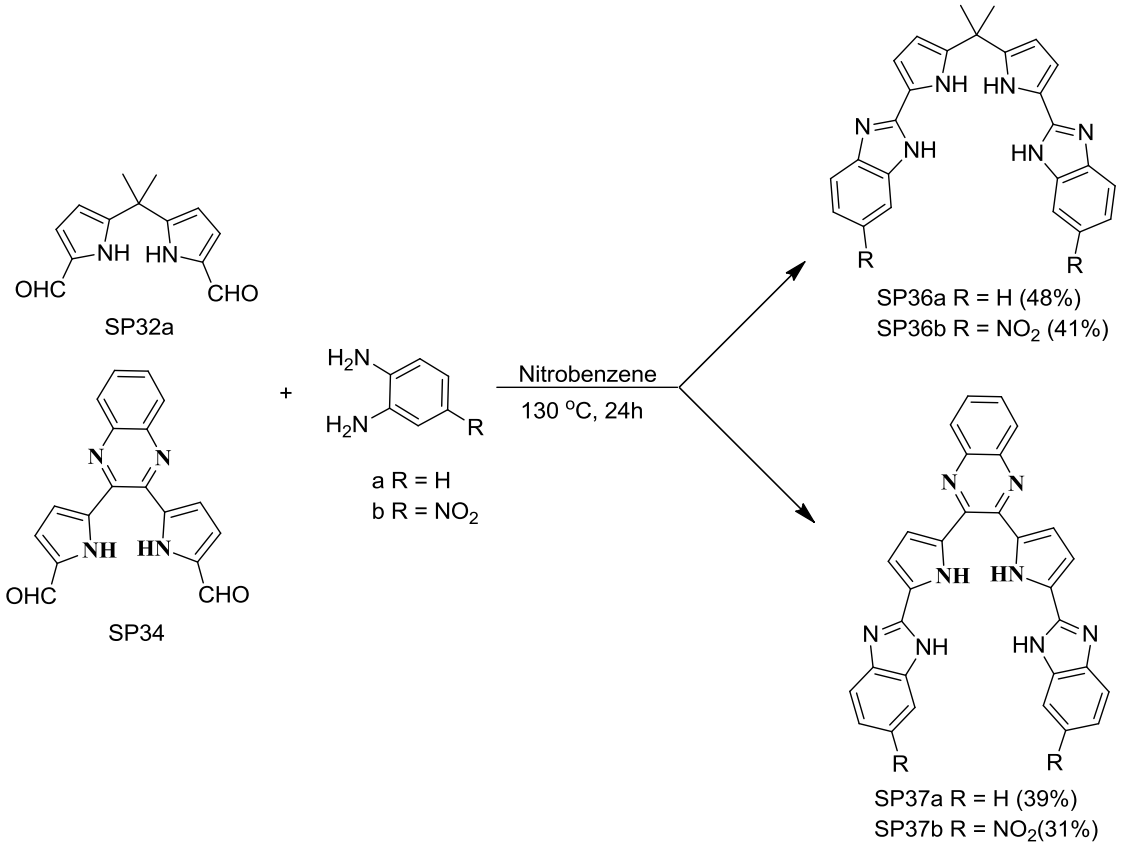

Scheme 6.2 Syntheses of **SP36a-b** and **SP37a-b**.

reaction mixture at 130 °C for 24 h. Purification by column chromatography on silica gel using 5% methanol in chloroform as eluent and subsequent recrystallization yielded the pyrrole-benzimidazole conjugates in reasonably good yields. The compounds **SP35a** and **SP35b** were further purified by sublimation at 150 and 180 °C respectively at high vacuum (~ 0.1 mm Hg).

The syntheses of receptors **SP36** and **SP37** is shown in scheme 6.2. The dialdehydes were reacted with *o*-phenylenediamine and 4-nitro-*o*-phenylenediamine separately, in nitrobenzene using the above mentioned condition, to yield the desired compound **SP36a-b** in 48 and 41%, and **SP37a-b** in 39 and 31% respectively. All compounds were purified on silica gel column

chromatography using 5% MeOH in $CHCl_3$ as eluent. Our further attempt to purify the compounds by sublimation unfortunately led to their degradation. These compounds were further purified by recrystallization with 1:1 methanol and acetone solution for analytical purpose.

6.3.2 Characterization of the receptors

All compounds were characterized by standard spectroscopic techniques including ^{1}H, ^{13}C NMR spectroscopy, mass and elemental analysis. The ^{1}H NMR spectra recorded in DMSO-d_6 at 298 K shows two NH signals above 12 ppm while the pyrrole α- and β-Hs resonate around 6 and 7 ppm respectively for all the receptors. In case of **SP36b**, the benzimidazole NH signal was split into a doublet, which may be attributed to the NH tautomerism of benzimidazole moiety that become slower in presence of the nitro group. On the other hand, the rotation is probably too fast in case of **SP36a**, to be detected in the NMR time scale, therefore it appears as a broad signal. Interestingly in case of **SP37b,** both pyrrole and benzimidazole NHs were split into doublets. This indicates in this case the NH tautomerization is even slower. All our attempts to obtain single crystals for these compounds remain unsuccessful so far.

UV-Vis spectrum of compound **SP35a** in DMSO (Figure 6.3) revealed two absorption maxima at 312 and 327 nm (not much resolved). In addition, it showed fluorescence, with emission maxima at 336 and 349 nm (Figure 6.3). On the other hand, insertion of nitro derivative (*i.e.* **SP35b**) resulted in well resolved absorption bands with maxima at 299 and 387 nm. As expected, this molecule did not display fluorescence owing to the intramolecular photoinduced electron transfer (PET) from the excited fluorophore to the electron withdrawing nitro group (donor-excited PET; d-PET).[18]

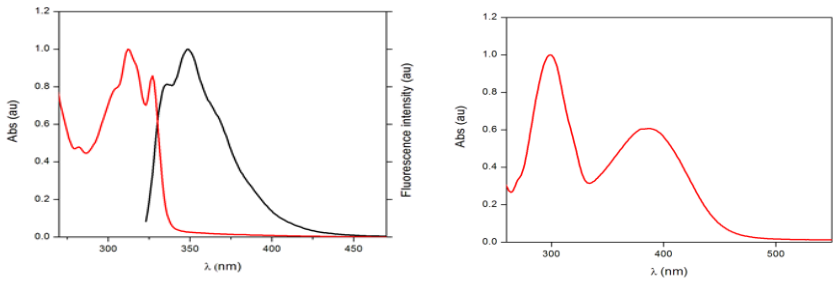

Figure 6.3 Normalized absorption (red) and emission spectra (black) of **SP35a** (left) and **SP35b** (right) respectively.

In case of sp^3-C bridged dimer **SP36a,** the absorption spectrum in DMSO showed slight broadening compared to **SP35a** with maxima at 313 and 337 nm and showed featureless emission band with maxima at 370 nm (Figure 6.4). Again substitution of nitro group (*i.e.*

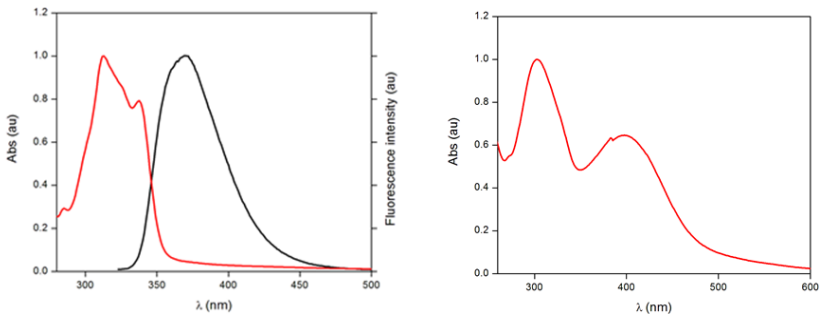

Figure 6.4 Normalized absorption (red) and emission spectra (black) of **SP36a** (left) and **SP36b** (right) respectively.

SP36b), led to two well resolved bands with absorption maxima at 302 and 398 nm, with concomitant quenching of fluorescence. The absorption spectra of quinoxaline bridged dimeric conjugate **SP37a** in DMSO, revealed two absorption bands with maxima at 318 and 402 nm and it showed a relatively large red shifted emission at 560 nm (Figure 6.5). This indicates greater conjugation between the two pyrrole-benzimidazole conjugates via quinoxaline both in the ground as well as the excited state. Interestingly, the nitro analogue *i.e.* **SP37b** displayed broad absorption profile, where the higher energy band is blue shifted (to 296 nm) and on the other hand the lower energy band is red shifted (to 422 nm) compared to **SP37a**. Again, as expected it did not display any observable fluorescence (Figure 6.5). The photophysical data of all the conjugates are shown in table 6.1.

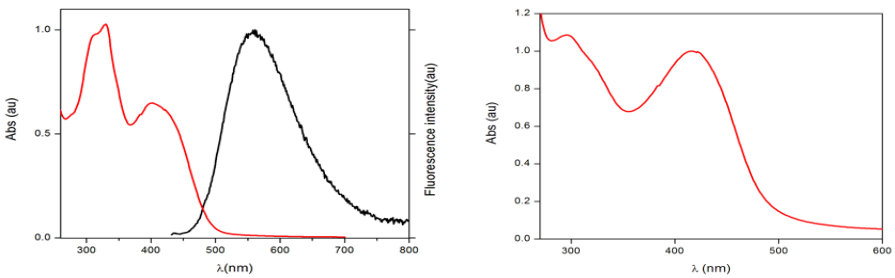

Figure 6.5 Normalized absorption and emission spectra of **SP37a** (left) and **SP37b** (right) respectively.

6.3.3 Anion binding investigation

UV-Visible, fluorescence and ^{1}H NMR spectroscopic titration methods were used to study the anion binding affinities of the synthesized receptors with various anions. Tetrabutylammonium salts of fluoride (as its trihydrate), chloride, bromide, iodide, dihydrogenphosphate, nitrate, bisulfate, perchlorate, acetate, and azide ions were used during the anion binding study. Due to the poor solubility of the compounds, all studies were carried out in DMSO.

6.3.3.1 UV-Vis method

Initial anion binding studies of the receptors were carried out at 298 K, in DMSO, using UV-Vis spectroscopic titration method. The studies were done with 20 μM solution of the receptor. Further their binding affinities were evaluated from the UV-Vis titration data by following Benesi-Hildebrand method.[19]

Table 6.1 Photophysical data of the receptors **SP35-37** in DMSO at 25 °C.

Receptors	Absorption λ_{max} in nm (log ε)	Emission λ_{max} (nm)
SP35a	312 (4.56), 327 (4.49)	337, 349
SP35b	299 (4.35), 387 (4.13)	-
SP36a	313 (4.68), 338 (4.58)	361 (broad)
SP36b	303 (4.55), 398 (4.36)	-
SP37a	318 (4.49), 404 (4.27)	160
SP37b	295 (4.59), 416 (4.55)	-

The anion screening experiment of **SP35a** showed an appreciable change in the absorption spectrum for fluoride ion only, among the tested anions. Addition of TBAF resulted in ~9 nm red shift of the two absorption bands (Figure 6.6). In order to evaluate the affinity of fluoride ion towards **SP35a**, systematic spectrophotometric titration was carried out in DMSO with varying concentration of fluoride ion, which indicated the onset of a weak binding event, accompanied by a gradual shift of the absorption profile, towards higher wavelength with an isobestic point at 325 nm. Job's plot analysis confirmed the formation of 1:1 complex. From the titration data the association constant (K_a) for fluoride ion was found to be 8.45×10^2 M^{-1} using Benesi-Hildebrand plot.[19] On the other hand, the anion scanning

experiment of receptor **SP35b** (*i.e.* the nitro analogue of **SP35a**) displayed significant change in UV-Vis spectrum, upon addition of F^-, CH_3COO^- and $H_2PO_4^-$ ions among the studied ions (Figure 6.7). The color of the solution changed from light yellow to red with varying intensity

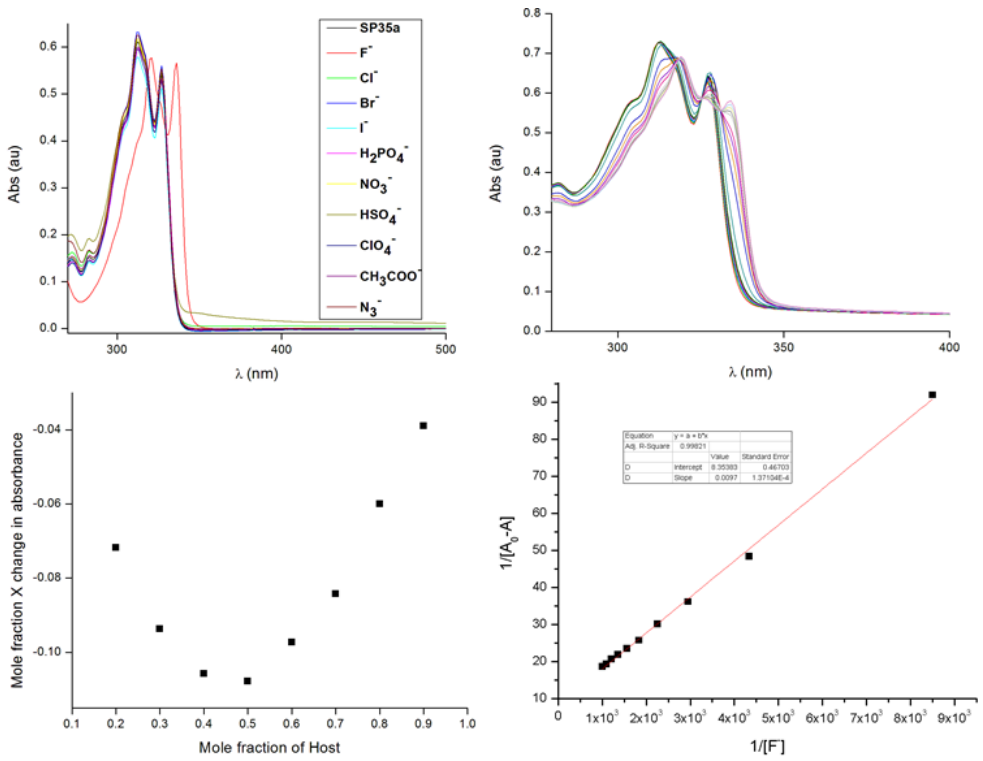

Figure 6.6 Top left: UV-Vis spectra of **SP35a** (20 μM) in DMSO in absence and presence of different anions; top right: evolution of UV-Vis spectra of **SP35a** (20 μM) upon gradual addition of TBAF (15 mM); bottom left: Job's plot of **SP35a** (20 μM) vs. TBAF (20 μM); bottom right: Benesi-Hildebrand plot of the titration data of **SP35a** vs. TBAF.

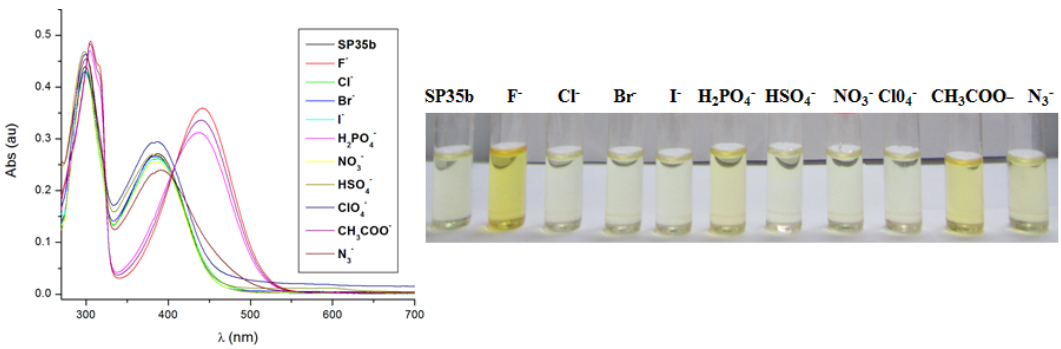

Figure 6.7 Left: UV-Vis spectra of **SP35b** (20 μM) in DMSO in absence and presence of different anions; right: naked eye view of the color upon addition of different anions.

upon addition of these three anions. UV-Vis titration were conducted to quantify anion induced colorimetric response of **SP35b**, which exhibits with gradual addition of fluoride and acetate ions, the intensities of absorption bands at 299 and 387 nm decreases, while concomitantly two new peaks appear at 305 and 439 nm (Figures 6.8 and 6.9). The titration revealed two clear isobestic points at 324 and 404 nm. Dihydrogenphosphate ion displayed similar response (Figure 6.10), with slight change in the peak maxima (304 and 431 nm). Job's plot analysis indicated the formation of 1:1 stoichiometric complexes, in case of all of them (Figures 6.8 to 6.10). The corresponding K_a values obtained from Benesi-Hildebrand plot are 1.20×10^4, 6.03×10^4 and 6.30×10^3 M^{-1} for F^-, CH_3COO^- and $H_2PO_4^-$ respectively. The change in color from light yellow to dark yellow may be ascribed to charge transfer from anion to the nitro group. Here, the complexation results in charge-transfer from the donor (*i.e.* anion) to the acceptor moiety ($-NO_2$ of benzimidazole), which stabilize the excited state and

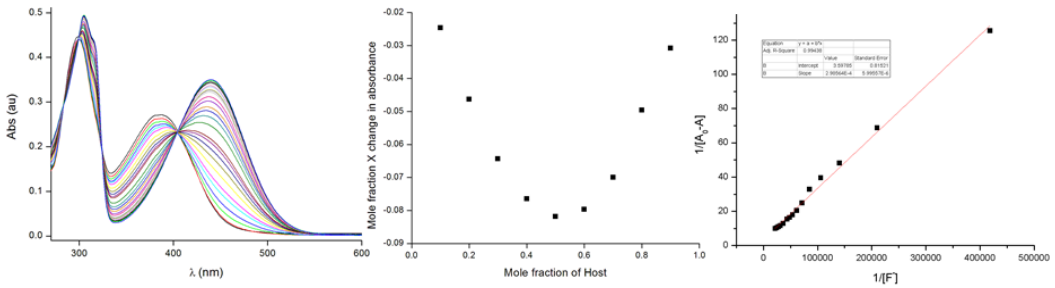

Figure 6.8 Left: Evolution of UV-Vis spectra of **SP35b** (20 μM) in DMSO upon gradual addition of TBAF (3.5×10^{-4} M); middle: Job's plot of **SP35b** (20 μM) vs. TBAF (20 μM); right: Benesi-Hildebrand plot of the titration data of **SP35b** vs. TBAF.

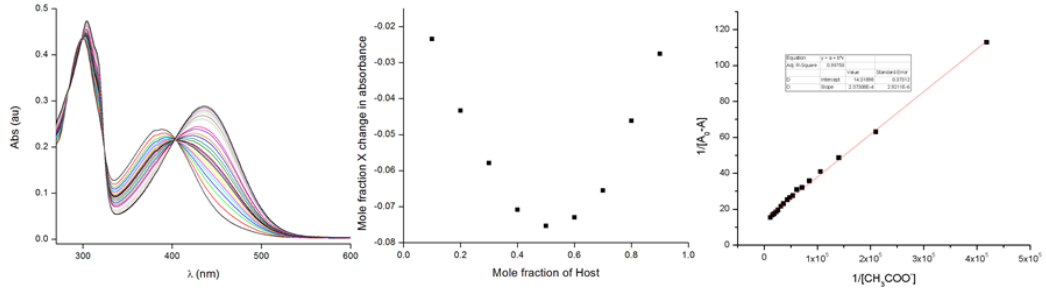

Figure 6.9 Left: Evolution of UV-Vis spectra of **SP35b** (20 μM) in DMSO upon gradual addition of TBA(CH_3COO) (4.3×10^{-4} M); middle: Job's plot of **SP35b** (20 μM) vs. TBA(CH_3COO) (20 μM); right: Benesi-Hildebrand plot of the titration data of **SP35b** vs. TBA(CH_3COO).

hence causes a bathochromic shift in the absorption maxima, as well as the color change.[15,20] This clearly reflects that changing the substituent at the benzimidazole moiety of **SP35a** from hydrogen to nitro (in compound **SP35b**), led to the colorimetric change upon addition of anions, however with a compromise on its selectivity towards anions.

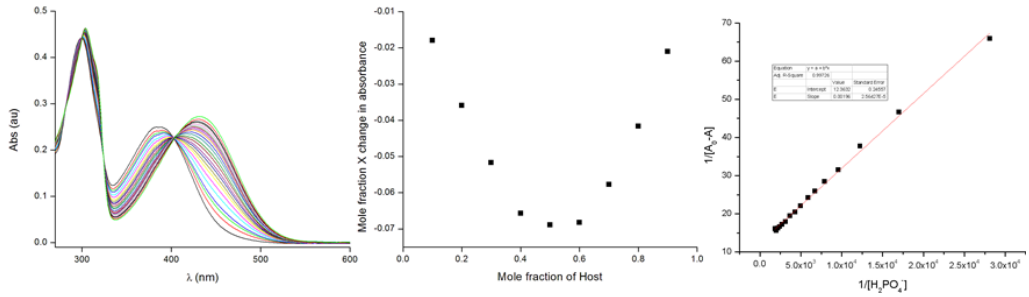

Figure 6.10 Left: Evolution of UV-Vis spectra of **SP35b** (20 μM) in DMSO upon gradual addition of $TBAH_2PO_4$ (1.3×10^{-3} M); middle: Job's plot of **SP35b** (20 μM) vs. $TBAH_2PO_4$ (20 μM); right: Benesi-Hildebrand plot of the titration data of **SP35b** vs. $TBAH_2PO_4$.

Anion screening study of receptor **SP36a** displayed selectivity towards fluoride ion, among the tested anions (Figure 6.11). UV-Visible titration study showed that like **SP35a**, with gradual addition of TBAF, the intensity of the peaks at 313 and 337 nm decreases with concomitant evolution of two new peaks at 324 and 342 nm. Job's plot analysis indicated the formation of a 1:1 complex and the fitting of the experimental absorption data in Benesi-Hildebrand plot yielded the affinity constant (K_a) as 1.90×10^3 M^{-1}. This clearly indicated **SP36a** has a higher affinity for fluoride ion than **SP35a**, which may be attributed to the presence of the higher number of binding sites (*i.e.* NH donors). The anion scanning experiment of receptor **SP36b** showed interaction with F^-, CH_3COO^- and $H_2PO_4^-$ ions only but unlike **SP35b**, in this case the color change was not significant (Figure 6.12). Upon addition of fluoride ion, the intensity of the peaks at 302 and 398 nm decreases while two new peaks appeared at 310 and 445 nm with two isobestic points at 304 and 414 nm (Figure 6.13). In case of acetate, the two new peaks appeared at 308 and 427 nm, while that in case of dihydrogenphosphate emerged at 306 and 422 nm (Figures 6.14 and 6.15). Job's plot analysis indicated the formation of 1:1 stoichiometric complexes, in case of all three anions and fitting of the titration data, using Benesi-Hildebrand plot gives their affinity constants as 3.62×10^4, 1.24×10^4 and 7.84×10^3 M^{-1} for fluoride, acetate and dihydrogenphosphate ions respectively.

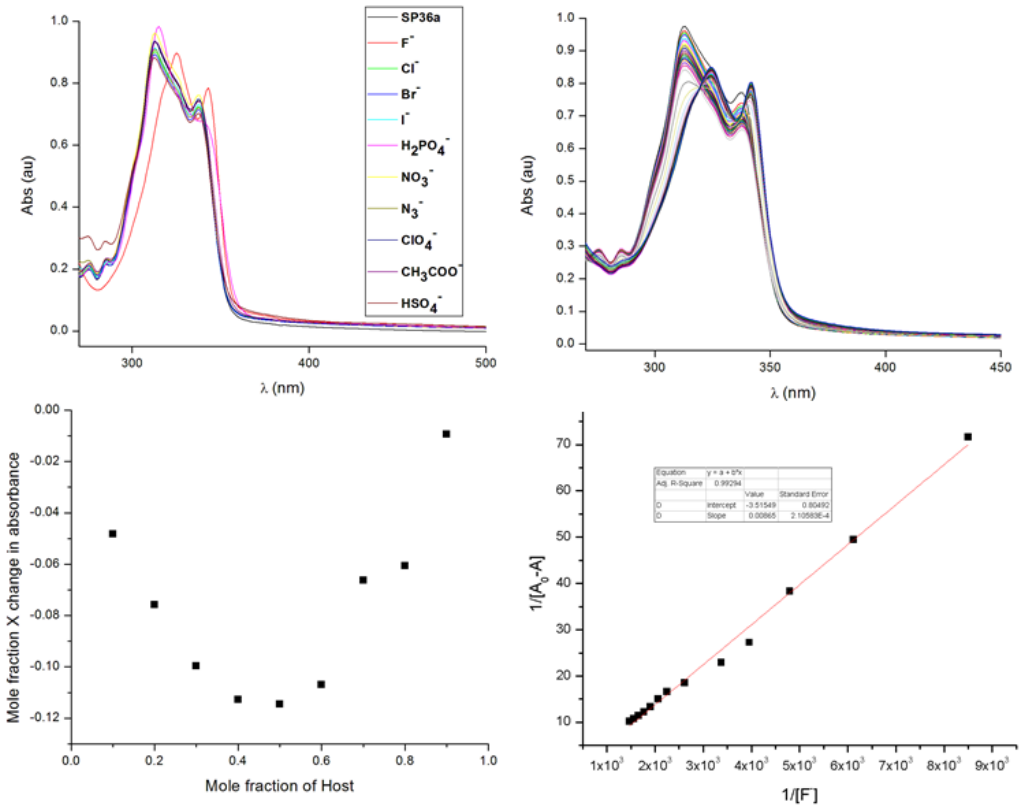

Figure 6.11 Top left: UV-Vis spectra of **SP36a** (20 μM) in DMSO in absence and presence of different anions; top right: evolution of UV-Vis spectra of **SP36a** (20 μM) upon gradual addition of TBAF (12 mM); bottom left: Job's plot of **SP36a** (20 μM) vs. TBAF (20 μM); bottom right: Benesi-Hildebrand plot of the titration data of **SP36a** vs. TBAF.

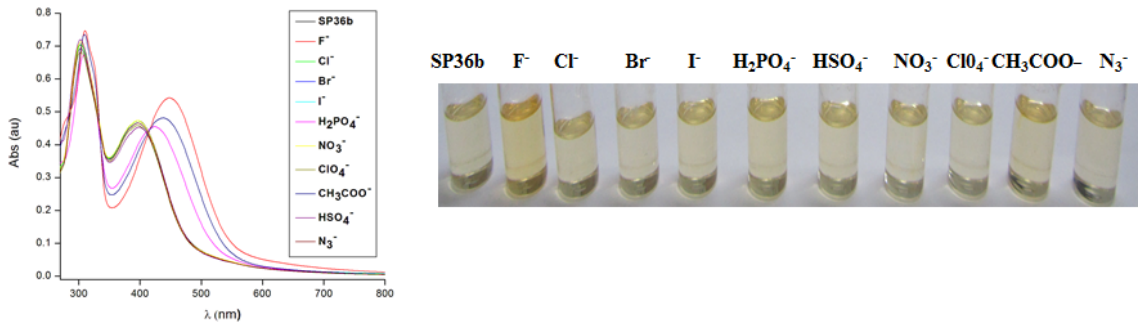

Figure 6.12 Left: UV-Vis spectra of **SP36b** (20 μM) in DMSO in absence and presence of different anions; right: Naked eye view of the color change while addition of different anions as their tetrabutylammonium salt to the solution of **SP36b** in DMSO.

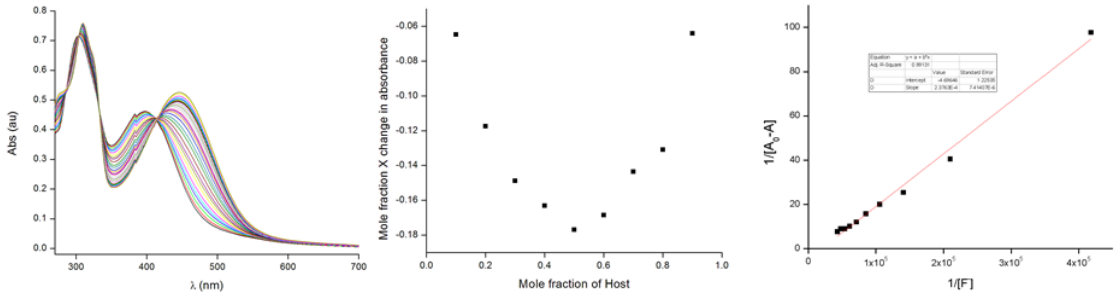

Figure 6.13 Left: Evolution of UV-Vis spectra of **SP36b** (20 μM) in DMSO upon gradual addition of TBAF (6.13×10^{-4} M); middle: Job's plot of **SP36b** (20 μM) vs. TBAF (20 μM); right: Benesi-Hildebrand plot of the titration data of **SP36b** vs. TBAF.

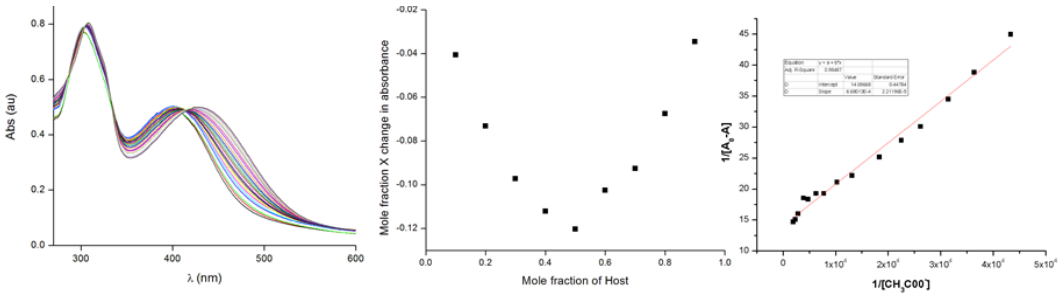

Figure 6.14 Left: Evolution of UV-Vis spectra of **SP36b** (20 μM) in DMSO upon gradual addition of TBA(CH_3COO) (5.2×10^{-4} M); middle: Job's plot of **SP36b** (20 μM) vs. TBA(CH_3COO) (20 μM); right: Benesi-Hildebrand plot of the titration data of **SP36b** vs. TBA(CH_3COO).

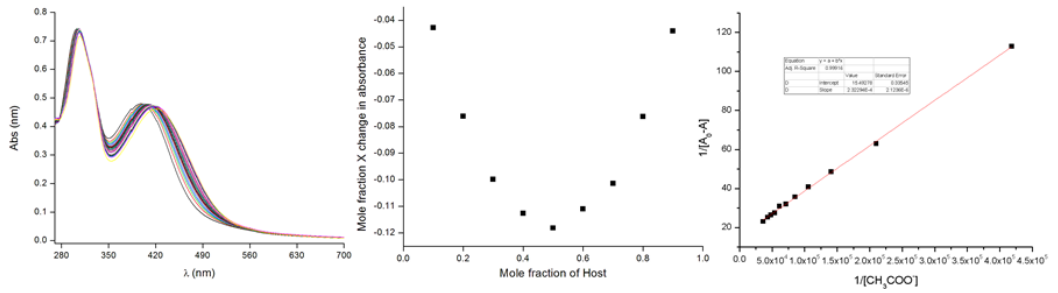

Figure 6.15 Left: Evolution of UV-Vis spectra of **SP36b** (20 μM) in DMSO upon gradual addition of $TBAH_2PO_4$ (1.0×10^{-3} M); middle: Job's plot of **SP36b** (20 μM) vs. $TBAH_2PO_4$ (20 μM); right: Benesi-Hildebrand plot of the titration data of **SP36b** vs. $TBAH_2PO_4$.

The anion binding study of pyrrole-benzimidazole conjugates bridged via quinoxaline moiety, **SP37a** and **SP37b** showed similar selectivity towards anions like **SP35b** and **SP36b**. Both displayed appreciable change in the absorption profile upon addition of F^-, CH_3COO^-

and $H_2PO_4^-$ ions only, among the tested anion (Figure 6.16). The addition of these three anions, led to a change in the color from yellow to red with varying intensities (Figure 6.16). The titration of receptor **SP37a** with fluoride showed the evolution of an absorption band at 506 nm with slight split in the higher energy band and the color changing from yellow to red. Three isobestic points at 318, 496 and 433 nm are noticed (Figure 6.17). The appearance of the peak at 506 nm may be attributed to anion to receptor charge transfer in the complex. Acetate and dihydrogenphosphate ions also induced similar changes in the absorption profile of **SP37a**, like seen in case of fluoride ion (Figures 6.18 and 6.19). Job's plot analysis showed the plateau at 0.5, indicating the formation of 1:1 complexes in these cases. Fitting the titration data to Benesi-Hildebrand plot resulted in binding constants 2.01×10^4, 8.72×10^4 and 9.4×10^3 M^{-1} for fluoride, acetate and dihydrogenphosphate ions, respectively.

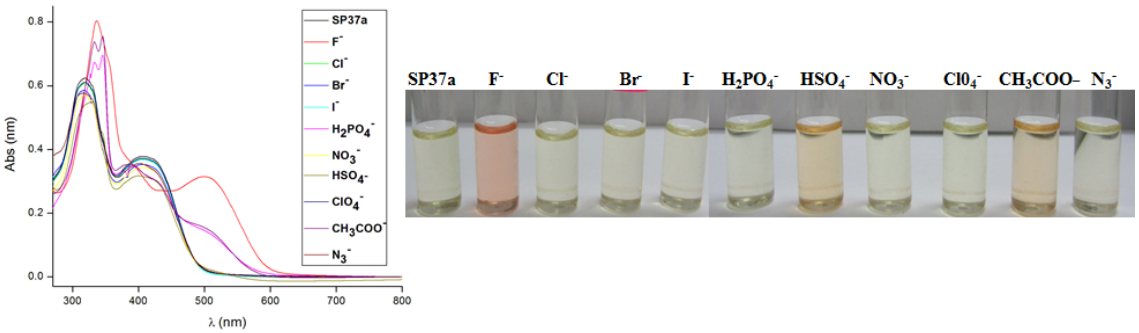

Figure 6.16 Left: UV-Vis spectra of **SP37a** (20 μM) in DMSO in absence and presence of different anions; right: Naked eye view of the color change while addition of different anions as their tetrabutylammonium salt to the solution of **SP37a** in DMSO.

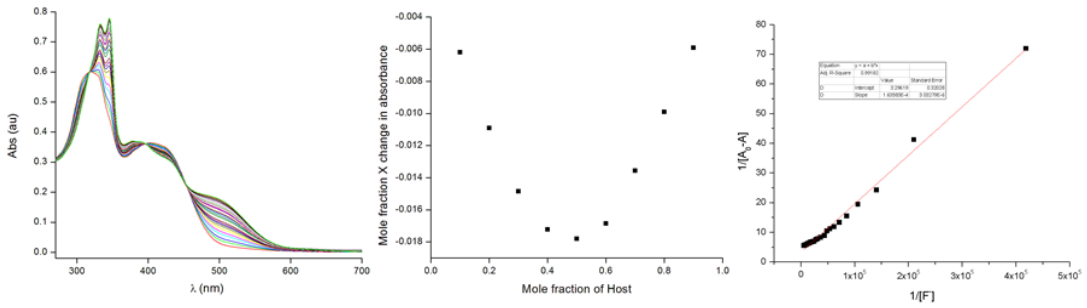

Figure 6.17 Left: Evolution of UV-Vis spectra of **SP37a** (20 μM) in DMSO upon gradual addition of TBAF (2.2×10^{-4} M); middle: Job's plot of **SP37a** (20 μM) vs. TBAF (20 μM); right: Benesi-Hildebrand plot of the titration data of **SP37a** vs. TBAF.

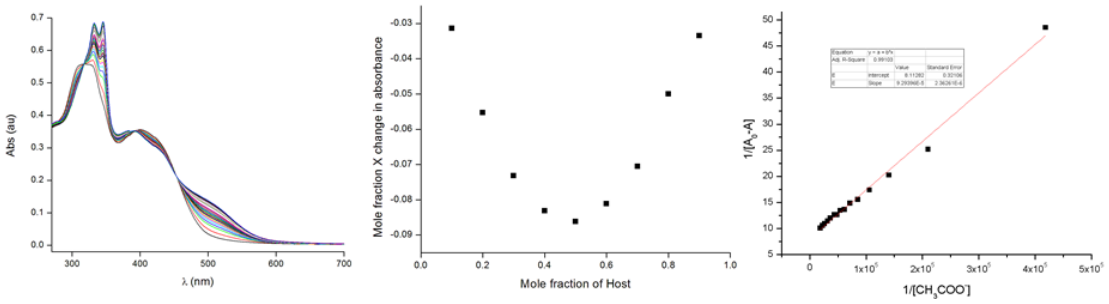

Figure 6.18 Left: Evolution of UV-Vis spectra of **SP37a** (20 μM) in DMSO upon gradual addition of TBA(CH_3COO) (6.3×10^{-4} M); middle: Job's plot of **SP37a** (20 μM) vs. TBA(CH_3COO) (20 μM); right: Benesi-Hildebrand plot of the titration data of **SP37a** vs. TBA(CH_3COO).

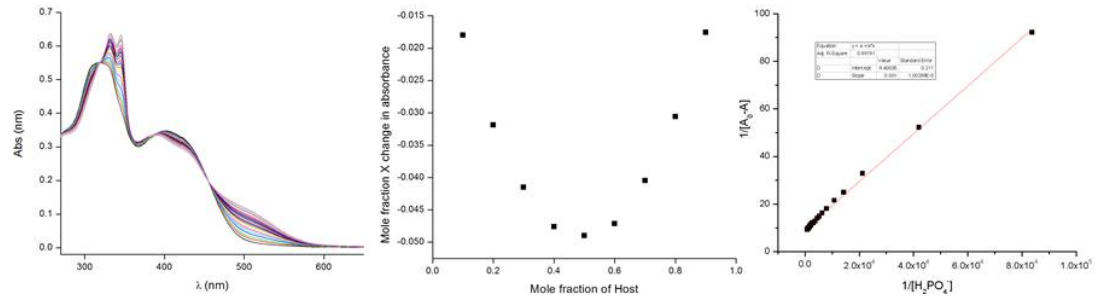

Figure 6.19 Left: Evolution of UV-Vis spectra of **SP37a** (20 μM) in DMSO upon gradual addition of $TBAH_2PO_4$ (1.3×10^{-3} M); middle: Job's plot of **SP37a** (20 μM) vs. $TBAH_2PO_4$ (20 μM); right: Benesi-Hildebrand plot of the titration data of **SP37a** vs. $TBAH_2PO_4$.

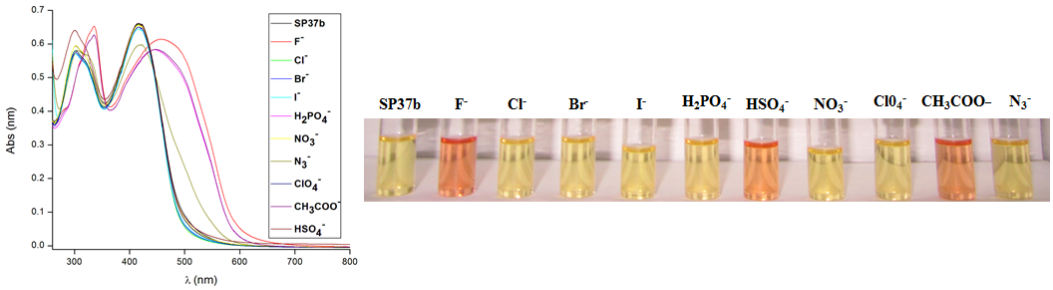

Figure 6.20 Left: UV-Vis spectra of **SP37b** (20 μM) in DMSO in absence and presence of different anions; right: naked eye view of the color change while addition of different anions as their tetrabutylammonium salts to the solution of **SP37b** in DMSO.

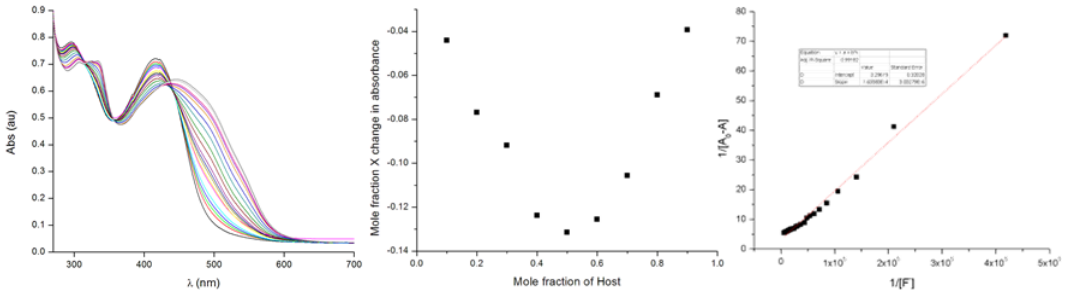

Figure 6.21 Left: Evolution of UV-Vis spectra of **SP37b** (20 μM) in DMSO upon gradual addition of TBAF (1.5×10^{-4} M); middle: Job's plot of **SP37b** (20 μM) vs. TBAF (20 μM); right: Benesi-Hildebrand plot of the titration data of **SP37b** vs. TBAF.

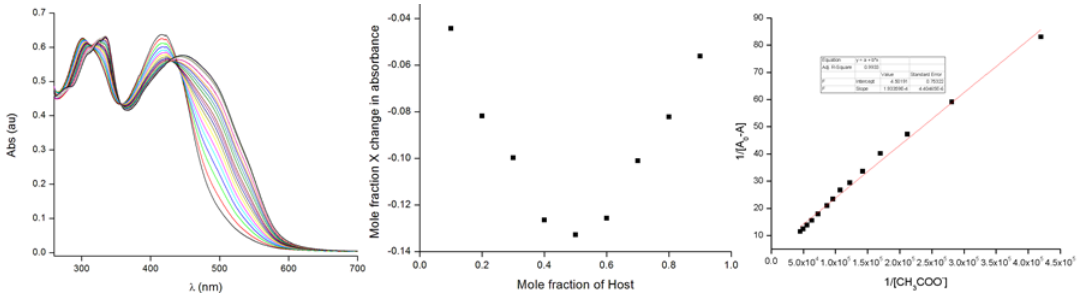

Figure 6.22 Left: Evolution of UV-Vis spectra of **SP37b** (20 μM) in DMSO upon gradual addition of TBA(CH_3COO) (5.2×10^{-4} M); middle: Job's plot of **SP37b** (20 μM) vs. TBA(CH_3COO) (20 μM); right: Benesi-Hildebrand plot of the titration data of **SP37b** vs. TBA(CH_3COO).

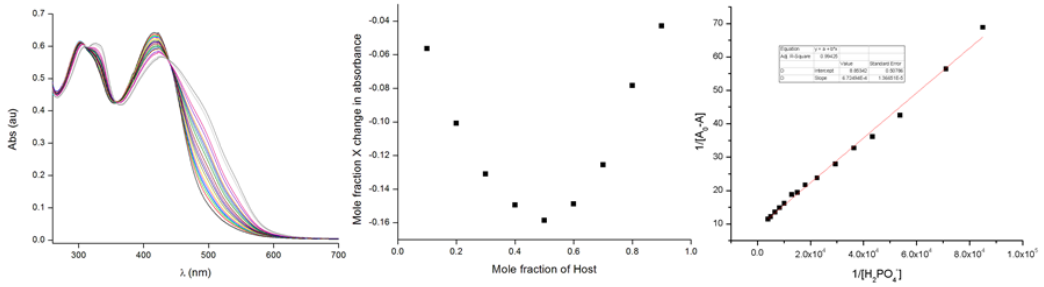

Figure 6.23 Left: Evolution of UV-Vis spectra of **SP37b** (20 μM) in DMSO upon gradual addition of $TBAH_2PO_4$ (2.5×10^{-4} M); middle: Job's plot of **SP37b** (20 μM) vs. $TBAH_2PO_4$ (20 μM); right: Benesi-Hildebrand plot of the titration data of **SP37b** vs. $TBAH_2PO_4$.

Like **SP37a**, receptor **SP37b** also showed affinity towards F^-, $H_2PO_4^-$ and CH_3COO^- ions and in addition, this receptor also had very weak affinity towards azide ion (Figure 6.20). Titration with fluoride ion showed the evolution of a broad peak at ~500 nm, with two

isobestic points at 335 and 444 nm and turned the color from dark yellow to red (Figure 6.21). The other two anions also induced similar changes in the absorption profile of **SP37b** like fluoride ion (Figures 6.22 and 6.23). The affinity constants of the receptors with different anions determined by UV-Vis spectroscopy are shown in table 6.2.

Table 6.2 Affinity constant, K_a (M^{-1}) of the receptors **SP35-37** towards the interacting anions as determined by UV-Vis spectroscopy in DMSO at 25 °C.

Host	F^-	CH_3COO^-	$H_2PO_4^-$
SP35a	8.45×10^2	-	-
SP35b	1.20×10^4	6.03×10^4	6.30×10^3
SP36a	1.90×10^3	-	-
SP36b	3.62×10^4	1.24×10^4	7.84×10^3
SP37a	2.01×10^4	8.72×10^4	9.4×10^3
SP37b	3.4×10^4	2.32×10^4	1.31×10^4

6.3.3.2 Fluorescence method

Fluorescence spectroscopic titration studies were also performed in order to check the ability of these receptors to operate as fluorometric anion sensors. Among the receptors synthesized nitro analogues are nonfluorescent (fluorescence is below detection limit). The studies were carried out with 1 μM solution of the remaining three hosts *i.e.* **SP35a**, **SP36a** and **SP37a**.

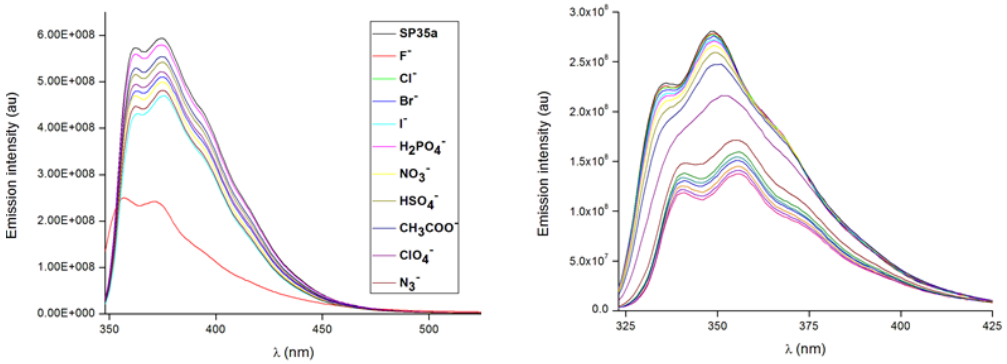

Figure 6.24 Left: fluorescence spectra of **SP35a** (1 μM) in DMSO in absence and presence of different anions; right: changes in the fluorescence spectra of **SP35a** (1 μM) upon gradual addition of TBAF (1.5 mM).

Remarkable quenching of fluorescence of receptors **SP35a** and **SP36a** was observed upon addition of F^- ion, whereas no significant change in fluorescence intensity could be noticed in case of the other anions (Figures 6.24 and 6.25).

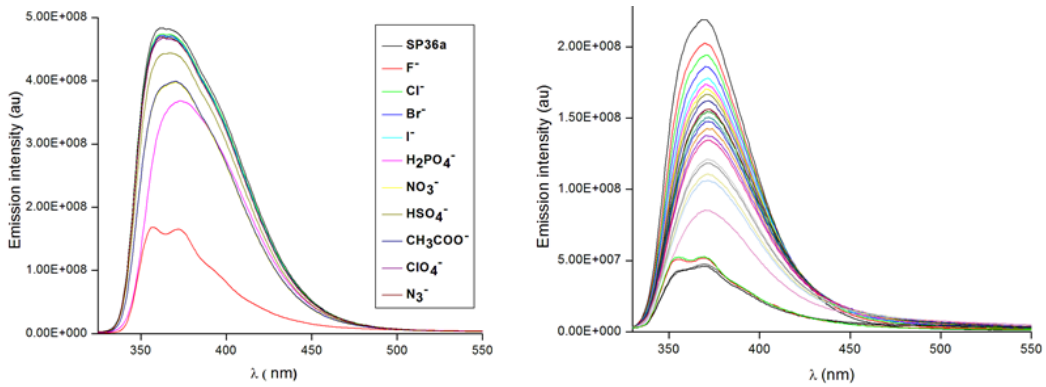

Figure 6.25 Left: Fluorescence spectra of **SP36a** (1 μM) in DMSO in absence and presence of different anions; right: changes in the fluorescence spectra of **SP36a** (1 μM) upon gradual addition of TBAF (2.0 mM).

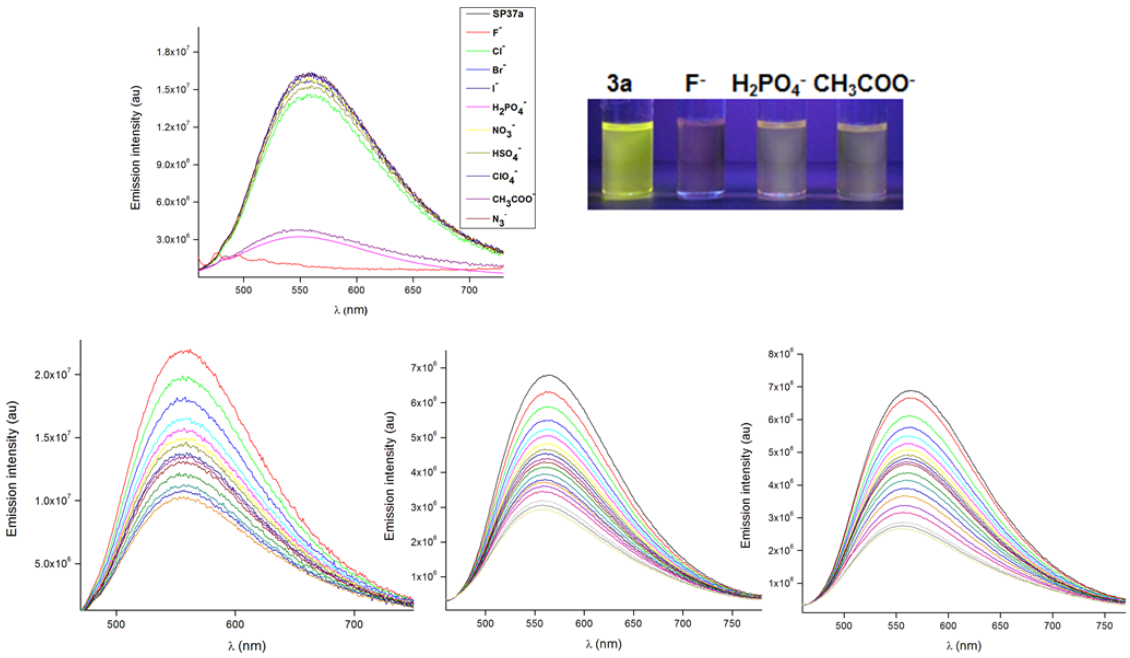

Figure 6.26 Top left: Fluorescence spectra of **SP37a** (1 μM) in DMSO in absence and presence of different anions; top right: visual changes in the fluorescence of **SP37a** upon addition of F^-, $H_2PO_4^-$ and CH_3COO^- ions; bottom left: changes in the fluorescence spectra of **SP37a** (1 μM) upon gradual addition of left: TBAF (5 μM); middle: changes TBA(CH_3COO) (3.4×10^{-4} M) and right: TBAH_2PO_4 (4.2×10^{-4} M).

Addition of F^- ion to **SP37a** resulted in almost complete quenching of its fluorescence. Further, addition of CH_3COO^- and $H_2PO_4^-$ ions also exerted substantial quenching of the fluorescence of the host (Figures 6.26). This may be ascribed to intramolecular photoinduced electron transfer (PET), from the quinoxaline residue to the benzimidazole moiety, triggered by anion complexation.

6.3.3.3 NMR titration method

To get a better insight regarding the nature of the interaction involved in the complexation process, ^{1}H NMR titrations were performed in DMSO-d_6 for some of the receptors, with fluoride and acetate ions.

The ^{1}H NMR titration of **SP35a** with TBAF revealed that with the addition of 0.17 equiv. of TBAF, both the NH resonances become broad with very little shift in their positions and subsequent addition of TBAF resulted in complete disappearance of the NH signals (Figure 6.27). After addition of ~1.2 equiv. of anion, a new broad triplet appeared at 16 ppm, indicating the formation of HF_2^- ion, which indicated the deprotonation of benzimidazole NH. However NMR spectra did not provide any conclusive inference about the pyrrolic NHs, indicating the presence of some very fast events w.r.t. the NMR time scale (Figure 6.27). On the other hand, the *β*-pyrrole CH and benzene-Hs display slightly up field shift upon addition

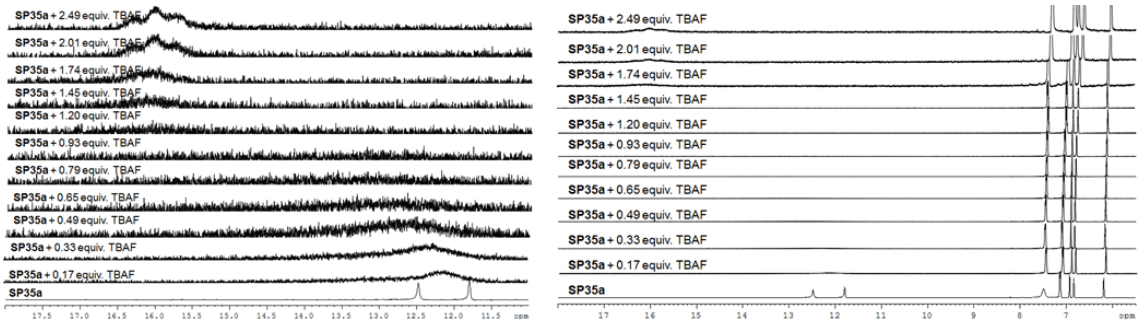

Figure 6.27 Selected portions of ^{1}H NMR indicating changes in the ^{1}H NMR spectra of **SP35a** (5 mM) upon gradual addition of TBAF in DMSO-d_6.

of fluoride ion, indicating the increase in the electron density on the receptor due to deprotonation. On the other hand, titration of **SP35b** with fluoride ion showed deprotonation of the benzimidazole NHs, while the pyrrole NH became broad with a little upfield shift (Figure 6.28). This indicated that pyrrole NH did not take part in the binding event and the upfield shift of the pyrrole NH may be attributed to the increase in the electron density in the

pyrrole-benzimidazole conjugate scaffold, owing to the deprotonation of the benzimidazole NH by the fluoride ion. This confirmed that the complexation of fluoride ion with **SP35b** is driven by the acidity of the NHs. Further, titration of **SP35b** with acetate ion revealed

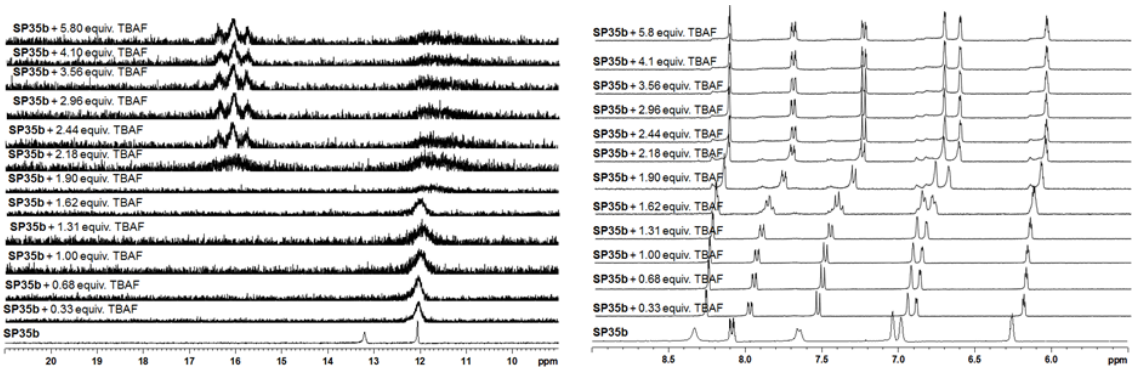

Figure 6.28 Selected portions of ^{1}H NMR indicating changes in the ^{1}H NMR spectra of **SP35b** (5 mM) upon gradual addition of TBAF in DMSO-d_6.

disappearance of the benzimidazole NH with concomitant downfield shift of the pyrrole NHs, indicating the participation of the two NHs in interaction with the two oxygen moiety of acetate ion (Figure 6.29). This suggests that the acetate binding is governed by the shape complementarity of the H-bonding sites and in this case both the NHs oriented in such a way to utilize the maximum number of H-bonding sites. Titration of **SP36b** with fluoride and

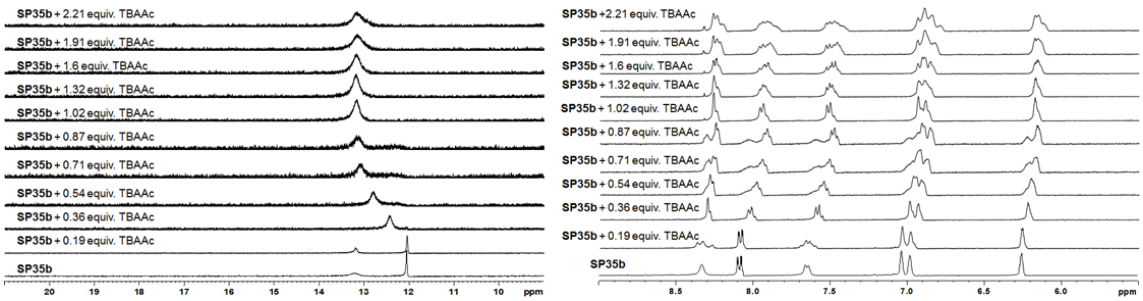

Figure 6.29 Selected portions of ^{1}H NMR indicating changes in the ^{1}H NMR spectra of **SP35b** (5 mM) upon gradual addition of TBA(CH_3COO) in DMSO-d_6.

acetate ions displayed similar binding patterns, as observed in case of **SP35b** (Figures 6.30 and 6.31). This clearly indicated that the binding mode of **SP36** and **SP35** are similar, where the anion complexation is governed by the acidity of the NHs for fluoride and acetate ions and in addition, the latter also influenced by shape complementarity. Besides, the enhanced affinity may be ascribed to the presence of higher number of binding sites. Interestingly, titration of receptor **SP37a**, the new peaks at 20.5 and at 16 ppm, along with a very broad

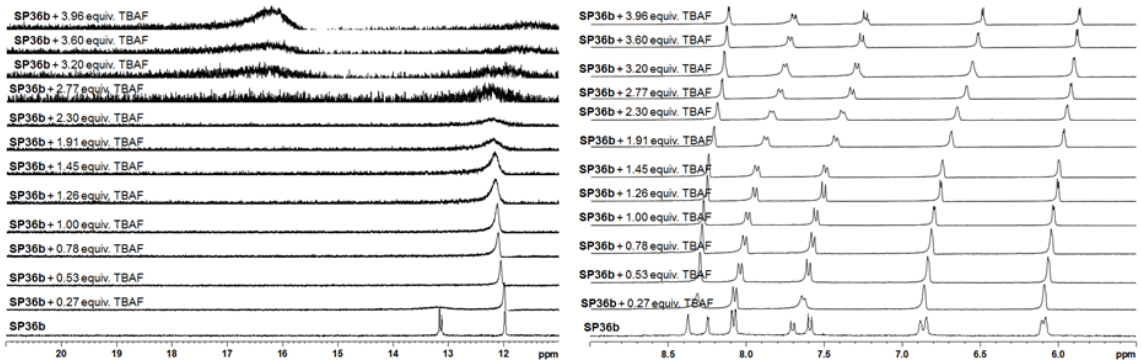

Figure 6.30 Selected portions of ^{1}H NMR indicating changes in the ^{1}H NMR spectra of **SP36b** (5 mM) upon gradual addition of TBAF in DMSO-d_6.

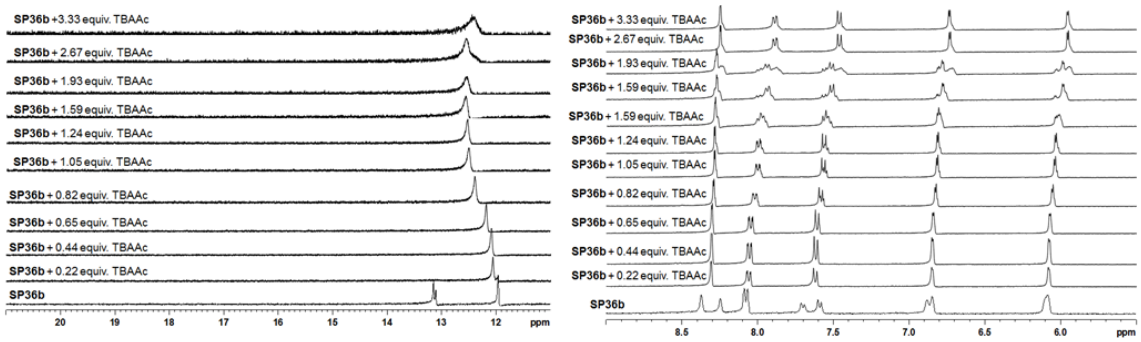

Figure 6.31 Selected portions of ^{1}H NMR indicating changes in the ^{1}H NMR spectra of **SP36b** (5 mM) upon gradual addition of TBA(CH_3COO) in DMSO-d_6.

peak between 12 and 16 ppm indicates the very slow nature of the complexation-decomplexation equilibrium (Figure 6.32). Besides, the study revealed the downfield shift with concomitant disappearance of the pyrrolic CH signal with addition of 1 equiv. of TBAF, which was quite unexpected. This signal might be merged with the benzene signals. Interestingly, gradual addition of TBAF upto ~2 equiv. resulted in sharpening of the peaks at 21 and 16 ppm with concomitant loss of the broad peak between 12 to 16 ppm. Further, the CH signal reappeared between 6.7-7.7 ppm (Figure 6.32). Subsequent addition of more TBAF resulted in upfield shift of the peak at 21 ppm to 18 ppm, while the broad peak at 16 ppm resolved into a triplet without undergoing shift. The later may be assigned to the formation of HF_2^-, owing to the deprotonation of the benzimidazolic proton. However, the appearance of peak at ~21 ppm and its subsequent shift to ~18 ppm is not completely understood by us and efforts are on in this direction. To the best of our knowledge, this type of observation is unprecedented. Further, titration of **SP37a** with acetate ion showed similar type of changes in the β-CH pyrrolic region while no new signal is observed in the downfield

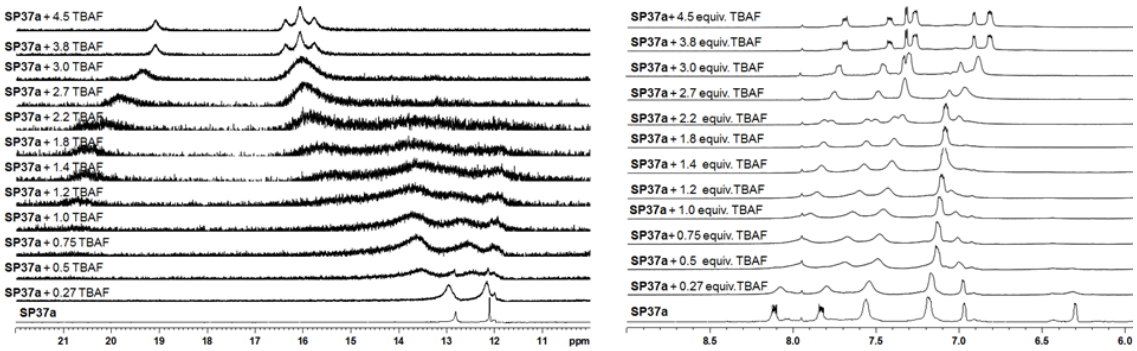

Figure 6.32 Selected portions of ^{1}H NMR indicating changes in the ^{1}H NMR spectra of **SP37a** (5 mM) upon gradual addition of TBAF in DMSO-d_6.

region as seen in case of fluoride binding. Moreover, addition of acetate ion induced broadening of the NH signals, which subsequently disappeared (Figure 6.33). Like fluoride, in this case also one of the pyrrole CH signals disappeared after addition of ~1 equiv. of anion and the other one slowly merged with the phenyl protons. The above observations led us to conclude that the unusual peak ~18 ppm in case of **SP37a** vs. fluoride titration can be ascribed to fluoride ion complexation only and on the other hand, the overall interaction mechanism of fluoride and acetate were almost similar. The titration of **SP37b** with TBAF exhibited comparatively faster complexation-decomplexation equilibrium than that in case of **SP37a** (Figure 6.34). Interestingly like **SP37a**, here also a new broad peak appeared at ~19 ppm with concomitant appearance of the HF_2^- signals at 16 ppm. However, this highly deshielded peak, never resolved further as noticed in case of **SP37a**. Further, here one of the pyrrolic CH gradually shifted downfield with gradual addition of fluoride ion and finally with ~1.5 equiv. of TBAF, it merged with the benzene CH signals, while the other pyrrole CH proton remained intact. Again, further experiments can only explain the origin of the peak at 19 ppm.

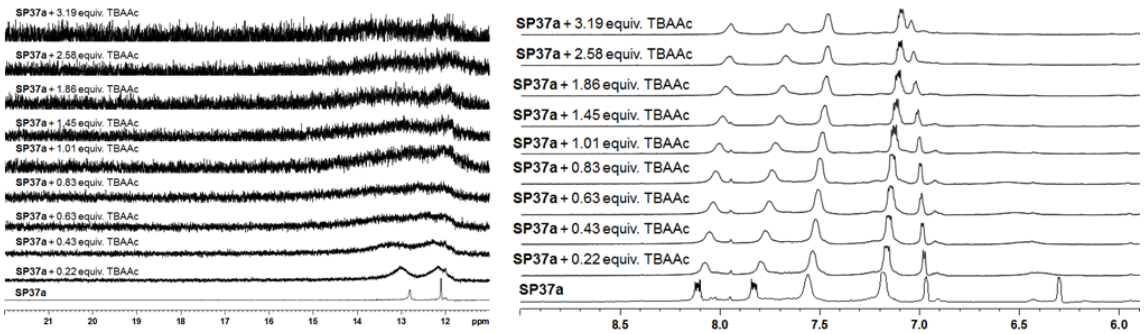

Figure 6.33 Selected portions of ^{1}H NMR indicating changes in the ^{1}H NMR spectra of **SP37a** (5 mM) upon gradual addition of TBA(CH_3COO) in DMSO-d_6.

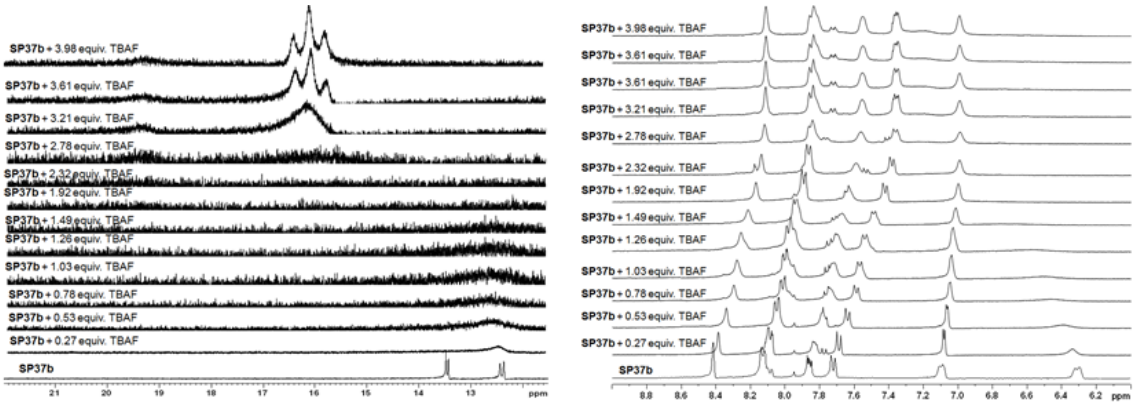

Figure 6.34 Selected portions of ^{1}H NMR indicating changes in the ^{1}H NMR spectra of **SP37b** (5 mM) upon gradual addition of TBAF in DMSO-d_6.

6.4 Conclusion

In conclusion, we have presented a new anion binding motif, based on pyrrole-benzimidazole conjugate, which included two competitive H-bonding sites with a remarkable pK_a difference. Herein, we have demonstrated how suitable substitution in the benzimidazole moiety can lead to a remarkable change in their affinity towards anion. Further, we have synthesized two different types of oligopyrrole-benzimidazole conjugates; one with localized and the other with delocalized π-cloud by incorporating sp^3- carbon and quinoxaline bridge respectively and studied their anion binding behavior. The study showed that pyrrole-benzimidazole conjugate receptors **SP35a** and **SP36a** exhibited good fluoride selectivity, whereas incorporation of nitro group led to increase in affinity along with a naked eye colorimetric response, however at the expense of selectivity. Receptors **SP35a** and **SP36a** could also act as dual sensor (UV-Vis as well as fluorescence). The nitro analogues bind acetate and dihydrogenphosphate ions as well. Moreover, both derivatives of quinoxaline bridged oligopyrrole-benzimidazole conjugates bind to fluoride, acetate and dihydrogenphosphate ions. The binding constant data obtained by fitting the UV-Vis titration data according to Benesi-Hildebrand method demonstrated that in case of fluoride and dihydrogenphosphate ions the order is **SP35a** < **SP36a** < **SP37a** and **SP35b**< **SP36b** < **SP37b** respectively due to the increase in the number of H-bonding moiety. Further, as expected the affinity also increased with the introduction of the nitro group, for fluoride and dihydrogenphosphate ions. On the other hand, acetate ion did not follow any generalized trend, indicating its affinity is driven by shape and size complementarity than acidity and number of the donor NHs. Further, ^{1}H NMR titration studies of **SP37a** and **SP37b** indicated some unusual phenomena, which are at present beyond our comprehension and efforts to

understand them are underway. These preliminary observations again highlighted the complex nature of the anion recognition event, which depends on size, shape and more pronouncedly on the acidity of the H-bond donors.

6.5 Experimental details

6.5.1 General procedure

To a solution of diamine derivative (1 mmol) in nitrobenzene, aldehyde derivative (1 mmol) was added. The reaction mixture was heated at 130 °C for 24 h. The precipitated solid was filtered, washed with first hexane and then diethyl ether and purified by column chromatography on silica gel with 5 % MeOH in $CHCl_3$ as eluent. Subsequently, the product was recrystallized from 1:1 acetone and methanol mixture.

6.5.2 Spectral data of SP35a

Yield: 55 %; ^{1}H NMR (400 MHz, DMSO-d_6): δ in ppm 12.48 (s, 1H, NH), 11.79 (s, 1H, NH), 7.48 (m, 2H, CH), 7.12 (q, 2H, CH, J = 2.88Hz), 6.92 (m, 1H, α-CH), 6.84 (m, 1H, β-CH), 6.19 (m, 1H, β-CH); ^{13}C NMR (100 MHz, DMSO-d_6): δ in ppm 147.24, 123.13, 121.88, 121.79, 109.61, 109.50; LCMS m/z calcd. for $C_{11}H_9N_3$ (M+H) 184, found 184; Elemental analysis for $C_{11}H_9N_3$ calcd. C: 72.11, H: 4.95, N: 22.94; found C: 72.26, H: 4.89, N: 22.85.

6.5.3 Spectral data of SP35b

Yield: 46 %; ^{1}H NMR (400 MHz, DMSO-d_6): δ in ppm 13.22 (br s, 1H, NH), 12.04 (s, 1H, NH), 8.31 (s, 1H, CH), 8.08 (d, 1H, CH, J = 8.8Hz), 7.65 (s, 1H, CH), 7.03 (m, 2H, α,β-CH), 6.25 (s, 1H, β-CH); ^{13}C NMR (100 MHz, DMSO-d_6): δ in ppm 151.08, 142.22, 123.04, 121.54, 117.7, 111.11, 109.84; LCMS m/z calcd. for $C_{11}H_8N_4O_2$ (M+H) 229, found 229; Elemental analysis for $C_{11}H_8N_4O_2$ calcd. C: 57.89, H: 3.53, N: 24.55, found C: 57.76, H: 3.45, N: 24.61.

6.5.4 Spectral data of SP36a

Yield: 48 %; ^{1}H NMR (400 MHz, DMSO-d_6): δ in ppm 12.43 (br s, 2H, NH), 11.79 (s, 2H, NH), 7.55 (br s, 4H, CH), 7.42 (s, 4H, CH), 7.12 (m, 2H, α-CH), 6.71 (s, 2H, β-CH), 1.78 (s, 6H, CH_3); ^{13}C NMR (100 MHz, DMSO-d_6): δ in ppm 147.28, 143.18, 122.78, 121.84, 109.11, 105.68, 35.42, 28.26; LCMS m/z calcd. for $C_{25}H_{22}N_6$ (M+H) 407, found 407;

Elemental analysis for $C_{25}H_{22}N_6$ calcd. C: 73.87, H: 5.46, N: 20.67; found C: 73.69, H: 5.58, N: 20.42.

6.5.5 Spectral data of SP36b

Yield: 41%; ^{1}H NMR (400 MHz, DMSO-d_6): δ in ppm 13.15 (m, 2H, NH), 11.97 (m, 2H, NH), 8.37 (s, 1H, CH), 8.25 (s, 1H, CH), 8.08 (d, 2H, CH, J = 8Hz), 7.71 (s, 1H, CH), 7.69 (s, 1H, CH), 6.86 (d, 2H, α-CH, J = 12Hz), 6.09 (t, 2H, β-CH, J = 4Hz), 1.81 (s, 6H, CH_3); ^{13}C NMR (100 MHz, DMSO-d_6): δ in ppm 150.51, 144.03, 143.39, 142.42, 141.80, 139.76, 117.73, 112.96, 110.72, 106.82, 106.19, 35.21, 17.68; LCMS m/z calcd. for $C_{25}H_{20}N_8O_4$ (M+H) 497, found 497; Elemental analysis for $C_{25}H_{20}N_8O_4$ calcd. C: 60.48, H: 4.06, N: 22.57; found C: 60.36, H: 4.12, N: 22.68.

6.5.6 Spectral data of SP37a

Yield: 39 %; ^{1}H NMR (400 MHz, DMSO-d_6): δ in ppm 12.79 (s, 2H, NH), 12.08 (s, 2H, NH), 8.11 (m, 2H, CH), 7.82 (d, 2H, CH, J = 4Hz), 7.56 (t, 4H, CH, J = 8Hz), 7.17 (s, 4H, CH), 6.96 (s, 2H, α-CH), 6.30 (d, 2H, β-CH, J = 4Hz); ^{13}C NMR (100 MHz, DMSO-d_6): δ in ppm 146.13, 145.17, 140.30, 132.04, 130.41, 128.80, 125.79, 122.39, 113.14, 111.19; LCMS m/z calcd. for $C_{30}H_{20}N_8$ (M+H) 493, found 493; Elemental analysis for $C_{30}H_{20}N_8$ calcd. C: 73.16, H: 4.09, N: 22.75, found C: 73.28, H: 4.15, N: 22.61.

6.5.7 Spectral data of SP37b

Yield: 31 %; ^{1}H NMR (400 MHz, DMSO-d_6): δ in ppm 13.43 (m, 2H, NH), 12.40 (m, 2H, NH), 8.42 (s, 2H, CH), 8.13 (d, 4H, CH, J = 8.8Hz), 7.87 (d, 2H, CH, J = 4Hz), 7.74 (s, 2H, CH), 7.10 (d, 2H, α-CH, J = 6.4Hz), 6.32 (d, 2H, β-CH, J = 11.2Hz); ^{13}C NMR (100 MHz, DMSO-d_6): δ in ppm 162.82, 144.90, 143.13, 140.32, 133.19, 130.67, 128.85, 124.5, 118.28, 113.38, 112.84; LCMS m/z calcd. for $C_{30}H_{18}N_{10}O_4$ (M+H) 583, found 583; Elemental analysis for $C_{30}H_{18}N_{10}O_4$ calcd. C: 61.85, H: 3.11, N: 24.04, found C: 61.76, H: 3.18, N: 24.15.

6.6 References

1. (a) Katayev, E. A.; Ustynyuk, Y. A.; Sessler, J. L. *Coord. Chem. Rev.* **2006**, *250*, 3004. (b) Gale, P. A. *Acc. Chem. Res.* **2006**, *39*, 465. (c) Amendola, V.; Esteban-Gomez, D.; Fabbrizi, L.; Licchelli, M. *Acc. Chem. Res.* **2006**, *39*, 343. (d) Yoon, J.;

Kim, S. K.; Kim, K. S. *Chem. Soc. Rev.* **2006**, *35*, 355. (e) Bowman-James, K. *Acc. Chem. Res.* **2005**, *38*, 671. (f) Gale, P. A. Coord. *Chem. Rev.* **2003**, *240*, 167. (g) Sessler, J. L.; Camiolo, S.; Gale, P. A. *Coord. Chem. Rev.* **2003**, *240*, 17. (h) Sun, S. -S.; Lees, A. J. *Coord. Chem. Rev.* **2002**, *230*, 170.

2. (a) In *Supramolecular Chemistry of anions*, Eds. Bianchi, A.; Garcia-Epsána, E.; Bowman-James, K. Wiley-VCH, New York, 1997. (b) In *Anion Receptor Chemistry*, Eds. Sessler, J. L.; Gale, P. A.; Cho, W. -S. RSC Publishing, Cambridge, UK, 2006. (c) Gale, P. A. *Chem. Commun.* **2011**, 82. (d) In *Frontiers in Supramolecular Organic Chemistry and Photochemistry*, Eds. Schneider, H. -J.; Dürr, H.VCH Publishing: Weinheim, Germany, 1991.
3. Schmidtchen, F. P. *Coord. Chem. Rev.* **2006**, *250*, 2918.
4. Wichmann, K.; Antonioli, B.; Söhnel, T.; Wenzel, M.; Gloe, K.; Price, J. R.; Lindoy, L. F.; Blake, A. J.; Schröder, M. *Coord. Chem. Rev.* **2006**, *250*, 2987.
5. Li, A. -F.; Wang, J. -H.; Wang, F.; Jiang, Y. -B. *Chem. Soc. Rev.* **2010**, *39*, 3729.
6. (a) Bondy, C. R.; Loeb, S. J. *Coord. Chem. Rev.* **2003**, *240*, 77. (b) Kang, S. O.; Begum, R. A.; Bowman-James, K. *Angew. Chem. Int. Ed.* **2006**, *45*, 7882. (c) Kang, S. O.; Hossain, Md. A.; Bowman-James, K. *Coord. Chem. Rev.* **2006**, *250*, 3038.
7. Amendola, V.; Fabbrizzi, L.; Mosca, L.; Schmidtchen, F. P. *Chem. Eur. J.* **2011**, *17*, 5972.
8. Sessler, J. L.; Camiolo, S.; Gale, P. A. *Coord. Chem. Rev.* **2003**, *240*, 17.
9. Shang, X. F.; Lin, H.; Xu, X. F.; Jiang, P.; Lin, H. K. *Appl. Organometal. Chem.* **2007**, *21*, 821.
10. Gale, P. A. *Chem. Commun.* **2008**, 4525.
11. Singh, N.; Jang, D. O. *Org. Lett.* **2007**, *9*, 1991.
12. Mc. Donald, K. P.; Hua, Y.; Lee, S.; Flood, A. H. *Chem. Commun.* **2012**, 5065.
13. Das, P.; Kesharwani, M. K.; Mandal, A. K.; Suresh, E.; Ganguly, B.; Das, A. *Org. Biomol. Chem.* **2012**, *10*, 2263.
14. (a) Okhuma, S.; Sato, T.; Okamoto, M.; Matsuya, H.; Arai, K.; Kataoka, T.; Nagai, K.; Wassermann, H. H. *Biochem. J.* **1998**, *334*, 731. (b) Sato, T.; Konno, H.; Tanaka, Y.; Kataoka, T.; Nagai, K.; Wasserman, H. H.; Ohkuma, S. *J. Biol. Chem.***1998**, *273*, 2145. (c) Yamamoto, D.; Kiyozuka, T.; Uemura, Y.; Yamamoto, C.; Takemot, H.; Hirata, H.; Tanaka, K.; Hiokoi, K.; Tsubura, A. J. *Cancer Res. Clin. Oncol.* **2000**, *126*, 191. (d) Furstner, A.; Grabowski, J.; Lehmann, C. W.; Kataoka, T.; Nagai. K.

Chem. Biochem. **2001**, *2*, 60. (e) Sessler, J. L.; Eller, L. R.; Cho, W. -S.; Nicolaou, S.; Aguilar, A.; Lee, J. T.; Lynch, V. M.; Magda, D. J. *Angew. Chem. Int. Ed.* **2005**, *44*, 5989. (f) Gale, P. A.; Light, M. E.; McNally, B.; Navakhun, K.; Sliwinski, K. E.; Smith, B. D. *Chem. Commun.* **2005**, 3773.

15. (a) Suksai, C.; Tuntulani, T. *Chem. Soc. Rev.* **2003**, *32*, 192. (b) Martínez-Mánèz, R.; Sanceńon, F. *Coord. Chem. Rev.* **2006**, *250*, 3081. (c) Martínez-Mánèz, R.; Sanceńon, F. *Chem. Rev.* **2003**, *103*, 4419.
16. (a) Sato, K.; Arai, S.; Yamagishi, T. *Tetrahedron Lett.* **1999**, *40*, 5219. (b) Kang, G.; Kim, H. S.; Jang, D. O. *Tetrahedron Lett.* **2005**, *46*, 6079. (c) Peng, X.; Wu, Y.; Fan, J.; Tian, M.; Han, K. *J. Org. Chem.* **2005**, *70*, 10524. (d) Kim, H. S.; Moon, K. S.; Jang, D. O. *Supramol. Chem.* **2006**, *18*, 97. (e) Singh, N.; Jang, D. O. *Org. Lett.* **2007**, *9*, 1991. (f) Moon, K. S.; Singh, N.; Lee, G. W.; Jang, D. O. *Tetrahedron* **2007**, *63*, 9106. (g) Lee, G. W.; Singh, N.; Jang, D. O. *Tetrahedron Lett*. **2008**, *49*, 1952. (h) Zapata, F.; Caballero, A.; Tarraga, A.; Molina, P. *J. Org. Chem.* **2010**, *75*, 162 (i) Kumari, N.; Jha, S.; Bhattacharya, S. *J. Org. Chem.* **2011**, *76*, 8215. (j) Abraham, Y.; Salman, H.; Suwinska, K.; Eichen, Y. *Chem. Commun.* **2011**, *47*, 6087.
17. Bordwell, F. G. *Acc. Chem. Res.* **1988**, *21*, 456.
18. Ueno, T., Urano, Y., Kojima, H., Nagano, T. *J. Am. Chem. Soc.* **2006**, *128*, 10640.
19. (a) Connors, K. A. In *Binding Constant Determination*; Wiley, New York, 1987. (b) Benesi, H.; Hildebrand, H. *J. Am. Chem. Soc.* **1949**, *71*, 2703.
20. Moon, K. S.; Singh, N.; Lee, G. W.; Jang, D. O. *Tetrahedron* **2007**, *63*, 9106.

CHAPTER 7

Conclusion

7.1 Summary

The thesis entitled "*Cyclic and acyclic oligopyrrole derivatives towards anion binding*" describes the syntheses of several acyclic and cyclic oligopyrrolic derivatives and their anion binding study. The thesis contains seven chapters. The first chapter gives an overview regarding anions and their recognition, followed by second chapter dealing with materials and methods employed for the dissertation work. Subsequently, there are four chapters, which deal with the anion binding study of the newly synthesized oligopyrrolic derivatives. The final chapter *i.e.* the present one provides a brief summary of the work carried out.

Anions drew wide attention of researcher in the last few decades owing to the important roles they play in biology and environment. Therefore, the major objective is to carry out selective recognition of anions, if possible with higher affinity. Several synthetic receptors have been reported in literature in this direction. Among them, pyrrole based receptors emerged as an attractive target over the last two decades. Again, cooperative anion binding is an upcoming research topic with very few reports in the literature. Owing to the difficulties involved in anion binding, design of receptors which can show cooperativity while binding

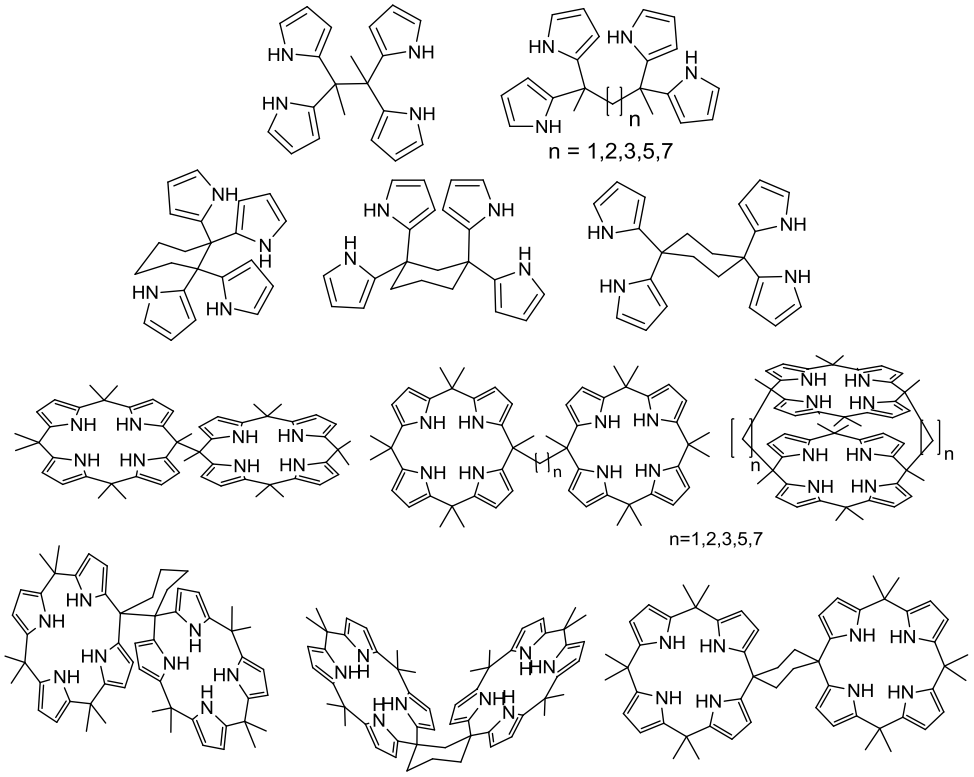

Figure 7.1 Structure of the proposed bisDPMs and biscalix[4]pyrroles.

anions appears to be extremely challenging. We envisaged biscalix[4]pyrroles, with flexible linkers can provide the desired attributes. In this direction, we designed several biscalixpyrroles (chapter 3), using bisDPMs as precursor, that in turn to be made from different type of aliphatic diketones with different organic scaffolds (cyclic and acyclic, flexible and rigid). We choose acyclic diketones to make biscalix[4]pyrroles, where one calix[4]pyrrole is strapped over another through flexible linker, *meso-meso* linked biscalixpyrroles and cyclohexanediones to have two calix[4]pyrrole at closer proximity with comparatively lesser flexibility (Figure 7.1).

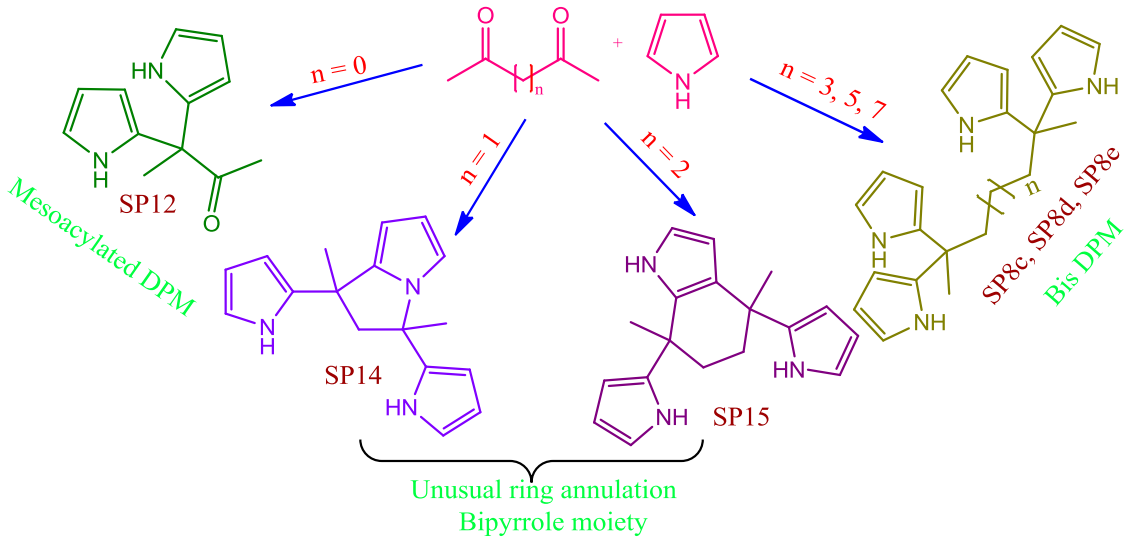

Figure 7.2 Pictorial representation of the outcome of the reaction of different acyclic diketones with pyrrole under acidic condition.

In case of acyclic *i.e.* flexible diketones, bisDPM could be achieved only when the two carbonyl groups are apart with a minimum propylene unit. Shorter linear aliphatic diketones viz. 2,4-pentandione and 2,5-hexanedione yielded ring annulated products, whereas the smallest one *i.e.* 2,3-butandione yielded monocondensed product only (Figure 7.2). The selective formation of **SP14** and **SP15** and the asymmetric nature of the three pyrrole units in the molecule may find its use as an interesting building block in porphyrinoid chemistry. **SP8c-e** can be used as building blocks towards the synthesis of biscalixpyrroles and other related macrocycles. However, so far we have not been able to isolate the desired biscalixpyrrole and efforts are still on this direction. The monoacyl dipyrromethane **SP12** and diacyl tripyrrane **SP13** can be used as building blocks towards functionalized calix[4]pyrrole which is described in chapter 4.

Among the cyclic rigid diketones the 1,4-isomer appeared to be most reactive towards pyrrole under acidic condition and the 1,2-isomer showed least reactivity (absence of the formation of bisDPM) (Figure 7.3). Further we could find a simple strategy to obtain 3-(1H-pyrrol-2-yl)cyclohex-2-enone **SP17**, which may provide a new route towards the transition

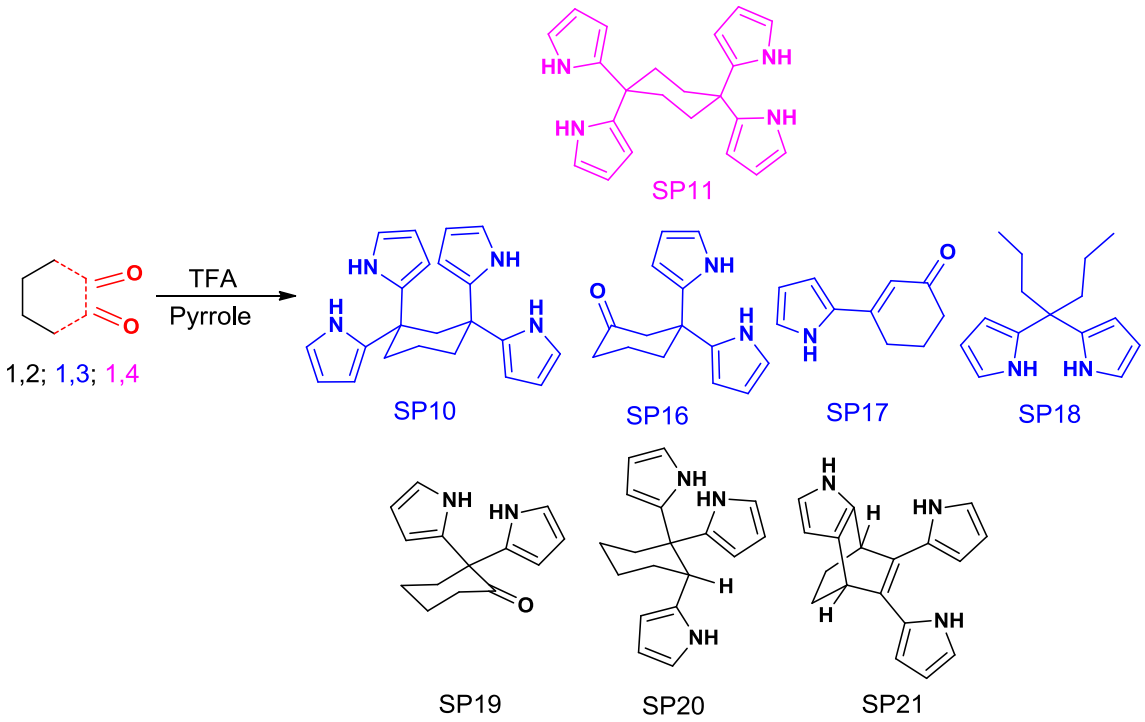

Figure 7.3 Pictorial representation of the outcome of the reaction of different isomers of cyclohexanedione with pyrrole under acidic condition.

metal-free C-C bond formation reaction. The surprising formation of 5,5′-dipropyldipyrromethane **SP18** (from 1,3-cyclohexanedione), the tripyrrole derivative **SP20** and the pyrrole substituted bicyclic dihydroindole **SP21** (from 1,2-cyclohexanedione) will be of greater interest in order to understand their mechanism. Again, so far our attempt to obtain biscalix[4]pyrrole is yet to succeed and efforts are still on in this direction. In spite of these failures, we could draw an important conclusion that the reaction of ketones with pyrrole need not always result in dipyrromethanes. Recently, Thompson *et al.* reported the reaction of substituted pyrroles with ketones and they obtained several annulated bispyrroles. Combinedly, we could infer that the reaction depends on the nature of both the ketones and the type of pyrrole used.[1]

Functionalized calix[4]pyrroles are known to display better selectivity towards anions. In this direction, the amalgamation of appropriate flexible hydrogen bonding complementary functional group to the calix[4]pyrrole periphery leads to enhanced binding affinity toward selected anions. Toward this, we have designed and synthesized two positional isomers of *meso*-diacylcalixpyrrole (5,10- and 5,15-) and subsequently isolated their individual conformational isomers (*cis* and *trans*) and studied the effect of position and orientation of the acyl group towards anion discrimination (chapter 4) .

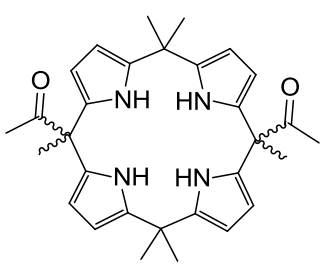

SP23

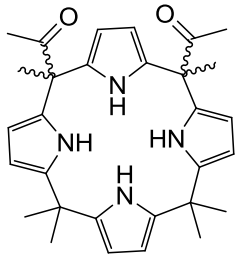

SP24

During the investigation, we have standardized the synthesis of 5,10-diacyltripyrrane and found that the condensation reaction of 2,3-butandione with pyrrole is dependent on the concentration of acid catalyst *i.e.* trifluoroacetic acid. At low acid concentration, it leads to a pyrrole-2-carbinole derivative, which may find importance as a precursor for designer porphyrinoids. Further, we have demonstrated that with proper hydrogen bonding functionalization at calix[4]pyrrole periphery, can lead to kinetically stable other conformers (1,2-conformation of *trans*-5,15-diacylcalix[4]pyrrole), along with interesting solid state structures, which, can expand the domain of host-guest chemistry of calix[4]pyrroles in solid state. The anion binding study of these designer macrocycles showed that when the two acyl groups are placed at the 5,10-positions in *cis*-orientation w.r.t. the calix[4]pyrrole periphery, their preference toward halides increased (fluoride displays largest enhancement), on the other hand, their placement at the 5,15-positions led to relatively higher affinity towards dihydrogenphosphate ion. In addition, it is noticed that the *cis*-isomers are remarkably better anion receptors than their *trans*-counterparts, which in turn displayed lesser affinity towards anions than the parent *meso*-octamethylcalix[4]pyrrole. Further, the study revealed that insertion of diacyl moiety in *cis*-orientation at the periphery, increased affinity towards dihydrogenphosphate ion than *meso*-octamethylcalix[4]pyrrole due to the formation of additional O-H…O hydrogen bonds with the anion.

Another interesting observation we found is, how a small change in the size of the cavity can lead to a drastic change in anion selectivity and sensing. Here we have designed and synthesized three new *meso*-expanded calix[4]pyrroles *i.e.* calix[2]bispyrrolylalkenes where the expansion is achieved via the replacement of two of the opposite *meso* carbons by ethene moieties (chapter 5). The synthesis was achieved by following the McMurry strategy, which

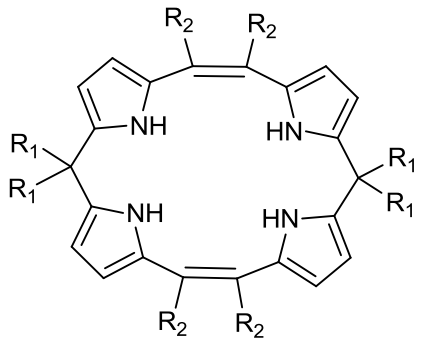

SP26 R_1,R_2 = Me
SP27 R_1 = Cy, R_2 = Me
SP28 R_1 = Me, R_2 = H

is employed for the first time in calix[4]pyrrole chemistry. These macrocycles represent a new class of the smallest expanded calix[4]pyrrole reported so far. Anion binding studies revealed that these molecules are highly selective for fluoride ion only, in contradiction with anion binding behaviour of the smaller octamethylcalix[4]pyrrole and its higher expanded calixpyrrole. Among them, calix[2]bispyrrolylethene **SP28** exhibited easy to observe colorimetric sensing of fluoride ion (colourless to dark red), in polar aprotic solvents through anion-π interaction. This study reflects that it is not always true that increasing the core size will increase the affinity towards the larger anions. Presently, efforts are underway in our laboratory to enhance its response.

Finally, we have developed pyrrole-benzimidazole conjugates as a new acyclic anion binding motif, which contains two competitive H-bonding sites with a remarkable different p*K*a. Herein, we have demonstrated how appropriate substitution on the benzimidazole moiety can lead to remarkable changes in their affinity towards anions. We have synthesized two different types of oligopyrrole-benzimidazole conjugates, one with localized and another one with delocalized π-cloud, by incorporating sp^3-carbon and quinoxaline bridge respectively and studied their anion binding behavior. The study demonstrated that pyrrole-imidazole conjugates **SP35a** and **SP36a** showed good fluoride selectivity among the tested anions, whereas incorporation of nitro group leads to increase in affinity accompanied by a naked eye colorimetric response, however with a compromise in selectivity. **SP35a** and

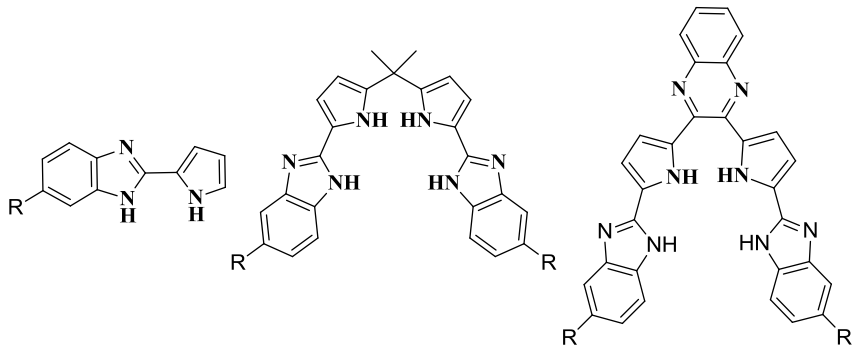

SP35a R = -H
SP35b R = -NO_2

SP36a R = -H
SP36b R = -NO_2

SP37a R = -H
SP37b R = -NO_2

SP36a can act as dual sensor (UV-Vis as well as fluorescence), although their response is not satisfactory w.r.t. naked eye observation. The nitro analogues bind acetate and dihydrogenphosphate ions as well. Again, quinoxaline bridged oligopyrrole-benzimidazole conjugates showed affinity towards fluoride, acetate and dihydrogenphosphate ions. As expected, the affinity of the receptors increased towards fluoride and dihydrogenphosphate ions upon introduction of the nitro group. On the other hand, acetate anion did not follow any generalized trend indictating the complicated nature of its interaction involving shape and size complementarity, than acidity and number of donors (*i.e.* NHs here). Further, ^{1}H NMR titration study of the quinoxaline bridged pyrrole-benzimidazole conjugates revealed some unusual phenomena, which are presently beyond our comprehension and we are trying to understand through additional experimental studies. Preliminary observations indicated the complex nature of the anion recognition phenomenon, which depends on complementarity of size, shape of the interacting partners and more pronouncedly, on the acidity of the H-bond donors.

7.2 Reference

1. Smithen, D.A.; Cameron, T.S.; Thompson, A. *Org. Lett.* **2011**, *13*, 5846.

Appendix

Appendix

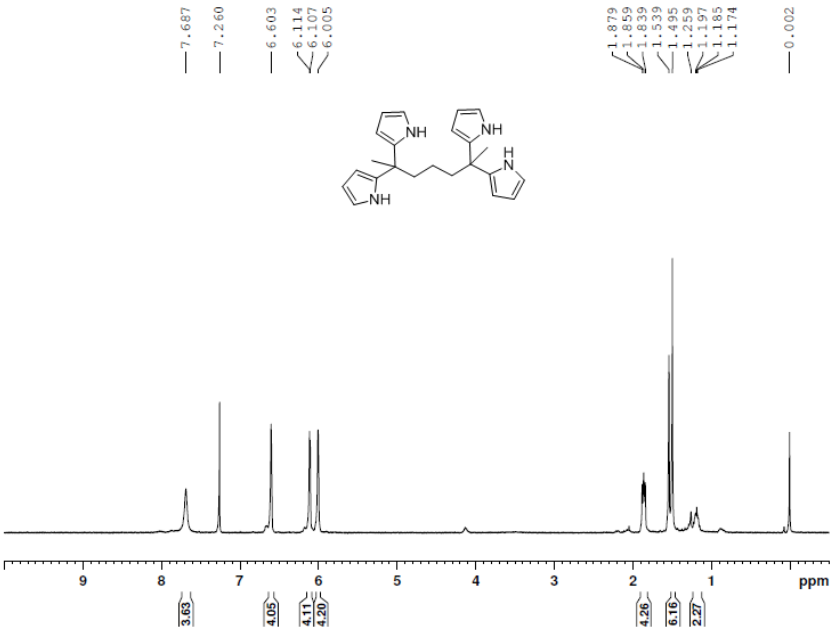

Figure A1 ^{1}H NMR spectrum of **SP8c**.

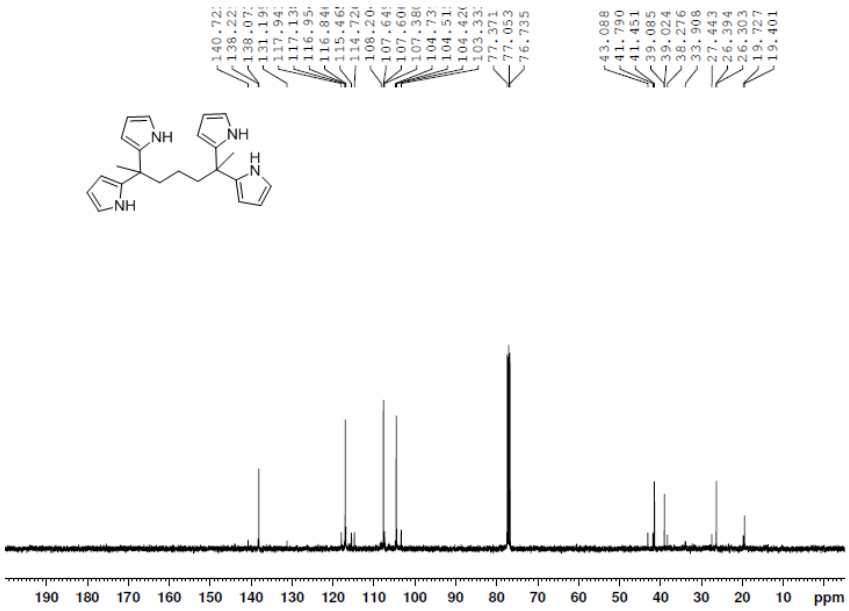

Figure A2 ^{13}C NMR spectrum of **SP8c**.

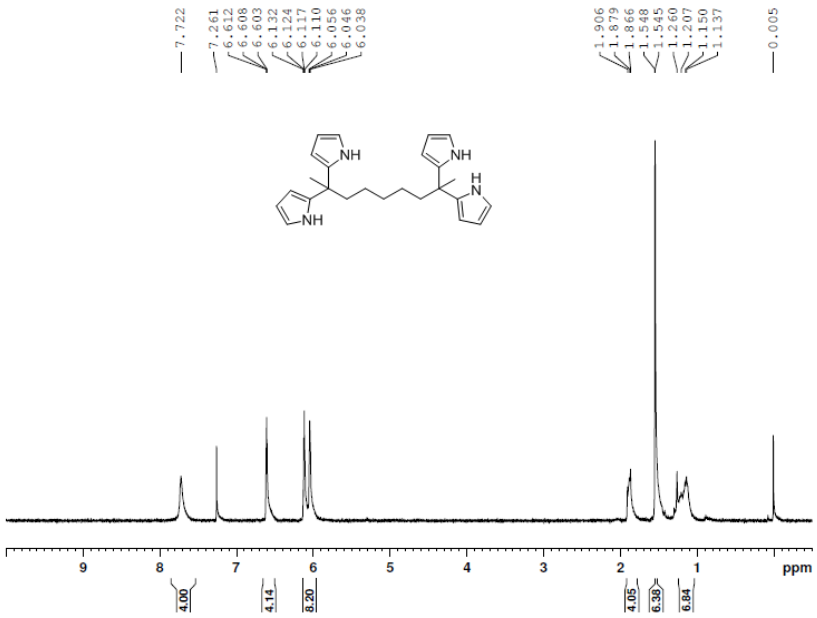

Figure A3 ^{1}H NMR spectrum of **SP8d**.

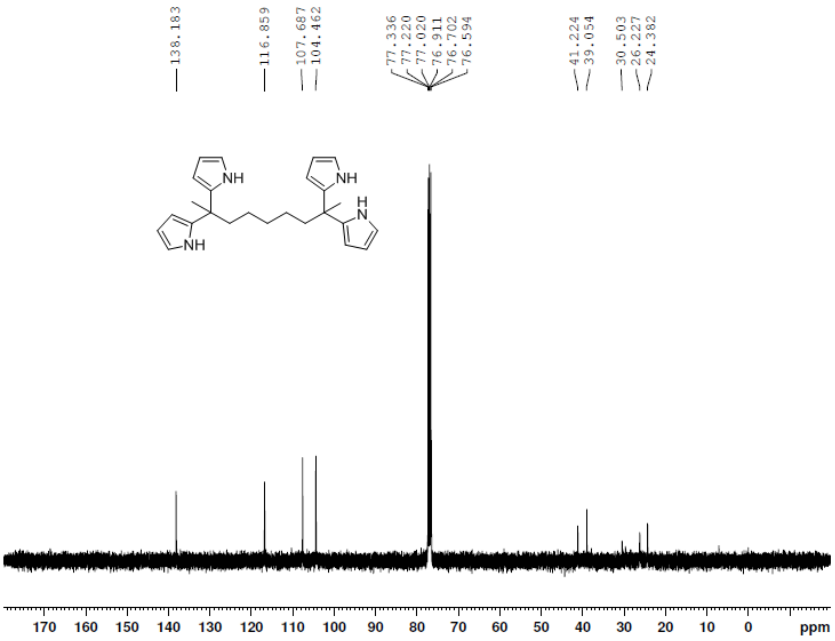

Figure A4 ^{13}C NMR spectrum of **SP8d**.

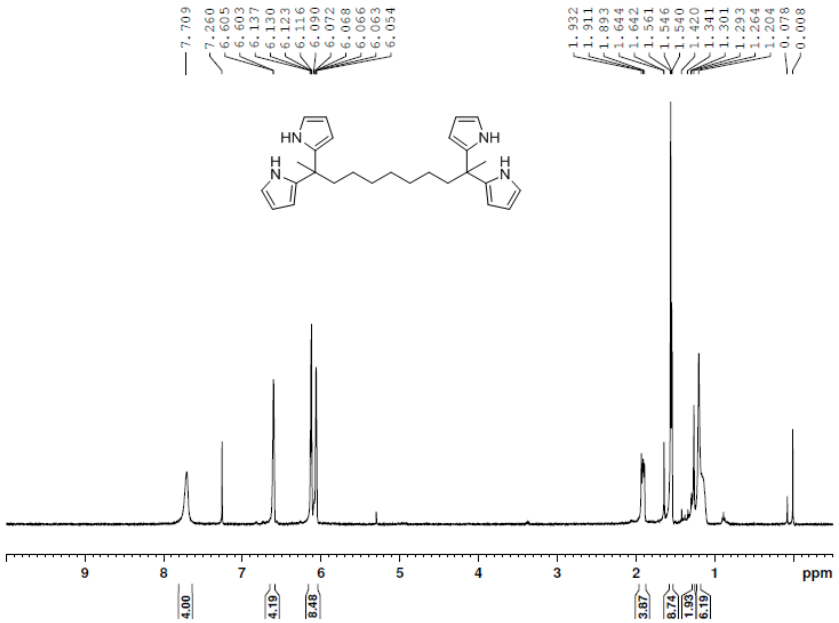

Figure A5 ^{1}H NMR spectrum of **SP8e**.

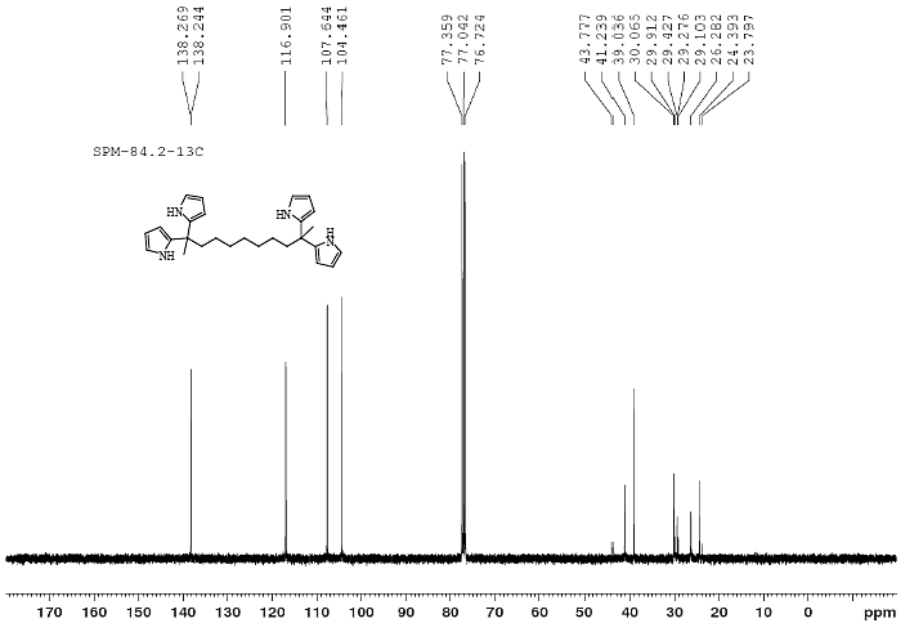

Figure A6 ^{13}C NMR spectrum of **SP8e.**

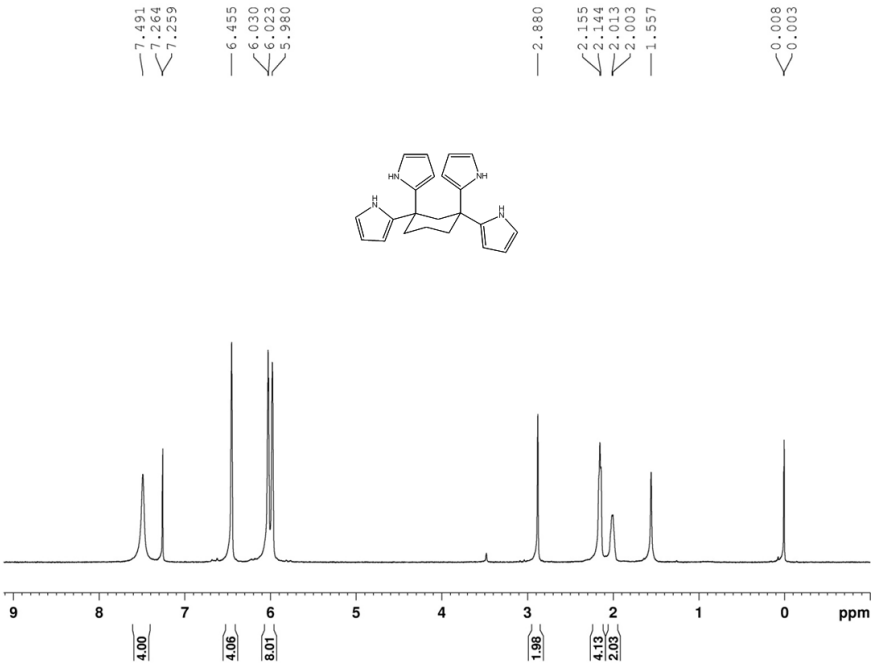

Figure A7 ^{1}H NMR spectrum of **SP10**.

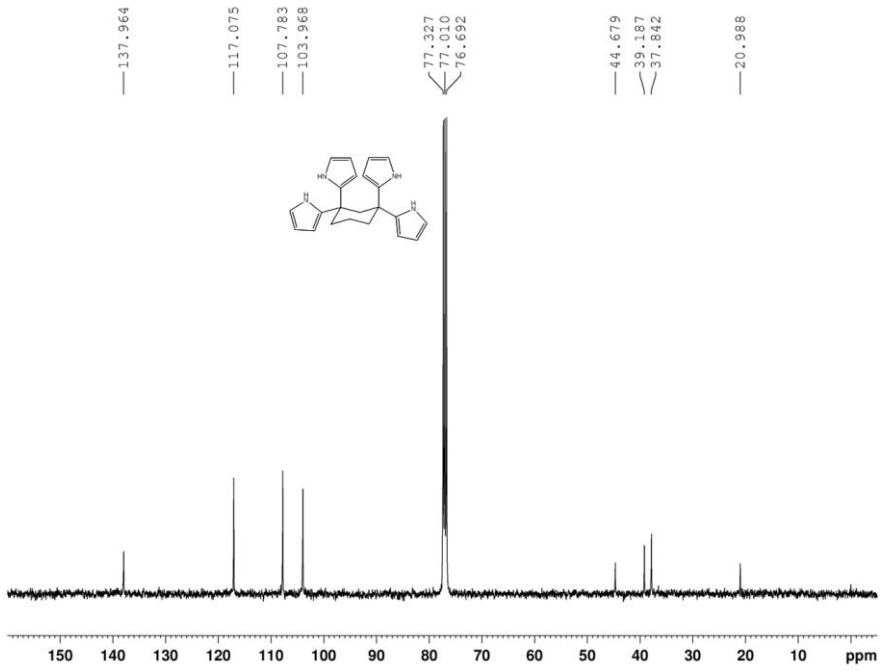

Figure A8 ^{13}C NMR spectrum of **SP10**.

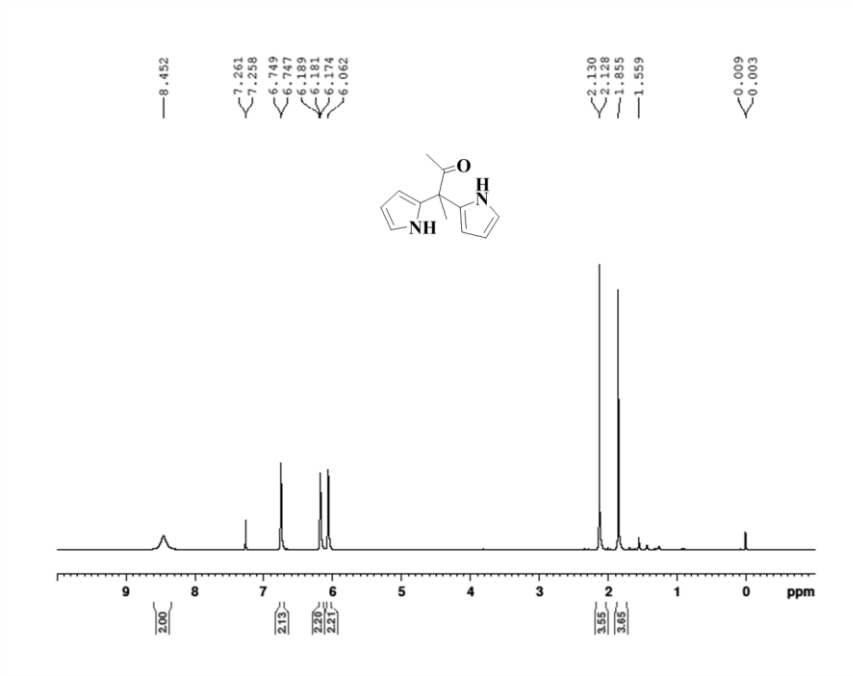

Figure A9 ^{1}H NMR spectrrum of **SP12**.

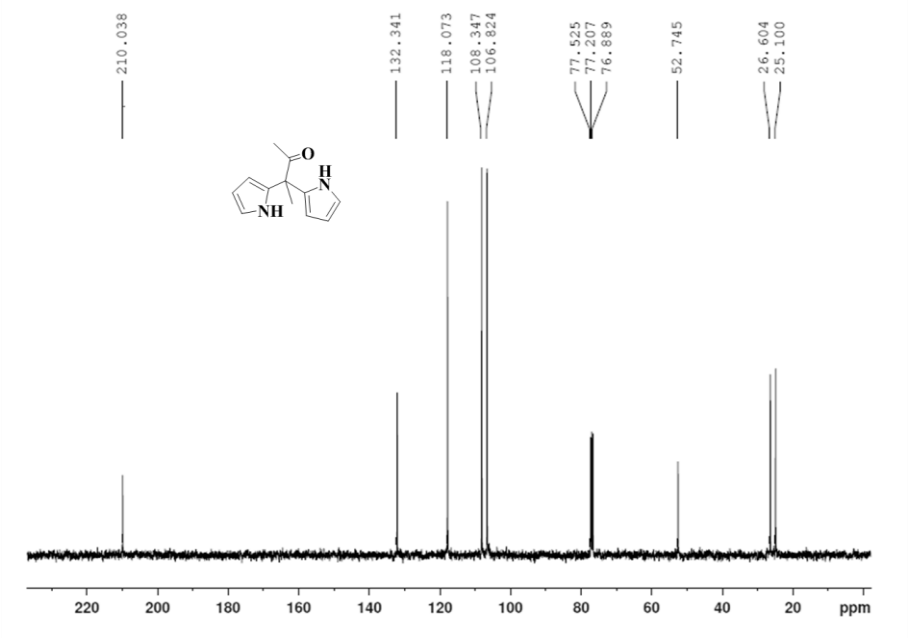

Figure A10 ^{13}C NMR spectrum of **SP12**.

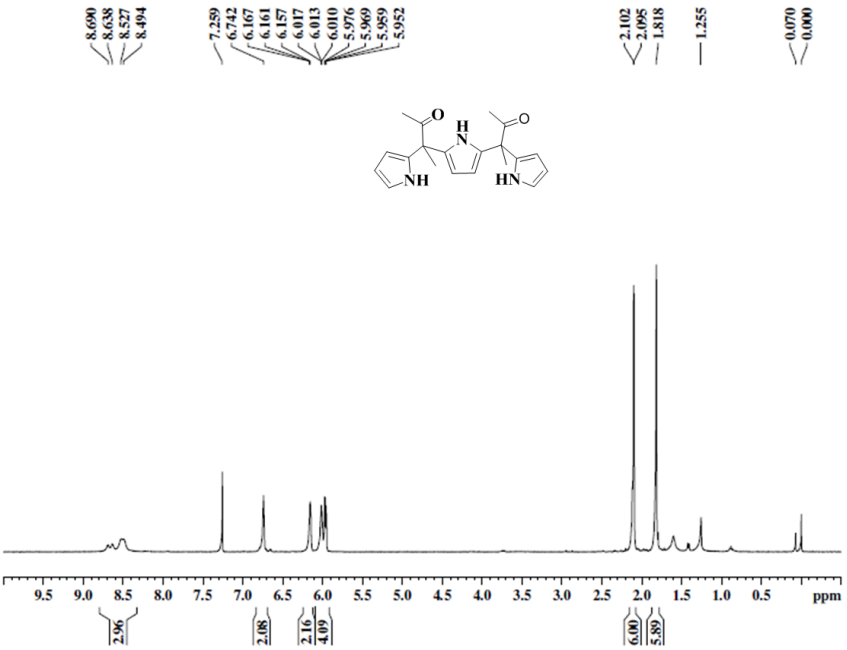

Figure A11 ^{1}H NMR spectrum of **SP13**.

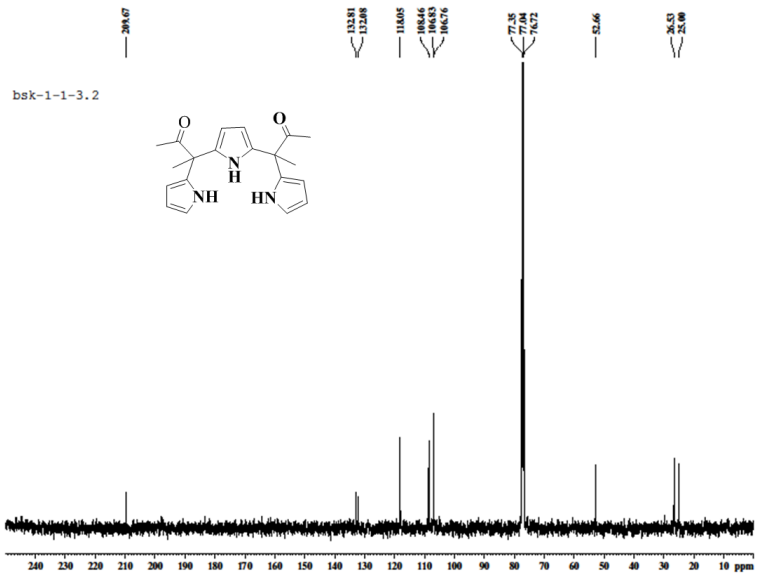

Figure A12 ^{13}C NMR spectrum of **SP13**.

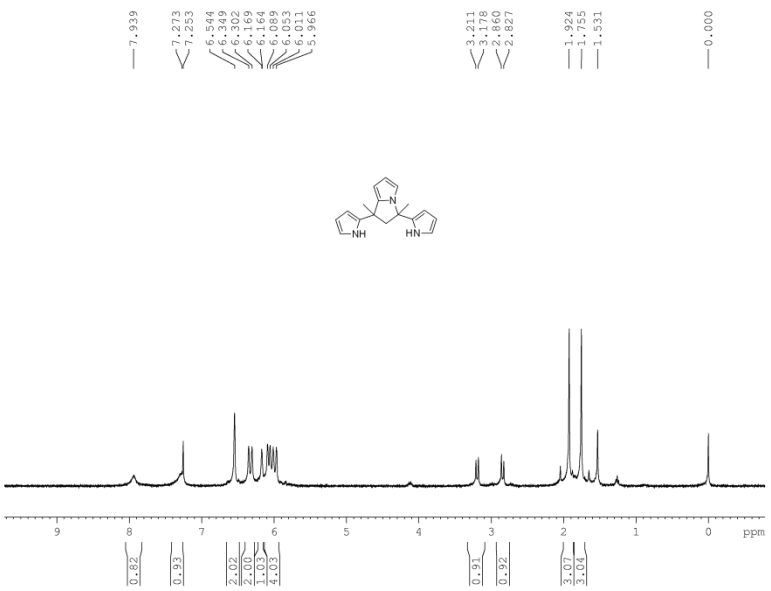

Figure A13 ^{1}H NMR spectrum of **SP14**.

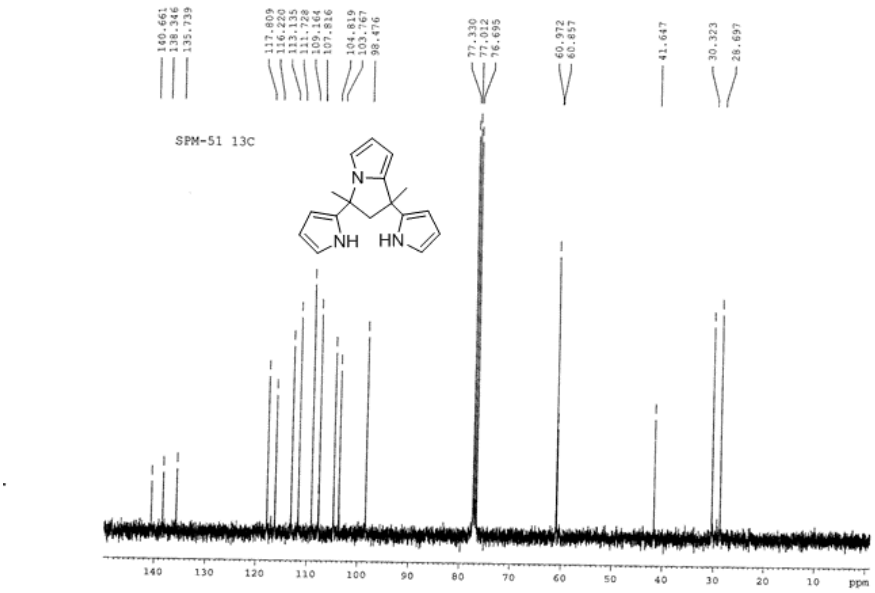

Figure A14 ^{13}C NMR spectrum of **SP14**.

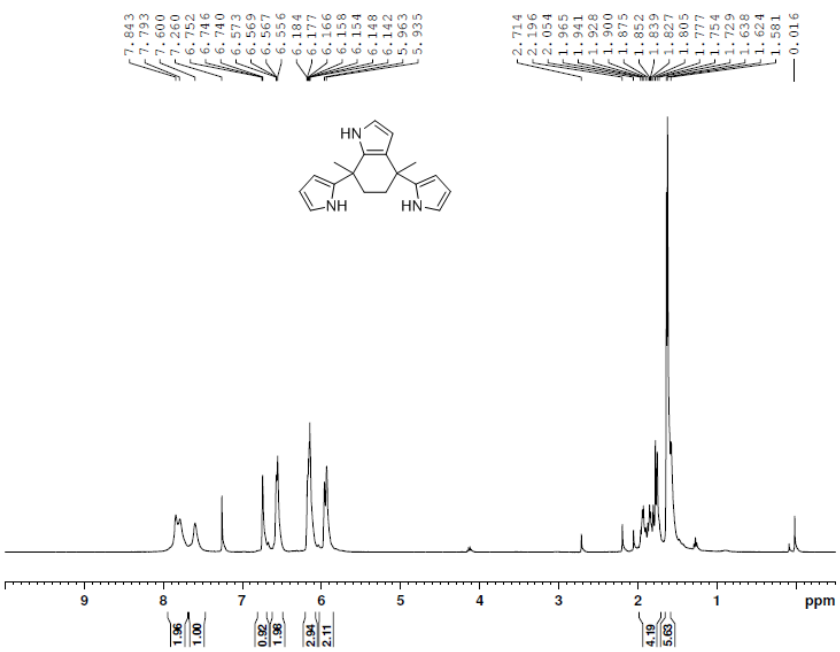

Figure A15 ^{1}H NMR spectrum of **SP15**.

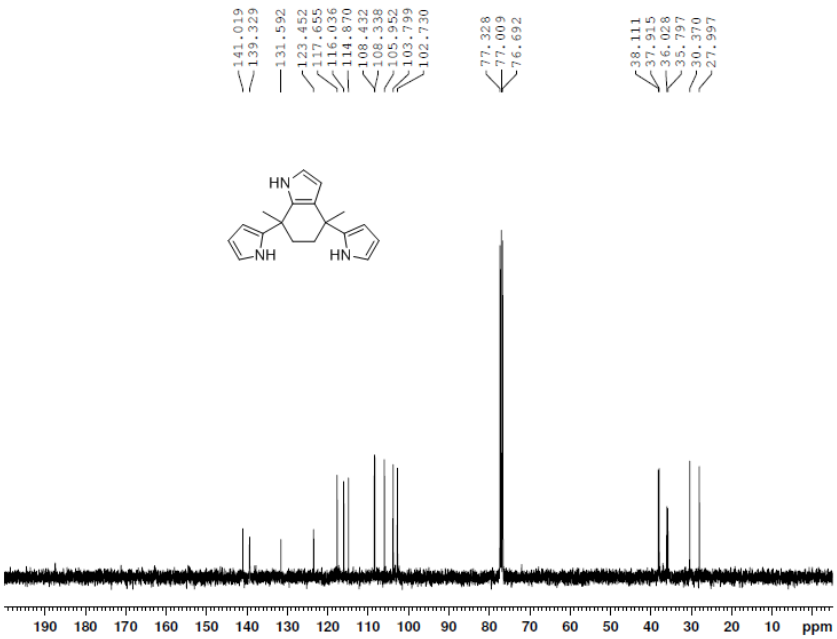

Figure A16 ^{13}C NMR spectrum of **SP15**.

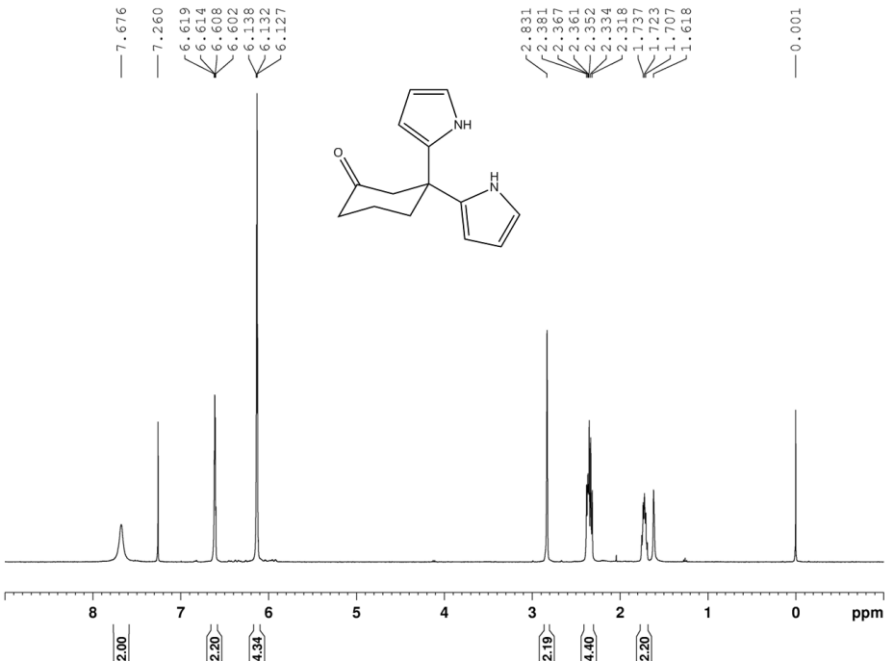

Figure A17 ^{1}H NMR spectrum of **SP16**.

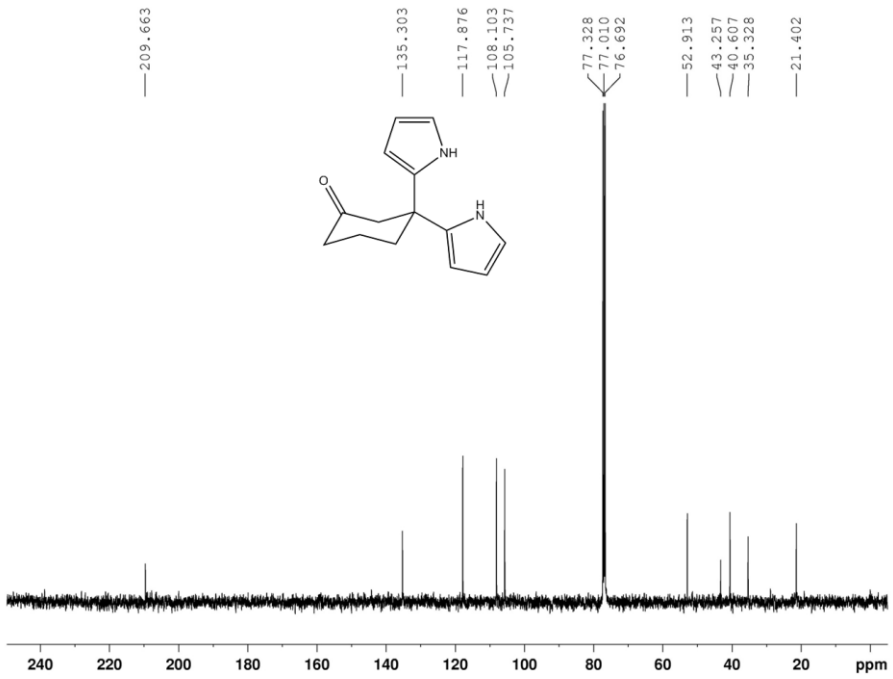

Figure A18 ^{13}C NMR spectrum of **SP16**.

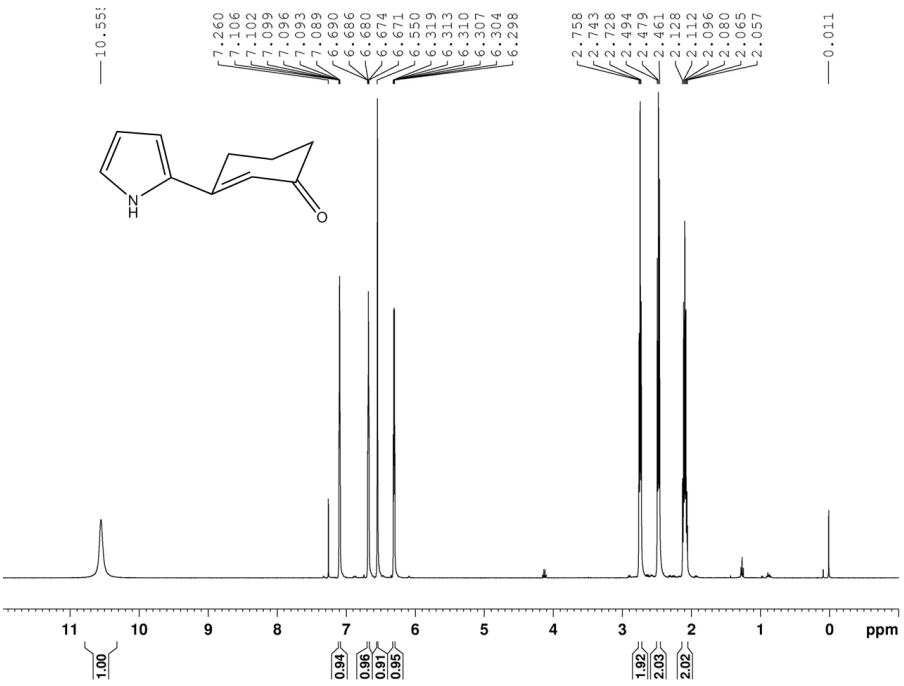

Figure A19 ^{1}H NMR spectrum of **SP17**.

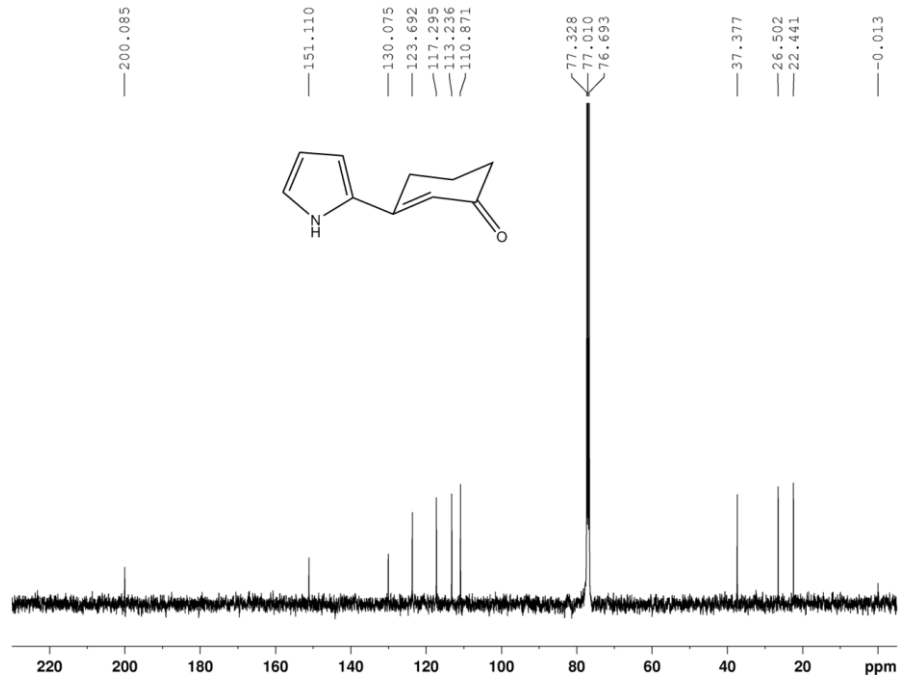

Figure A20 ^{13}C NMR spectrum of **SP17**.

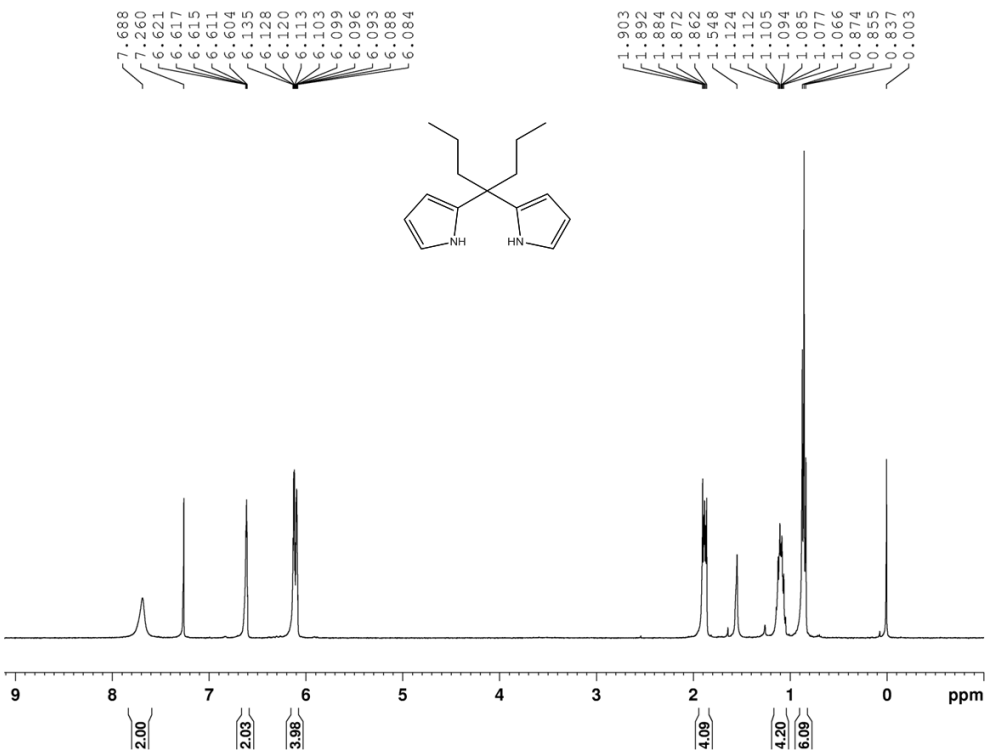

Figure A21 ^{1}H NMR spectrum of **SP18**.

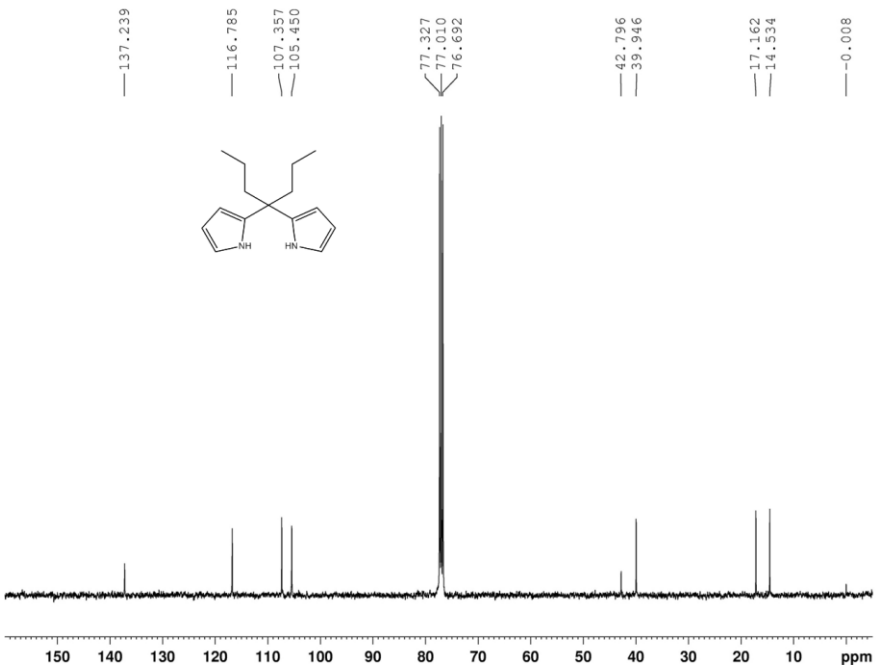

Figure A22 ^{13}C NMR spectrum of **SP18**.

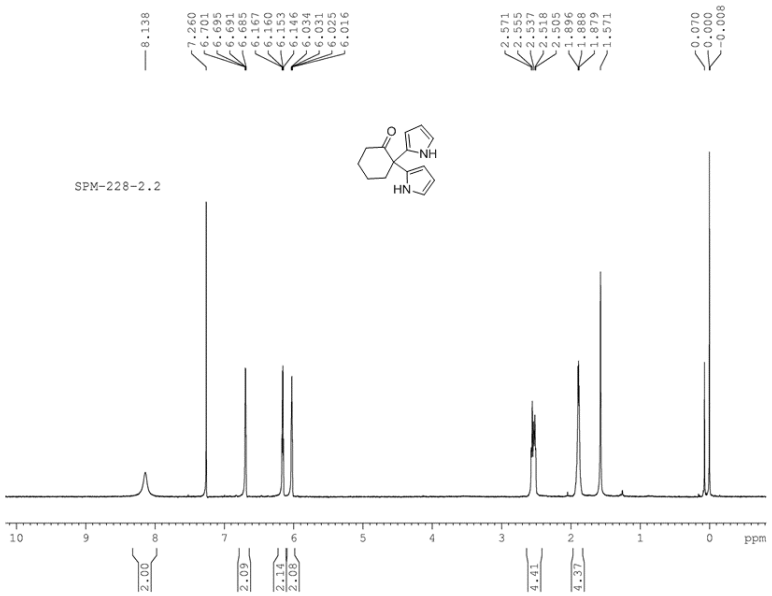

Figure A23 ^{1}H NMR spectrum of **SP19**.

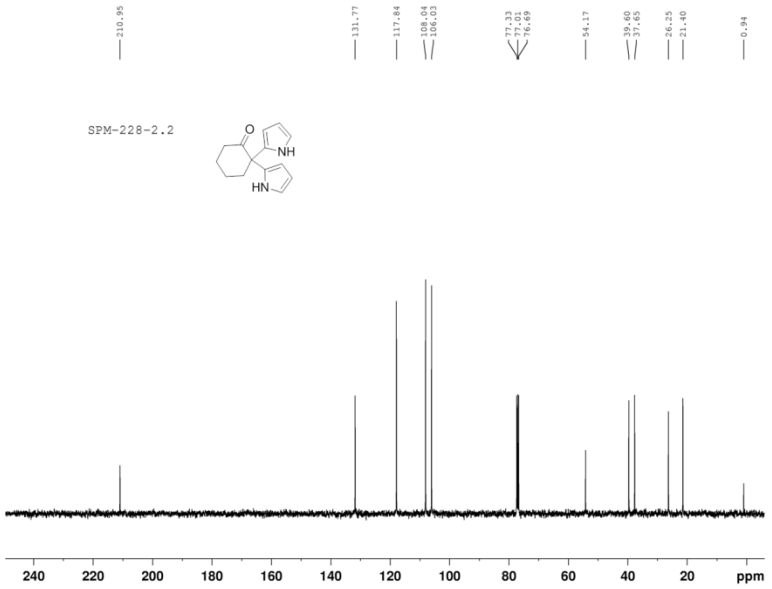

Figure A24 ^{13}C NMR spectrum of **SP19**.

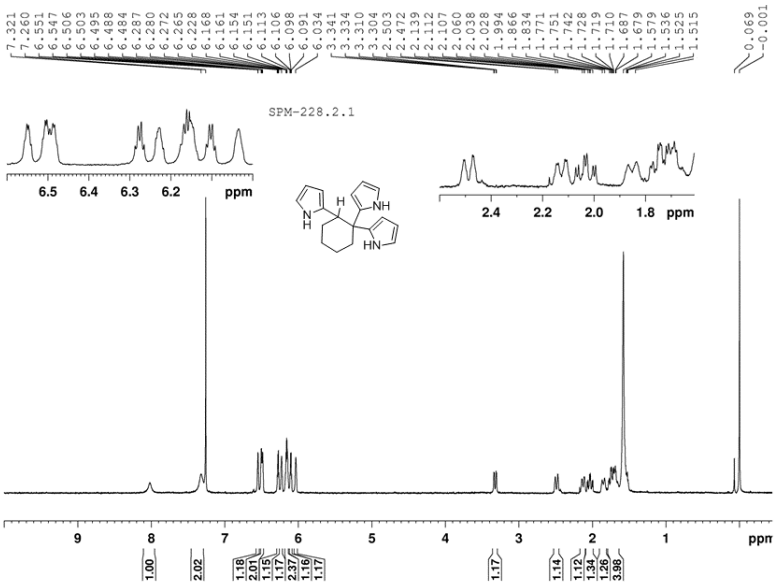

Figure A25 ^{1}H NMR spectrum of **SP 20**.

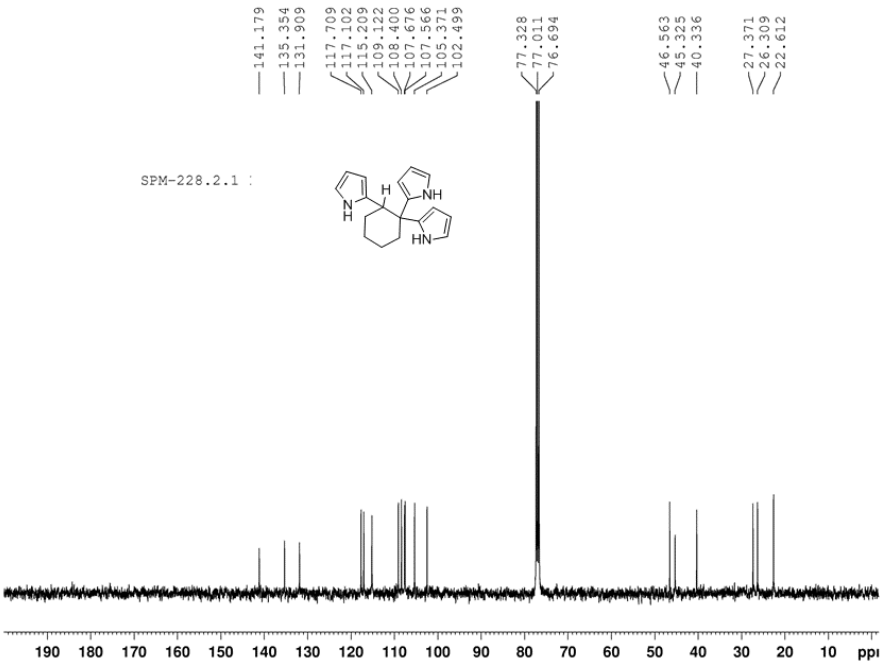

Figure A26 ^{13}C NMR spectrum of **SP 20**.

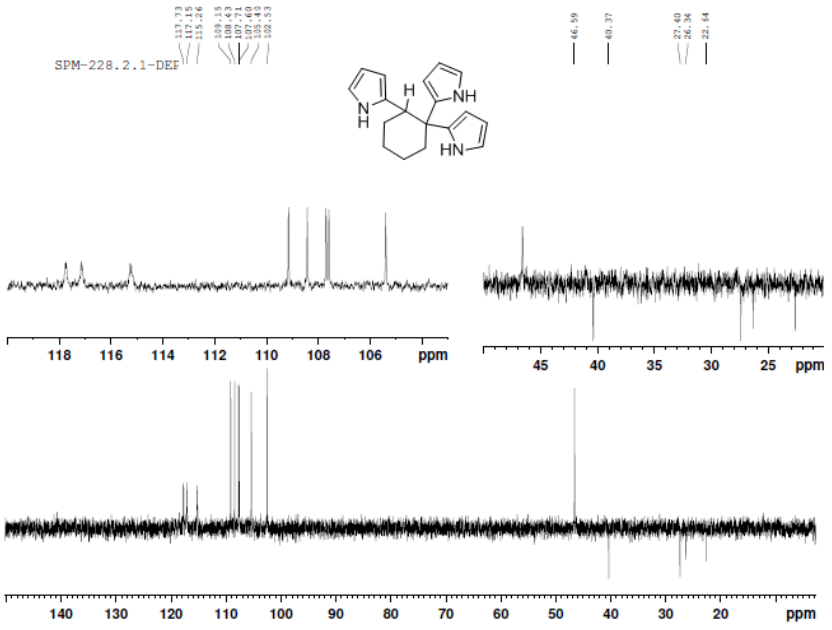

Figure A27 DEPT-135 spectrum of **SP20**.

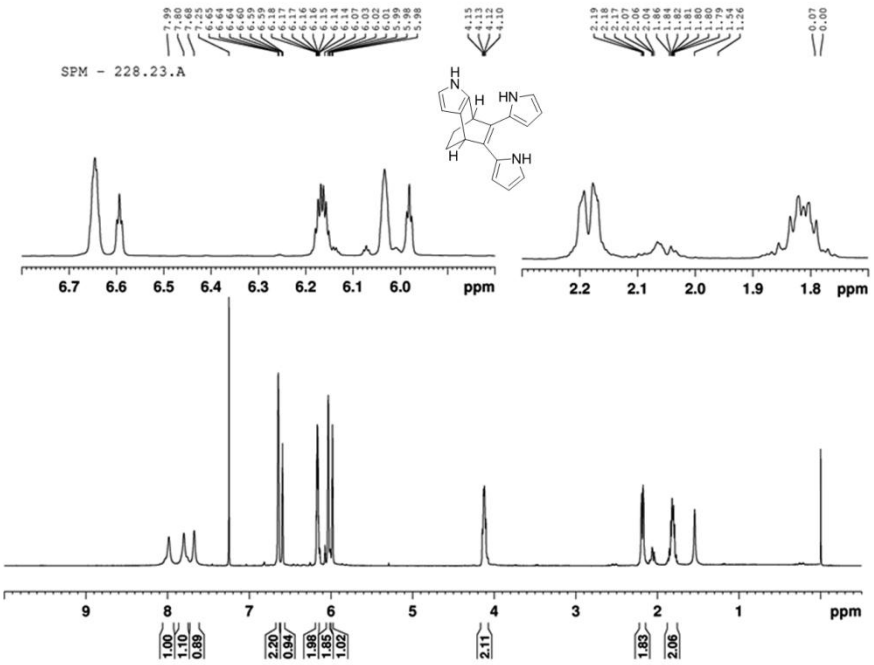

Figure A28 ^{1}H NMR spectrum of **SP21**.

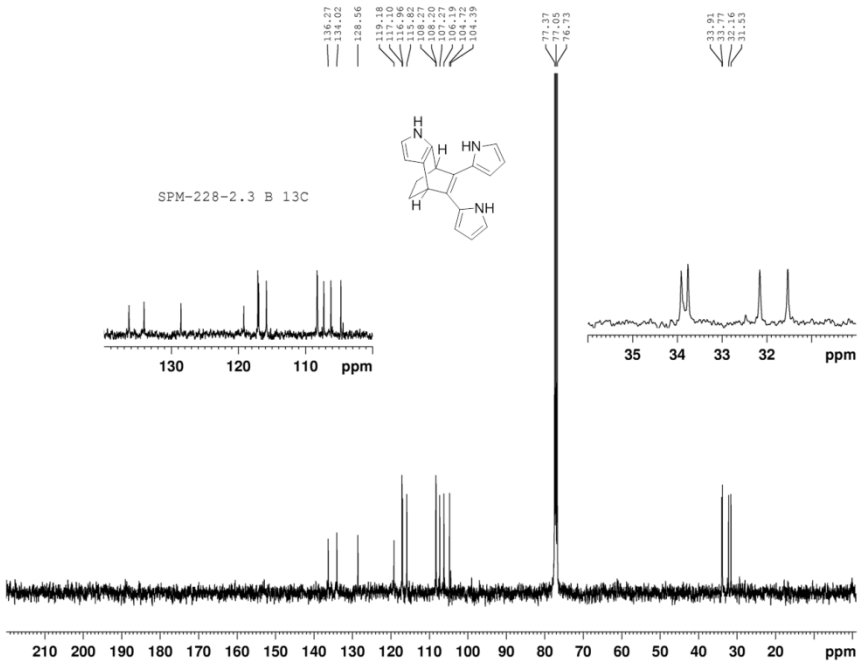

Figure A29 ^{13}C NMR spectrum of **SP21**.

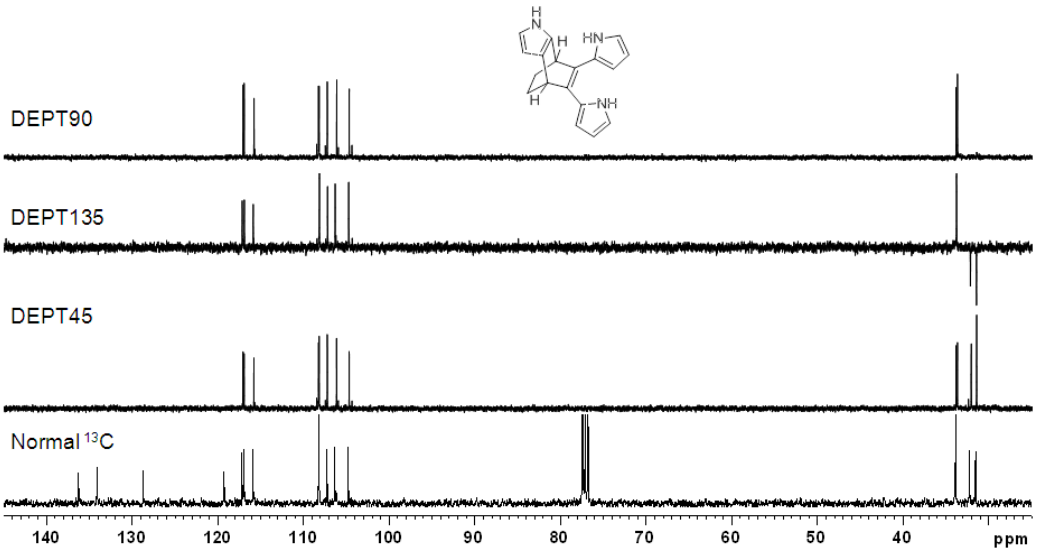

Figure A30 DEPT spectra of **SP21**.

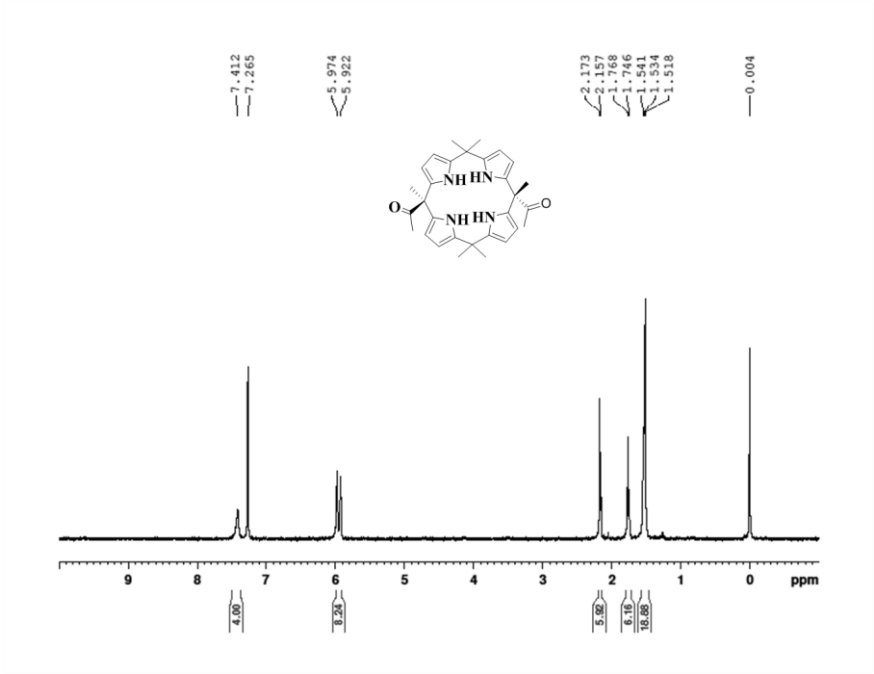

Figure A31 ^{1}H NMR spectrum of *trans*-**SP23**.

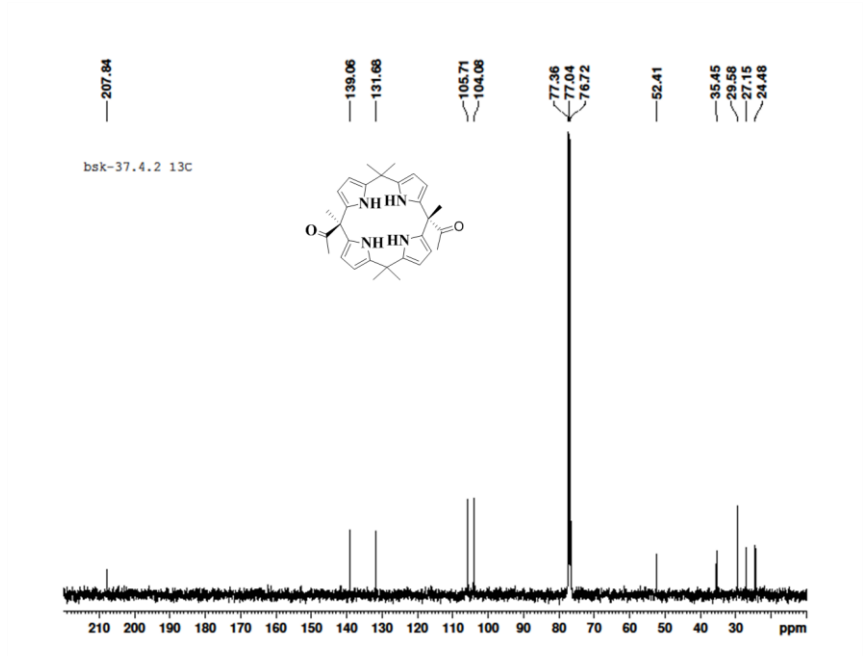

Figure A32 ^{13}C NMR spectrum of *trans*-**SP23**.

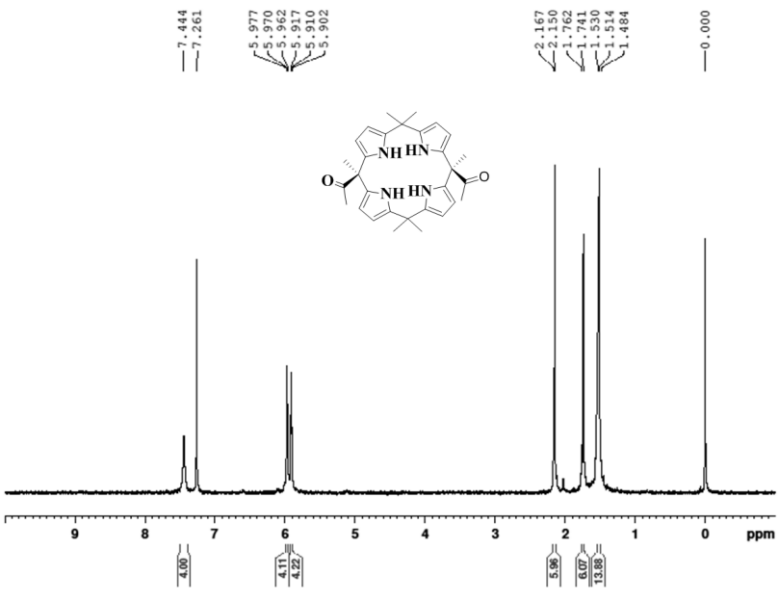

Figure A33 ^{1}H NMR spectrum of *cis*-**SP23**.

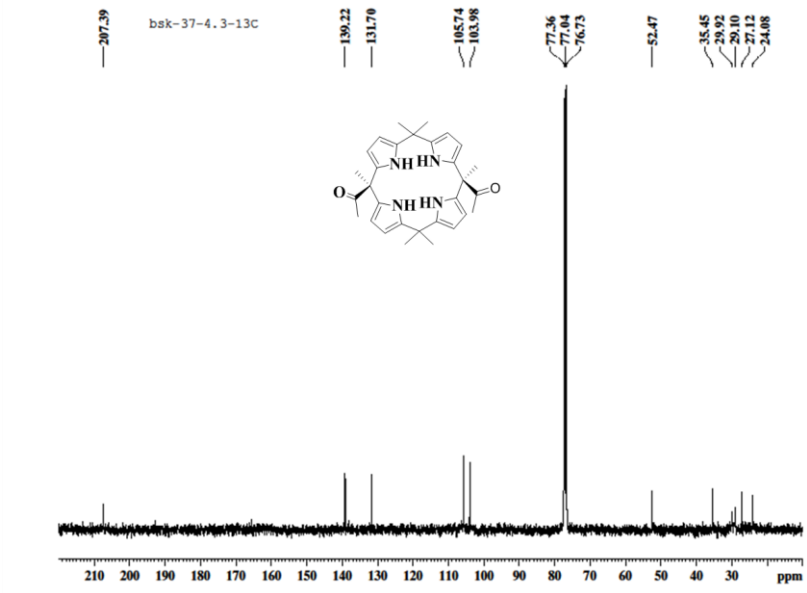

Figure A34 ^{13}C NMR spectrum of *cis*-**SP23**.

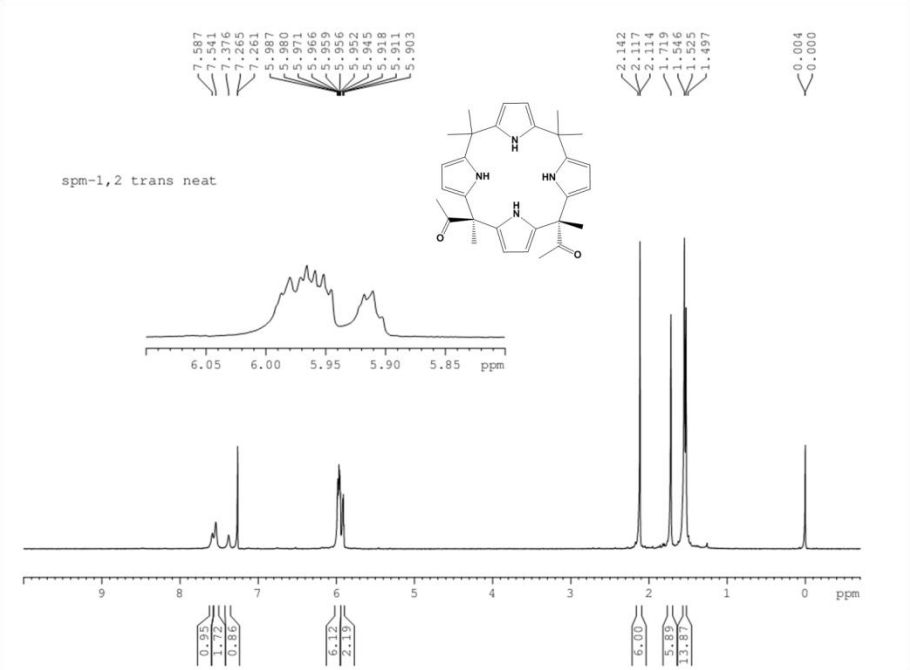

Figure A35 ^{1}H NMR spectrum of *trans*-**SP24**.

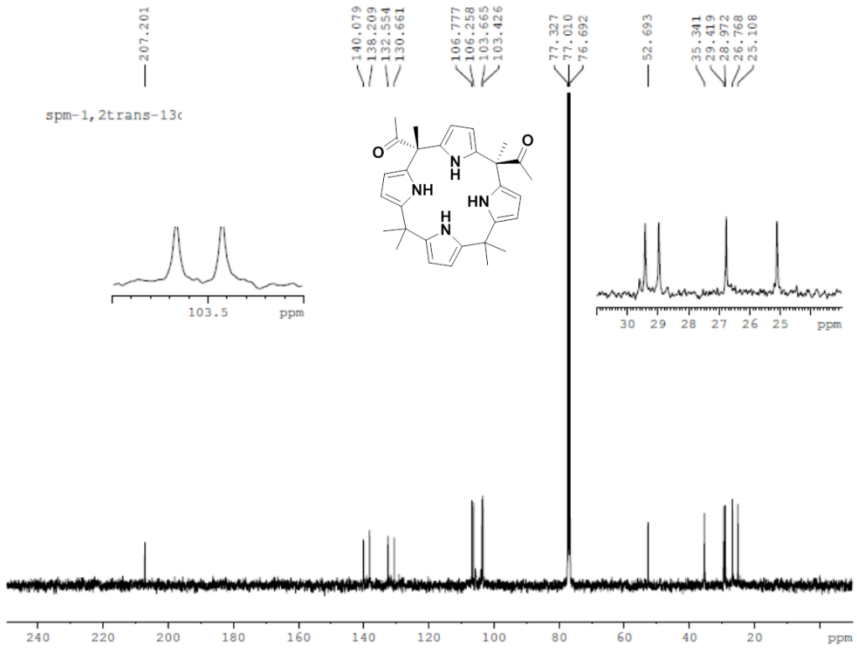

Figure A36 ^{13}C NMR spectrum of *trans*-**SP24**.

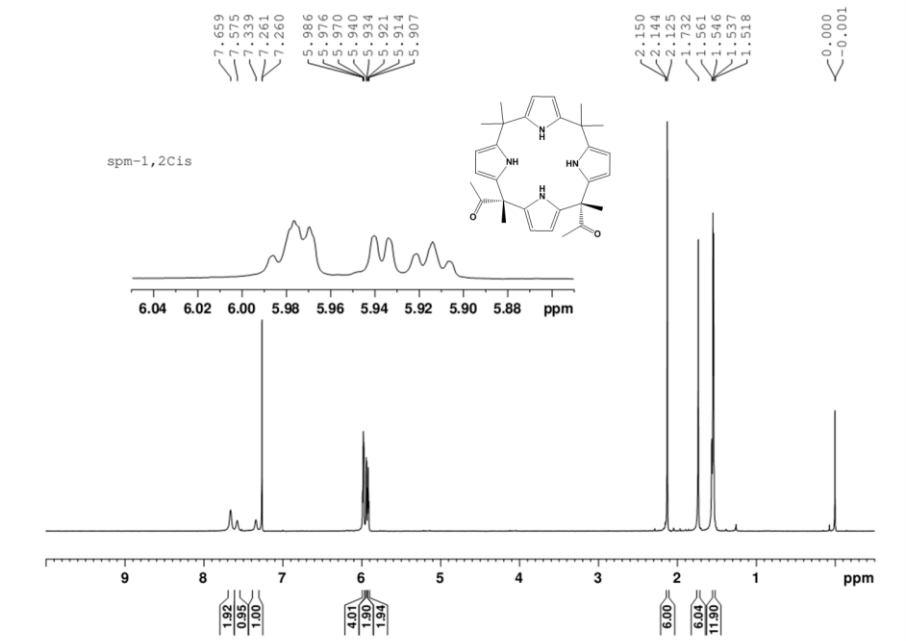

Figure A37 ^{1}H NMR spectrum of *cis*-**SP24**.

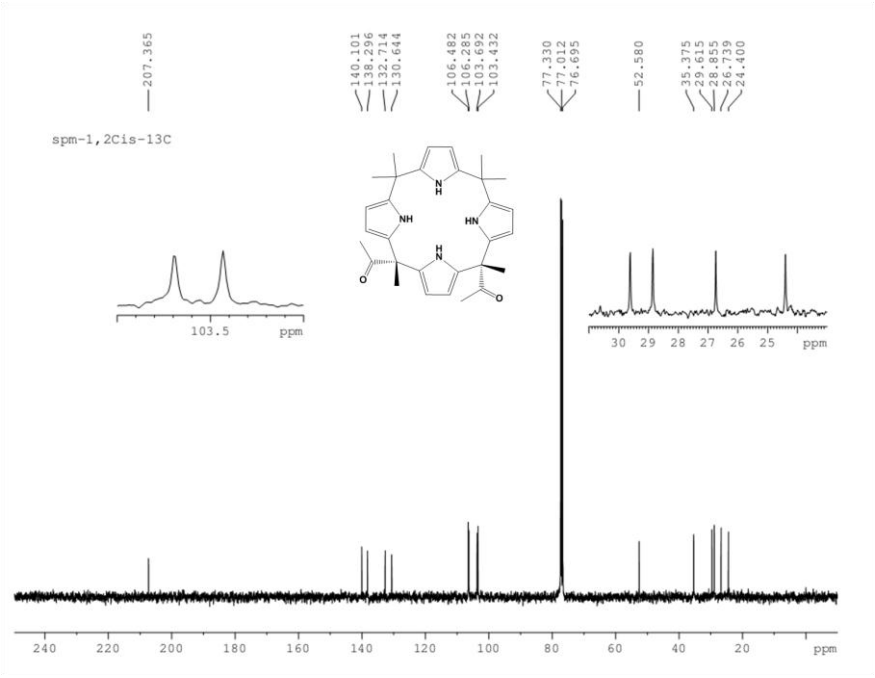

Figure A38 ^{13}C NMR spectrum of *cis*-**SP24**.

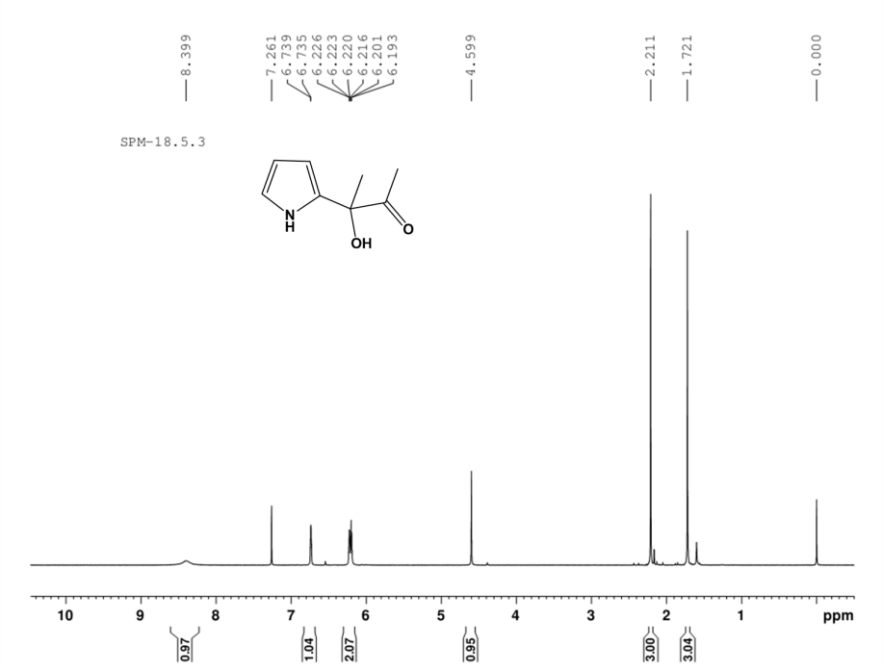

Figure A39 ^{1}H NMR spectrum of **SP25**.

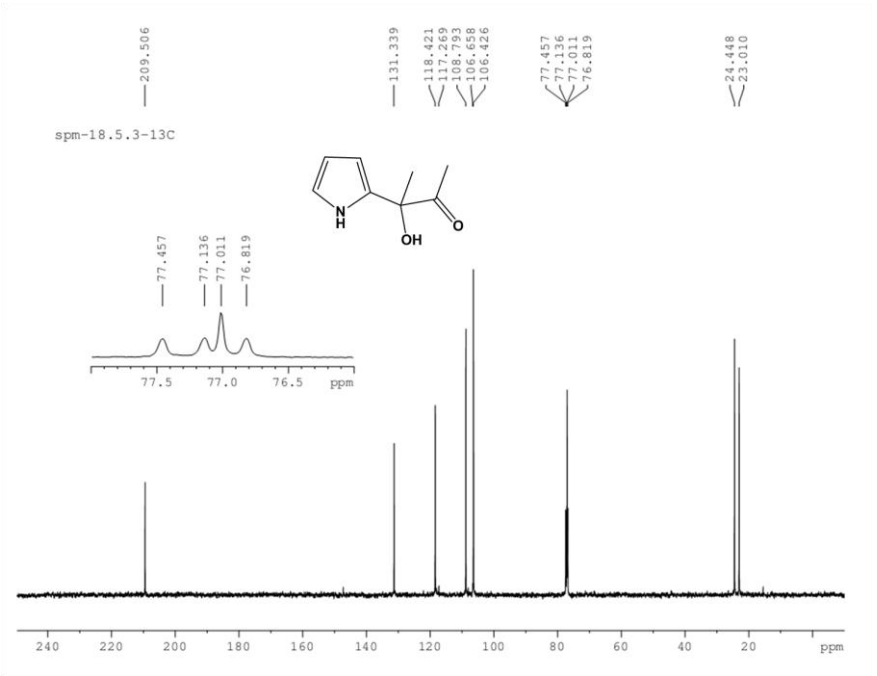

Figure A40 ^{13}C NMR spectrum of **SP25**.

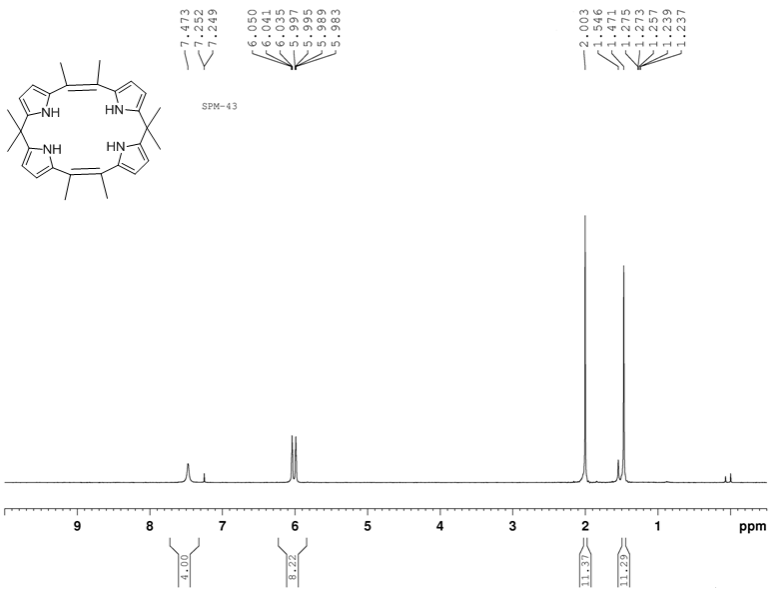

Figure A41 ^{1}H NMR spectrum of **SP27**.

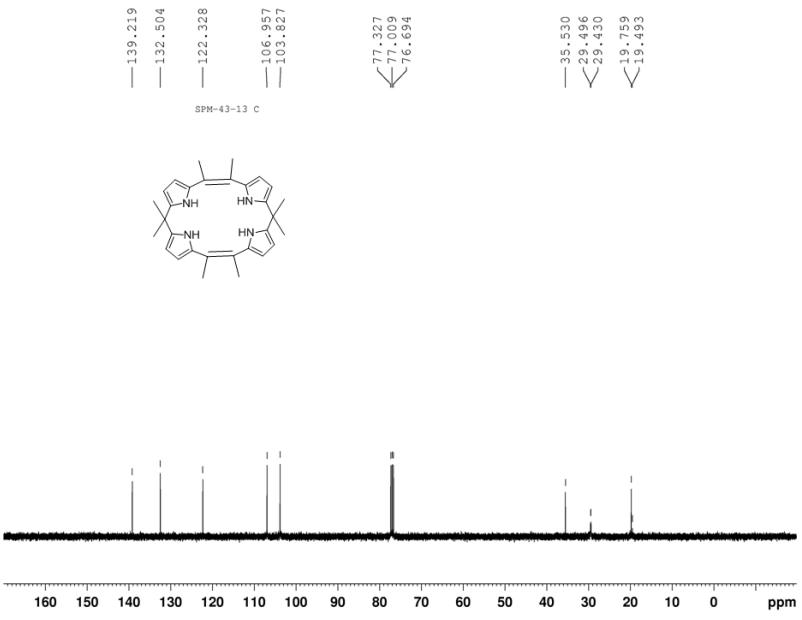

Figure A42 ^{13}C NMR spectrum of **SP27**.

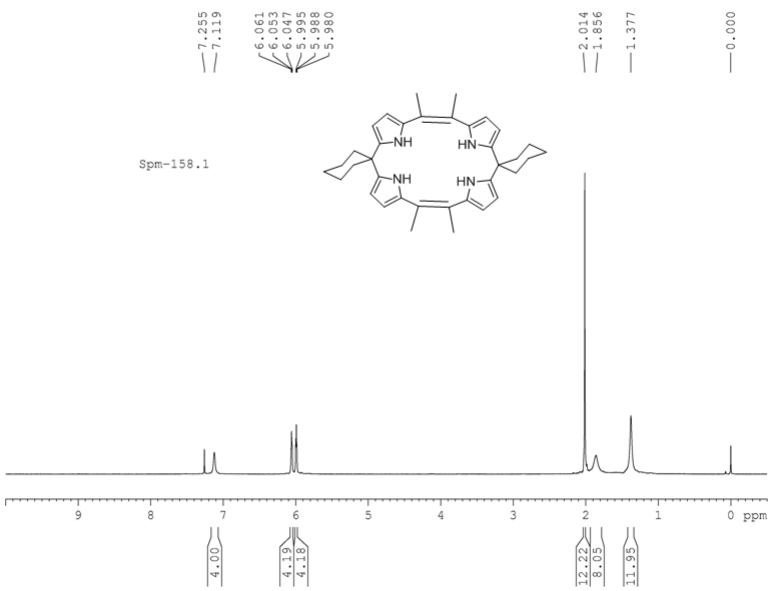

Figure A43 ^{1}H NMR spectrum of **SP28**.

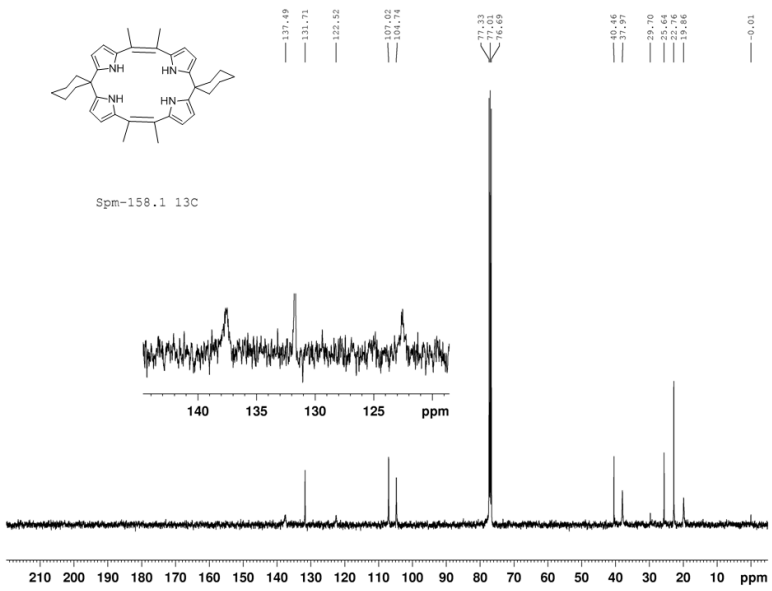

Figure A44 ^{13}C NMR spectrum of **SP28**.

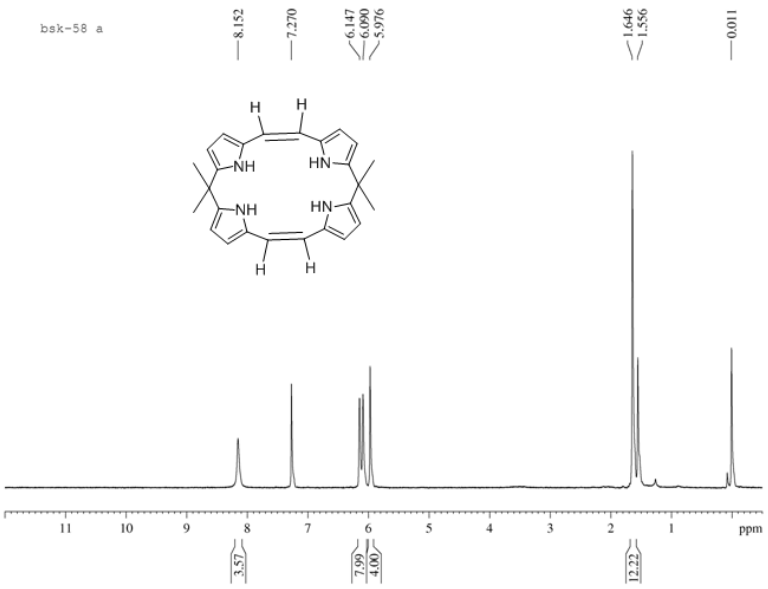

Figure A45 ^{1}H NMR spectrum of **SP29**.

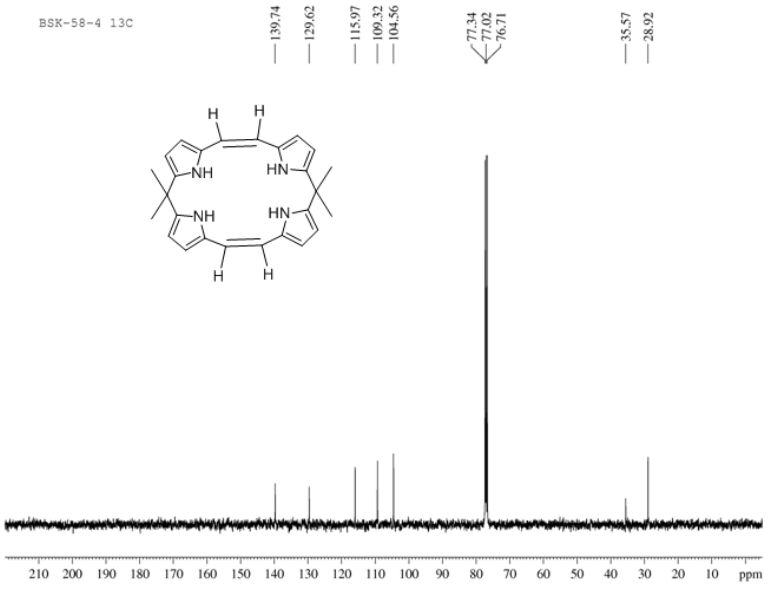

Figure A46 ^{13}C NMR spectrum of **SP29**.

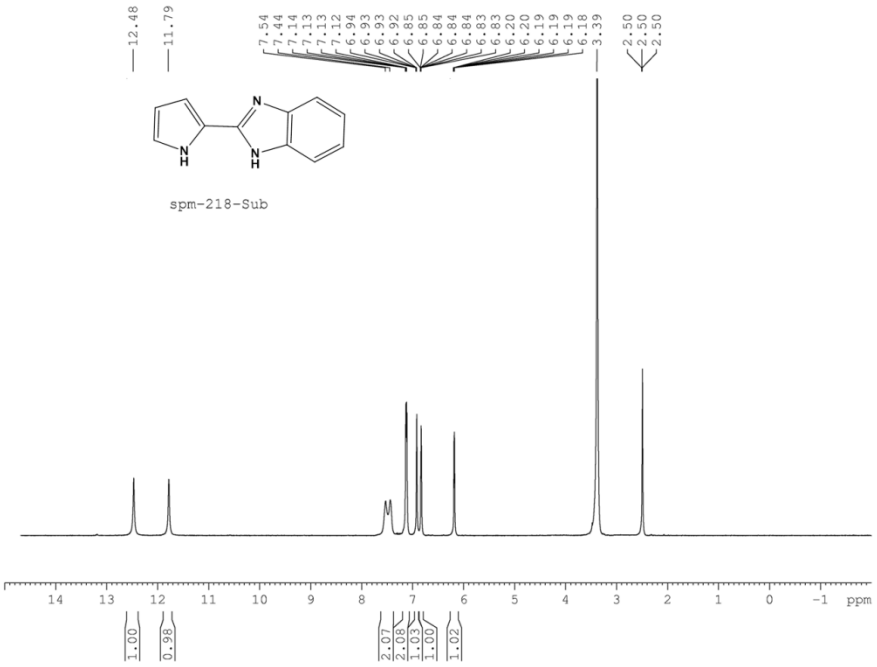

Figure A47 ^{1}H NMR spectrum of **SP35a**.

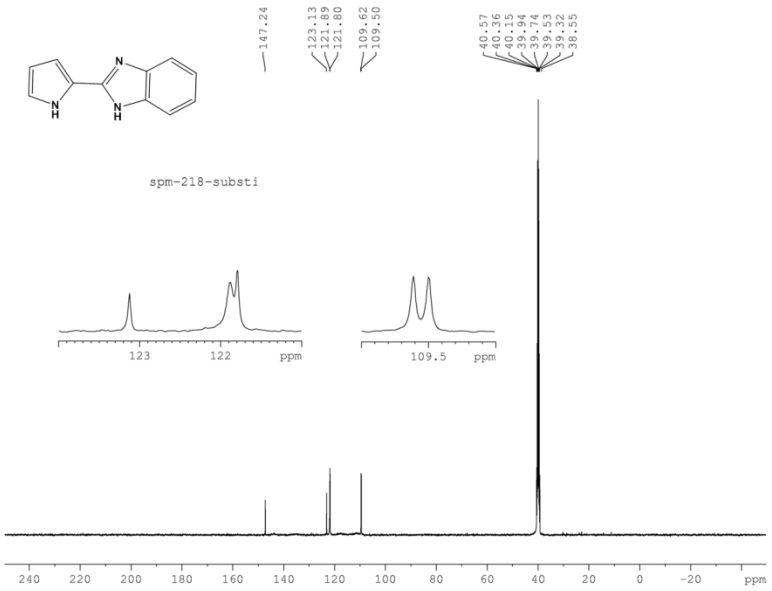

Figure A48 ^{13}C NMR spectrum of **SP35a**.

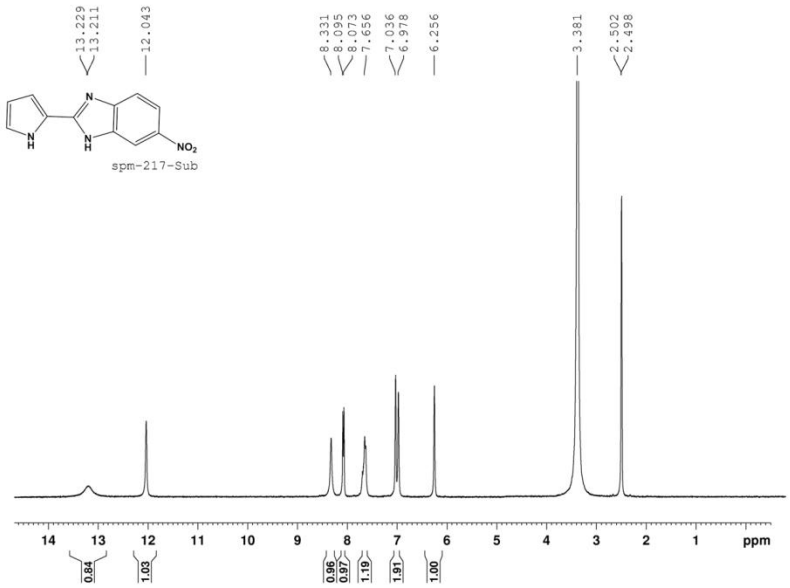

Figure A49 ^{1}H NMR spectrum of **SP35b**.

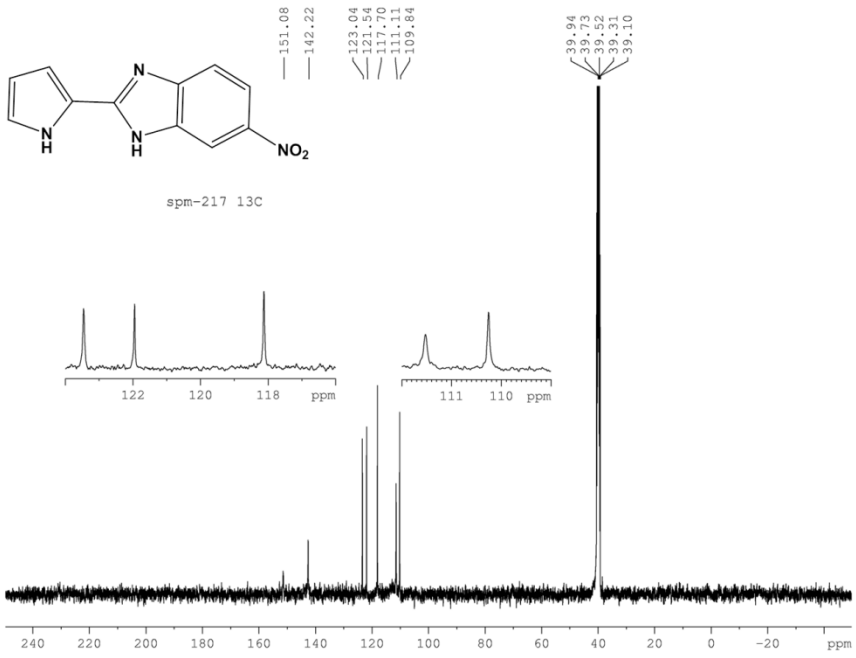

Figure A50 ^{13}C NMR spectrum of **SP35b**.

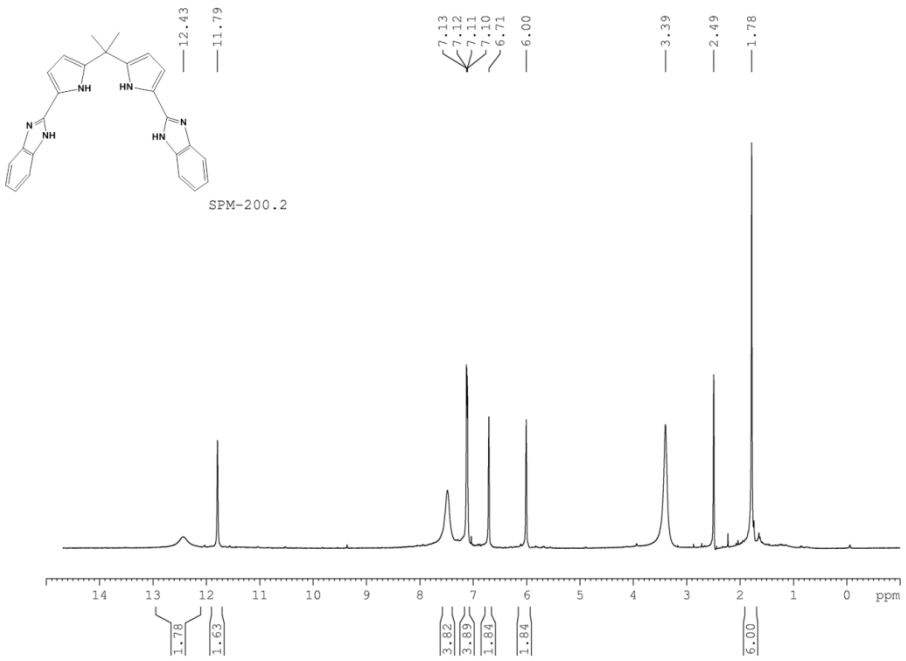

Figure A51 ^{1}H NMR spectrum of **SP36a**.

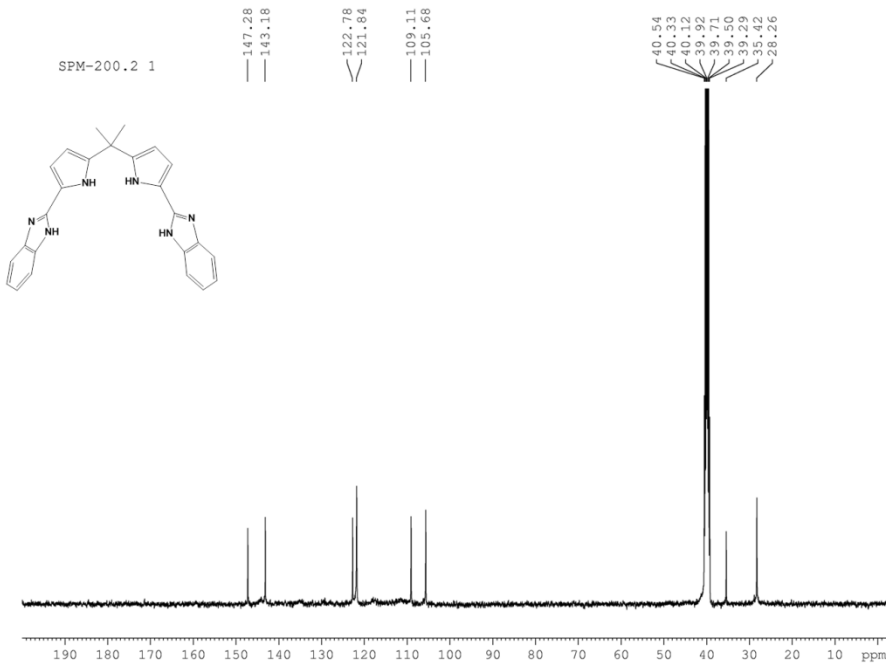

Figure A52 ^{13}C NMR spectrum of **SP36a**.

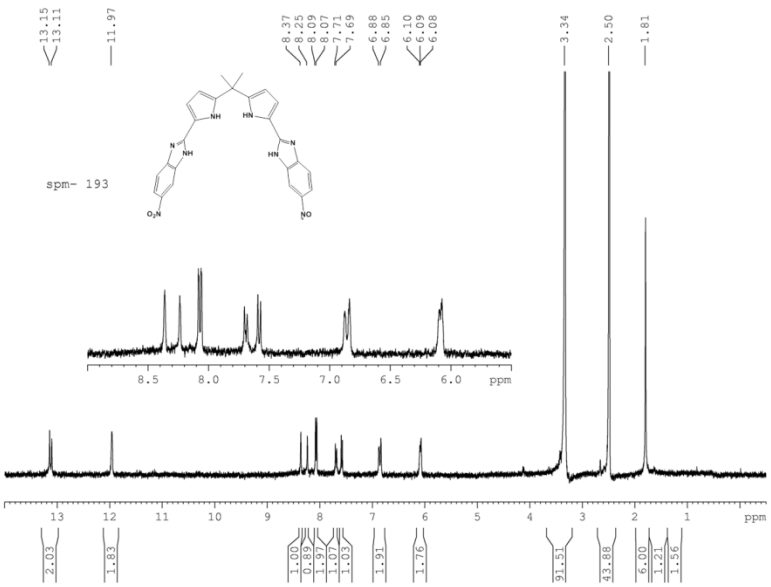

Figure A53 ^{1}H NMR spectrum of **SP36b**.

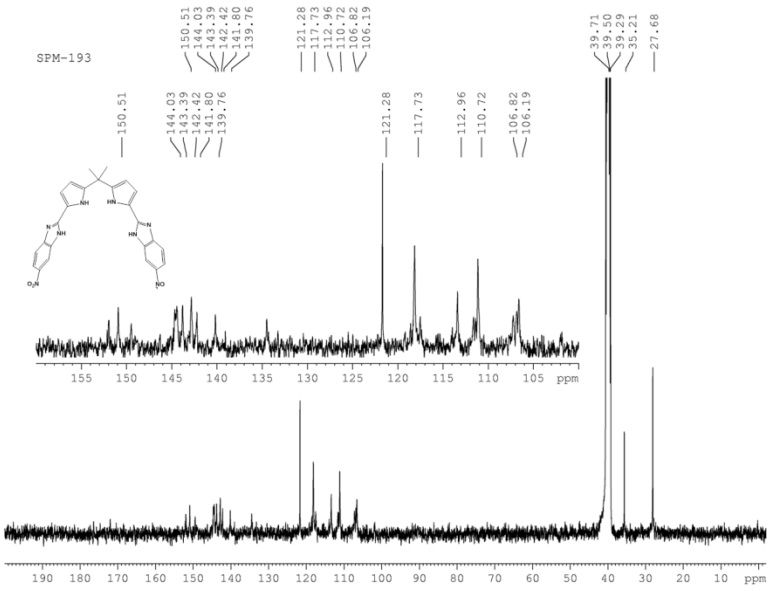

Figure A54 ^{13}C NMR spectrum of **SP36b**.

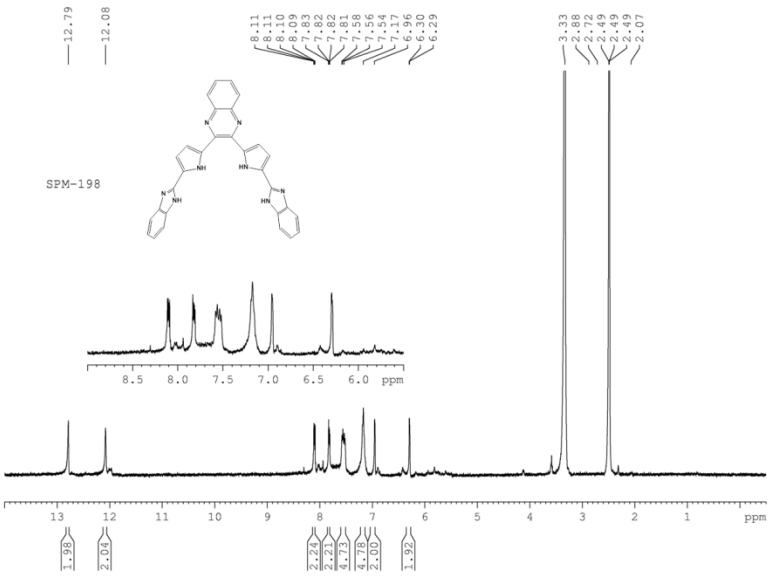

Figure A55 ^{1}H NMR Spectrum of **SP37a**.

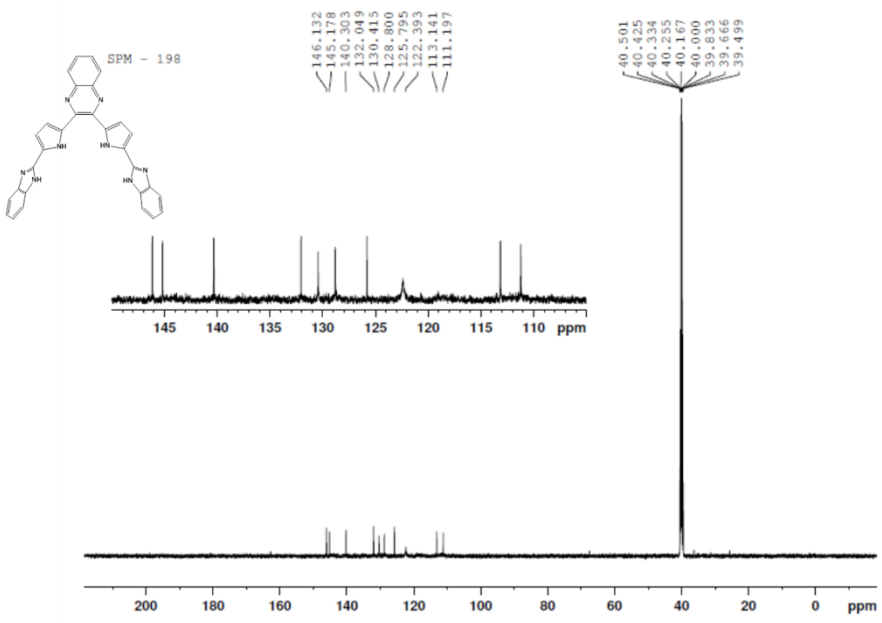

Figure A56 ^{13}C NMR Spectrum of **SP37a**.

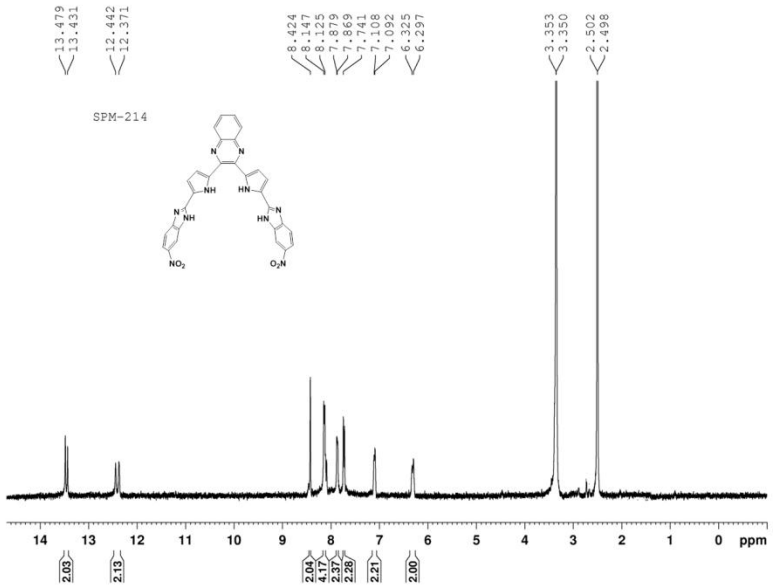

Figure A57 ^{1}H NMR Spectrum of **SP37b**.

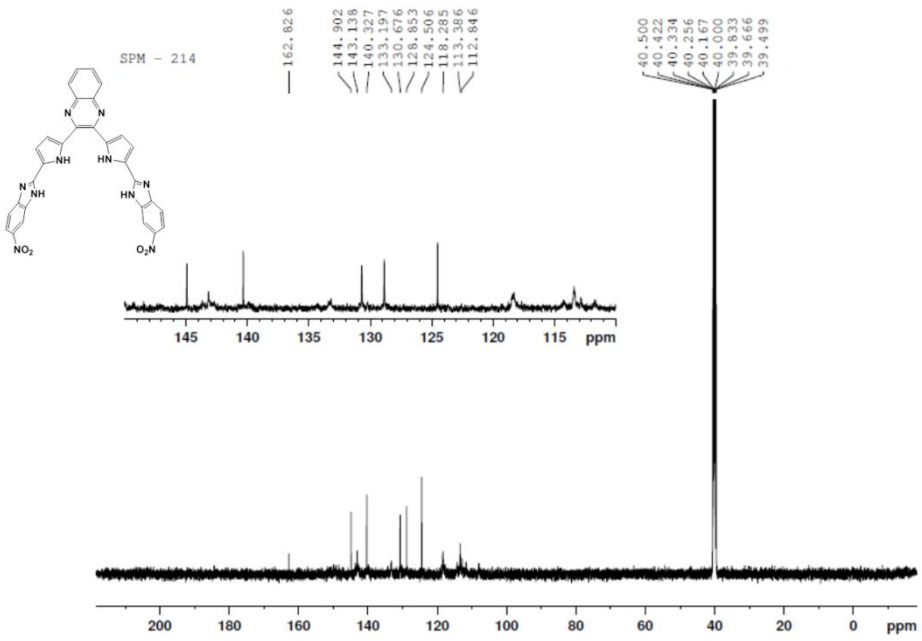

Figure A58 ^{13}C NMR Spectrum of **SP37b**.

Publications

1. Unusual ring annulation during condensation of acetylacetone with pyrrole, **Mahanta, S. P.**; Panda, P. K. *Tetrahedron Lett.* **2009**, *50*, 890-892.

2. New strapped calix[4]pyrrole based receptors for anions, Samanta, R.; **Mahanta, S. P.**; Chaudhari, S.; Panda, P.; Narahari, A. *Inorg. Chim. Acta* **2011**, *372*, 281-285.

3. *Meso*-diacylated calix[4]pyrrole: Structural diversities and enhanced binding towards dihydrogenphosphate ion, **Mahanta, S. P.**; Kumar, B. S.; Panda, P. K. *Chem. Commun.* **2011**, *47*, 4496-4498.

4. Interesting reactivity of diketones with pyrrole under acidic condition, **Mahanta, S. P.**; Panda, P. K. *J. Chem. Sci*. **2011**, *123*, 593-599.

5. Colorimetric sensing of fluoride ion by new expanded calix[4]pyrrole through anion-π interaction, **Mahanta, S. P.**; Kumar, B. S.; Sambath, B.; Sivasankar, C.; Panda, P. K. *Org. Lett.* **2012**, *14*, 548-551.

6. Naphthalene strapped fluorescent calix[4]pyrrole isomers: halide ion selectivity based on strap topography, Samanta, R.; **Mahanta, S. P.**; Ghanta, S.; Panda, P. K. *RSC Advances* **2012**, *2*, 7974-7977.

7. Calix[2]bispyrrolylarenes: New expanded calix[4]pyrroles for fluorometric sensing of anions via extended π-conjugation, Chandra, B.; **Mahanta, S. P.**; Pati, N. N; Baskaran, S.; Kanaparthi, R. K.; Sivasankar, C.; Panda, P. K. *Org. Lett.* **2013**, *15*, 306-309.

8. Condensation of cyclohexanediones with pyrrole under acidic conditions: Unusual products and interesting structural features, **Mahanta, S. P.**; Panda, P. K. (Communicated)

9. 5,10-Diacylcalix[4]pyrroles: Synthesis and anion binding studies, **Mahanta, S. P.**; Panda, P. K. (Communicated)

10. Pyrrole-benzimidazole conjugates: a new H-bonding motif towards anion binding, Mahanta, S. P.; Panda, P. K. (Manuscript under preparation)

Conference presentations

1. Poster presented on "Towards synthesis of bisdipyrromethanes: interesting reactivity of diketones with pyrrole under acidic condition", 11th National Symposium in Chemistry (NSC 11), **2009**, NCL, Pune, India.

2. Poster presented on "Towards synthesis of bisdipyrromethanes: interesting reactivity of diketones with pyrrole under acidic condition", 6th Annual in-house symposium CHEMFEST **2009**, School of Chemistry, University of Hyderabad, Hyderabad, India.

3. Poster presented (with Narendra Nath Pati, Brijesh Chandra) on "Calix[4]phycene: An efficient host for dihydrogenphosphate anion", 12th National Symposium in Chemistry (NSC 12), **2010**, IICT, Hyderabad, India.

4. Poster presented on "*Meso*-acylated Calix[4]pyrroles: a neutral host for dihydrogenphosphate" 6th International Conference on Porphyrins and Phthalocyanines (ICPP-6), **2010**, Santa Ana Pueblo, New Mexico, USA.

5. Oral presentation on "Modification of Calix[4]pyrrole moiety towards anion binding" 9th Annual in-house symposium CHEMFEST **2012**, School of Chemistry, University of Hyderabad, Hyderabad, India.